SEPARATION OF MIXTURES OF PROTEINS

USING CRYSTALLIZATION

Somchai Maosoongnern

A Thesis Submitted in Partial Fulfillment of the Requirements for the

Degree of Doctor of Philosophy in Chemical Engineering

Suranaree University of Technology

Academic Year 2015

การแยกสารผสมของโปรตีนโดยกระบวนการตกผลึก

นายสมชาย เมาสูงเนิน

วิทยานิพนธ์นี้เป็นส่วนหนึ่งของการศึกษาตามหลักสูตรปริญญาวิศวกรรมศาสตรดุษฎีบัณฑิต
สาขาวิชาวิศวกรรมเคมี
มหาวิทยาลัยเทคโนโลยีสุรนารี
ปีการศึกษา 2558

SEPARATION OF MIXTURES OF PROTEINS USING CRYSTALLIZATION

Suranaree University of Technology has approved this thesis submitted in partial fulfillment of the requirements for the Degree of Doctor of Philosophy.

Thesis Examining Committee

_____

(Asst. Prof. Dr. Atichat Wongkoblab)

Chairperson

_____

(Asst. Prof. Dr. Chalongsri Flood)

Member (Thesis Advisor)

_____

(Prof. Dr. Adrian E. Flood)

Member

_____

(Dr. Terasut Sookkumnerd)

Member

_____

(Asst. Prof. Dr. Sopark Sonwai)

Member

_____   _____

(Prof. Dr. Sukit Limpijumnong)   (Assoc. Prof. Flt. Lt. Dr. Kontorn Chamniprasart)

Vice Rector for Academic Affairs   Dean of Institute of Engineering

and Innovation

สมชาย เมาสูงเนิน : การแยกสารผสมของโปรตีนโดยกระบวนการตกผลึก
(SEPARATION OF MIXTURES OF PROTEINS USING
CRYSTALLIZATION) อาจารย์ที่ปรึกษา : ผู้ช่วยศาสตราจารย์ ดร.ฉลองศรี ฟลัด,
212 หน้า.

ปัญหาหลักสำคัญในการที่จะได้มาซึ่งผลิตภัณฑ์โปรตีนบริสุทธิ์คือ การแยกโปรตีนที่
ต้องการออกมาจากโปรตีนที่มีอยู่ตามธรรมชาติ โดยให้มีความบริสุทธิ์อยู่ในระดับที่อุตสาหกรรม
ต้องการใช้ กระบวนการตกผลึกของโปรตีนเป็นประบวนการแยกและทำโปรตีนให้บริสุทธิ์วิธีหนึ่ง
ที่ถูกใช้น้อยมากในอุตสาหกรรมทางชีวเคมี ถึงแม้ว่าผลิตภัณฑ์ที่แยกออกมาได้จะมีความบริสุทธิ์สูง
มีอัตราการผลิตที่สูงและง่ายที่จะขยายขนาดการผลิต เนื่องจากมีข้อเสียในเรื่องของการขาดข้อมูล
ทางด้านอุณหพลศาสตร์และจลนศาสตร์ ที่จะทำให้กระบวนการตกผลึกเป็นไปอย่างมีประสิทธิภาพ
งานวิจัยนี้มีวัตถุประสงค์เพื่อศึกษา ความเป็นไปได้ที่จะแยกโปรตีนไลโซไซม์บริสุทธิ์ออกจากสาร
ผสมของไลโซไซม์และโอวัลบูมิน โดยศึกษาและทำความเข้าใจอุณหพลศาสตร์ จลนศาสตร์ และ
พฤติกรรมการตกผลึกของไลโซไซม์จากสารละลายเดี่ยวและสารผสม

ความสามารถในการละลายเป็นคุณสมบัติพื้นฐานของโปรตีนและสาร โดยทั่วไป ความรู้
และความเข้าใจในความสามารถในการละลายของโปรตีน นั้นจำเป็นอย่างยิ่งในการออกแบบและ
ปฏิบัติการการตกผลึกของผลิตภัณฑ์ต่างๆ ในระดับอุตสาหกรรม ความสามารถในการละลายของ
โปรตีนไลโซไซม์จะเพิ่มขึ้นเมื่ออุณหภูมิเพิ่มขึ้น ลดลงเมื่อความเข้มข้นของเกลือโซเดียมคลอไรด์
เพิ่มขึ้น และมีค่าลดลงเล็กน้อยเมื่อค่าความเป็นด่างของสารละลาย (pH) มากขึ้น สำหรับการวัดค่า
ความเข้มข้นขึ้นของโปรตีนในสารละลายผสมนั้นมีวิธีการวัดที่ปรับปรุงขึ้นมาสองวิธีการคือ การใช้
อิเล็คโตรโฟรีซีสแบบโซเดียมโดเดคซิลซัลเฟตโพลีอะคริลาไมด์เจลร่วมกับการดูดกลืนแสงยูวี และ
การใช้การดูดซับแสงยูวีสำหรับโปรตีนผสม การวัดค่าความสามารถในการละลายของโปรตีนที่ขึ้น
อยู่กับตัวแปรต่าง ๆ มีความสำคัญเป็นอย่างมากในการศึกษากระบวนการตกผลึกทั้งในระบบ
โปรตีนเดี่ยวและระบบโปรตีนผสม

เพื่อศึกษาทำความเข้าใจการตกผลึกของโปรตีนให้มากยิ่งขึ้น ผู้วิจัยได้ศึกษาจลนศาสตร์
ของโปรตีนด้วยการสร้างแผนภาพวัฏภาคของโปรตีนไลโซไซม์ โดยใช้เครื่องสเต็มอินทิกริตี้แบบ
สิบหลุม (STEM integrity 10 system) ซึ่งความกว้างของพื้นที่กึ่งสเถียรของแผนภาพวัฏภาคจะ
ขึ้นอยู่กับสภาพของสารละลาย เช่น จะแคบลงเมื่อเติมเกลือเพิ่มลงไป ข้อมูลที่ได้จากแผนภาพวัฏ
ภาคนี้สามารถนำมาใช้เพื่อช่วยออกแบบและควบคุมกระบวนการตกผลึกได้

        การตกผลึกแบบกะของไลโซไซม์ทั้งระบบโปรตีนชนิดเดียวและระบบโปรตีนผสมถูก
ศึกษาโดยการตกผลึกโดยใช้ตัวล่อ โดยการตกผลึกจะเกิดขึ้นภายในพื้นที่กึ่งสเถียรของแผนภาพวัฏ
ภาค เพื่อให้แน่ใจว่าไม่มีการเกิดผลึกใหม่เกิดขึ้น ซึ่งกระบวนการตกผลึกประสบความสำเร็จในการ
ตกผลึกแยกโปรตีนไลโซไซม์ออกมาจากทั้งระบบโปรตีนชนิดเดียวและระบบโปรตีนผสม ผลการ
ทดลองพบว่ากลไกการเติบโตของผลึกถูกควบคุมด้วยกระบวนการการรวมตัวกันที่พื้นผิวของผลึก
อัตราการเติบโตของผลึกขึ้นอยู่กับกำลังสองของค่าความเข้มข้นยิ่งยวดสัมพัทธ์ โอวัลบูมินที่เจือปน
ลงไปในสารละลายจนถึงความเข้มข้น 67.5% ของความเข้มข้นของโปรตีนรวม ไม่มีผลกระทบ
สำคัญอะไรกับการเติบโตของผลึก รวมทั้งความแตกต่างของความเข้มข้นของเกลือโซเดียมคลอไรด์
สามและสี่เปอเซ็นต์ก็ไม่มีผลกระทบสำคัญอะไรกับการเติบโตของผลึกด้วยเช่นกัน อย่างไรก็ดี
อุณหภูมิมีผลกระทบต่อการเติบโตของผลึกเป็นอย่างมาก ค่าคงที่ของการเติบโตของผลึกมีค่า
เพิ่มขึ้นตามการเพิ่มขึ้นของอุณหภูมิและเป็นไปตามความสัมพันธ์ของอาร์รีเนียส

สาขาวิชา <u>วิศวกรรมเคมี</u>   ลายมือชื่อนักศึกษา<u>   </u>

ปีการศึกษา 2558   ลายมือชื่ออาจารย์ที่ปรึกษา<u>   </u>

                          ลายมือชื่ออาจารย์ที่ปรึกษาร่วม<u>   </u>

SOMCHAI MAOSOONGNERN : SEPARATION OF MIXTURES OF
PROTEINS USING CRYSTALLIZATION. THESIS ADVISOR : ASST.
PROF. CHALONGSRI FLOOD, Ph.D., 212 PP.

PROTEIN SEPARATION/BATCH CRYSTALLIZATION/MIXED
PROTEINS/SOLUBILITY/PHASE DIAGRAMS/CRYSTALLIZATION
KINETICS/LYSOZYME

The main difficulty in accessing protein products is purifying the many proteins involved in natural products into pure protein fractions on an industrial scale. Protein crystallization is a separation/purification technique little used in the bioprocess industry despite the high purity levels and good separation factors obtained. One of the major drawbacks has been the lack of thermodynamic and kinetic data required for efficient crystallization. This thesis aims to study the possibility to separate pure lysozyme out of the mixtures of lysozyme and ovalbumin by understanding the thermodynamic and kinetic behavior of the crystallization of lysozyme from both pure and mixed solution.

Solubility is a fundamental thermodynamics property of proteins and other species, and is essential knowledge to be able to design and operate industrial crystallizers for any product. The solubility of lysozyme increases with increasing temperature, decreases with increasing sodium chloride concentration, and is slightly reduced at higher values of the pH. Two modified techniques, SDS-PAGE gel + UV-Vis and the UV-Vis for mixtures, were introduced for use in measurement of the concentration of proteins in mixtures. The measurement of solubility as a function of

the parameters is very important in studying the crystallization process in both pure and mixed protein systems.

To extend the understanding of protein crystallization, the kinetics of protein crystallization were studied, with the phase diagrams of lysozyme being determined using the STEM integrity 10 system. The width of the metastable zone depends on the solution conditions, i.e. it is narrower when more salt is added to the mixture. The presence of the phase diagram offers the possibility to use the information for design and control the crystallization process.

The batch crystallization of lysozyme for both pure and mixed systems was studied via a seeded crystallization process. The crystallization was performed within the metastable region to ensure that no nucleation occurs. The successful crystallization of tetragonal lysozyme crystal was performed for both pure and mixed protein systems. The growth kinetics is controlled by the surface integration mechanism. The crystal growth rates were found to be second order with respect to the relative supersaturation. There is no significant effect of ovalbumin impurity, up to the concentration of 67.5% (based on total protein), and NaCl concentrations of 3 and 4%, on the growth of lysozyme crystal. The temperature has a greater effect on the growth of the crystal. The growth rate constants increase with increasing temperature and follow an Arrhenius relationship.

School of Chemical Engineering   Student's Signature _____

Academic Year 2015   Advisor's Signature _____

                                        Co-Advisor's Signature _____

ACKNOWLEDGEMENTS

First and foremost, with the achievement of this degree I would like to express my sincere gratitude to my thesis advisor and co-advisor, Asst. Prof. Dr. Chalongsri Flood and Prof. Dr. Adrian E. Flood for providing me with the opportunity to undertake a Ph.D., supporting information, invaluable advice and for the limitless patience and encouragement that have helped me pass through my difficult times. It has always been a great honor to be their Ph.D. student. I appreciate their contributions of time, ideas, and funding in order to make my Ph.D. experience very productive and enormously stimulating. I could not have imagined having any better advisor for my study for the Ph.D. Without their patience and insightful suggestion, I would not have achieved this far and this thesis would not have been completed.

I would like to express my gratitude to Asst. Prof. Dr. Atichat Wongkoblab, Dr. Terasut Sookkumnerd, Asst. Prof. Dr. Sopark Sonwai, Prof. Dr. Chaiyot Tangsathitkulchai, and Assoc. Prof. Dr. Wipa Sujinta for their kind agreement to serve on my committee for the thesis examination and thesis proposal, and also for their wonderful questions and guidance.

I would like to thank all of the lecturers at the School of Chemical Engineering, Suranaree University of Technology (SUT) for their superb attitude and advice. Especially, I would like to thank Asst. Prof. Dr. Chalongsri Flood. She has taught me, both consciously and unconsciously, from the beginning of how a good chemical engineer should be. I would also like to thank all of the academic members

in the School of Chemical Engineering, for their teaching, support and encouragement. Also, thanks go to my friends who are graduate students in the School of Chemical Engineering, who shared the experience of graduate student life, and who have made this experience very joyous and memorable.

I would also like to acknowledge Prof. Dr. Joachim Ulrich from the Institute of Thermal Process Technology at the Martin Luther University Halle-Wittenberg, Halle (Saale), Germany, for his invaluable guidance during my research experience in Germany, and also thanks to all of the group members there.

The assistance from the technical staff in the Center for Scientific and Technology Equipment, SUT, are appreciated, especially Mr. Anuchit Ruangvittayanon and Miss Kanravee Issarangkul Na Ayuthaya. Many thanks go to Mrs. Amporn Ladnongkhun for her skillful secretarial work and Mr. Saran Dokmaikun for his skillful technical work and assistance. I would also like to thank all members in the School of Biochemistry for their assistance.

Finally, I would like to express my honest gratefulness to everyone in my family, especially my parents for their love and care, and also gratefully acknowledge the invaluable help of everyone I may have forgotten to mention here.

Somchai Maosoongnern

TABLE OF CONTENTS

TABLE OF CONTENTS (Continued)

TABLE OF CONTENTS (Continued)

TABLE OF CONTENTS (Continued)

TABLE OF CONTENTS (Continued)

TABLE OF CONTENTS (Continued)

TABLE OF CONTENTS (Continued)

TABLE OF CONTENTS (Continued)

Page

LIST OF TABLES

LIST OF TABLES (Continued)

LIST OF TABLES (Continued)

LIST OF TABLES (Continued)

LIST OF TABLES (Continued)

LIST OF TABLES (Continued)

LIST OF TABLES (Continued)

LIST OF FIGURES

LIST OF FIGURES (Continued)

LIST OF FIGURES (Continued)

LIST OF FIGURES (Continued)

LIST OF FIGURES (Continued)

LIST OF FIGURES (Continued)

LIST OF FIGURES (Continued)

LIST OF FIGURES (Continued)

LIST OF FIGURES (Continued)

SYMBOLS AND ABBREVIATIONS

Symbols

$\Delta A_{450nm}/\min \text{Blank}$ = Change in an absorbance of the reference solution at 450 nm

$\Delta A_{450nm}/\min \text{Test}$ = Change in an absorbance of the test solution at 450 nm

E_G = Activation energy of growth, (kJ/mol)

σ_G = Geometric standard deviation, μm

v = Growth layer velocity in the presence of an impurity, μm/hr

v_0 = Growth layer velocity in the pure solution, μm/hr

x_{mV} = Volume-based geometric mean crystal size, μm

L = Characteristic dimension, μm

k_d = Coefficient of mass transfer by diffusion, μm/hr

c = Concentration, mg/mL

ΔH_{diss} = Enthalpy of dissolution, kJ/mol

ΔH_{fus} = Enthalpy of fusion, kJ/mol

ΔS_{diss} = Entropy of dissolution, kJ/(mol·K)

ΔS_{fus} = Entropy of fusion, kJ/(mol·K)

T_{fus} = Fusion temperature (melting point) of the solute, K

k_G = Growth rate constant, μm/hr

$\bar{L}$ = Number mean crystal size, μm

SYMBOLS AND ABBREVIATIONS (Continued)

x_{NL}	=	Number-based mean crystal size, µm
l	=	Path length of the light (the width of the cuvette), cm
k_g^0	=	Pre-exponential constant (µm/hr)
k_r	=	Rate constant for the surface integration, µm/hr
V	=	Volume the solution, mL
θ_{eq}	=	Fractional surface coverage by adsorbed impurity at equilibrium
A	=	Surface area of crystal, µm^2
A250	=	Absorbance at 250 nm
A260	=	Absorbance at 260 nm
A270	=	Absorbance at 270 nm
A280	=	Absorbance at 280 nm
A290	=	Absorbance at 290 nm
A3000	=	Absorbance at 300 nm
A_{B+S}	=	Constant in birth and spread growth model, µm/hr
A_{BCF}	=	Constant in Burton-Caberra-Frank growth model, µm/hr
B_{B+S}	=	Constant in birth and spread growth model, -
B_{BCF}	=	Constant in Burton-Caberra-Frank growth model, -
$c*$	=	Solubility, mg/mL
G	=	Growth rate, µm/hr
IR	=	Infrared

SYMBOLS AND ABBREVIATIONS (Continued)

K	=	Langmuir constant
k_a	=	Area shape factor, -
k_v	=	Volume shape factor, -
m	=	Mass of crystal, mg
n	=	Growth rate order
pKa	=	Acid dissociation constant
R	=	Ideal gas constant, 8.314 J/mol·K.
R_i	=	Side chain of the i-th amino acid
Rxn	=	Reaction
S	=	Super saturation ratio, -
t	=	Time, hr or min ot sec
T	=	Temperature, K or °C

Greek Symbols

γ	=	Activity coefficient, -
ε	=	Extinction coefficient, mL·mg^{-1}·cm^{-1}
α	=	Impurity effectiveness factor, -
λ	=	Wavelength, nm
Δ	=	Change in a variable
ρ	=	Density
σ	=	Relative supersaturation, -

SYMBOLS AND ABBREVIATIONS (Continued)

σ_g	=	Geometric standard deviation of the volume distribution, μm

Superscripts

*	=	Equilibrium

Subscripts

0	=	Initial
$cryst$	=	Crystal
D	=	Dissolution
$diss$	=	Dissolution
eq	=	Equilibrium
fus	=	Fusion
G	=	Growth
i	=	Initial conditions
lys	=	Lysozyme
$oval$	=	Ovalbumin
p,l	=	Protein in liquid phase
s	=	Seed crystal
t	=	Time

SYMBOLS AND ABBREVIATIONS (Continued)

Abbreviations

Abs	=	Absorbance
AFM	=	Atomic force microscopy
Ave. Abs.	=	Average absorbance
CSD	=	Crystal size distribution
Exp. No.	=	Experimental Number
HEWL	=	Hen egg white lysozyme
LLPS	=	Liquid – liquid phase separation
Lys	=	Lysozyme
MZW	=	Metastable zone widths
ODu	=	Uncalibrated Optical Density
Oval	=	Ovalbumin
pI	=	Isoelectric point
RSSE	=	Residual sum of squared errors of prediction
S.D.	=	Standard deviation
SDS-PAGE	=	Sodium dodecyl sulphate - Polyacrylamide gel electrophoresis
SNT	=	Secondary nucleation threshold
UV-Vis	=	UV Visible spectrophotometer

CHAPTER I

INTRODUCTION

1.1 Introduction to Proteins

Proteins are organic compounds composed of amino acids arranged in a linear chain and joined together by peptide bonds between the carboxyl and amine groups of adjacent amino acid residues as shown in Figure 1.1 (a). The polypeptide chain of a protein molecule can be represented by the overall formula given in Figure 1.1 (b), where R_i represents the side chain of the i-th amino acid.
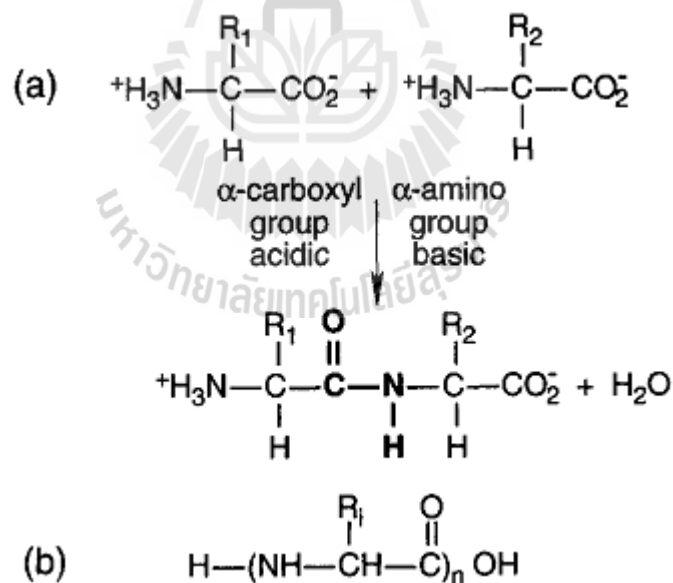
Figure 1.1 Primary structures of proteins. (a) Formation of a peptide bond (outlined

in bold) between two amino acids that differ in their side chains

(residues, R_1, R_2). (b) Overall formula for polypeptide chain

(backbone) with residues R_i (Rosenberger, 1996).

Natural proteins contain only 20 standard amino acids. The side chains or residues consist of simple hydrocarbon groups, that may contain aromatic rings, nitrogen, oxygen and sulfur as shows in Figure 1.2.
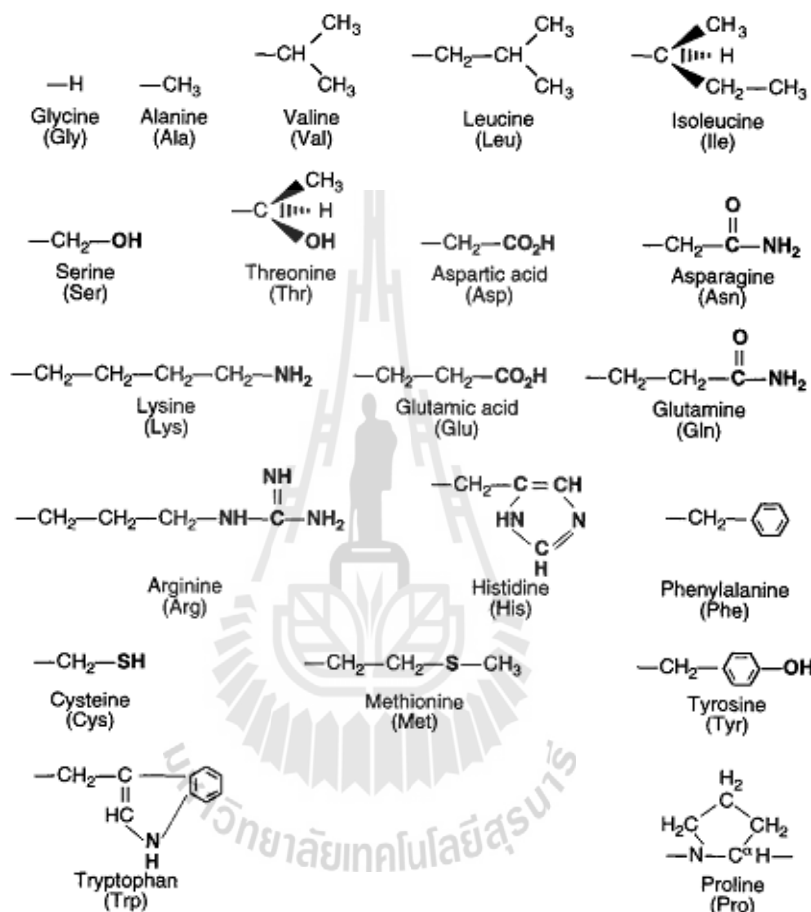
Figure 1.2 Chemical structures of the residues of the 20 amino acids that form

proteins. Charged (polar) functional groups in bold (Rosenberger,

1996).

A significant characteristic for the biological function as well as for the crystallization of proteins is that the residues consist of polar functional groups, indicated in bold in the figure, and nonpolar functional groups. The polar groups

prefer to associate with water. In contrast to these hydrophilic groups, the nonpolar hydrophobic groups prefer to associate with themselves. The hydrophilic groups result in proteins having finite water solubility despite being very large molecules.

The main proteins used in this study is hen egg-white (HEW) lysozyme, an enzyme that damages bacterial cell walls, and ovalbumin, a protein that has a molecular weight of 45 kDa and an isoelectric point (pI) of 4.58 (Stadelman and Cotterill, 1990). Lysozyme has a molecular weight of 14.4 kDa and an isoelectric point (pI) of 11.3 (Tanford and Roxby, 1972). The amino acid side chains glutamic acid (Glu) and aspartic acid (Asp) have been found to be critical to the activity of this enzyme. Glu acts as a proton donor to the glycosidic bond, cleaving the C-O bond in the substrate, whilst Asp acts as a nucleophile to generate a glycosyl enzyme intermediate. The glycosyl enzyme intermediate then reacts with a water molecule, to give the product of hydrolysis and leaving the enzyme unchanged.

1.2   Background and Significance of the Study

Proteins are value added products from simple agricultural materials and appear all around in our life. The examples of existing uses of proteins are in food (Motoki and Seguro, 1998; Proctor and Cunningham, 1998; Yokoyama, Nio, and Kikuchi, 2004), in cosmetic products (Anton, Nau, and Nys, 2006; Chvapli and Eckmayer, 2007), in medicine, and in other products such as packing film (Mecitoglu, Yemenicioglu, Arslanoglu, ElmacI, Korel, and Cetin, 2006; Stolte, Frohberg, Pietzsch, and Ulrich, 2010). The specific examples are proteins such as lysozyme, an enzyme that damages bacterial cell walls and is found (among other places) in chicken egg white, subtilisin, an enzyme used in commercial products, for example in

laundry and dishwashing detergents, cosmetics, and food processing, and can be found in many Bacillus species. The main difficulty in accessing these products is purifying the many proteins involved in natural products into pure protein fractions on an industrial scale. The most commonly used methods for protein purification is ion exchange chromatography (Li-Chan, Nakai, Sim, Bragg, and Lo, 1986; Porter and Ladisch, 1992) and precipitation by salting-out (Wiencek, 1999). Ion exchange chromatography involves high investment and operating costs and it is accompanied often by additional steps until a protein with high purity and stability is obtained (Chisti and Mooyoung, 1990) while precipitation by salting-out requires high amounts of salts (Alderton and Fevold, 1946). The industrial processes demand the opposite to these processes; processes with low investment, low operating costs, which are environmentally friendly. Therefore, this research attempts to show that this separation is possible using crystallization, a simpler and lower cost technique than many currently used.

The solubility and phase diagram is a fundamental property of proteins and other species, and is essential knowledge to be able to design and operate industrial crystallizers of any product. Most solubility data for pure and mixed protein systems published in the literature have used the well-known classical dissolution and crystallization methods (Ataka and Asai, 1988; Howard, Twigg, Baird, and Meehan, 1988; Retailleau, Ries-Kautt, and Ducruix, 1997) and a miniature column method (Cacioppo and Pusey, 1991; Cacioppo, Munson, and Pusey, 1991; Forsythe, Judge, and Pusey, 1999; Pusey and Gernert, 1988; Pusey and Munson, 1991). These two methods have different benefits and drawback, however use the same UV absorbance technique. For the solubility measurement of pure proteins it is a reliable technique,

but for a mixture of proteins this technique has some weak points; several proteins can absorb light at the same wavelength resulting in unreliable solubility data for the protein mixtures. Therefore, the solubility data, phase diagram, and the improvement of the solubility measurement technique for protein mixtures are the first consideration.

Although techniques used for protein crystallization have been progressing greatly, successful crystallization is still largely empirical and operator dependent. The crystallization of a protein is a complicated process involving numerous parameters, thus detailed understanding of the effect of crystallization conditions on the crystallization is essential. Investigation of the effect of supersaturation, temperature, pH, salt concentration, and protein impurity on the crystallization process must be clearly understood in order to design a successful crystallization system.

In the crystal growth kinetic studies of protein crystallization there are three groups of techniques that have been used: The first technique is crystal growth kinetics based on individual crystal size measurements, which are studies in which the growth rates of individual crystal faces of a single growing crystals are measured microscopically. Most of the kinetic studies in protein crystallization fall into this category (Ataka and Tanaka, 1986; DeMattei and Feigelson, 1989; Forsythe, Ewing, and Pusey, 1994; Li, Nadaraj, and Pusey, 1995; Monaco and Rosenberger, 1993; Pusey and Naumann, 1986; Pusey, Snyder, and Naumann, 1986). The second technique is crystal growth kinetics based on crystal size distribution (CSD) studies, which deal with the crystal growth rates in bulk crystallizations (Judge, Johns, and White, 1995). The third technique is crystallization kinetic studies based on

measurements of solute concentration with time. This method obtains kinetic parameters by plotting a kinetic model to concentration-time data (Ataka and Asai, 1990; Bessho, Ataka, Asai, and Katsura, 1994). Each method is different, and has differences in the strong and weak points. Accurate measurement of nucleation rate is still often very difficult, and there are many types of methods to attempt this, although all have strong drawbacks. Crystal growth kinetic studies without nucleation should be used where possible if reliable and accurate results are necessary.

These ideas raise the author to address the fundamental significance and practical importance in studying thermodynamics (solubility) and kinetics (phase diagram and crystal growth) of protein crystallization and attempts to show that both crystallization from pure protein solutions and crystallization of a protein from mixed protein solutions is possible using seeded batch crystallization (crystallization without nucleation, where only crystal growth occurs), a simpler and lower cost technique than many currently used.

1.3　Research Objectives

This thesis research will use experimental data to study the crystallization of lysozyme from both pure lysozyme solutions and mixed lysozyme-ovalbumin solutions containing salt and sodium acetate buffer using seeded batch crystallization. This includes measurement and analysis of the thermodynamic and kinetic properties, and studying the effect of the solution conditions or process conditions on these properties. The specific objectives of this research are as follows:

1.3.1　To determine the solubility of protein as a function of temperature, salt concentration, and solution pH and correlate the experimental data to the chemical

thermodynamic equation to predict the behavior of the solubility. Modifications of current techniques used to measure the concentration of mixed protein during crystallization will be presented.

1.3.2   To investigate the concentration − temperature phase diagram of lysozyme and determine the metastable zone width as a function of salt concentration and solution pH by collection of data on the phase diagram. The metastable zone width is prepared and used to ensure that the crystallization occurs only by growth, and thus is operated under non nucleating conditions.

1.3.3   To study the isothermal seeded batch crystallization of pure lysozyme to demonstrate the growth kinetics of the crystallization process and demonstrate the ability to crystallize pure lysozyme from solution. The growth kinetics were determined based on the measurement of the lysozyme concentration decay with time. The results demonstrate that this crystallization process is possible.

1.3.4   To separate mixtures of two proteins in aqueous solutions using seeded batch crystallization in two cases; where only one protein was supersaturated, or where both proteins were supersaturated, to produce a commercial product from a complex mixture. The effects of solution conditions and/or experimental conditions on the growth kinetics are investigated.

1.4   Scope and Limitation of the Research

1.4.1   Thermodynamics studies of protein crystallization

The solubility of protein as a function of temperature, salt concentrations, and solution pH is required to be measured in order to compare with the previous data and for use in the crystallization of protein from mixed-protein

solution (where the existing data are not sufficient). The solubility was measured using both the well-known classical dissolution methods and a miniature column method. The concentrations of pure protein solutions were measured using the UV absorbance technique while the concentrations in mixed protein solutions require a modified technique. The combinations of SDS-PAGE gel and UV-Vis technique, and UV-Vis for mixed protein were introduced to measure the concentration of mixed protein solutions.

1.4.2 Kinetics studies of protein crystallization

The concentration – temperature phase diagram of lysozyme are measured using the turbidity technique by the use of a STEM Integrity 10 system (Electro Thermal, England). This phase diagram allowed collecting the solubility and nucleation data to determine the metastable zone width.

The possibility of separation of pure lysozyme from the mixed solution of lysozyme – ovalbumin using crystallization was studied in two cases. (1) Separation of lysozyme from solution where only lysozyme was supersaturated. (2) Using preferential crystallization (seeding with only lysozyme) to achieve pure lysozyme under conditions where both proteins are supersaturated.

In the growth kinetics study, the crystallization experiments were performed in a batch crystallizer to demonstrate the growth kinetics of the crystallization process and the ability to crystallize pure lysozyme from solution. The growth kinetics were measured by measurement of the lysozyme concentration decay with time (observation of the desupersaturation curve) by assuming no nucleation, no breakage, and no agglomeration occur during the crystallization process. The assumption of no nucleation, breakage or agglomeration was confirmed by

observation of the process using micrographs. The purity and remaining activity of the product crystal are determined using standard techniques, SDS-PAGE gel and the activity test. The dependence of crystal growth on parameters including the supersaturation, temperature, protein impurity, and salt concentration were investigated for crystallization of mixtures of two proteins to produce a commercial product.

1.5 Research Development

This thesis is divided into 6 chapters. **Chapter I** is introduction part; it gives some introduction to proteins and describes the background, significance, objectives, and scope of the research. **Chapter II** reports the solubility data as a function of temperature, NaCl concentration, and solution pH. The solubility data were correlated with the van't Hoff equation to predict the phase behavior. In this part, the modifiied techniques used for measurement of concentrations in mixed protein solutions are also introduced. The phase diagrams that contain the thermodynamic data (solubility, either obtained from literature or self-measured) and the kinetic data (nucleation points) are measured using the turbidity technique and reported in **Chapter III.** These include determination of the metastable zone width as a function of supersaturation, temperature, NaCl concentration, and solution pH. In **Chapter IV**, the possibility of crystallization of lysozyme using seeded isothermal batch crystallization was investigated. The growth kinetics was measured by measurement of lysozyme concentration decay with time and described by the power-law model. **Chapter V** studied the crystallization of lysozyme from mixed protein solutions and describes the effects of supersaturation, temperature, protein impurity, and salt concentration on the

growth of the crystal. The purity of the product crystal was confirmed by SDS-PAGE gel and an activity test with micrococcus lysodeikticus bacteria. Finally, **Chapter VI** concludes the results from this thesis and gives some recommendations for future study.

1.6 References

Alderton, G., and Fevold, H.L. (1946). Direct crystallization of lysozyme from egg white and some crystalline salt of lysozyme. **J. Biol. Chem.** 164: 1-5.

Anton, M., Nau, F., and Nys, Y. (2006). Bioactive egg components and their potential uses. **World's Poultry Science Journal** 62: 429-438.

Ataka, M., and Asai, M. (1988). Systematic studies on the crystallization of lysozyme. Dtermination and use of phase diagrams. **J. Cryst. Growth** 90: 86-93.

Ataka, M., and Asai, M. (1990). Analysis of the nucleation and crystal growth kinetics of lysozyme by a theory of self-assembly. **Biophys. J.** 58: 807-811.

Ataka, M., and Tanaka, S. (1986). The growth of large single crystals of lysozyme, **Biopolymers** 25(2): 337-350.

Bessho, Y., Ataka, M., Asai, M., and Katsura, T. (1994). Analysis of the crystallization kinetics of lysozyme using a model with polynuclear growth mechanism. **Biophys. J.** 66(2): 310-313.

Cacioppo, E., and Pusey, M.L. (1991). The solubility of the tetragonal form of hen egg white lysozyme from pH 4.0 to 5.4. **J. Cryst. Growth** 114: 286-292.

Cacioppo, E., Munson, S., and Pusey, M.L. (1991). Protein solubilities determined by a rapid technique and modification of that technique to a micro-method. **J. Cryst. Growth** 110: 66-71.

Chisti, Y., and Mooyoung, M. (1990). Large scale protein separations: Engineering aspects of chromatography. **Biotechnol. Adv.** 8(4): 699-708.

Chvapli, M., and Eckmayer, Z. (2007). Role of protein in cosmatics. **Int. J. Cosmatic Sci.** 7(2): 41-49.

DeMattei, R.C., and Feigelson, R.S. (1989). Growth rate study of canavalin single crystals. **J. Cryst. Growth** 97(2): 333-336.

Forsythe E.L., Judge R.A., and Pusey M.L. (1999). Tetragonal chicken egg white lysozyme solubility in sodium chloride solutions. **J. Chem. Eng. Data.** 44: 637-640.

Forsythe, E.L., Ewing, F., and Pusey, M.L. (1994). Studies on tetragonal lysozyme crystal growth rates. **Acta Crystallogr.** D50: 614-619.

Howard, S.B., Twigg, P.J., Baird, J.K., and Meehan, E.J. (1988). The solubility of hen egg-white lysozume. **J. Cryst. Growth** 90: 94-104.

Judge, R.A., Johns, M.R, and White E.T. (1995). Protein Purification by Bulk Crystallization: The Recovery of Ovalbumin. **Biotechnol. Bioeng.** 48(4): 315-323.

Li, M., Nadaraj, A., and Pusey, M.L. (1995). Modeling the growth rates of tetragonal lysozyme crystals. **J. Cryst. Growth** 156(1-2): 121-132.

Li-Chan, E., Nakai, S., Sim, J., Bragg, D.B., and Lo, K.V. (1986). Lysozyme separation from egg white by cation exchange column chromatography. **J. Food Sci.** 51: 1032-1036.

Mecitoglu, c., Yemenicioglu, A., Arslanoglu, A., ElmacI, Z.S., Korel, F., and Cetin, A.E. (2006). Incorporation of partially purified hen egg white lysozyme into zein films for antimicrobial food packaging. **Food Res. Int.** 39(1): 12-21.

Monaco, L.A., and Rosenberger, F. (1993). Growth and etching kinetics of tetragonal lysozyme. **J. Cryst. Growth** 129: 465-484.

Motoki, M., and Seguro, M. (1998). Transglutaminase and its use for food processing**. Trends Food Sci. Tech.** 9: 204–210.

Porter, J.E., and Ladisch, M.R. (1992). Ion-exchange and affinity chromatography costs in α-galactosidase purification. **Biotechnol. Bioeng.** 39: 717-724.

Proctor, V.A., and Cunningham, F.E. (1998). The chemistry of lysozyme and its use as a food preservative and a pharmaceutical. **Crit. Rev. Food Sci. Nutr.** 26(4): 359-95.

Pusey, M.L., and Gernert, K. (1988). A method for rapid liquid-solid phase solubility measurements using the protein lysozyme. **J. Cryst. Growth** 88: 419-424.

Pusey, M.L., and Munson, S. (1991). Micro-apparatus for rapid determinations of protein solubilities. **J. Cryst. Growth** 113: 385-389.

Pusey, M.L., and Naumann, R. (1986). Growth kinetics of tetragonal lysozyme crystals. **J. Cryst. Growth** 76(3): 593-599.

Pusey, M.L., Snyder, R.S., and Naumann, R. (1986). Protein crystal growth: growth kinetics for tetragonal lysozyme crystals. **J. Biol. Chem.** 261(14): 6524-6529.

Retailleau, P., Ries-Kautt, M., and Ducruix, A. (1997). No salting-in of lysozyme chloride observed at low ionic strength over a Large range of pH. **Biophys. J.** 73: 2156-2163.

Rosenberger, F. (1996). Protein Crystallization, **J. Cryst. Growth** 166: 40-54.

Stadelman, W.J., and Cotterill, O.J. (1990). **Egg Science and Technology** (3rd ed.). New York: Food Products Press.

Stolte, I., Frohberg, F., Pietzsch, M., and Ulrich, J. (2010). Crystal in protein films: what are they good for?. **Chem. Eng. Res. Des.** 88: 1148-1152.

Tanford, C., and Roxby, R. (1972). Interpretation of protein titration curves: Application to lysozyme. **Biochem.** 11: .2192-2198.

Wiencek, J.M. (1999). New strategies for protein crystal growth. **Annu. Rev. Biomed. Eng.** 1: 505-534.

Yokoyama, K., Nio, N., and Kikuchi, Y. (2004). Properties and applications of microbial transglutaminase. **Appl. Microbiol. Biotechnol.** 64: 447–454.

CHAPTER II

SOLUBILITY AND THERMODYNAMIC OF

LYSOZYME AND OVALBUMIN PROTEIN

2.1   Abstract

The solubilties of pure lysozyme powder and lysozyme crystal were determined for the temperature range $5 - 30°C$, sodium chloride concentration 3 - 7%, and pH $4 - 6$ using 0.1M sodium acetate buffer as a buffer. The solubility of lysozyme increases with increasing temperature, decreases with increasing sodium chloride concentration, and is slightly reduced at higher values of the pH. A third-order polynomial equation was used to correlate the solubility as a function of temperature and can fit the data very well, with the coefficient of determination greater than 0.99 for the solubility of the powder and greater than 0.999 for the solubility of the crystal. The enthalpy and entropy of dissolution were estimated by the use of the van't Hoff equation. The results fit the van't Hoff equation and predict average enthalpies of dissolution of 74.84 ± 6.03 and 84.56 ± 3.84 kJ/mol and entropies of dissolution of 266.05 ± 21.81 and 292.97 ± 15.05 J/mol·K for lysozyme powder and crystal, respectively. Several modifications of the solubility and concentration measurement technique for protein mixtures were introduced. The combination of the SDS-PAGE gel and UV-Vis techniques has the advantage that the composition of protein in the mixture can be determined via the SDS-PAGE gel to estimate the purity and thus the UV absorbance can be measured at only one wavelength. However, the use of this

method was limited at the composition of lysozyme in mixed solution lower than 60%. The modification of using UV-Vis at six different wavelengths has the advantage that it only requires UV photometer measurements, which are fast, and the result shows no detection limit until 1 mg/mL of total protein (depending on the UV photometer).

2.2 Introduction

The solubility is a fundamental property of protein and other substances. Understanding the solubility behavior is a major requirement for the successful design and operation of crystallization processes. The solubility of a protein strongly depends on the protein-protein interactions as well as the protein-solvent interactions (Curtis and Lue, 2006). Protein solubility is affected by the properties of the molecule itself (e.g. net charge, charge ratio, polar, neutral amino acids, hydrophobicity or hydrophilicity, …) and also depends on the solution conditions such as temperature, salt concentration, and solution pH. In general, the effect of these parameters on the solubility can be determined by experimentally measuring the solubility as a function of each parameter. In this study, hen egg white lysozyme has been chosen as a model protein since it is a well-studied protein and has often been used in thermodynamic and kinetic crystallization studies (Ataka and Asai, 1988; Cacioppo and Pusey, 1991; Cacioppo, Munson, and Pusey, 1991; Curtis and Lue, 2006; Forsythe, Judge, and Pusey, 1999; Howard, Twigg, Baird, and Meehan, 1988; Retailleau, Ries-Kautt, and Ducruix, 1997; Pusey and Gernert, 1988; Ildefonso, Revalor, Punniama, Salmon, Candoni, Veesler, 2012; Diaz Borbon and Ulrich, 2012; Elgersma, Ataka and Katsura, 1992; Liu, Wang, and Ching, 2010; Apgar, 2008; Ries-Kautt and Ducruix, 1989;

Muschol and Rosenberger, 1997; Jolles and Berthou, 1972; Berthou and Jolies, 1974; Ewing, Forsythe, and Pusey, 1994) which is a large set of reported data.

Several methods have been used to measure the solubility of pure lysozyme. Examples of such methods are the well-known classical dissolution and crystallization methods (Ataka and Asai, 1988; Howard, Twigg, Baird, and Meehan, 1988; Retailleau, Ries-Kautt, and Ducruix, 1997). These methods have the advantage that we can carry out more than one experiment at the same time. However, there are some disadvantages - the requirement for long times to reach equilibrium due to the slow diffusivity of proteins in the solution, and also imprecise measurements if sufficient equilibrium time is not allowed. The measured solubility data by these methods might have a concentration higher or lower than the equilibrium concentration depending on whether the method involved crystallization or dissolution. An alternative method for measuring the solubility of pure proteins is the use of a miniature column technique (Cacioppo and Pusey, 1991; Cacioppo, Munson, and Pusey, 1991; Forsythe, Judge, and Pusey, 1999; Pusey and Gernert, 1988; Pusey and Munson, 1991). This technique is known as a rapid determination technique with high reliability; the solubility data can be obtained within 24 h with an error less than ± 0.2 mg/mL at salt content of 3% and ± 0.1 mg/mL at salt content of $3 - 5.7\%$ (Forsythe, Judge, and Pusey, 1999) and requires only a small amount of material. Therefore, using this method allows a larger number of experiments with the same amount of materials, and a better set of data. However, it is not possible to carry out more than one experiment at once and it can't be used for measurement of high viscosity solutions due to the flow of the solution is needed in the operation. Both methods have used the UV absorbance technique to estimate the concentration of

protein in the final step. For the solubility measurement of pure proteins it is a reliable technique, but for mixture of proteins this technique has some weak points. Several proteins can absorb light at the same wavelength resulting in unreliable solubility data for the protein mixtures. Therefore, improvement of the solubility measurement technique for protein mixtures is required.

In this work, the solubility data of lysozyme were measured using both the classical method and the miniature column technique. The solubility data were determined by the dissolution of both lysozyme powder form (the classical method) and the lysozyme crystal form (the miniature column method). The solubility data cover the temperature range 5 – 30°C, sodium chloride concentration 3 - 7%, and pH 4 – 6 using 0.1M sodium acetate buffer as a buffer. A third-order polynomial equation was used to fit the data to observe the change in solubility as a function of temperature. Moreover, the enthalpy and entropy of dissolution were estimated by the use of the van't Hoff equation.

Furthermore, the modifications of the concentration measurement techniques for mixture of protein are presented. The first method is the combination of SDS-PAGE gel and the UV-Vis technique. In this modified technique the composition of protein in the mixture will be analyzed by SDS-PAGE gel and Gel Doc analyzer, and the concentration of each protein will be estimated by UV absorbance. Another method is the UV-Vis technique. In general, the concentration of protein will be determined by measurement of the UV absorption ability at one wavelength. In this modified technique six different wavelengths were used to measure the absorbance of the protein. These two techniques offer the opportunity to measure the change in protein concentration during crystallization.

2.3   Theory

2.3.1   Definition of Solubility

The solubility is a physical property of a chemical substance. It is the ability of a solute to dissolve in a solvent, and is defined as the maximum amount of solute dissolved in a solvent at equilibrium at a particular set of conditions (e.g. temperature, pressure, and pH). Understanding the solubility behavior is an indispensable requirement for the successful development of crystallization processes (Tung, Paul, Midler, and McCauley, 2009). The solubility of a substance fundamentally depends on the physical and chemical properties of the solute and solvent as well as on temperature and pressure, and the concentrations of any other solutes that may be present. There are many parameters having an effect on the solubility of a substance. In most cases determining the solubility as a function of temperature is sufficient (Beckmann, 2000). However for proteins there are three parameters that strongly affect the solubility, temperature, salt concentration, and solution pH. Another parameter that has an effect on solubility and should be investigated is protein impurity, for further understanding of the crystallization of protein mixtures.

2.3.2   Effect of temperature on the solubility of protein

The solubility of a given solute in a given solvent typical strongly depends on temperature. As shown in Figure 2.1, the solubility of lysozyme increases with increasing temperature. This solubility behavior is commonly observed in organic compounds. Many correlations and predictions have been proposed for solubility data as a function of temperature. One of the most commonly used is the polynomial (Mullin, 2001), as expressed in equation (2.1).

$$c = A + BT + CT^2 + ... \tag{2.1}$$

where c is the solution composition, expressed in any convenient units. T is the temperature and A, B, C etc. are constants that depend on the units used. In previous work, the third order polynomial was proposed to fit the solubility data of lysozyme in sodium acetate buffer well (Cacioppo and Pusey, 1991; Forsythe and Pusey, 1996).
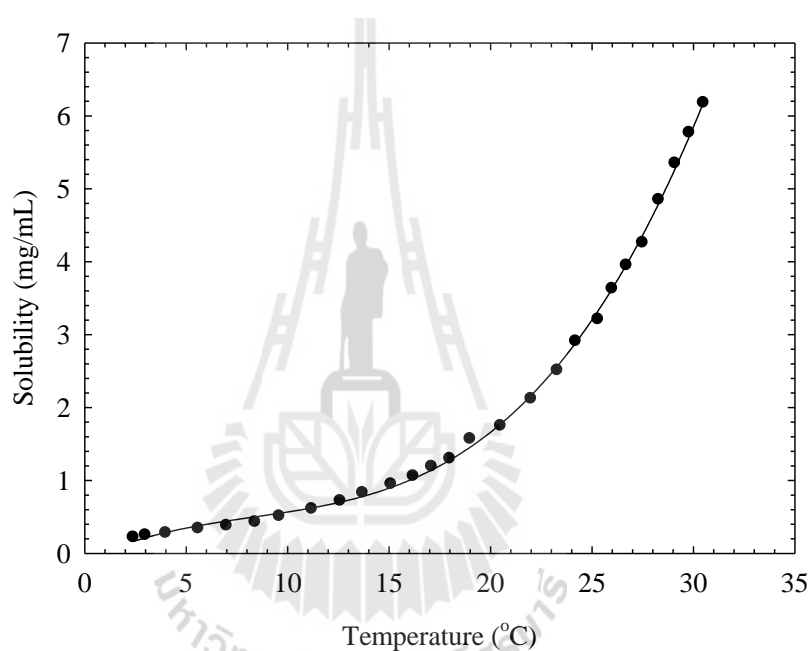
Figure 2.1 Lysozyme solubility as a function of temperature at pH 4.0 and 5.0%

sodium chloride concentration (Forsythe, Judge, and Pusey, 1999).

2.3.3 Effect of salt concentration on the solubility of protein

The effect of salt concentration on protein crystallization has focused on protein solubility. Figure 2.2 shows the lysozyme solubility as a function of temperature for various sodium chloride concentrations. As shown in the Figure 2.2, the solubility of lysozyme decreases with an increasing concentration of sodium chloride.
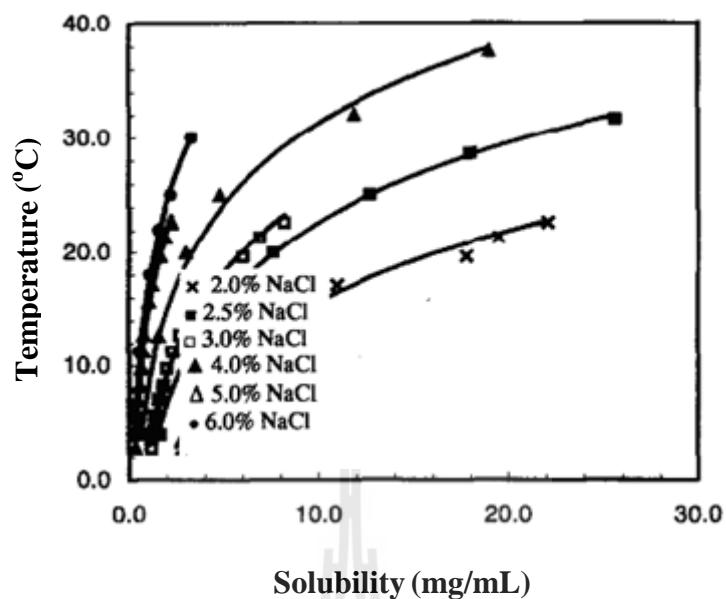
Figure 2.2 Lysozyme solubility as a function of temperature for various sodium

chloride concentrations (Lu, Wang, and Ching, 2002).

This is due to the salting out effect. There are hydrophobic amino acids and hydrophilic amino acids in protein molecules. Lysozyme folding in aqueous solution causes hydrophobic amino acids to form protected hydrophobic areas, while hydrophilic amino acids interact with the molecules of solvation and allow proteins to form hydrogen bonds with the surrounding water molecules. When the salt concentration is increased, some of the water molecules are attracted by the salt ions, which decreases the number of water molecules available to interact with the charged part of the lysozyme molecule. As a result of the increased demand for solvent molecules, the protein-protein interactions are stronger than the solvent-solute interactions; the protein molecules coagulate by forming hydrophobic interactions with each other and not with the aqueous solution, thus reducing the solubility.

Characterization of the effectiveness of various salts in crystallizing (salting out) proteins has been determined (Ducruix, 1992; Collins, 1985) when Hofmeister established the lyotropic series that ranked various salts according to their ability to precipitate hen egg white proteins; the series is given by

<u>cations</u>: $Li^+ > Na^+ > K^+ > NH_4^+ > Mg_2^+$

<u>anions</u>: $SO_4^{2-} > HPO_4^{2-} > CH_3COO^- > C_6H_5O_7^{3-} > C_3H_2O_5^{2-} > HCO_3^- > CrO_4^{2-}$
$> Cl^- > NO_3^- > ClO_3^- > SCN^-$
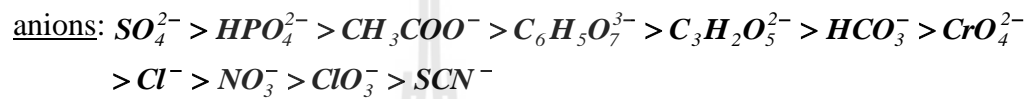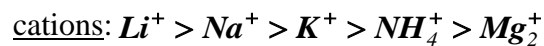
2.3.4   Effect of pH on the solubility of protein

Knowledge of the isoelectric point (pI) is important to understand the effect of pH on the solubility of a protein. The isoelectric point (pI), is the pH at which a particular molecule or surface carries no net electrical charge. The pI value can affect the solubility of a molecule at a given pH. Such molecules often have a minimum solubility in water or salt solutions at the pH which corresponds to their pI and often precipitate out of solution at this pH. Figure 2.3 shows the effect of pH on ovalbumin solubility. The solubility of ovalbumin decreases when the pH approaches to the pI value.
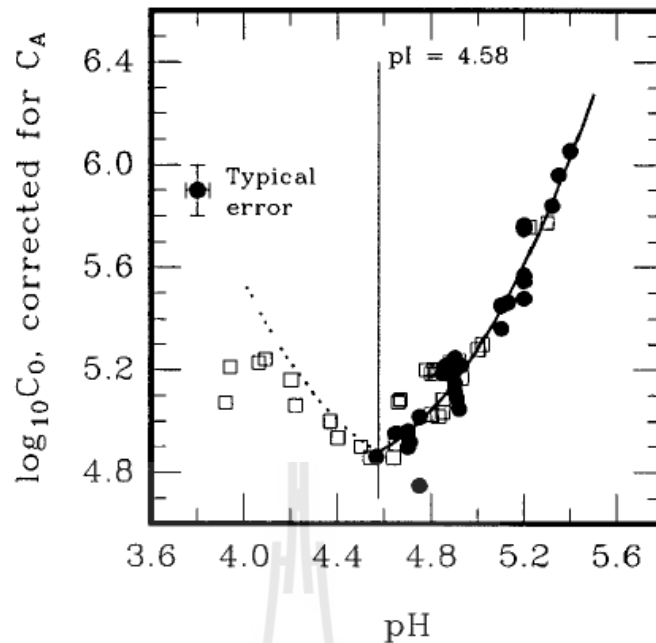
Figure 2.3 Effect of pH on ovalbumin solubility in ammonium sulfate solutions at

18°C (The solubility data are from: (□) Sorensen and Hoyrup, 1915-17;

(●) Judge, Johns, and White, 1996).

This behavior is due to the fact that proteins are biological molecules containing both acidic and basic functional groups. The amino acids which make up proteins may be positive, negative, neutral or polar in nature, and together give a protein its overall charge. At a pH below their pI, proteins carry a net positive charge; above their pI they carry a net negative charge. When the pH is far from the pI, proteins have more positive or negative charge and then can dissolve more in solution. As the pH approaches to the pI, proteins have less positive or negative charge resulting in a decrease in solubility. For lysozyme, the protein that has a pI value of 11.3 (Tanford and Roxby, 1972), the effect of pH on solubility is the same as for

ovalbumin as shown in Figure 2.4 but there is no literature report for the data in the region above the pI because it is outside the range of many common buffers.
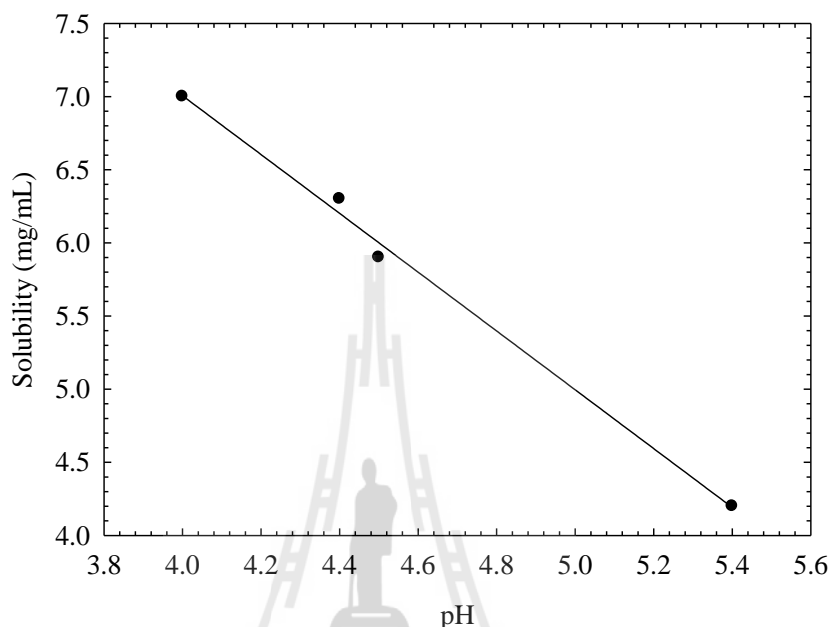
Figure 2.4 Effect of pH on lysozyme solubility at 20°C, and 3% NaCl in 0.1M
sodium acetate buffer (The solubility data are from: Forsythe, Judge,
and Pusey, 1999).

2.3.5 Effect of protein impurity on the solubility of protein

A study on the effect of macromolecule impurities on lysozyme solubility has focused on ovalbumin and conalbumin as impurities, as both are typically identified in commercial lysozyme preparations (Thomas, Vekilov, and Rosenberger, 1996) and are likely to be present in lysozyme crystallization solutions. Figure 2.5 and 2.6 shows the effect of ovalbumin and conalbumin on lysozyme solubility respectively.
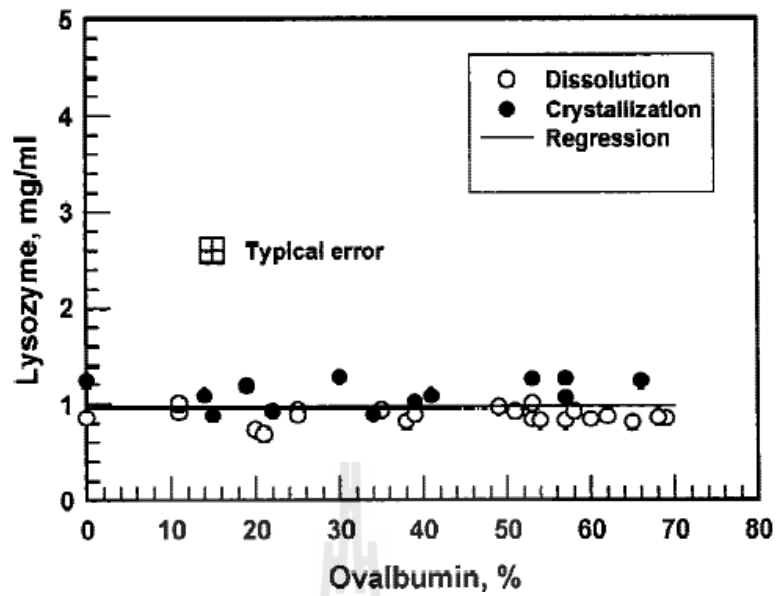
Figure 2.5 The effect of ovalbumin on lysozyme solubility at 18°C, pH 4.0, and 5%

NaCl in 0.1M sodium acetate buffer (Judge, Forsythe, and Pusey, 1998).
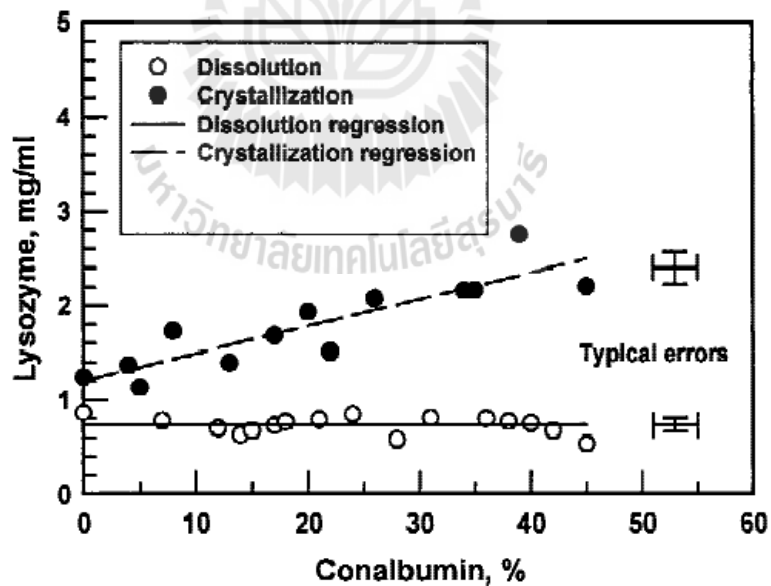
Figure 2.6 The effect of conalbumin on lysozyme solubility at 18°C, pH 4.0, and 5%

NaCl in 0.1M sodium acetate buffer (Judge, Forsythe, and Pusey, 1998).

In the case of ovalbumin impurity, the lysozyme solubility was found to be independent of impurity concentration and not statistically significantly different to the pure lysozyme solubility, measured by dissolution and crystallization.

In the case of conalbumin impurity, there appears to be no significant effect of conalbumin for solubility determined by dissolution. However, for the solubility measurement by crystallization, the crystals appear to stop growing before the solubility is reached. This trend increases with increasing conalbumin concentration. Therefore solubility results from crystallization experiments are likely to be incorrect − due to poisoning of the crystal growth process rather than being a true equilibrium state.

2.3.6 Solubility and Thermodynamics of Protein

The solubility of as a function of temperature can be determined via the van't Hoff equation (Broide, Tominc, and Saxowsky 1996; Flood 2009) as expressed in equation (2.2).

$$\ln(c\gamma) = -\frac{\Delta H_{fus}}{RT}\left(1 - \frac{T}{T_{fus}}\right)$$
(2.2)

Where c is the concentration of solute in the solution is, γ is the activity coefficient of the solute, T is the saturated solution temperature (K), T_{fus} is the fusion temperature (melting point) of the solute (K), ΔH_{fus} is the enthalpy of fusion (J/mol), and R is the ideal gas constant and is equal to 8.314 J/mol·K.

Assuming the solution is ideal, the activity coefficient of the solute is equal to 1. Then equation (2.2) reduces to

$$\ln(c) = -\frac{\Delta H_{fus}}{RT} + \frac{\Delta S_{fus}}{R} \tag{2.3}$$

Where $\Delta S_{fus} = \Delta H_{fus} / T_{fus}$ is the entropy of fusion. In general, the solubility is solvent dependent. Therefore ΔH_{fus} and ΔS_{fus} can be replaced by with ΔH_{diss} and ΔS_{diss} (Mullin, 2001). Equation (2.3) becomes

$$\ln(c) = -\frac{\Delta H_{diss}}{RT} + \frac{\Delta S_{diss}}{R} \tag{2.4}$$

where ΔH_{diss} and ΔS_{diss} are the enthalpy and entropy of dissolution, respectively. The plot of $\ln(c)$ versus $1/T$ gives a straight line for which the slope is equal to $-\Delta H_{diss}/R$ and the intercept of the Y axis is equal to $\Delta S_{diss}/R$.

The value of the dissolution enthalpy for proteins can be negative or positive as given in reviews by Cohn (1965) and Cohn and Ferry (1965). Aldolase protein from rabbit muscle is an example; the enthalpy of crystallization is positive when crystallized as one form and negative when crystallized as another form (Czok and Bucher, 1960). The values of ΔH_{diss} from some literature are summarized and compared in Table 2.1. As expected, the change in enthalpy $(-\Delta H_{diss})$ of lysozyme is negative, meaning that heat is released when a lysozyme crystal forms.

Table 2.1 The heat of crystallization $\left(-\Delta H_{diss}, kJ/mol\right)$ of lysozyme in 0.1M

sodium acetate buffer.

Protein	Solution conditions	$\left(-\Delta H_{diss}\right)$	Reference
Lysozyme	2.0% NaCl, pH 4.2	-81.8	Haas,1999
Lysozyme	2.5% NaCl, pH 4.8	-73.7	Lu, 2002
Lysozyme	4.0% NaCl, pH 4.8	-73.2	Lu, 2002
Lysozyme	6.0% NaCl, pH 4.8	-62.3	Lu, 2002
Lysozyme	0.3M NaCl, pH 4.0	-87.0	Cacioppo, 1991
Lysozyme	0.5M NaCl, pH 4.0	-32.0	Ries-Kautt, 1989

2.4 Materials and Methods

2.4.1 Materials

In the solubility measurement of lysozyme powder, hen egg white lysozyme (HEWL, product No. DR0308) was purchased from Bio Basic Inc. and ovalbumin (product No. A5503) was purchased from Sigma-Aldrich. These two proteins were used without further purification since no other proteins were detected in a SDS-PAGE gel electrophoresis analysis (15% acrylamide).

In the solubility measurement of tetragonal lysozyme crystal, Hen egg white lysozyme (HEWL, product No. 62971) and ovalbumin (product No. 05461) were purchased from Fluka and used without further purification.

Sodium chloride (purity ≥99.5%), sodium acetate trihydrate (purity ≥99.5%) and acetic acid (100%) were purchased from Carl Roth. All chemicals and deionized water were used without further purification.

2.4.2   Preparation of Sodium Acetate Buffer and Salt Solution

0.1 M sodium acetate buffer stock solutions were prepared with sodium acetate trihydrate and acetic acid based on the method of Dawson et al. (1986). A 0.2 g/mL salt stock solution was prepared by dissolving 4 g of NaCl into enough 0.1 M sodium acetate buffer to obtain a final volume of 20 mL at the desired pH.

2.4.3   Solubility Measurement Using Classical Technique

In this section, the solubility of lysozyme powder was measured. The measurements were performed at various temperatures (10, 15, 20, 25, and 30°C), pH values (4.0, 4.4, 4.6, 5.0, 5.4 and 6.0), and salt concentrations (3%, 4%, and 5%). Solution with the desired pH and salt concentration were prepared by appropriate mixing of sodium acetate buffer and salt solutions. To start the experiment a 1.5 mL micro tube which contained the specific solution (at the desired pH and salt concentration) were put into the float comb (which held 18 different micro tube samples). Excess amounts of lysozyme powder were put into the solution within the micro tube and then the cover of the micro tube was closed. The float comb was placed inside a constant temperature water bath, where the temperature was controlled within ±0.5°C. The concentrations of dissolved lysozyme were measured after 1, 2, and 3 weeks using a UV photometer (HP 8453, Agilent) at 280 nm wavelength. An extinction coefficient of 2.3337 mL·mg^{-1}·cm^{-1} was used (which was obtained from a calibration curve of 5 measurements).

2.4.4   Solubility Measurement using The Miniature Column Technique

In this section, the solubility of tetragonal lysozyme crystals was measured. Tetragonal lysozyme crystals were prepared by mixing equal volumes of

100 mg/mL lysozyme solution and 8 wt% sodium chloride solution and keeping the mixture at 4-8°C overnight. The solubility of tetragonal lysozyme crystals was measured at temperature of 5, 10, 15, 20, and 25°C, sodium chloride concentration of 3, 4, 5 and 7 wt%, and pH of 5.0, 5.6, and 6.0 using the miniature column technique as described by Cacioppo and Pusey, (1991); Cacioppo, Munson, and Pusey, (1991); Forsythe, Judge, and Pusey, (1999); Pusey, and Gernert, (1988); Pusey, and Munson, (1991). The temperature of the column was maintained within ± 0.1°C using a thermostat (F12 ED, Julabo).

The concentrations of dissolved lysozyme were measured using a UV photometer (Carry 50, Varian) at 280 nm. An extinction coefficient of 2.4321 mL·mg^{-1}·cm^{-1} was used (obtained from a calibration curve of 9 measurements).

2.4.5 Concentration Measurement of Mixed Proteins

2.4.5.1 The Combination of SDS-PAGE gel and UV-Vis method

In this method, the calibration curve for UV absorbance of mixed protein with known composition of each protein was prepared as shown in Figure 2.7. The lysozyme and ovalbumin in sodium acetate buffer were mixed at the desired proportion and the UV absorbance was measured at 280 nm wavelength using a UV photometer (HP 8453, Agilent). The unknown solution concentration of the mixed lysozyme and ovalbumin solution was measured by a combination of UV absorbance and SDS-PAGE gel and Gel Doc analysis (UV light transillumination, with Fluor-S^{TM} MultiImager + Quantity One 1-D Analysis software) to find the composition of each protein in the solution. After the SDS-PAGE gel was performed the gel with apparent lysozyme and ovalbumin bands was put into the UV light transillumination, with the Fluor-S^{TM} MultiImager. The intensity volume of each band

was determined by the Quantity One 1-D Analysis software. The compositions of each protein were estimated by the plot of intensity volume ratio versus composition of protein. Then, the total protein concentration can be determined by locating the composition point on the calibration curve for the UV absorbance of the mixed protein. Finally, the concentrations of pure protein were estimated from the total protein concentration and composition.
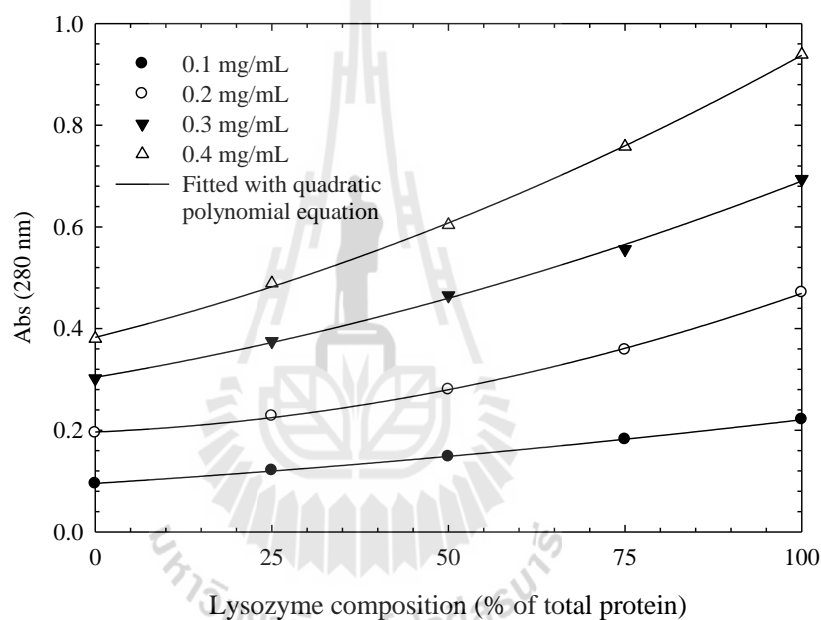
Figure 2.7 Calibration curve for UV absorbance at 280 nm as various composition

of lysozyme and total protein concentration.

2.4.5.2 UV-Vis method

Applying Beer-Lambert's law to analyze the concentration of each component in the mixed solution, it is possible to define the absorbance of the mixed solution as a summation of the absorbance of each pure component as given by

$$A(\lambda) = \sum_{i=1}^{n} \varepsilon_i(\lambda) c_i l \qquad (2.5)$$

In the case of the two components mixture (lysozyme + ovalbumin) equation (2.5) can be written as

$$A(\lambda) = \varepsilon_{lys}(\lambda) c_{lys} l + \varepsilon_{oval}(\lambda) c_{oval} l \qquad (2.6)$$

where $A(\lambda)$ is the absorbance of the mixed solution at wavelength λ, $\varepsilon_{lys}(\lambda)$ and $\varepsilon_{oval}(\lambda)$ are the extinction coefficients of lysozyme and ovalbumin at wavelength λ, respectively, c_{lys} and c_{oval} are the concentrations of lysozyme and ovalbumin, and l is the path length of the light (the width of the cuvette). Equation (2.6) can be used to determine the concentration of lysozyme and ovalbumin by measuring the absorbance of the solution at two wavelengths as long as the extinction coefficient of the pure components, $\varepsilon_{lys}(\lambda)$ and $\varepsilon_{oval}(\lambda)$, are known at both wavelengths. Normally, the wavelengths that will be used for the measurement of absorbance of the mixture should be the maximum value of absorbance for one component and the minimum value for the others (Benesch, Benesch, and Yung, 1973). In the case of mixtures of lysozyme and ovalbumin both proteins have the same absorption behavior (have their maximum absorbance at the same wavelength, see Figure 2.8). Therefore it is hard to choose the best two wavelengths that give the maximum accuracy of measurement. To solve this problem the linear least squares mathematical method (Spiegel, Lipschutz, and Liu, 2009) was applied to determine the concentrations from the UV

measurement made at more than two wavelengths to minimize the error of the measurement.
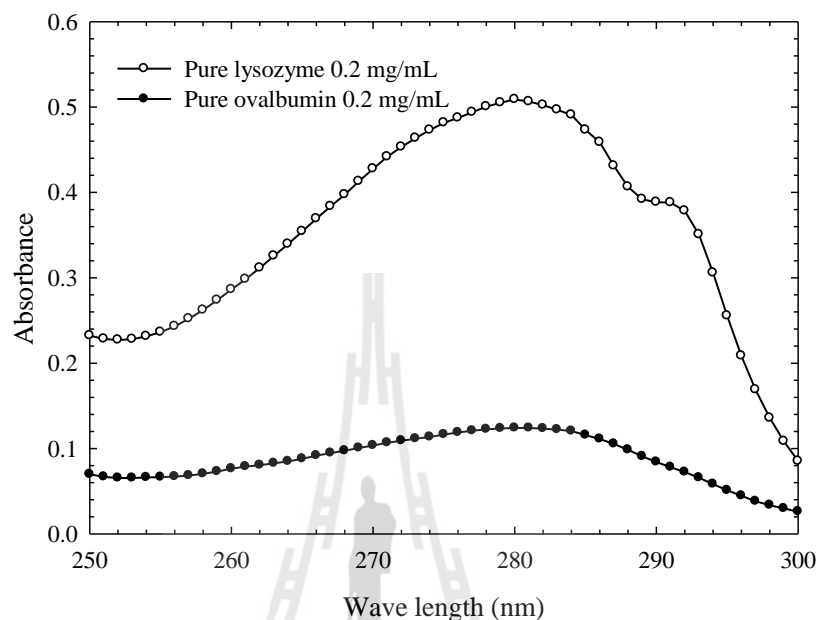
Figure 2.8 Absorption behavior of lysozyme and ovalbumin in 0.1 M sodium
acetate buffer pH 5.

Solutions of 1 mg/mL of lysozyme and ovalbumin were prepared by dissolving 20 mg of lysozyme or ovalbumin into enough buffer to obtain a final volume of 20 ml. Two proteins solutions were mixed at the desired proportion in buffer to prepare the total concentration of proteins ranging from 0 to 1 mg/mL with 0.2 mg/mL increments. The composition of each protein in the mixture was varied from 0 to 100%. The absorbance of the solutions were measured three times at six different wavelengths; 250, 260, 270, 280, 290 and 300 nm. An extinction coefficient obtained from a calibration curve was used.

2.5   Results and Discussions

2.5.1   Solubility of Lysozyme Powder

The measured solubility data of lysozyme powder are listed in table 2.2 and shown in Figures 2.9 - 2.14. Each data point is the average of three concentrations at equilibrium (constant concentration with time, within 3 weeks). The calculated standard deviations were found to be varied with sodium chloride concentration. The average values of the standard deviation of the distribution of measured values are 0.24, 0.11, and 0.07 at 3%, 4%, and 5% sodium chloride concentration, respectively.

Table 2.2 Lysozyme solubility at various temperature, pH, and salt concentration using the classical technique.

Temp. (°C)	NaCl (%)	Solubility (mg/mL)					
		pH 4.0	pH 4.4	pH 4.6	pH 5.0	pH 5.4	pH 6.0
10	3	2.50	2.50	2.56	2.45	1.52	1.72
	4	0.97	1.22	1.14	1.48	1.04	1.25
	5	0.60	0.79	0.85	0.92	0.82	0.94
15	3	4.62	4.25	4.90	3.82	2.54	3.25
	4	1.62	2.11	1.75	2.13	1.79	2.12
	5	0.97	1.23	1.12	1.60	1.40	1.56
20	3	8.04	7.14	8.87	6.59	4.35	5.70
	4	2.68	3.55	3.16	3.47	2.86	4.78
	5	1.75	1.98	2.01	2.64	2.18	2.98
25	3	15.00	11.15	14.52	11.22	7.88	10.64
	4	4.76	5.70	5.28	5.48	4.75	6.32
	5	3.32	3.40	3.22	3.98	3.74	4.16
30	3	28.75	17.08	22.23	17.28	11.86	17.25
	4	9.00	9.24	8.52	8.78	8.24	12.64
	5	6.30	6.33	5.26	6.52	6.15	8.68
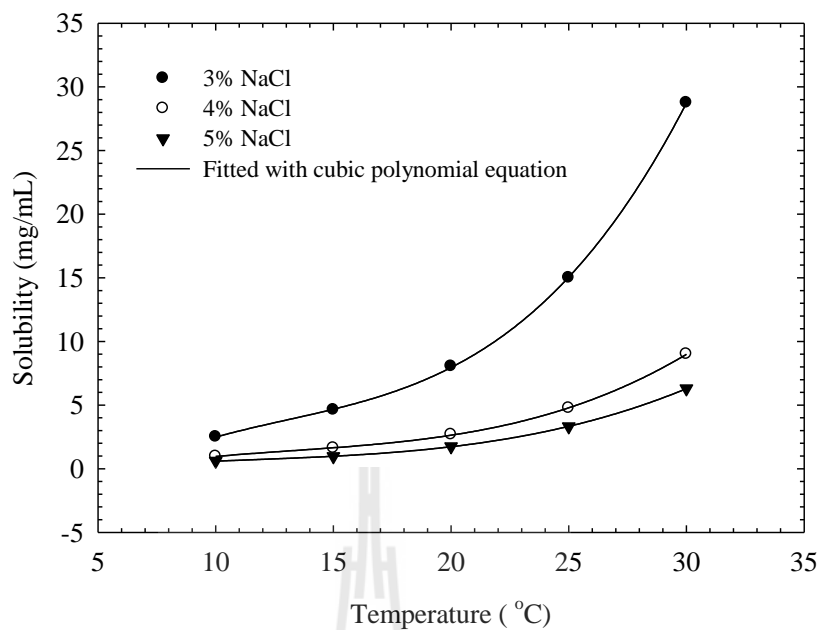
Figure 2.9 Solubility of lysozyme powder at pH 4.0 as a function of temperature and

NaCl concentrations.
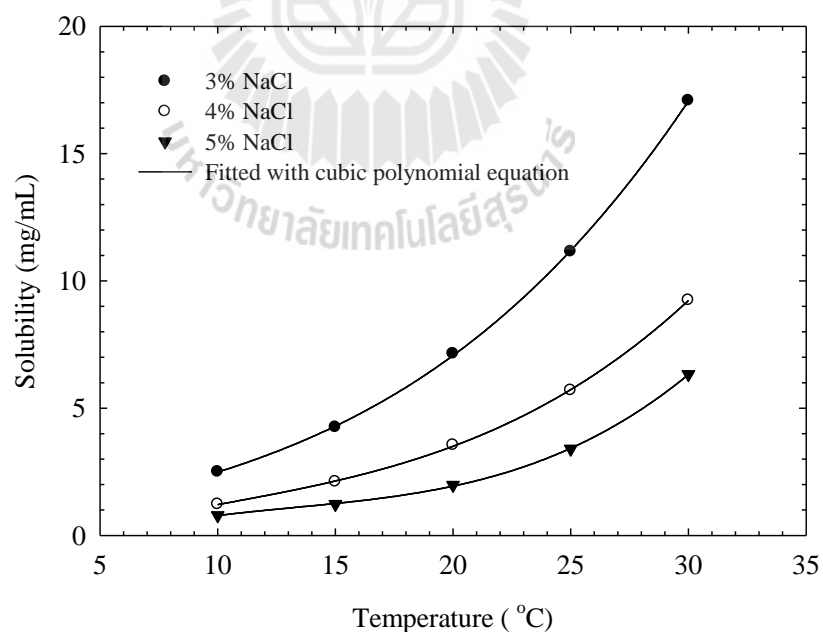
Figure 2.10 Solubility of lysozyme powder at pH 4.4 as a function of temperature

and NaCl concentrations.
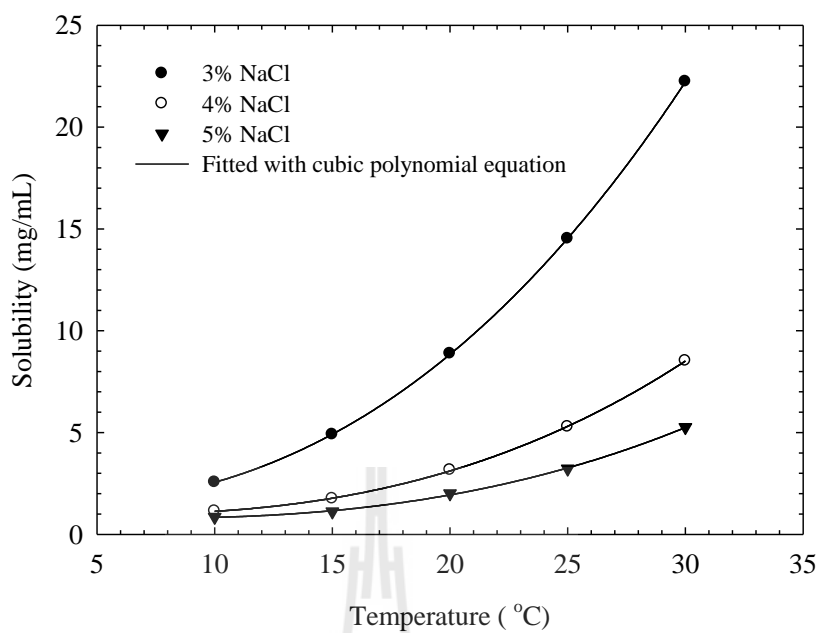
Figure 2.11 Solubility of lysozyme powder at pH 4.6 as a function of temperature

and NaCl concentrations.
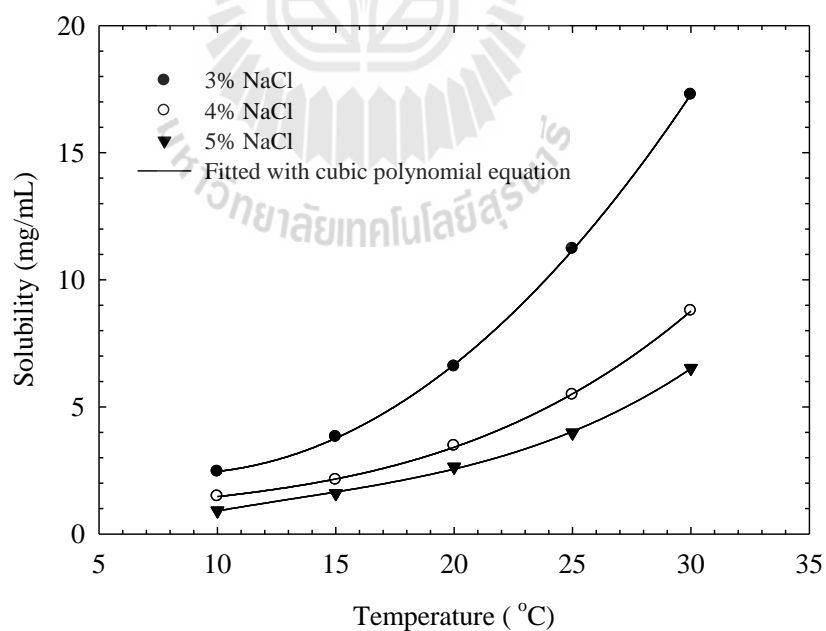
Figure 2.12 Solubility of lysozyme powder at pH 5.0 as a function of temperature

and NaCl concentrations.
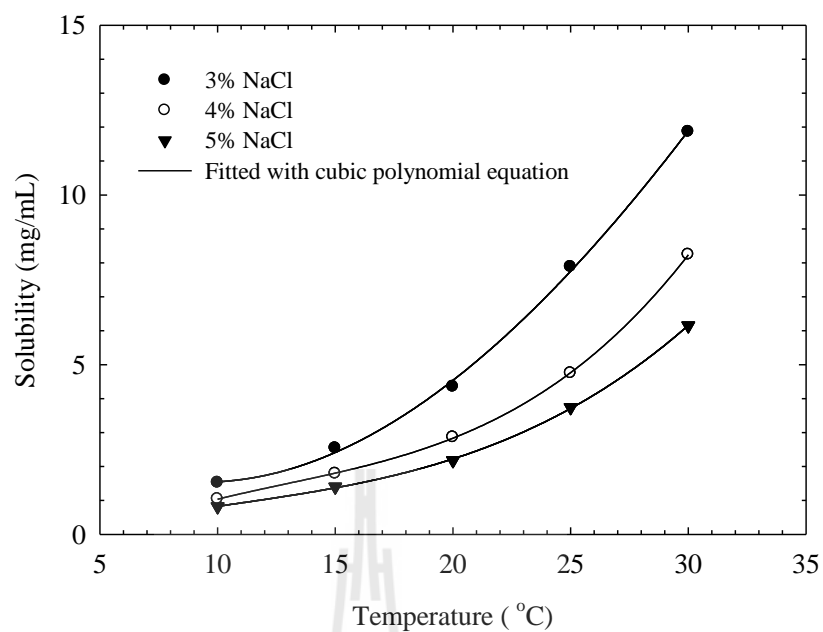
Figure 2.13 Solubility of lysozyme powder at pH 5.4 as a function of temperature

and NaCl concentrations.
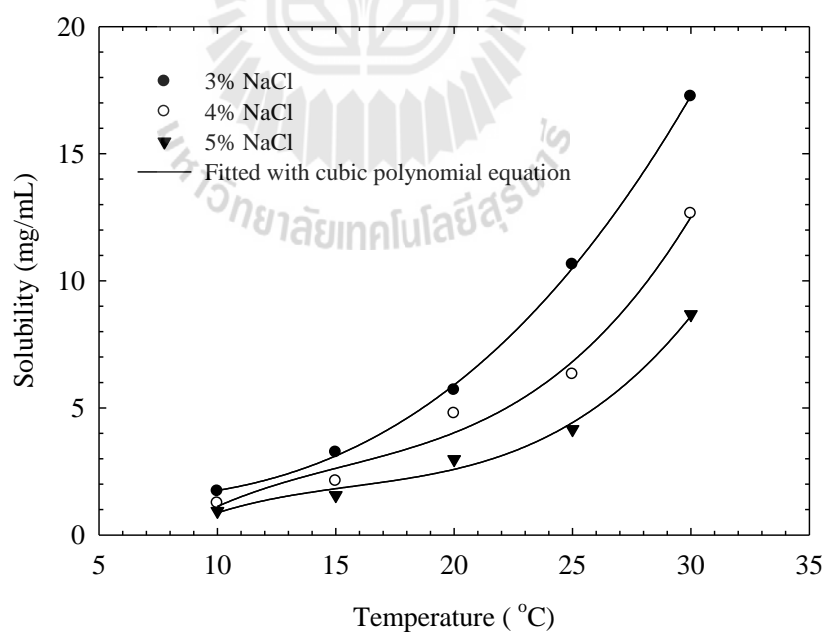
Figure 2.14 Solubility of lysozyme powder at pH 6.0 as a function of temperature

and NaCl concentrations.

The solubility curves show the solubility of lysozyme increases with increasing temperature, and decreases with increasing NaCl concentration. This solubility behavior is commonly observed in organic compounds and consistent with other work on proteins (Forsythe and Pusey 1996). The solubility data as a function of temperature were fitted using a third-order polynomial equation; the results of the constants in equation (2.1) are listed in Table 2.3. All of the fitted lines have the coefficient of determination (R^2) greater than 0.99 and the average residual sum of squared errors of prediction (RSSE) is only 0.091 indicating that the third-order polynomial can fit the solubility data well. Careful observation of the effect of pH show the solubility seems to be slightly reduced at higher values of the pH (the effect is not very clear). Although solubility is mostly increasing with increasing pH, there are some points where the solubility decreases with increasing pH.

Table 2.3 Constant of solubility data of lysozyme powder fitted to the third-order

polynomial, $c = A + BT + CT^2 + DT^3$

pH	NaCl (%)	Constant of a third-order polynomial fit			
		A	B	C	D
4.0	3	-9.62800	2.27560	-0.14300	0.00370
	4	-3.02400	0.74770	-0.04660	0.00120
	5	-1.10200	0.33150	-0.02280	0.00070
4.4	3	0.20400	0.21760	-0.00410	0.00050
	4	-1.00600	0.33010	-0.01640	0.00060
	5	-1.94400	0.51130	-0.03190	0.00080
4.6	3	1.64600	-0.12060	0.01830	0.00030
	4	1.28000	-0.07860	0.00430	0.00020
	5	1.10200	-0.06660	0.00260	0.00010
5.0	3	4.56200	-0.52110	0.03090	0.00002
	4	0.53800	0.12270	-0.00690	0.00040
	5	-1.80800	0.43660	-0.02210	0.00060
5.4	3	4.29000	-0.60550	0.03540	-0.00020
	4	-2.28400	0.57870	-0.03320	0.00090
	5	-0.63200	0.23570	-0.01330	0.00040
6.0	3	1.83200	-0.11920	0.00610	0.00050
	4	-8.14800	1.64450	-0.09170	0.00200
	5	-6.67600	1.38570	-0.08000	0.00170

2.5.2 Solubility of Tetragonal Lysozyme Crystal

Examples of dissolution profiles of tetragonal lysozyme crystal in sodium acetate buffer are shown in Figure 2.15. The plot shows the increasing of solution absorbance as a function of time. The lysozyme concentration can be directly

calculated from the solution absorbance. Therefore, lysozyme solubilities were determined by averaging the concentrations at equilibrium (the constant concentration with time in Figure 2.15). The dissolution curve in Figure 2.15 shows that the approximate times required to reach equilibrium are around 800 minute at 5°C, 400 minute at 10°C, and 300 minute at 15°C. This indicates that the dissolution rate is increased with increasing solute on temperature. The solubilities of tetragonal lysozyme crystal are listed in Table 2.4 and shown in Figures 2.16 - 2.18.
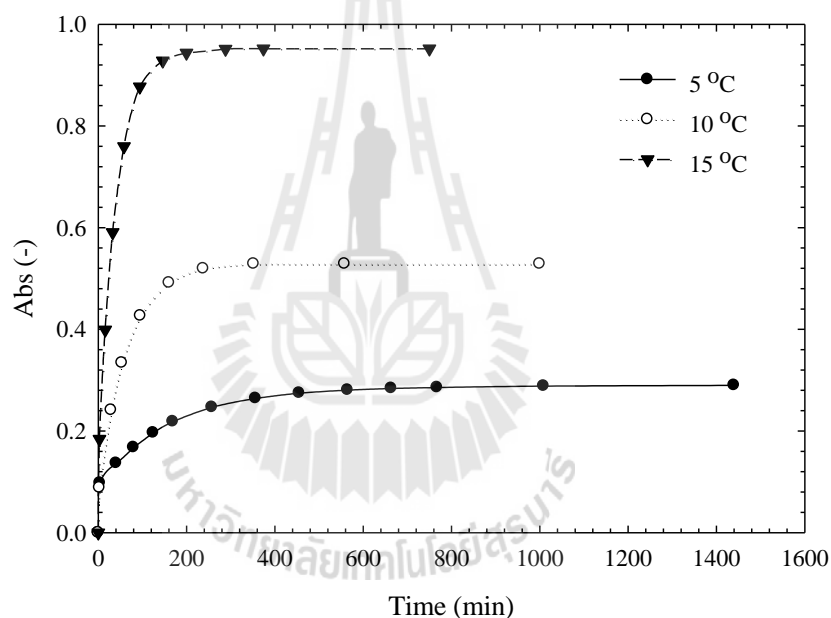
Figure 2.15 Examples of dissolution profiles of tetragonal lysozyme crystal

(4% NaCl, pH 5.0, and 2 mm path length cuvette for UV

measurement).

Table 2.4 Lysozyme solubility at various temperature, pH, and salt concentration

using the miniature column technique**.**

Temp. (°C)	NaCl (%)	Solubility (mg/mL)		
		pH 5.0	pH 5.6	pH 6.0
5	3	1.09	0.90	0.95
	4	0.58	0.62	0.61
	5	0.37	0.49	0.48
	7	0.29	0.35	0.46
10	3	2.10	1.55	1.63
	4	1.11	1.07	1.07
	5	0.72	0.86	0.87
	7	0.49	0.60	0.69
15	3	4.02	3.72	3.61
	4	2.03	2.05	1.90
	5	1.22	1.43	1.49
	7	0.88	1.04	1.16
20	3	7.21	5.72	5.52
	4	4.02	4.04	3.87
	5	2.35	2.47	3.10
	7	1.48	1.69	2.24
25	3	14.74	10.50	9.98
	4	7.08	6.95	6.16
	5	4.52	5.07	4.70
	7	2.58	3.20	3.92

The calculated standard deviation associated with the presented solubility data were
found to be varied with sodium chloride concentration. The average values of the
standard deviation of the distribution of measured values are 0.20, 0.10, 0.05, and
0.03 at 3%, 4%, 5%, and 7% sodium chloride concentration, respectively. This
indicated that the dissolution rate is higher at the higher salt concentrations.
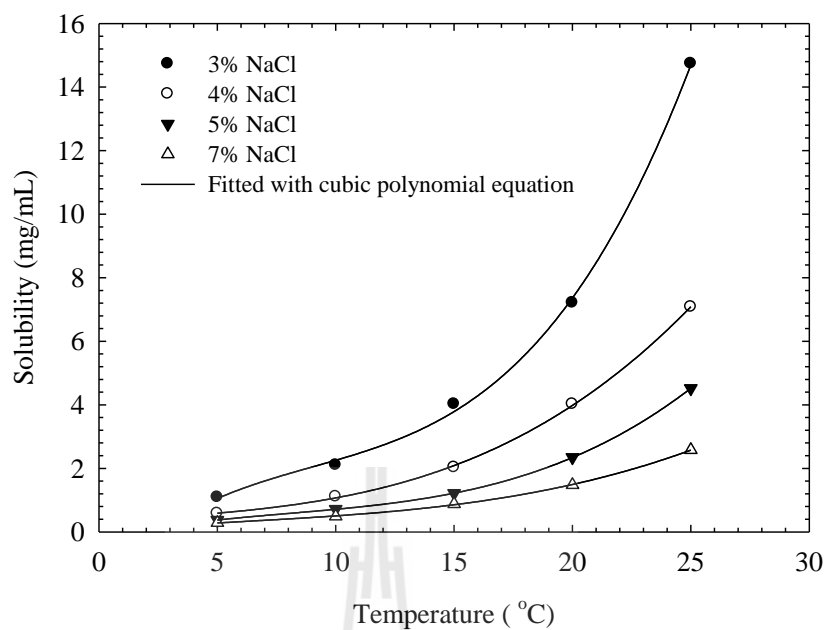
Figure 2.16 Solubility of tetragonal lysozyme crystal at pH 5.0 as a function of

temperature and NaCl concentrations.
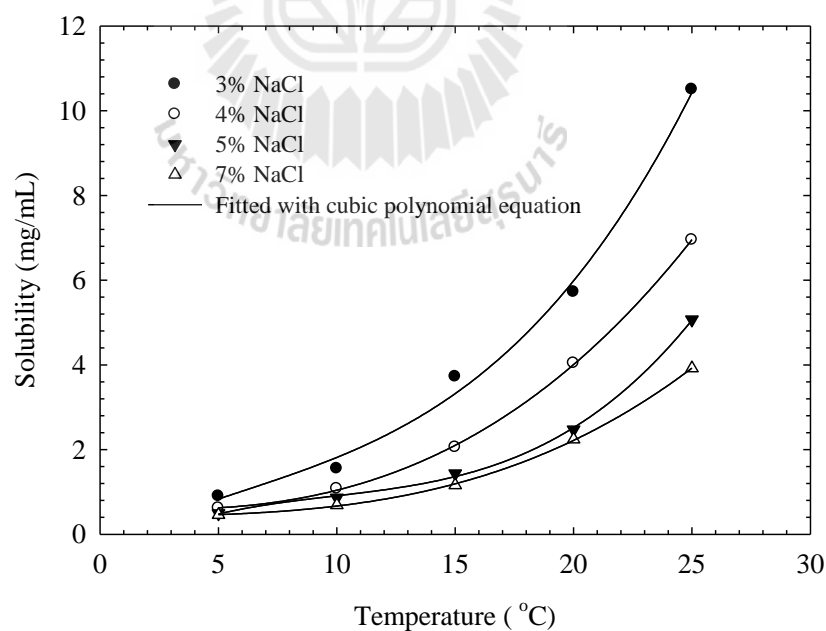
Figure 2.17 Solubility of tetragonal lysozyme crystal at pH 5.6 as a function of

temperature and NaCl concentrations.
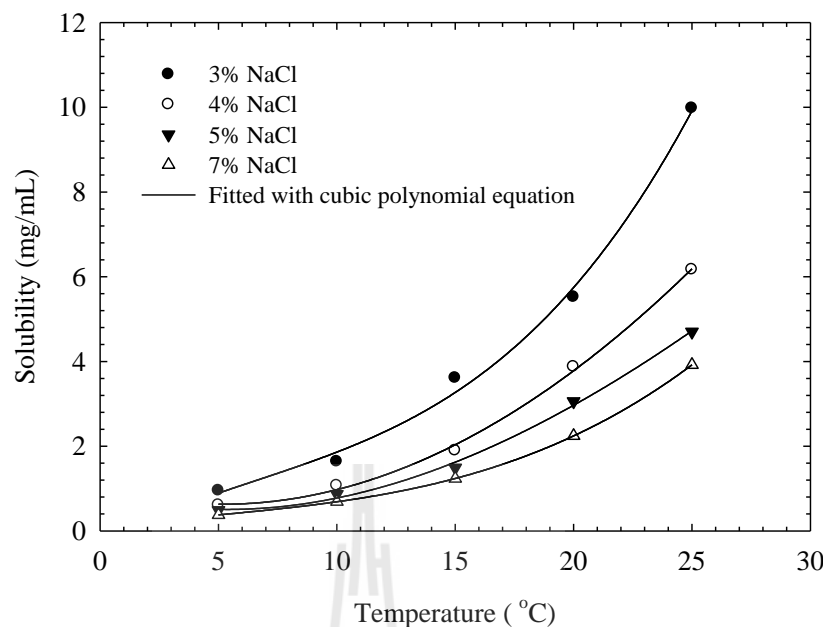
Figure 2.18 Solubility of tetragonal lysozyme crystal at pH 6.0 as a function of
temperature and NaCl concentrations.

Similarly to the previous section, the solubility plot showed the
solubility of lysozyme increases with temperature and decreases with increasing NaCl
concentration. The solubility data were also consistent with previous work (Forsythe
and Pusey, 1996). The third-order polynomial equation fit with a function of
temperature gives the constants in equation (2.1) listed in Table 2.5. All of the fitted
lines have the average coefficient of determination (R^2) greater than 0.999 and the
average residual sum of squared errors of prediction (RSSE) is only 0.062 indicating
that the third-order polynomial can also fit these solubility data well. The major
advantage of this method is a reduction in the time required to reach equilibrium, with
this time being reduced from several weeks to within one day (Pusey, 1988).

Table 2.5 Constants for the solubility data of lysozyme crystal fitted to a third-order

polynomial, $c = A + BT + CT^2 + DT^3$

pH	NaCl (%)	Constant of a third-order polynomial fit			
		A	B	C	D
5.0	3	-1.53800	0.77080	-0.06200	0.00230
	4	0.30400	0.06020	-0.00290	0.00050
	5	-0.23600	0.17890	-0.01430	0.00060
	7	0.03160	0.06370	-0.00370	0.00020
5.6	3	-0.25200	0.26960	-0.01470	0.00080
	4	0.65700	-0.03740	0.00490	0.00030
	5	-0.60780	0.32890	-0.02680	0.00090
	7	0.40400	0.01010	-0.00080	0.00020
6.0	3	-0.26660	0.29260	-0.01640	0.00080
	4	1.03010	-0.15620	0.01540	-0.00004
	5	0.90720	-0.15150	0.01500	-0.00010
	7	0.09230	0.06950	-0.00390	0.00030

2.5.3   Thermodynamics

Fitting the solubility data in Table 2.2 and 2.4 to equation (2.4) (*ln(c)*

against 1/*T*) gives a straight line approximation, as shown in Figures 2.19-2.27. The

ΔH_{diss} and ΔS_{diss} values can be obtained from the slope of the line and the intercept of

y axis, respectively. The plot showed the equation fitted the experimental solubility

data very well. The estimated values of the ΔH_{diss} and ΔS_{diss} are listed in Tables 2.6

and 2.7.   The example of fitting the equation is shown in equation (2.7) for the

dissolution of tetragonal lysozyme crystal in 0.1M sodium acetate buffer pH 5.0 and

4% NaCl concentration.

$$\ln(c) = -\frac{1.27 \times 10^3}{T} + 36.37 \qquad (2.7)$$

where *T* is in K.

The average enthalpy and entropy of dissolution are 74.84 ± 6.03 kJ/mol and 266.05 ± 21.81 J/mol·K for lysozyme powder (Table 2.5) and 84.56 ± 3.84 kJ/mol and 292.97 ± 15.05 J/mol·K for tetragonal lysozyme crystal (Table 2.6), respectively. However, the value of enthalpy and entropy for the two type of lysozyme might be the same. The difference may result from the experimental errors. The average of values enthalpy and entropy for the two type lysozyme are 78.69 ± 7.12 kJ/mol and 276.82 ± 23.85 kJ/mol, respectively. The estimated enthalpies are consistent with other work (Howard et al., 1988; Ries-Kautt, 1989; Cacioppo, 1991; Haas, 1999; Lu, 2002). As expected, the change in enthalpy of dissolution(ΔH_{diss}) of lysozyme is positive indicating that the endothermic reaction of breaking the hydrogen bonds to create a cavity for the solutes within the aqueous solution occurs (Anuar et al., 2009); heat is required when a lysozyme crystal dissolves.
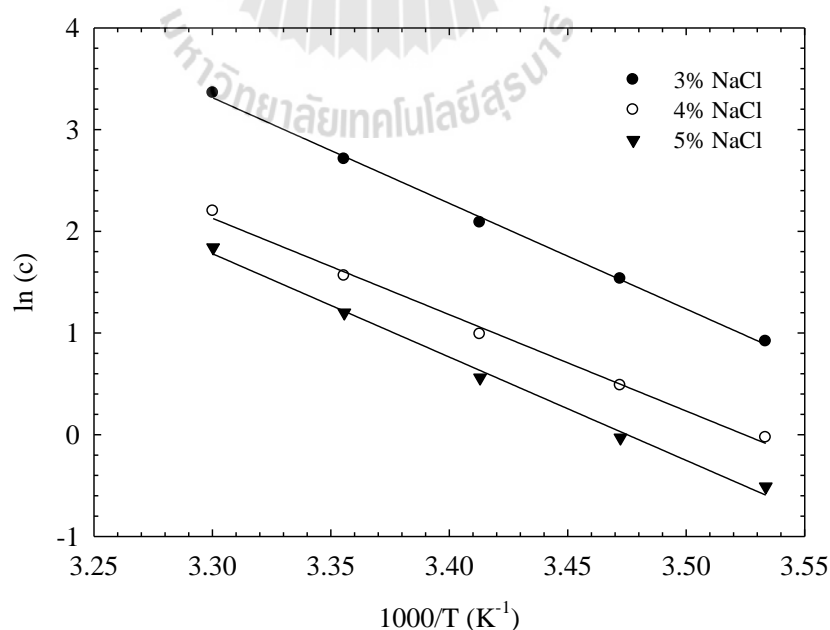
Figure 2.19 Van't Hoff plot, solubility data of lysozyme powder pH 4.0
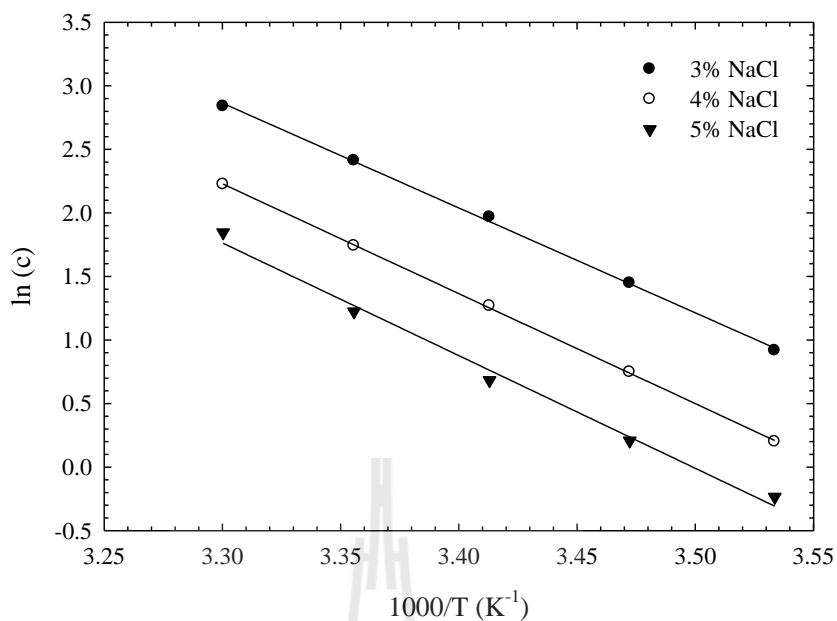
Figure 2.20 Van't Hoff plot, solubility data of lysozyme powder pH 4.4
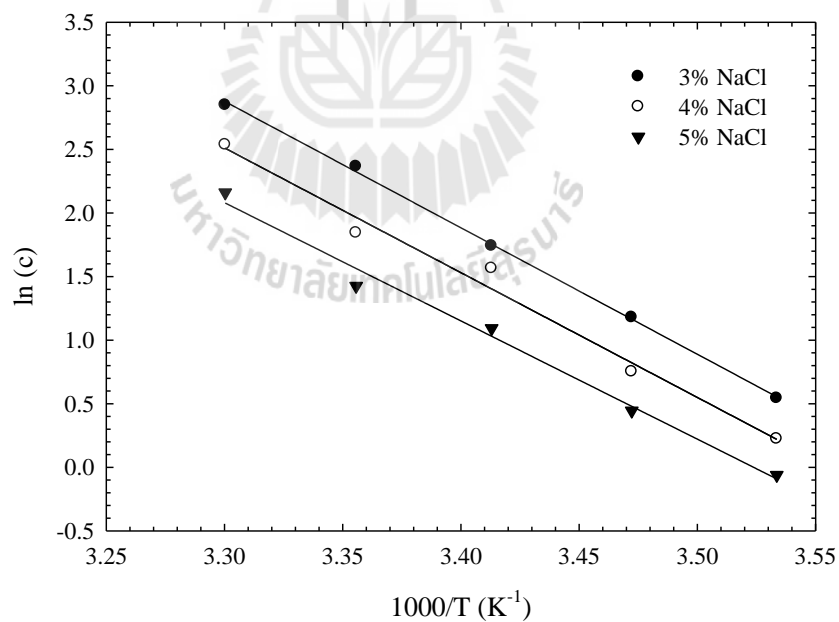
Figure 2.21 Van't Hoff plot, solubility data of lysozyme powder pH 4.6
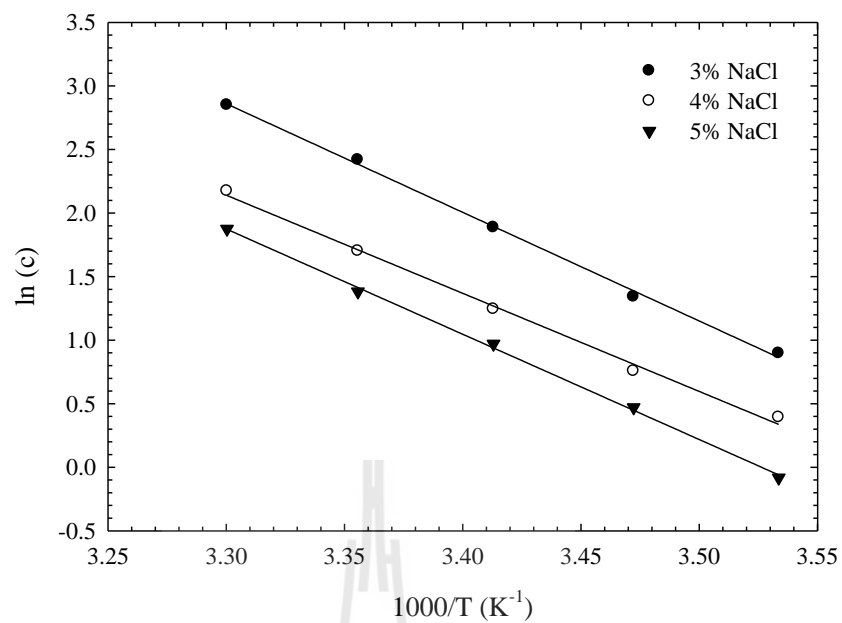
Figure 2.22 Van't Hoff plot, solubility data of lysozyme powder pH 5.0
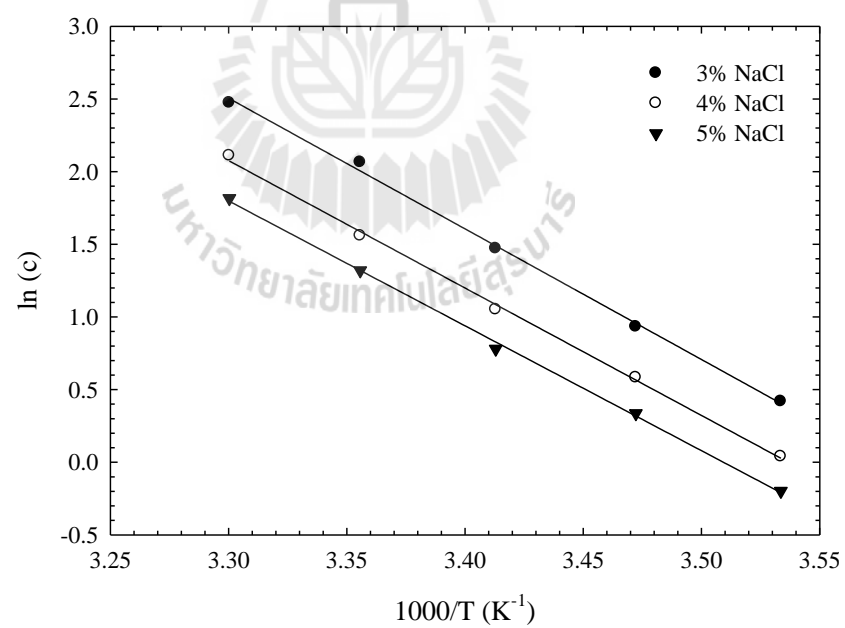
Figure 2.23 Van't Hoff plot, solubility data of lysozyme powder pH 5.4
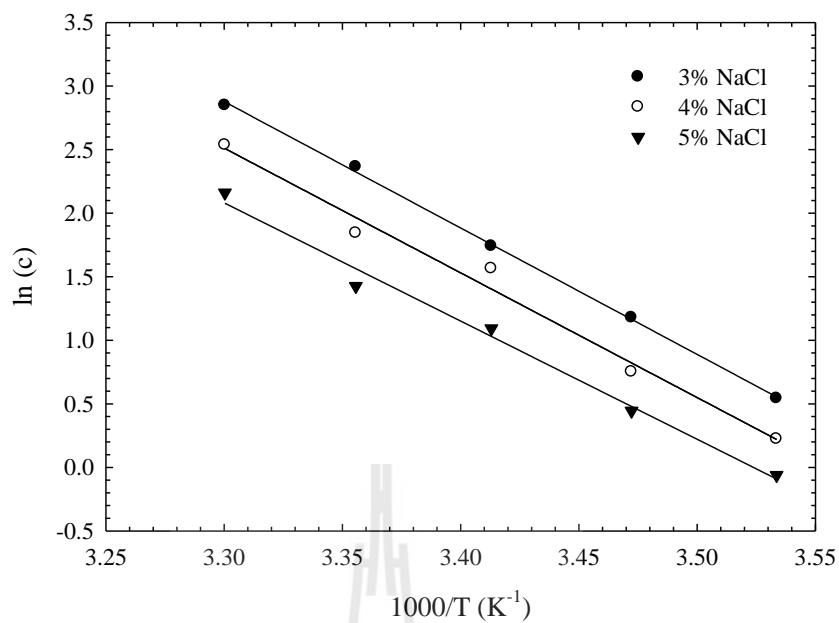
Figure 2.24 Van't Hoff plot, solubility data of lysozyme powder pH 6.0
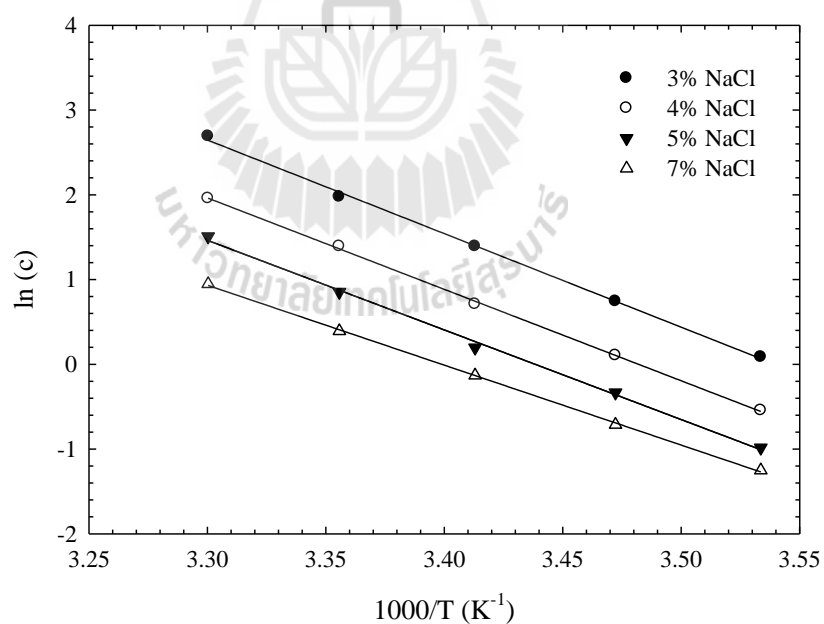
Figure 2.25 Van't Hoff plot, solubility data of tetragonal lysozyme crystal pH 5.0
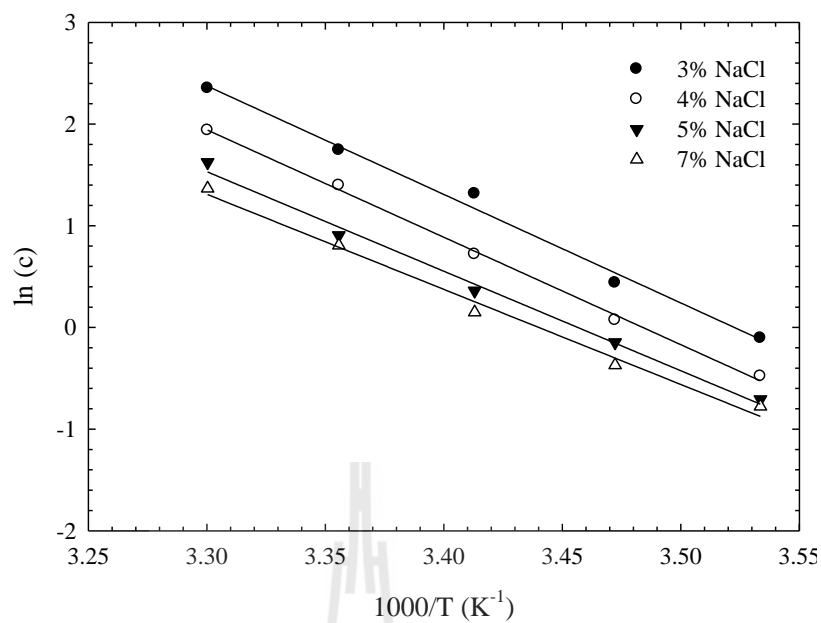
Figure 2.26 Van't Hoff plot, solubility data of tetragonal lysozyme crystal pH 5.6
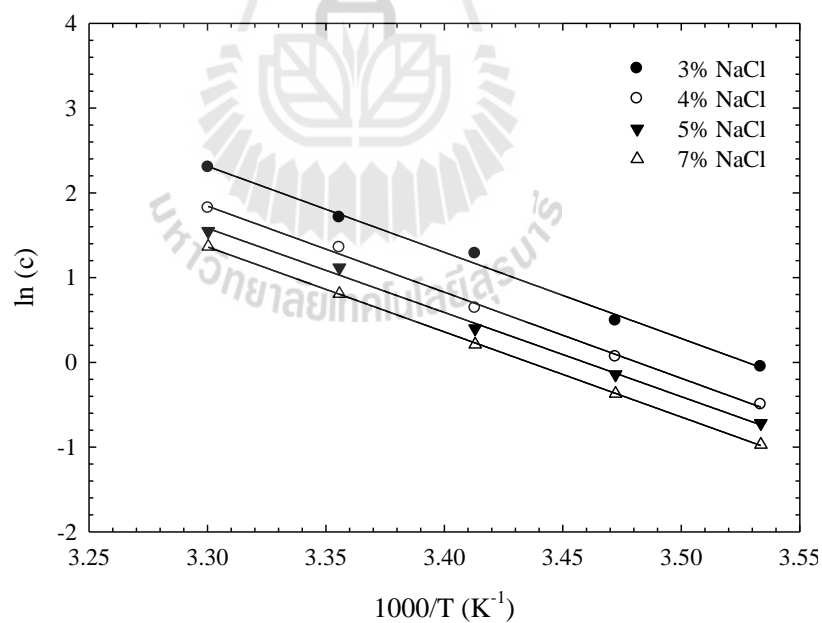
Figure 2.27 Van't Hoff plot, solubility data of tetragonal lysozyme crystal pH 6.0

Table 2.6 The enthalpy and entropy of dissolution of lysozyme powder in 0.1M

      sodium acetate buffer.

pH	NaCl (%)	Constant parameters	
		ΔH_{diss} (kJ/mol)	ΔS_{diss} (J/mol·K)
4.0	3	86.38	312.62
	4	78.80	277.73
	5	84.49	293.60
4.4	3	68.60	250.20
	4	71.93	255.92
	5	73.72	257.95
4.6	3	77.24	281.22
	4	73.08	258.96
	5	66.94	234.38
5.0	3	71.06	258.28
	4	64.19	229.61
	5	68.87	242.87
5.4	3	74.75	267.50
	4	72.91	257.86
	5	71.45	250.73
6.0	3	82.69	296.82
	4	81.59	290.12
	5	77.32	272.47

Table 2.7 The enthalpy and entropy of dissolution of tetragonal lysozyme crystal in

      0.1M sodium acetate buffer.

pH	NaCl (%)	Constant Parameters	
		ΔH_{diss} (kJ/mol)	ΔS_{diss} (J/mol·K)
5.0	3	89.70	312.33
	4	87.95	302.40
	5	87.95	302.40
	7	78.41	266.52
5.6	3	88.73	312.56
	4	87.85	306.07
	5	81.39	281.32
	7	77.76	267.51
6.0	3	84.49	298.07
	4	84.46	294.04
	5	82.60	285.74
	7	83.46	286.75

2.5.4 Concentration Measurement of Mixed Proteins using The Combination of SDS-PAGE gel and UV-Vis Technique.

In preliminary experiments, the intensity volume which is defined as the intensity of the color stained on the protein band per area of the band in the gel of pure lysozyme and ovalbumin were measured as shown in Figure 2.28. Intensity volume per amount of protein are constant for ovalbumin but it was divided into two sections for lysozyme As shown, a small composition of lysozyme gives a large slope of the plotted line, and at a larger slope at a high composition of lysozyme.
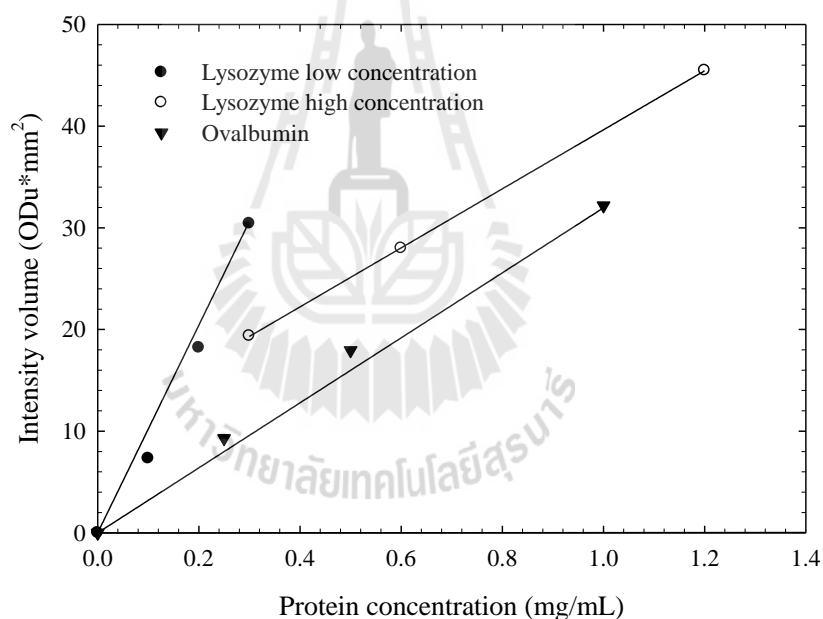
Figure 2.28 Intensity volume of pure protein.

Performing the SDS-PAGE gel of mixed lysozyme – ovalbumin solution analyzed with the Gel Doc analyzer gives the results between intensity volume ratio and protein composition as shown in Figure 2.29; (an example of the raw data for SDS-PAGE gel and intensity volume analysis are shown in Appendix A).

The results showed that the straight line plot of intensity volume ratio and lysozyme composition can be divided into two parts.

The first part is the plot from 0 - 60% lysozyme composition and fitted well with the linear equation

$$y = 3.1372x \qquad (2.8)$$

The second part is the plot of lysozyme composition more than 60% and this data can be fitted well with the linear equation

$$y = -14.6266 + 24.306x \qquad (2.9)$$

This behavior resulted from the difference in the extinction coefficient (parameters defining how strongly a substance absorbs light at a given wavelength) of lysozyme and ovalbumin. Lysozyme has a higher value of the extinction coefficient than ovalbumin, and these results in it having higher ability to absorb light.
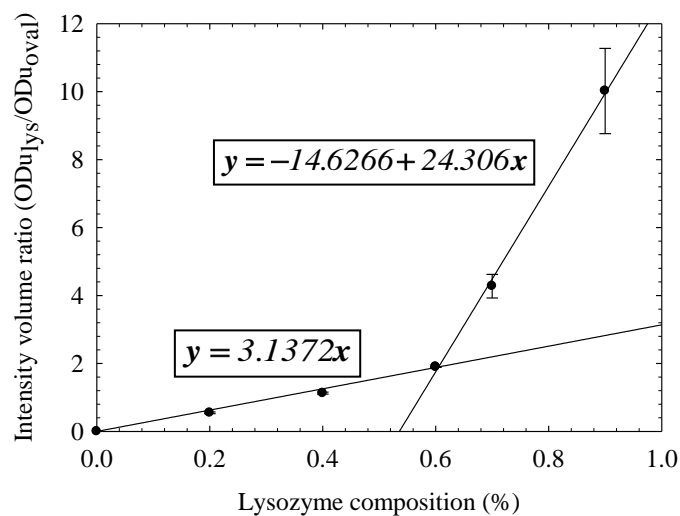
Figure 2.29 Intensity volume ratios as a function of lysozyme composition.

The calculated compositions of each protein were estimated using the relation between intensity volume ratio and protein composition in Figure 2.29 and equations (2.8) and (2.9). The total protein concentration can be estimated using the calibration curve shown in Figure 2.7. Finally, the concentrations of pure protein were estimated from the total protein concentration and composition. This method has the advantage that the composition of protein in the mixture can be determined together with running SDS-PAGE gel to observe the purity of the protein and require the measurement of UV absorbance at only one wavelength. However, lysozyme has no consistency in intensity volume between low and high concentration.

2.5.5 Concentration Measurement of Mixed Proteins using the UV-Vis method.

The extinction coefficients of pure lysozyme and ovalbumin were obtained from the calibration curves as described in section 2.4.5.2 and shown in Table 2.8. Both proteins have the same absorption behavior. A maximum absorption occurs at 280 nm and the absorption decreases from this point with either an increase or a decrease of the wavelength.

Table 2.8 Summary of the extinction coefficients used in the calculation (obtained from the calibration curve).

Wave length (nm)	Extinction coefficient (mL/mg·cm)	
	Lysozyme	Ovalbumin
250	1.1052	0.3598
260	1.4135	0.4127
270	2.0987	0.5607
280	2.4121	0.6559
290	1.8551	0.4359
300	0.3673	0.1312

The measurements of the absorbance of the mixture of lysozyme and ovalbumin at six different wavelengths (measured three times for each wavelength) are listed in Table 2.8 together with the use of extinction coefficients of pure protein results in six equations with two unknowns (in the form of equation (2.6)), the lysozyme and ovalbumin concentrations. These concentrations could be calculated by the use of the linear least squares method. The calculated results of protein concentrations for different compositions and total concentrations were plotted against the prepared concentrations to observe the detection limit and accuracy of the measurement, as shown in Figure 2.30 - 2.32. The detection limits of this method were presented by the coefficient of determination (R^2) of the linear fit. No detection limits were observed in the case of the composition of proteins in the mixture and for the total concentration lower than to 1 mg/mL since a very good fit of the data; $R^2 = 0.9990$ for lysozyme (Figure 2.30), $R^2 = 0.9882$ for ovalbumin (Figure 2.31), and $R^2 = 0.9989$ for total protein concentrations (Figure 2.32), were recorded.

The slope of the linear fits indicated the accuracy of calculations (absolute accuracy is indicated by the slope = 1). The errors of measurements were calculated from the slope of the fitted line and defined as equation (2.10)

$$Error\,(\%) = |1 - slope| \times 100\% \tag{2.10}$$

The observational errors (errors from measurements and calculations) and including the experimental errors are summarized in Table 2.9.
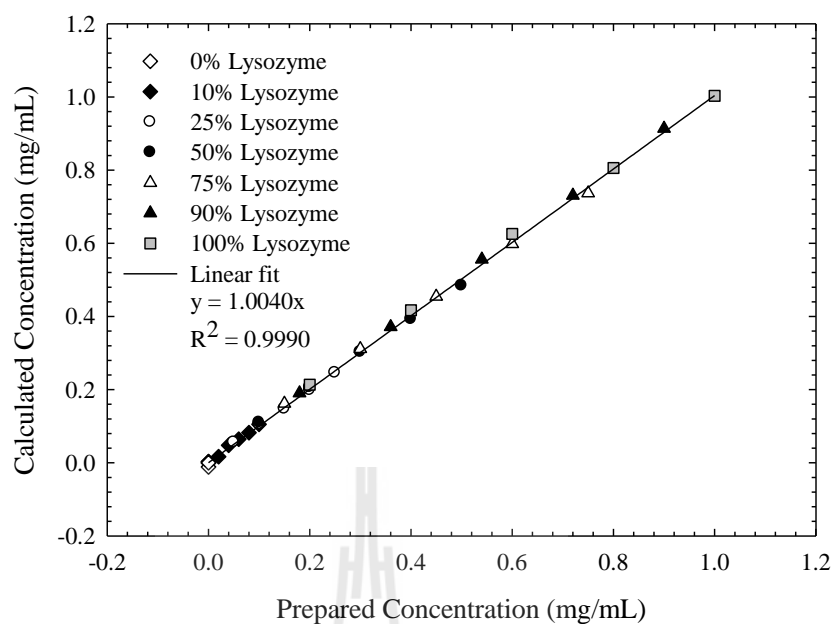
Figure 2.30 Comparison of the calculated and prepared concentration of lysozyme

in the mixed solutions of lysozyme and ovalbumin.
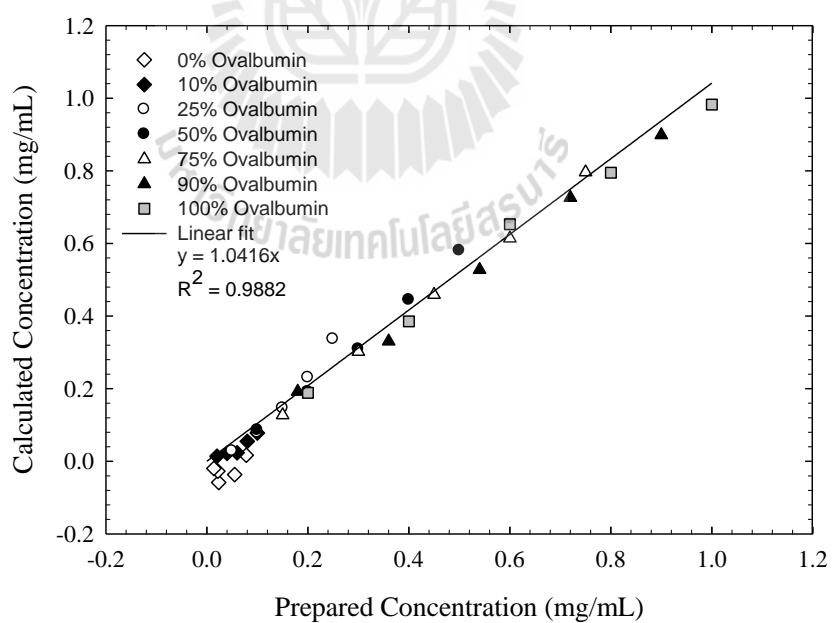
Figure 2.31 Comparison of the calculated and prepared concentration of ovalbumin

in the mixed solutions of lysozyme and ovalbumin.
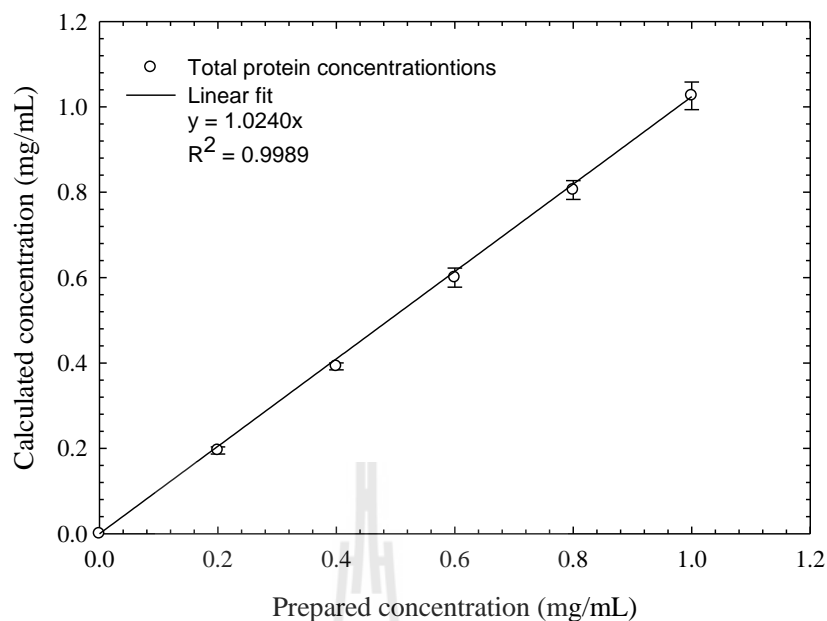
Figure 2.32 Comparison of the calculated and prepared concentrations of total

proteins (lysozyme + ovalbumin) in the mixed solutions.

Table 2.9 Summary of the errors from both measurements and experiments.

Components	Observational errors (%)	Including experimental errors (%)
Lysozyme	0.40	1.19
Ovalbumin	4.16	7.91
Total protein	2.40	5.38

The observational error values indicated that the error from

measurements and calculations depend on the absorption ability of the substance in

the mixture. The protein that has a higher extinction coefficient should have a smaller

error from the calculation. In the case of mixed lysozyme and ovalbumin, lysozyme

has a higher value of the extinction coefficient than ovalbumin. Therefore, the error of

concentration from calculation for pure lysozyme is lowest. Three independent

experiments were performed to investigate the experimental errors. The standard deviation of experiment is highest at 1 mg/mL total protein (±0.0457 mg/mL) and reduces with decreasing of concentration. The R^2 of the linear fit of the plots of calculated and prepared concentration are 0.9969 for lysozyme, 0.9822 for ovalbumin and 0.9999 for total protein. However the plots are not shown here. The observational errors and the experimental errors are shown in the third column of Table 2.9. These values consist of the error from measurements, calculations, and experiments. This method is advantageous in the measurement requires only a UV photometer, which is a fast measurement, and the detection limit is less than 1 mg/mL of total protein (depending on the UV photometer). It has only some difficulty, solving 6 equations together is not easy with an analytical method. However, using a numerical program (e.g. Matlab, Maple) solves this problem.

2.6   Conclusions

The lysozyme solubility data which is necessary to use for the design and development of a crystallization process were determined as a function of temperature, sodium chloride concentration and, solution pH using both the classical technique and the miniature column technique. The results are consistent with previous work (Forsythe and Pusey, 1996). The solubility data are well fitted with both a third – order polynomial equation and the van't Hoff equation. Therefore both correlations can be used to predict the behavior of the solubility as function of temperature. The enthalpy of dissolution of the powder form and crystal form can be estimated and gives a positive value. This means that an endothermic reaction occurs and heat is required to make lysozyme dissolve.

The modified techniques used to measure the concentration of mixed protein during crystallization were presented. These two techniques involve measuring the concentration in the solution phase and require only a few microliters of the solution. Using very small samples results in smaller disturbance on the crystallization process which is necessary for the crystallization of protein (which is sensitive to experimental and solution conditions). Although there are some limitations for use, the techniques offer the opportunity to be used depending on the requirement of each project.

2.7   References

Apgar, M.C. (2008). The influence of pH on nucleation, solubility and structure of lysozyme protein crystals. Ph.D Thesis. **University of South Florida (USF).** Florida, USA.

Ataka, M., and Asai, M. (1988). Systematic studies on the crystallization of lysozyme. Dtermination and use of phase diagrams. **J. Cryst. Growth** 90: 86-93.

Beckmann, W. (2000). Seeding the desired polymorph: background, possibilities, limitations, and case studies. **Org. Process Res. Dev.** 4(5): 372-383.

Benesch, R.E., Benesch, R., and Yung, S. (1973). Equations for the Spectrophotometric Analysis of Hemoglobin Mixtures. **Anal. Biochem.** 55: 245-248.

Berthou, J., and Jolies, P.A. (1974). Phase transition in a protein crystal: the example of hen lysozyme. **Biochim. Biophys. Acta.** 36: 222-227.

Broide, M.L., Tominc, T.M., and Saxowsky, M.D., (1996). Using phase transitions to investigate the effect of salts on protein interactions. **Phys. Rev**. 53: 6325-6335.

Cacioppo, E., and Pusey, M.L. (1991). The solubility of the tetragonal form of hen egg white lysozyme from pH 4.0 to 5.4. **J. Cryst. Growth** 114: 286-292.

Cacioppo, E., Munson, S., and Pusey, M.L. (1991). Protein solubilities determined by a rapid technique and modification of that technique to a micro-method. **J. Cryst. Growth** 110: 66-71.

Collins K.D., and Washabaugh M.W., (1985). The Hofmeister effect and the behaviour of water at interfaces. **Q. Rev. Biophys.** 18: 323-422.

Curtis, R.A., and Lue, L. (2006). A molecular approach to bioseparations: Protein–protein and protein–salt interactions. **Chem. Eng. Sci.** 61(3): 907-923.

Czok, R., and Bucher, T. (1960). Crystallized enzymes from the myogen of rabbit skeletal muscle. **Adv. Protein Chem**. 15: 337.

Dawson, R.M.C., Elliot, D.C., Elliot, W.H., and Jones, K.M. (1986). **Data for Biochemical Research** (3rd ed.). Oxford: Science Publication.

Diaz Borbon, V., and Ulrich, J. (2012). Solvent freeze out crystallization of lysozyme from a lysozyme-ovalbumin mixture. **Cryst. Res. Technol**. 47(5): 541-547.

Ducruix A., and Giege R., (1992). **Crystallization of Nucleic Acids and Protein: A Practical Approach**. New York: Oxford University Press.

Elgersma, A.V., Ataka, M., and Katsura, T. (1992). Kinetic studies on the growth of three crystal forms of lysozyme based on the measurement of protein and Cl^{-} concentration changes. **J. Cryst. Growth** 122(1-4): 31-40.

Ewing, F., Forsythe, E., and Pusey, M.L. (1994). Orthorhombic Lysozyme Solubility. **Acta Cryst.** D50: 424-428.

Flood, A.E. (2009). **Industrial crystallization from solution: A primer**. Thailand: Suranaree University of Technology.

Forsythe E.L., and Pusey M.L. (1996). Tetragonal chicken egg white lysozyme solubility in sodium chloride solutions. **J. Cryst. Growth** 168: 112-117.

Forsythe E.L., Judge R.A., and Pusey M.L. (1999). Tetragonal chicken egg white lysozyme solubility in sodium chloride solutions. **J. Chem. Eng. Data.** 44: 637-640.

Haas C., Drenth J., and Wilson W.W., (1999). Distribution of the second virial coefficients of globular proteins**. J. Phys. Chem.** 103: 2808-2811.

Howard, S.B., Twigg, P.J., Baird, J.K., and Meehan, E.J. (1988). The solubility of hen egg-white lysozume. **J. Cryst. Growth** 90: 94-104.

Ildefonso, M., Revalor, E., Punniama, P., Salmon, J.B., Candoni, N., and Veesler, S. (2012). Nucleation and polymorphism explored via an easy-to-use microfluidic tool. **J. Cryst. Growth** 342: 9-12.

Jolles, P., and Berthou, J. (1972). High temperature crystallization of lysozyme: an example of phase transition. **FEBS Lett.** 23(1): 21-23.

Judge R.A., Forsythe E.L., and Pusey M.L., (1998). The Effect of Protein Impurities on Lysozyme Crystal Growth. **Biotechnol. Bioeng.** 59(6): 776-785.

Judge R.A., Johns M.R., and White E.T., (1996). Solubility of ovalbumin in ammonium sulfate solutions, **J. Chem. Eng. Data.** 41: 422-424.

Liu, Y., Wang, X., and Ching, C.B. (2010) Toward Further Understanding of Lysozyme Crystallization: Phase Diagram, Protein-Protein Interaction, Nucleation Kinetics, and Growth Kinetics. **Cryst. Growth. Des.** 10: 548-558.

Lu J., Wang X.J., and Ching C.B., (2002). Batch crystallization of soluble proteins: effect of precipitant, temperature, and additive. **Prog. Crystal Growth and Charact.** 45: 201-217

Mullin, J.W. (2001). **Crystallization** (4th ed.). Oxford: Butterworth-Heinemann.

Muschol, M., and Rosenberger F. (1997). Liquid–liquid phase separation in supersaturated lysozyme solutions and associated precipitate formation/crystallization. **J. Chem. Phys.** 107(6): 1953-1962.

Pusey, M.L., and Gernert, K. (1988). A method for rapid liquid-solid phase solubility measurements using the protein lysozyme. **J. Cryst. Growth** 88: 419-424.

Pusey, M.L., and Munson S. (1991). Micro-apparatus for rapid determinations of protein solubilities. **J. Cryst. Growth** 113: 385-389.

Retailleau, P., Ries-Kautt, M., and Ducruix, A. (1997). No salting-in of lysozyme chloride observed at low ionic strength over a Large range of pH. **Biophys. J.** 73: 2156-2163.

Ries-Kautt, M.M., and Ducruix, A.F. (1989). Relative Effectiveness of Various Ions on the Solubility and Crystal Growth of Lysozyme. **J. Biol. Chem.** 264(2): 745-748.

Sorensen S.P.L., and Hoyrup M., (1915-17). Studies on proteins, **Comt. Rend. Lab. Carlberg.** 12: 12-67.

Spiegel, M.R., Lipschutz, S., and Liu, J. (2009). **Mathematical Handbook of Formulas and Tables** (3rd ed.). New York: McGraw-Hill.

Tanford, C., and Roxby, R. (1972). Interpretation of protein titration curves: Application to lysozyme. **Biochem.** 11: 2192-2198.

Thomas B.R., Vekilov P.G., and Rosenberger F., (1996). Heterogeneity determination and purification of commercial hen egg-white lysozyme. **Acta Cryst.** D52: 785-798.

Tung, H.H., Paul, E.L., Midler, M., and McCauley J.A., (2009). **Crystallization of Organic Compounds: An Industrial Prespective.** New Jersey: John Wiley & Sons, Inc.

Benesch, R.E., Benesch, R., and Yung, S. (1973). Equations for the Spectrophotometric Analysis of Hemoglobin Mixtures. **Anal. Biochem.** 55: 245-248.
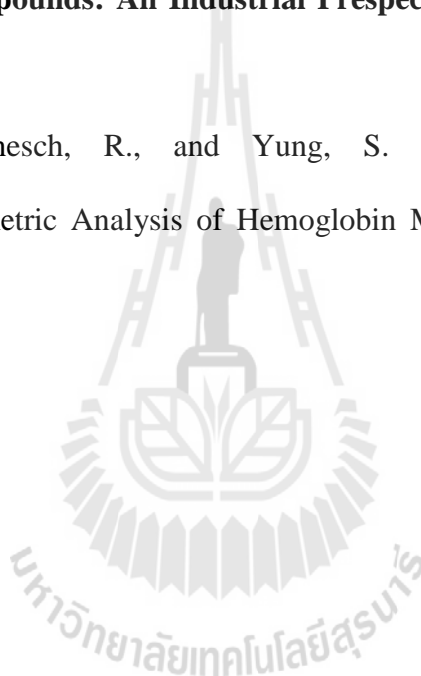
CHAPTER III

INTRODUCING A FAST METHOD TO DETERMINE
THE SOLUBILITY AND METASTABLE ZONE WIDTH
FOR PROTEIN: CASE STUDY LYSOZYME

3.1 Abstract

The phase diagrams of tetragonal hen egg white lysozyme containing besides thermodynamic (solubility) also kinetic (nucleation) data were determined for pH values of 4.4, 5.0 and 6.0, 3 to 7 wt% sodium chloride concentrations and lysozyme concentrations from 5 to 70 mg/mL by the use of a turbidity technique. This new technique offers a rapid, precise and reliable determination of nucleation and solubility points. These points can be obtained simultaneously within 6 h. The errors of measurements are less than $\pm$ 0.9°C for the solubility temperature and less than $\pm$ 1.0°C for the nucleation temperature. The solubility data obtained could be extended and described by a good correlation with literature data. The solubility of lysozyme was found to decrease with increasing salt concentration while the nucleation points were observed more early with respect to salt addition; as a consequence the metastable zone is more narrow. The solubility of lysozyme is slightly reduced at higher values of the pH, and the nucleation point is observed later in time. The result is an increase of the metastable zone width.

3.2   Introduction

Knowledge of the phase diagram has key importance when designing and controlling a crystallization process for a substance. In the case of proteins, accurate phase diagram data is limited due to the complexity of their structure caused by the diversity of the amino acid residue groups that form proteins, with this process being easily influenced by environmental conditions. Natural proteins contain 20 standard amino acids (Rosenberger, 1996). A significant characteristic for the biological function as well as for the crystallization of proteins is that the residues consist of polar functional groups and nonpolar functional groups. The polar groups prefer to associate with water. In contrast to these hydrophilic groups, the nonpolar hydrophobic groups prefer to associate with themselves. The hydrophilic groups result in proteins having finite water solubility despite being very large molecules. The solubility of a protein depends strongly on the protein-protein interactions as well as on the protein-solvent interactions (Curtis and Lue, 2006). Any slight modification of the composition can influence the solubility dramatically, or even alter the nature of these macromolecules. Independently of the complexity of protein behavior, the phase transformation is still governed by both the thermodynamics and the kinetics of the system. It is still possible to describe all this information in phase diagrams. In the case that crystallization conditions or nucleation points are identified the information can be plotted in phase diagrams, and in this case the information that is provided relates to both thermodynamics and kinetics.

There is a well studied protein from which a large set of reported data on solubility and crystallization conditions is available: hen egg white lysozyme (HEWL). This protein is composed of 129 amino acids and it has molecular weight of

14.3 kDa (Blake, Koenig, Mair, North, Phillips, and Sarma, 1965; Canfield, 1963; Jolles, 1969). It is a basic protein with an approximate isoelectric point value of 11.3 and belongs to the group of globular proteins (Wetter and Deutsch, 1951). HEWL has often been used in thermodynamic and kinetic crystallization studies (Apgar, 2008; Ataka and Asai, 1988; Berthou and Jolies, 1974; Borbon and Ulrich, 2012; Cacioppo, Munson, and Pusey, 1991; Cacioppo, and Pusey, 1991; Curtis, and Lue, 2006; Elgersma, Ataka, and Katsura, 1992; Ewing, Forsythe, and Pusey, 1994; Forsythe, Judge, and Pusey, 1999; Howard, Twigg, Baird, and Meehan, 1988; Ildefonso, Revalor, Punniama, Salmon, Candoni, and Veesler, 2012; Jollbs and Berthou, 1972; Liu, Wang, and Ching, 2010; Muschol and Rosenberger, 1997; Pusey and Gernert, 1988; Ries-Kautt and Ducruix, 1989; Retailleau, Ries-Kautt, and Ducruix, 1997). In order to control the isothermal batch crystallization within specific conditions the phase diagram of HEWL is required. Even though it is one of the most studied proteins, phase diagrams which contain solubility and nucleation curves (which is kinetic information rather than thermodynamic) for pH 4.4, 5.0 and 6.0, with NaCl from 3 to 7 wt% and with a temperature range of 2 to 45°C are not available. However, for instance, the solubility of HEWL at pH 4.4 and 5 and temperatures between 2 and 25°C have been reported (Cacioppo, Munson, and Pusey, 1991; Cacioppo, and Pusey, 1991; Forsythe, Judge, and Pusey, 1999), but for higher temperatures there is no data. This has been the impulse which brought the present work to be conducted. It is necessary to complete these solubility curves up to the operating temperatures of the desired batch crystallization process or any other further interest, as well as the nucleation points for the whole range of conditions in order to control the crystallization process.

Several methods have been used to measure the solubility of proteins, such as the well known classical dissolution and crystallization methods (Ataka and Asai, 1988; Howard, Twigg, Baird, and Meehan, 1988; Retailleau, Ries-Kautt, and Ducruix, 1997). These methods have the disadvantage of requiring long times due to the slow diffusivity of proteins in the solution and also resulting in very imprecise measurements. The measured solubility points by these methods might have a concentration higher or lower than the equilibrium concentration. One good alternative for measuring the solubility of proteins is the use of a miniature column technique (Cacioppo, Munson, and Pusey, 1991; Pusey and Gernert, 1988). This technique is known as a rapid determination technique with high reliability (the solubility data can be obtain within 24 h with an error less than ± 1 mg/mL, (Forsythe, Judge, and Pusey, 1999)) and requires only a small amount of material. Therefore the use of this method allows a larger number of experiments in the same amount of materials, and thus a better data set. However, it is not possible to carry out more than one experiment at once time. In order to measure the nucleation point, some methods such as microtitter plates or micofluidic tools are used (Ildefonso, Revalor, Punniama, Salmon, Candoni, and Veesler, 2012). Both crystallizations require only a small volume of solution. However, these methods have precision limitations because they are based on optical observations.

Here the turbidity measurement method for detection of the nucleation and solubility points of proteins is introduced using lysozyme as a model substance. The principle of this method consists of the application of an IR signal through a protein solution, and the detection of changes in the signal produced by changes in the mixture caused by thermal changes. This signal has 100% transmission when the

solution is clear. If the solution is cooled down and the nucleation temperature is reached, the transmission decreases due to the scattering of the signal by particles formed within the solution (protein nuclei). It is assumed that this corresponds to the formation of the protein crystals which may nucleate within the drops rich with protein. Images of the solution were acquired to ensure the formation of the crystal. The protein nuclei grow further during the cooling process, up to crystals with significant size. It is therefore possible to increase the temperature of the solution and induce the dissolution of the crystals until the equilibrium is reached. At this point the formed particles are totally dissolved and the transmission of the IR signal is again 100%. This temperature corresponds to the solubility point. The method offers furthermore the possibility to measure the nucleation and solubility points simultaneously in one experiment, and it is possible to carry out up to 10 experiments simultaneously. The required solution volume is only 1 mL and the duration for one cycle (nucleation and solubility measurement) is just 6 hr.

In the present work the phase diagrams are reported for lysozyme, and contain the thermodynamic data (solubility, either obtained from literature or self measured) and the kinetic data (nucleation points) for pH values of 4.4, 5.0 and 6.0, 3-7 wt% sodium chloride concentrations and lysozyme concentrations from 5 to 70 mg/mL. In the operation of a crystallization process the kinetic data are vital to observe the change in the crystallizing system over time, and are equally important as the thermodynamic data which are used to observe the behavior of the system at equilibrium. Therefore, the positioning of these data together in the phase diagram is very useful. For example, in the solvent freeze out crystallization process of lysozyme (Borbon and Ulrich, 2012) the particle size or size distribution of the crystals can be

controlled by changing the process conditions from the nucleating region to the middle of the metastable region, which is only possible if the phase diagram is known. In an isothermal crystallization the supersaturation value has a strong effect on the growth rate and the habit of the growing protein crystals (Elgersma, Ataka, and Katsura, 1992; Liu, Wang, and Ching, 2010). Therefore, the operation time, size and quality of the crystals can be directly controlled by the supersaturation value.

Furthermore, the metastable zone widths (MZW) are presented and offer the opportunity to be used to control isothermal or cooling crystallization processes.

3.3 Theory

It has been said that "crystallization from solution is usually the result of two processes; crystal nucleation and crystal growth. These two processes can proceed either consecutively (in series) or simultaneously (in parallel) throughout the whole, or during only part, of the crystallization period depending on supersaturation levels" (Mullin, 2001).

In this section the primary focus is on the theory of supersaturation, nucleation, and the metastable zone. Other important terms of crystallization from solution are described in other Chapters.

3.3.1 Supersaturation

Crystallization from solution occurs when supersaturation is generated. Supersaturation occurs when the solute concentration in a solution exceeds its solubility (Randolph and Larson, 1988). The state of supersaturation is an essential requirement for all crystallization operations.

The most common expressions of supersaturation are the concentration driving force, the supersaturation ratio, and the relative supersaturation as shown in following equations

$$\Delta c = c - c^{*} \tag{3.1}$$

$$S = \frac{c}{c^{*}} \tag{3.2}$$

$$\sigma = \frac{\Delta c}{c^{*}} = S - 1 \tag{3.3}$$

Where Δc is the concentration driving force, S is the supersaturation ratio, σ is the relative supersaturation, c is the solution concentration, and c^{*} is the equilibrium concentration at given temperature.

3.3.2 Nucleation

Nucleation involves the process of formation of new crystals in a liquid solution. Nucleation is classified into primary and secondary nucleation. Primary nucleation is the birth of new crystals from a liquid or solution that contains no solute crystal, and is divided into homogeneous primary nucleation and heterogeneous primary nucleation. In homogeneous primary nucleation the nuclei are formed without the external nucleation sites available (as could be caused by the walls of the vessel, dust particles, crystals or solids of other solutes, etc.). Heterogeneous primary nucleation occurs when the presence of such foreign surfaces assists in obtaining primary nuclei. Secondary nucleation is the formation of new nuclei which occurs due to the presence of crystals of the crystallizing material.

3.3.3 Metastable Zone

Crystals can grow without significant nucleation in a metastable zone which is often exhibited by supersaturated solutions. Nucleation is typically avoided or minimized in crystallization processes because it is difficult to control and gives a bad product size distribution. In batch crystallization processes the operation is usually undertaken in the metastable zone and crystallization is initiated through the addition of seed crystals, thus avoiding large amounts of nucleation. However, when the supersaturation is sufficiently high, secondary nucleation in the presence of prior crystals can occur. The limit of this supersaturation is referred to as the metastable limit for secondary nucleation or the secondary nucleation threshold (SNT). When the supersaturation is higher than the limit, the heterogeneous primary nucleation and homogeneous primary nucleation can occur, respectively as shown in Figure 3.1. The limits of supersaturation for each progressive nucleation are referred to as the metastable limit of nucleation for the particular mechanism.
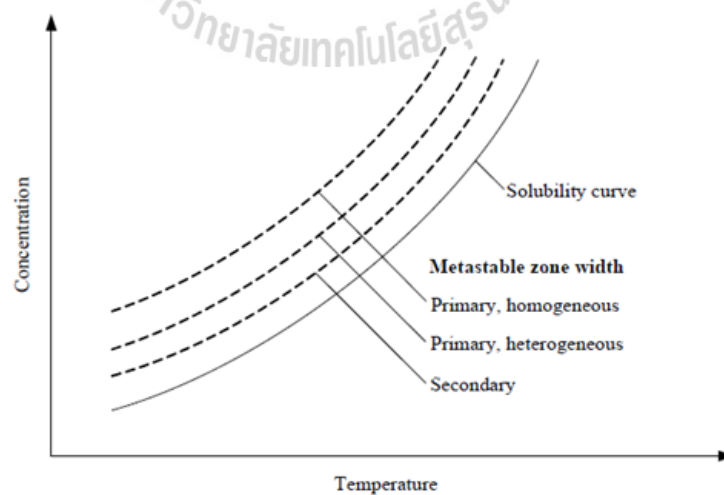
Figure 3.1 Metastable zone widths for different nucleation mechanisms

(adapted from Mersmann, 2001).

3.4   Materials and Methods

Hen egg white lysozyme (HEWL) (product No. 62971, Fluka) was used without further purification since no other proteins were detected in a SDS-PAGE gel electrophoresis analysis (15% acrylamide). Sodium chloride, NaCl ($\geq$99.5%, Carl Roth) was used as a crystallizing agent. 0.1 M sodium acetate buffer stock solutions were prepared with sodium acetate trihydrate ($\geq$99.5%, Carl Roth) and acetic acid (100%, Carl Roth) based on the method of Dawson et al. (1986). 100 mg/mL lysozyme stock solution was prepared by dissolving 2 g of lysozyme into enough 0.1 M sodium acetate buffer to obtain a final volume of 20 mL at the desired pH. After dissolution (approximately 3 hours), the solution was centrifuged at 9000 rpm for 15 min by the use of a 2-16K centrifuge (Sigma, Germany) in order to remove any undissolved particles that cannot be observed by the naked eye. There was no significant amount of protein removed by the centrifuge since the lysozyme concentration after centrifuge was 99.87 $\pm$ 0.21 mg/mL (using the UV absorbance technique, see section 2.2). The solution was then kept at 4-8°C in a refrigerator. A 0.2 g/mL salt stock solution was prepared by dissolving 4 g of NaCl into enough 0.1 M sodium acetate buffer to obtain a final volume of 20 mL at the desired pH. Solutions with pH of 4.4, 5.0, and 6.0, salt concentrations of 3, 4, 5, and 7 wt%, and with 5 to 70 mg/mL of lysozyme were prepared by appropriate mixing of the stock solutions (0.1 M sodium acetate buffer, lysozyme stock solution, and salt stock solution).

3.4.1 Measurements of Nucleation and Solubility Points via the Turbidity Method

The temperatures of nucleation and solubility points were measured by the detection of turbidity changes in the solutions through temperature variations. All experiments were performed in a STEM Integrity 10 system (Electro Thermal, England) depicted in Figure 3.2. This device can run up to 10 experiments (one experiment per cell of the STEM Integrity 10 reaction station) at the same time with independent control of temperature and stirring speed. The operating ranges of the device are stirring speed from 250 to 1200 rpm, temperature from -30 to 150°C and maximum cooling and heating rates of 5°C/min.
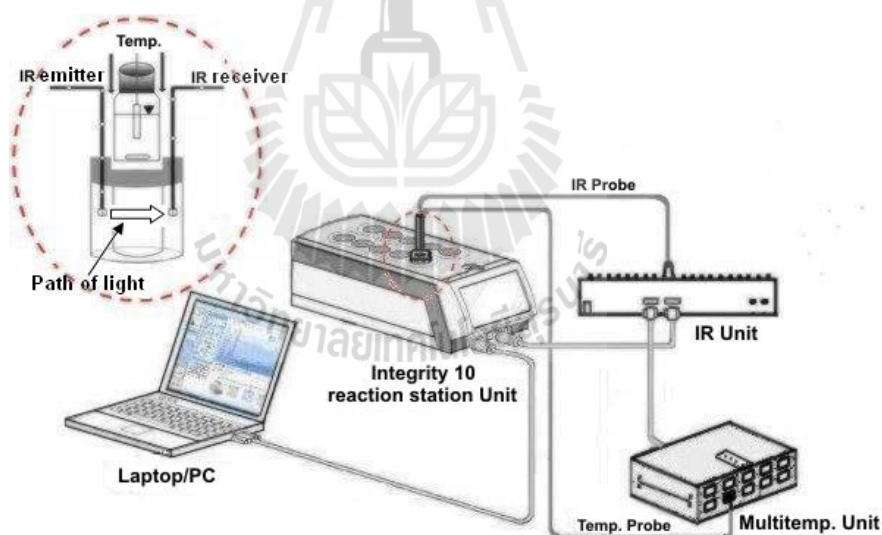
Figure 3.2 STEM Integrity 10 system (Electro Thermal).

To start the experiment a 1.5 mL glass bottle containing 1 mL of lysozyme solution (with known concentration) was inserted in an IR probe (part code ATS10360) which was placed in a cell of a STEM Integrity 10 reaction station. This IR probe was

designed as a miniature transmission probe for operation in the wavelength range of 920 to 960 nm and with a light pathway of 8 mm. The light was passed through the solution from the IR emitter channel to the IR receiver channel. The temperature sensor was immersed into the solution through the cap of the glass bottle. The solution was stirred at 350 rpm while it was cooled or heated. The STEM Integrity 10 reaction station is controlled by the STEM Integrity 10 software. The real time turbidity (the ratio of the light intensity before and after passing through the solution) and temperature of the solutions are collected by connecting the IR probe to the Multi-IR box (part code ATS10232) and the temperature sensor to the Multi-Temp 10 Module (part code ATS10001). Both IR Unit and Multi-Temp 10 Module were connected to the computer through the STEM Integrity 10 reaction station block.

To determine the nucleation point, the temperature of the determined solution is increased to 35, 40, 45 or 50°C (depending on pH, lysozyme concentration and salt concentration) and kept constant for 10 minutes. Then, the temperature is decreased to the set temperature of 0, 5, 10, or 15°C (depend on the nucleation point) and kept constant again at this set temperature for 10 minutes. Two cooling rates are applied to the system: 1.0 K/min and 0.1 K/min. The faster cooling rate is applied when the temperature of the solution is far from the set temperature and the slower cooling rate when the temperature of the system approaches it. The changing point of the cooling rate is approximately 5°C higher than the nucleation point. This is an approximation of the researcher based on preliminary experiments. The MZW changes with respect to a slower cooling rate. The example of a temperature profile for the experiment with lysozyme concentration of 25 mg/mL, 4 wt% NaCl and pH 4.4 is given in Figure 3.3 (left). The solution was heated up to 40°C for 10 minutes.

Then the temperature was decreased to 20°C within 20 minutes (cooling rate = 1 K/min). After that the solution was cooled again to 5°C within 150 minutes and kept at constant temperature at this point for 10 minutes. The nucleation point is defined as the first point at which a distinct drop in transmission is measured while the temperature is decreasing. A VHX-500F microscope (Keyence, Germany) was used to analyze the morphology of the nucleated crystals.

To determine the solubility point, after the cooling process and the formation of the crystals the solution is heated up to a set temperature (the same point as the start of the cooling process). The temperature profile was also divided into 2 steps, as in the cooling process (using a heating rate of 1.0 K/min when the temperature is far from the set point and 0.1 K/min when the temperature is near to the set point). The solubility point is defined as the point at which the transmission reaches a stable plateau while the temperature is increasing. The plot of transmission against temperature gives clear information on nucleation and solubility points (see Figure 3.3, right).
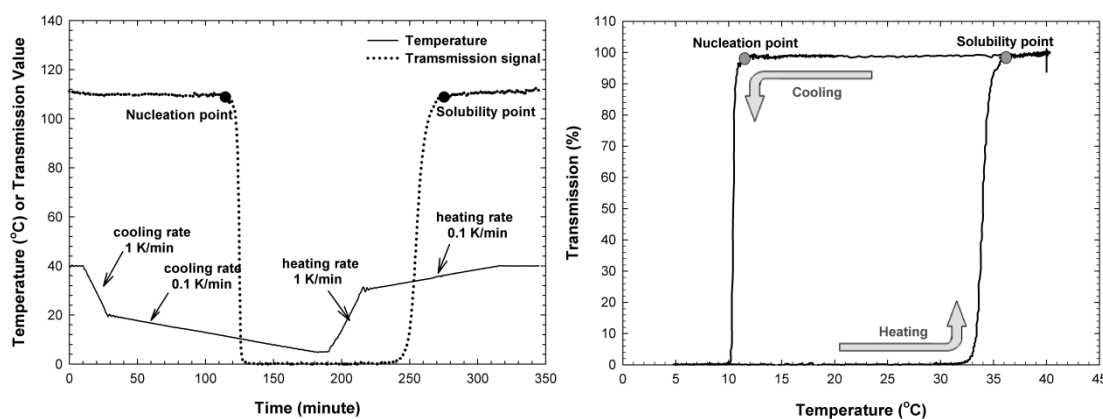
Figure 3.3 <u>Left</u>: Temperature profile. <u>Right</u>: Change in turbidity of a lysozyme solution with temperature. $C_{lys} = 25$ mg/mL, 4 wt% NaCl and pH 4.4.

3.4.2 Solubility measurement by the miniature column technique (low temperature, pH 6.0)

Tetragonal lysozyme crystals were prepared by mixing equal volumes of 100 mg/mL lysozyme solution and 8 wt% sodium chloride solution and keeping the mixture at 4-8°C overnight. The solubility of tetragonal lysozyme crystals at pH 6.0 was measured at 5, 10, 15, 20, and 25°C with sodium chloride concentration of 3, 4, and 5 wt% using the miniature column technique as described by Cacioppo, Munson, and Pusey (1991) and Pusey and Gernert (1988). The temperature of the column was maintained within ± 0.1°C using a thermostat (F12 ED, Julabo).

The concentrations of dissolved lysozyme were measured using a UV photometer (Carry 50, Varian) at 280 nm. An extinction coefficient of 2.4321 mL· $mg^{-1} \cdot cm^{-1}$ was used (obtained from a calibration curve of 9 measurements).

3.5 Results and Discussion

3.5.1 Phase Diagrams

The measured nucleation (kinetic) and solubility (thermodynamic) points for the lysozyme systems were plotted in phase diagrams. Each data point is the average of three replicate experiments (the samples used in each replicate experiment were fresh prepared from the stock solution). The nucleation points are corresponding to a cooling rate of 0.1 K/min since this cooling rate was applied to the system at least 5°C higher than the nucleation point.

The preliminary experiments showed that there is no effect of a cooling rate of 1 K/min on the MZW if the cooling rate was changed to 0.1 K/min at a point at least 5°C higher than the nucleation. We compared the result from this experiment to

the result of an experiment at a constant cooling rate equal to 0.1 K/min and obtained

the same nucleation temperature to within ±1.0 K.

Figure 3.4 Change in turbidity of a lysozyme solution with temperature. Different

cooling rates (0.1, 0.2, 0.3, and 0.4 K/min) were applied in the second

step of the cooling process. Lysozyme concentration 40 mg/mL, 4 wt%

NaCl and pH 4.4.

In Figure 3.4 the applied cooling rates in the second step of the cooling

process were 0.1, 0.2, 0.3 and 0.4 K/min. The detected nucleation and the solubility

temperatures are nearly the same (an error of less than 1°C is observed). In some

conditions the induction time is expected to be very long because the nucleation is

very difficult at high pH. This result shows that it is also possible to increase the

second cooling rate up to 0.4 K/min and still obtain results consistent with 0.1 K/min

cooling rate.

The maximum error (the difference between the measured value and the average value) of the measurement is $\pm$ 0.9°C for the solubility temperature and $\pm$ 1.0°C for the nucleation temperature. The phase diagrams of lysozyme for different sodium chloride concentrations at pH 4.4, 5.0 and 6.0 are shown in Figures 3.5, 3.6 and 3.7, respectively. The solubility data obtained from the turbidity measurements for pH values of 4.4 and 5.0 were plotted with the solubility data from the literature (Forsythe, Judge, and Pusey, 1999). The solubility for systems at pH 6.0 and low temperatures was measured as described in the previous section (3.4.2). There are no literature data for these conditions to be found. The reliability of the measurements was shown by a good correlation of the solubility data (solid line) with an exponential growth ($R^2 \geq 0.99$). The literature solubility data (Forsythe, Judge, and Pusey, 1999) which was obtained by the use of the miniature column technique has been compared with the solubility data of Apgar, (2008) (who determined the solubility of lysozyme crystals by observation of the rate of change of scattering intensity of the sample) and it was found to be in good agreement. Therefore, the solubility data measured in this work is consistent with the experimental results of Apgar. The solubility is a thermodynamic property of a substance, and the Van't Hoff equation can be used to describe the changes in solubility with temperature. The exponential growth equation can be linearized into the Van't Hoff equation. Therefore the solubility data can be represented with a curve of exponential type. A second order polynomial was used to fit the onset of the nucleation data, which are indicated as dotted lines in the phase diagrams.
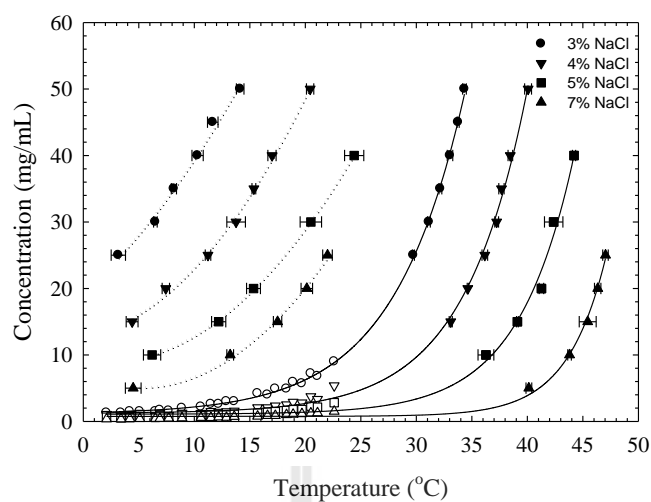
Figure 3.5 Phase diagram of HEWL for pH 4.4, open symbols are solubility data
from literature (Forsythe, Judge, and Pusey, 1999). The dashed lines
represent the fitted nucleation data. The solid lines represent the fitted
solubility data.
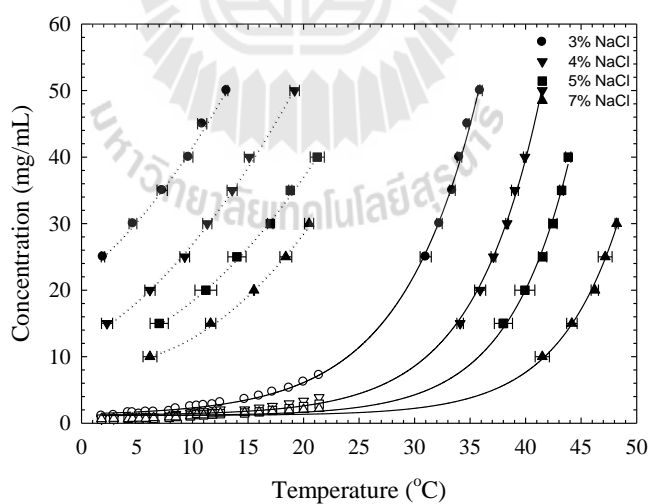
Figure 3.6 Phase diagram of HEWL for pH 5.0, open symbols are the solubility
datafrom literature (Forsythe, Judge, and Pusey, 1999). The dash lines
represent the fitted nucleation data. The solid lines represent the fitted
solubility data.
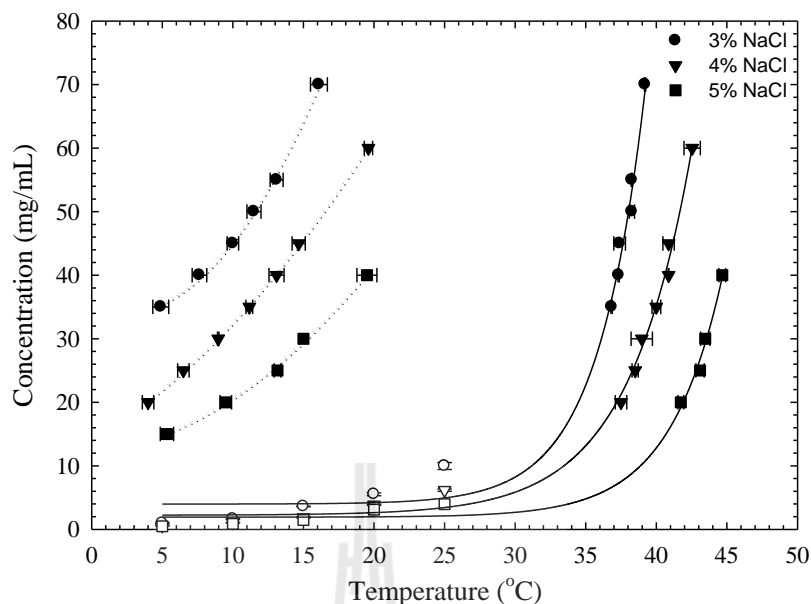
Figure 3.7 Phase diagram of HEWL for pH 6.0, open symbols are the solubility data

obtained by the use of a miniature column technique. The dash lines

represent the fitted nucleation data. The solid lines represent the fitted

solubility data.

To verify the morphology of the crystals formed during the cooling

step (nucleation), the crystals were observed under a microscope. In Figure 3.8 (a),

small crystals obtained shortly after the end of the cooling process are shown as an

example. The size of the crystals is less than 10 μm and it was difficult to identify

their morphology. Therefore, a sample of those crystals has been kept for three days at

4-8°C in order to let them grow. In Figure 3.8 (b), crystals with sizes around 100 μm

are shown. Due to the larger size of the crystals, the tetragonal shape is easily

recognized for this example as well as for almost all the crystals analysed in the

measurement of the nucleation points. However, for 7 wt% of NaCl and 40 mg/mL of

lyosozyme at pH 5.0, the crystals show an orthorhombic shape (see Figure 3.8 (c)).
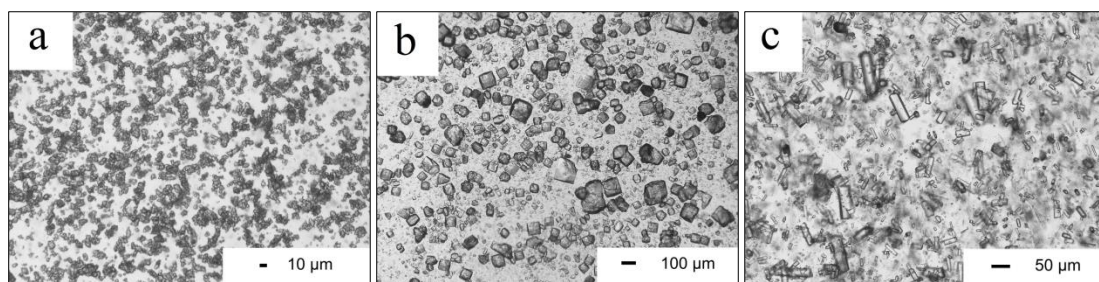
Figure 3.8 Lysozyme crystals (30 mg/mL, pH 5.0, 4 wt% NaCl): a) after end of

cooling process, b) after three days growth at 4°C. Lysozyme crystals

(40 mg/mL, pH 5.0, 7 wt% NaCl): c) after three days growth at 4°C.

In the phase diagrams (Figures. 3.5, 3.6, and 3.7) it can be observed that there is a concurrent shift in nucleation and solubility points with salt concentration. This phenomenon was also observed and reported by other authors (Cacioppo and Pusey, 1991; Muschol and Rosenberger, 1997; Ries-Kautt, and Ducruix, 1989). Therefore, with increasing salt concentration the nucleation temperature approaches to 25°C, the temperature at which there is a phase transformation from the tetragonal lysozyme crystals form into the orthorhombic form (Berthou and Jolies, 1974; Ewing, Forsythe, and Pusey, 1994; Jollbs and Berthou, 1972). This explains the formation of the orthorhombic crystals at higher concentrations of lysozyme for 7 wt% of NaCl at pH 5.0 (Figure 3.8 (c)).

As it can be observed in Figure 3.7 (pH 6.0), experimental data for 7 wt% sodium chloride are missing. Well shaped tetragonal crystals were not obtained after the end of the cooling process for these conditions. The formation of particles in the solution took place after the end of the cooling process, but once the temperature of the system was increased (the heating process) the particles were immediately

dissolved. In this case it was not possible to further analyze the particles by microscopy to determine which morphology they presented. The measured solubility and nucleation values are not reliable, and are therefore not reported for these conditions. The possible explanation of this phenomenon is the occurrence of liquid − liquid phase separation (LLPS) without nucleation of protein crystals. In general LLPS occurs at a very high supersaturation and can occasionally be observed by changing the solution condition (Asherie, 2004). When LLPS occurred liquid drops were formed containing a high concentration of protein. These drops may separate from the rest of the solution, which now contains a lower concentration of protein. The many small drops can scatter light, resulting in a drop in the transmission of light detected by the device, similar to the nucleation of a crystal. However, when the solution was heated up the solution immediately become clear liquid because LLPS is inherently a metastable transition in protein solution (Asherie, Lomakin, and Benedek, 1996). In this case it is considered that the LLPS occurred without the nucleation of protein crystals taking place within the protein-rich droplets.

At pH 6.0 it is barely possible to crystallize lysozyme in tetragonal shape from sodium acetate solutions. This behavior was also reported by Alderton and Fevold (1946). They observed a copious crystallization at pH 3.5, moderate at pH 4.8 and very slight at pH 5.8, by using 5 wt% sodium chloride and an initial lysozyme concentration of 40 mg/mL. It indicates that the crystallization of HEWL in the tetragonal form is less probable at high pH values and high salt concentrations (>5 wt%).

In all cases the nucleation point is reached more early with increasing salt concentration. The solubility decreases with increasing salt concentration. This is

due to the salting out effect, therefore, the crystallization is easier to perform (Ries-Kautt and Ducruix, 1989). The solution pH also has an influence on the nucleation point of lysozyme crystals as shown in the phase diagrams. The nucleation temperature and concentration decreases with increasing pH as can be observed if Figures 3.5, 3.6 and 3.7 are compared. The pH has a stronger effect on the nucleation points than on the solubility. The solubility slightly decreases with increasing pH due to the low ionic strength (Cacioppo and Pusey, 1991), a behavior that was also observed by Ataka and Tanaka, (1986).

The phase diagrams shown in Figures 3.5 and 3.6 as well as in Figure 3.7 supply information for a study of the behavior of the process when the experimental conditions change with respect to time. The location of the nucleation line indicates the border of the nucleation region and the upper limit of the metastable region. In the metastable region the nucleated crystals can grow without the formation of new crystals. In protein crystallization, the growth of a protein crystal to a suitable size for structural determination is still difficulty. The presence of the nucleation line in the phase diagram helps to know how to change the solution conditions to allow the crystals grow after they have been nucleated.

3.5.2 Metastable Zone Width (MZW)

Nucleation, one of the two phenomena in crystallization, gives one boundary of the metastable zone; the zone width is therefore strongly kinetically influenced. The information on the metastable zone is limited by the precision of the method to detect the presence of particles with determined size. There are no fluctuations of the turbidity signal during the cooling process. It is assumed that this corresponds to the formation of the protein crystals which probably nucleate within

the drops rich with protein. These nuclei probably have an inherent growth and this nucleation point should carry the inherent uncertainly of the exact nucleation point. Nevertheless, it is consider a good estimation of the nucleation point for phase diagrams that will be used as guide in crystallization.

The width of the metastable zone is determined as the distance between the solubility and the corresponding nucleation points. The MZW are shown in the phase diagrams for the evaluated pH values and sodium chloride concentrations in Figure 3.9. Depending on the arrangements of the axis, the width can be expressed, for example, with respect to temperature for 40 mg/mL of lysozyme (Figure 3.9, left) or concentration at 5°C (Figure 3.9, right).
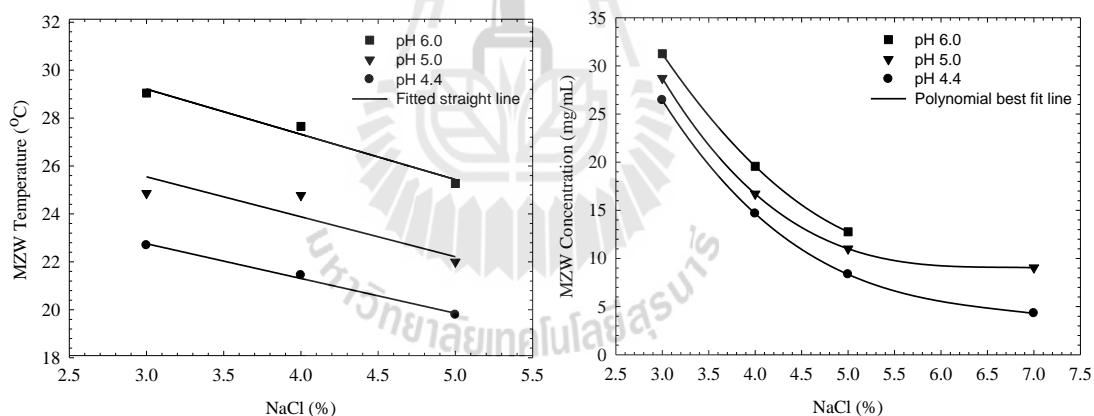
Figure 3.9 Left: Influence of NaCl concentration and solution pH on the MZW with respect to temperature level. Lysozyme concentration: 40 mg/mL. Right: Influence of NaCl concentration and solution pH on the MZW with respect to protein concentration at 5°C.

In Figure 3.9 it can be observed that the increasing of salt concentration causes the narrowing of the MZW. This phenomenon can be described by linking protein – protein interaction with the classical nucleation theory (Liu, Wang, and Ching, 2010). Increasing salt concentration can reduce the energy barrier of the diffusion of protein molecules from the bulk solution to the cluster (more ions represent less protein – solvent interaction). Therefore, the strength of protein – protein interaction is increased with increasing salt concentration. The increasing of pH value causes an increase in the width of the MZW. One explanation of this is that lysozyme is a protein that consists of a number of side-chain groups that have pKa values close to or within the pH range of 4.0–5.2 (Kuramitsu and Hamaguchi, 1980). The titration of side chains at increment of pH value can form intermolecular interactions which may increase the interfacial tension (Mullin, 1993). Therefore, the nucleation rate may be reduced. This behavior of the metastable zone width is expected and is to be found for all the other conditions evaluated in section 3.5.1. The narrowing of the metastable zone with increasing salt concentration results from a shift of the nucleation curve together with a smaller shift of the solubility line. This has been previously observed and reported by other authors (Borbon and Ulrich, 2012; Liu, Wang, and Ching, 2010; Muschol and Rosenberger, 1997).

3.6   Conclusions

The concentration-temperature phase diagrams enriched by the kinetic data necessary to design crystallization processes are here determined for lysozyme as a function of sodium chloride concentration and solution pH, by the use of a turbidity measurement technique. This technique shows a rapid and reliable determination of

nucleation and solubility points. The use of this technique allows the collection of data of the metastable zone width within a few hours rather than days, and with a high precision compared to conventional methods (Ataka and Asai, 1988; Howard, Twigg, Baird, and Meehan, 1988; Retailleau, Ries-Kautt, and Ducruix, 1997). The presence of the kinetic data in the phase diagram offers the possibility to use this information for design and control crystallization process. To maintain the right modification, tetragonal rather than orthorhombic, was an aim. The width of the metastable zone of lysozyme in sodium acetate buffer depends on the solution conditions (in this study: initial protein concentration, salt concentration, and solution pH). The knowledge of the influence of these variables on the metastable zone width can be used to predict the phase diagram for another set of conditions. For example, using seeded isothermal batch crystallization at 5°C, pH 5.4, and 4 wt% NaCl the upper limit of MZW concentration would be approximately 18 mg/mL higher than the solubility (see Figure 3.9, right). Or using the cooling batch crystallization for the 40 mg/mL initial lysozyme concentration, pH 5.4, and 4 wt% NaCl the MZW temperature is approximately 25°C lower than the solubility temperature (see Figure 3.9, left).

3.7 References

Alderton, G., and Fevold, H.L. (1946). Direct crystallization of lysozyme from egg white and some crystalline salts of lysozyme. **J. Biol. Chem.** 146: 1-5.

Apgar, M.C. (2008). The Influence of pH on nucleation, solubility and structure of lysozyme protein crystals. Ph.D Thesis. **University of South Florida (USF).** Florida, USA.

Asherie, N. (2004). Protein crystallization and phase diagrams. **Methods** 34: 266-272.

Asherie, N., Lomakin, A., and Benedek, G.B. (1996). Phase diagram of colloidal solutions. **Phys. Rev. Lett.** 77(23): 4832-4835.

Ataka, M., and Asai, M. (1988). Systematic studies on the crystallization of lysozyme: Determination and use of phase diagrams. **J. Cryst. Growth** 90: 86-93.

Ataka, M., and Tanaka, S. (1986). The Growth of Large Single Crystals of Lysozyme. **Biopolymers** 25: 337-350.

Berthou, J., and Jolies, P.A. (1974). Phase transition in a protein crystal: the example of hen lysozyme. **Biochim. Biophys. Acta** 336: 222-227.

Blake, C.C.F., Koenig, D.F., Mair, G.A., North, A.C.T., Phillips, D.C., and Sarma, V.R. (1965). Structure of Hen Egg-White Lysozyme: A Three-dimensional Fourier Synthesis at 2 Å Resolution. **Nature** 206(4986): 757-761.

Borbon, V.D., and Ulrich, J. (2012). Solvent freeze out crystallization of lysozyme from a lysozyme-ovalbumin mixture. **Cryst. Res. Technol.** 47(5): 541-547.

Cacioppo, E., and Pusey, M.L. (1991). The solubility of the tetragonal form of hen egg white lysozyme from pH 4.0 to 5.4. **J. Cryst. Growth** 114: 286-292.

Cacioppo, E., Munson, S., and Pusey, M.L. (1991). Protein solubilities determined by a rapid technique and modification of that technique to a micro-method. **J. Cryst. Growth** 110: 66-71.

Canfield, R.E. (1963). The Amino Acid Sequence of Egg White Lysozyme. **J. Biol. Chem.** 238 (8): 2698-2707.

Curtis, R.A., and Lue, L. (2006). A molecular approach to bioseparations: Protein–protein and protein–salt interactions. **Chem. Eng. Sci.** 61(3): 907-923.

Dawson, R.M.C., Elliot, D.C., Elliot, W.H., and Jones, K.M. (1986). **Data for Biochemical Research** (3rd ed.). Oxford: Science Publication.

Elgersma, A.V., Ataka, M., and Katsura, T. (1992). Kinetic studies on the growth of three crystal forms of lysozyme based on the measurement of protein and Cl$^-$ concentration changes. **J. Cryst. Growth** 122(1-4): 31-40.

Ewing, F., Forsythe, E., and Pusey, M.L. (1994). Orthorhombic Lysozyme Solubility. **Acta Cryst.** D50: 424-428.

Forsythe, E.L., Judge, R.A., and Pusey, M.L. (1999). Tetragonal Chicken Egg White Lysozyme Solubility in Sodium Chloride Solutions. **J. Chem. Eng. Data** 44: 637-640.

Howard, S.B., Twigg, P.J., Baird, J.K., and Meehan, E.J. (1988). The solubility of hen egg-white lysozyme. **J. Cryst. Growth** 90: 94-104.

Ildefonso, M., Revalor, E., Punniama, P., Salmon, J.B., Candoni, N., and Veesler, S. (2012). Nucleation and polymorphism explored via an easy-to-use microfluidic tool. **J. Cryst. Growth** 342: 9-12.

Jollbs, P., and Berthou, J. (1972). Hight temperature crystallization of lysozyme: an example of phase transition. **FEBS Lett.** 23(1): 21-23.

Jolles, P. (1969). Lysozymes: A Chapter of Molecular Biology. **Angew. Chem. Int. Ed.** 8(4): 227-239.

Kuramitsu, S., and Hamaguchi, K. (1980). Analysis of the acid-base titration curve of hen lysozyme. **J. Biochem.** 87(4): 1215–1219.

Liu, Y., Wang, X., and Ching, C.B. (2010). Toward Further Understanding of Lysozyme Crystallization: Phase Diagram, Protein-Protein Interaction, Nucleation Kinetics, and Growth Kinetics. **Cryst. Growth Des.** 10: 548-558.

Mersmann, A. (2001). **Crystallization technology handbook** (2nd ed.). New York: Marcel Dekker, Inc.

Mullin, J.W. (1993). **Crystallization** (3rd ed.). Oxford: Butterworth-Heinemann.

Mullin, J.W. (2001). **Crystallization** (4th ed.). Oxford: Butterworth-Heinemann.

Muschol, M., and Rosenberger, F. (1997). Liquid–liquid phase separation in supersaturated lysozyme solutions and associated precipitate formation/crystallization. **J. Chem. Phys.** 107(6): 1953-1962.

Pusey, M.L., and Gernert, K. (1988). A method for rapid liquid-solid phase solubility measurements usinf the protein lysozyme. **J. Cryst. Growth** 88: 419-424.

Retailleau, P., Ries-Kautt, M., and Ducruix, A. (1997). No Salting-In of Lysozyme Chloride Observed at Low Ionic Strength over a Large Range of pH. **Biophys. J.** 73: 2156-2163.

Ries-Kautt, M.M., and Ducruix, A.F. (1989). Relative Effectiveness of Various Ions on the Solubility and Crystal Growth of Lysozyme. **J. Biol. Chem.** 264(2): 745-748.

Rosenberger, F. (1996). Protein crystallization. **J. Cryst. Growth** 166(1-4): 40-54.

Wetter, L.R., and Deutsch, H.F. (1951). Immunological studies on egg white proteins. IV Immunochemical and physical studies of lysozyme. **J. Biol. Chem.** 192: 237-242.

CHAPTER IV

BATCH CRYSTALLIZATION AND GROWTH

KINETICS OF PURE LYSOZYME

4.1   Abstract

The batch crystallization and growth kinetics of pure lysozyme were studied in 0.1 M sodium acetate buffer in order to give background to the studies involving crystallization from mixed protein solutions. The batch crystallization experiments were performed isothermally at 20°C in a 100 mL agitated crystallizer that was modified from a Schott bottle. The experimental conditions used are initial lysozyme concentration approximately 25 mg/mL, sodium chloride concentration of 4%, solution pH 5, and the solution volume of 50 ml. The mean seed crystal size was 8.0 μm (number-based) and 120 mg were used in each experiment. The product crystal yields (the ratio of weight of lysozyme crystallized on the total weight of lysozyme that can crystallize at equilibrium) were 84.68% and 49.67% using 25 hr and 6 hr operation time, respectively. The growth kinetics of the crystallization process has been studied based on the measurement of the decline in lysozyme concentration with time. The crystal growth rate at higher supersaturation is higher than subsequent crystal growth rate at lower. The growth rates of lysozyme were found to be second order with respect to the relative supersaturation. Therefore the growth kinetics of the crystallization process is controlled by the surface integration mechanism. The calculated growth rate constants value was 5.65×10^{-6} cm/hr which is in good agreement with previous work.

4.2 Introduction

Crystallization processes are one of the most important separation and purification processes in the pharmaceutical, chemical, and food industries. In protein crystallization studies the presented thermodynamic and kinetic data is limited due to the differences in the methods of measurement employed and the complexity of their structure caused by the diversity of the amino acid residue groups that form proteins. The process is easily influenced by environmental and experimental conditions.

As described in Chapter II and III, the determinations of solubility, metastable zone wide, and growth kinetics are important for designing, controlling, and characterization of a crystallization process for any substance. The solubility was studied in Chapter II and the metastable zone wide was studied in Chapter III. In this chapter the crystal growth kinetics were studied.

In the crystal growth rate study for general substances, there are two main groups of techniques that have been used to measure the crystal growth rate (Myerson and Ginde, 2002). The first group is the growth kinetics measurement based on individual crystal size. This first group includes studies in which growth rates of individual crystal faces of single growing crystals are measured microscopically or using atomic force microscopy (AFM) (Gougazeh, Omar, and Ulrich, 2009; Kitamura and Ishizu, 1998; Pantaraks and Flood, 2005). In protein crystallization, most of the kinetic studies belong in this group (Ataka and Tanaka, 1986; DeMattei and Feigelson, 1989; Forsythe, Ewing, and Pusey, 1994; Li, Nadaraj, and Pusey, 1995; Monaco and Rosenberger, 1993; Pusey and Naumann, 1986; Pusey, Snyder, and Naumann, 1986). The growth rates of single faces of protein crystal were measured periodically to obtain the functional dependence of growth rate on supersaturation.

The second group is the growth kinetics measurement based on a suspension of seed crystals having a particular particle size distribution (a multiparticle system). These techniques usually relate to the measurement of change in mass or size of the seed crystals as a function of supersaturation. The examples and discussion of experimental methods can be found in a number of references (Flood, Johns, and White, 2000; Garside, Mersmann, and Nyvlt, 2002; Mullin, 2001; Randolph and Larson, 1988; Srisa-nga, Flood, and White, 2006; Tanrikulu, Eroğlu, Bulutcu, and Özkar, 1998). The growth rate study in bulk crystallization of protein using this technique was illustrated by Judge et al. (1995). They seeded ovalbumin crystal in the metastable zone region and from periodic measurements of the crystal size distribution the growth rate was evaluated as a function of supersaturation. However, there is another technique that has been used to measure the crystal growth rate; the growth kinetics measurement based on measurements of solute concentration with time (Garside, Mersmann, and Nyvlt, 2002; Glade, Ilyaskarov, and Ulrich, 2004; Schöll, Lindenberg, Vicum, Brozio, and Mazzotti, 2007). This method is usually used in seeded isothermal batch crystallization experiments. The growth rate studies of crystallization of proteins using this technique has been demonstrated (Ataka and Asai, 1990; Bessho, Ataka, Asai, and Katsura, 1994). In these studies the authors obtained the kinetic parameters by fitting a kinetic model to the concentration-time data. A two-parameter model was developed which combines the nucleation and growth rates in lysozyme crystallization to give a single rate equation based on the concentration profile. Unfortunately, the model is unable to separate nucleation from growth kinetics. However, another model for crystal growth only (without nucleation) has been proposed (Carbone and Etzel, 2006; Carbone, Judge, and Etzel, 2005). The

analysis for this model requires only the simple measurement of protein concentration using a spectrophotometer, made on the solution phase of batch crystallization experiments, but it must be confirmed that no nucleation occurs. The periodical measurements of concentration can be directly converted to crystal mass and fitted to the model. Therefore, the growth kinetics was estimated by the plot of the fitted model. This technique is advantageous in that the growth kinetics can be obtained from one experiment with simple measurements.

In this work, the isothermal seeded batch crystallization of pure lysozyme has been studied to demonstrate the growth kinetics of the crystallization process and the ability to crystallize pure lysozyme from solution. The growth kinetics was determined based on the measurement of lysozyme concentration decay with time (observation of the desupersaturation curve) by assuming no nucleation, no breakage, and no agglomeration occur during the crystallization process (only crystal growth occurs). The measured concentrations are converted to predicted crystal mass, crystal size, and finally to the crystal growth rate using the mass balance. A power-law model equation of the growth rate was used to fit the growth rate data as a function of relative supersaturation to determine the growth rate order and the growth rate constant. The batch crystallization experiments were performed at constant solution condition (i.e. temperature, initial lysozyme concentration, and salt concentration). The effects of these parameters will be studied in the next Chapter, the batch crystallization of mixed lysozyme – ovalbumin solutions.

4.3   Theory

In this section, the theory of crystal growth is summarized. Other important phenomena or theories relating to the crystallization from solution (e.g. solubility, supersaturation, nucleation, and metastable zone wide) are described in previous chapters.

4.3.1   Crystal Growth and Models

Crystal growth is the major process by which the crystal size becomes larger. In the theory of crystal growth there are two mechanisms that play an important role in crystal growth; a diffusion step and a surface integration step (Mersmann, 1995; Randolph and Larson, 1988). The first step (diffusion) occurs when the solute molecules diffuse to the surface of the crystal through a mass transfer mechanism, due to a concentration gradient between the bulk concentration and surface concentration. The second step (surface integration) concerns the insertion of molecules into the surface of the crystal where they can integrate into the crystal lattice if they find a suitable integration site via surface diffusion. The model of these mechanisms is illustrated in Figure 4.1. When the rate of mass transfer to the crystal surface is much slower than the rate of integration into the surface, growth of the crystal is controlled by the *mass diffusion mechanism*, and the converse process is growth of the crystal controlled by the *surface integration mechanism*.
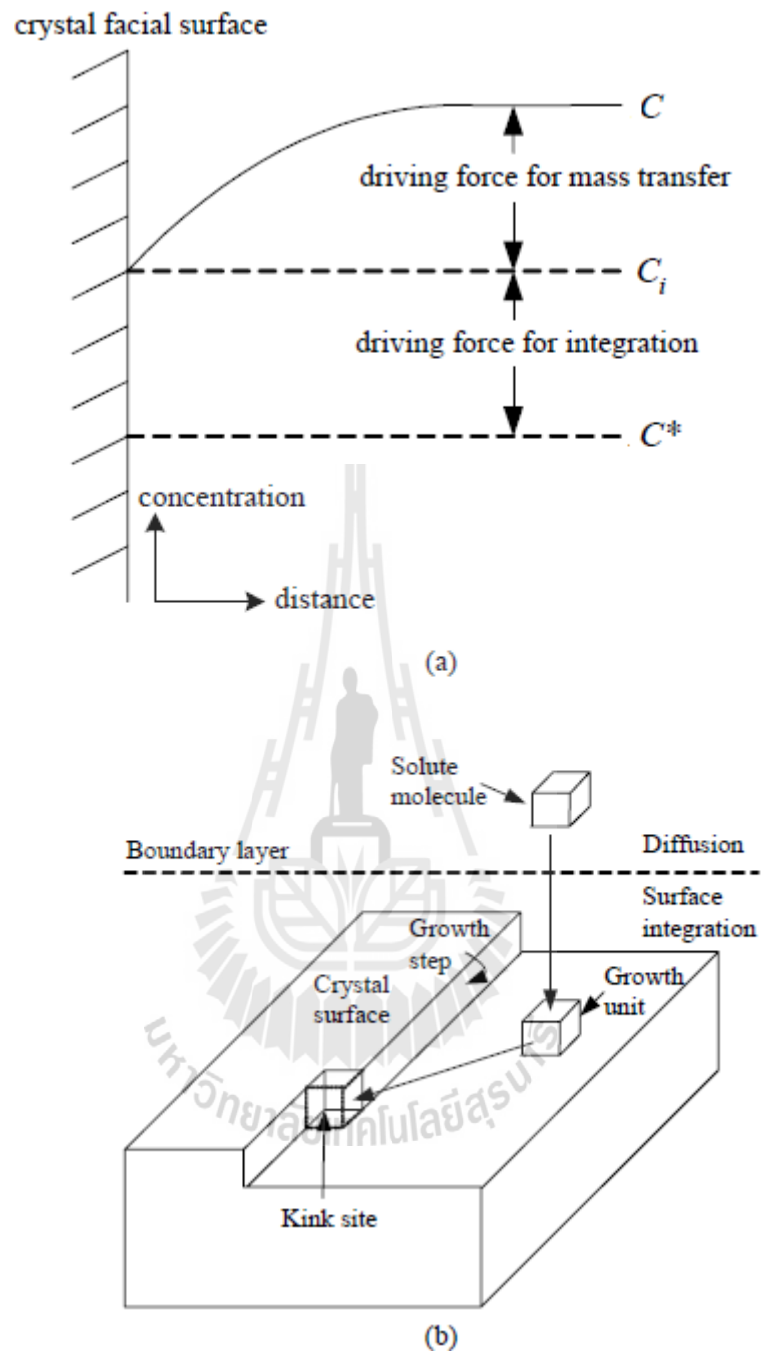
Figure 4.1 The diagram demonstration of the concentration driving force (a), and the

model of the two-mechanism crystal growth process (b) (adapted from

Strickland-Constable, 1968).

The crystal growth rate is normally described as a rate of linear increase in a characteristic dimension of the crystal with time, and expressed as the following equation.

$$G = \frac{dL}{dt} \qquad (4.1)$$

where G is the crystal growth rate, L is the characteristic dimension that is increasing, and t is the growth time. The units of time and the characteristic dimension depend on the units of the growth rate. Since the mass and surface area of the crystal can be estimated by $m = \rho k_v L^3$ and $A = k_a L^2$, respectively (Mullin, 2001; Randolph and Larson 1988), therefore the growth rate can be also represented as a rate of mass deposition (i.e. a mass flux) as described in equation (4.2) and (4.3).

$$\frac{dm}{dL} = 3\rho k_v L^2, \ \ dm = 3\rho k_v L^2 \, dL, \ \ \frac{dm}{dt} = 3\rho k_v L^2 \frac{dL}{dt} \qquad (4.2)$$

Thus

$$R_G = \frac{1}{A}\frac{dm}{dt} = 3\rho \frac{k_v}{k_a}\frac{dL}{dt} \qquad (4.3)$$

where R_G is the rate of mass deposition, m is the crystal mass, A is the surface area of crystal, ρ is the density of the crystal, k_v is the volume shape factor, and k_a is the area shape factor.

There are several theoretical models used to describe the mechanisms of crystal growth as have been reviewed in detail by Strickland-Constable (1968), Ohara and Reid (1973), and Mullin (2001).

4.3.1.1 Diffusion-reaction model

Due to the driving force between the bulk concentration and the concentration at the crystal surface, solute molecule must diffuse to the surface of the crystal through a mass transfer mechanism with the rate as expressed in the form

$$\frac{dm}{dt} = k_d A(c - c_i) \tag{4.4}$$

where k_d is a coefficient of mass transfer by diffusion, c is solute concentration in the solution, and c_i is the solute concentration in the solution at crystal-solution interface. The mass diffusion (a first-order reaction) and surface integration mechanism are occurring under the influence of different concentration driving forces but the same rate, equation (4.4) can be expressed in the form of equation (4.5) also.

$$\frac{dm}{dt} = k_r A(c_i - c^*) \tag{4.5}$$

where k_r is a rate constant for the surface integration (reaction) process, c^* is the equilibrium solute concentration. Assuming the unknown interfacial concentration c_i is equal to bulk concentration c gives

$$\frac{dm}{dt} = k_G A(c - c^*)^n \tag{4.6}$$

where k_G is the overall growth rate constant and n is the growth rate order.

4.3.1.2 Surface integration models

There are three surface integration models which have been proposed. The first model is the ***continuous growth model***. This is a model for a crystal surface which is rough on the molecular scale. When a solute molecule diffuses to the crystal surface, it is immediately integrated if they find a suitable integration site or desorb and return to the solution phase, as depicted in Figure 4.1 (b). This growth model is often occurs at high supersaturation, and always affects the purity of the crystal or induce more easily incorporated of the solvent molecules (Kramer and van Rosmalen, 2009).

A second model is the ***screw dislocation or Burton-Caberra-Frank (BCF) model***. This model is used to overcome the limitation of the continuous growth model by recognizing the significance of the screw dislocation, which presents as a continuous spiral during growth (Figure 4.2). The assumption for this model is that the surface nuclei cannot form on a smooth surface (or the attachment of new molecules is very difficult without the ledge created by the spiral dislocation), but the steps are self-perpetuating by propagating using a dislocation in the crystal, known as a screw dislocation. These steps grow continuously and the surface becomes a spiral staircase. The growth rate perpendicular to the surface can be expressed as equation (4.7) (Mullin, 2001; Randolph and Larson, 1988).

$$G = A_{BCF}\sigma^2 \tanh\left(\frac{B_{BCF}}{\sigma}\right) \tag{4.7}$$

Where A_{BCF} and B_{BCF} are constants, and σ is relative supersaturation.
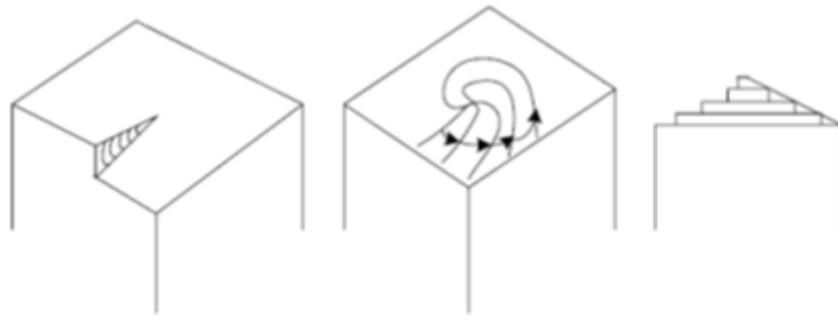
Figure 4.2 The crystal growth development by screw dislocation model

(Adapted from Mullin, 2001).

Lastly, the ***Birth and spread model***. This model assumes that the growth is based on nucleation on the crystal surface follow by the spread of the monolayers (Ohara and Reid, 1973). The model is illustrated as Figure 4.3. These steps are created by a mechanism of two dimensional (2D) nucleation followed by the layer growth. Since a high level of supersaturation is required for significant formation of 2D nuclei, the mechanism should only occur at high levels of supersaturation. The growth rate based on this model has been developed and expressed as equation (4.8) (Jones, 2002; Garside, Mersmann, and Nyvlt, 2002).

$$G = A_{B+S}\sigma^p \exp\left(-\frac{B_{B+S}}{\sigma}\right) \tag{4.8}$$

where A_{B+S}, B_{B+S}, and p are constants.
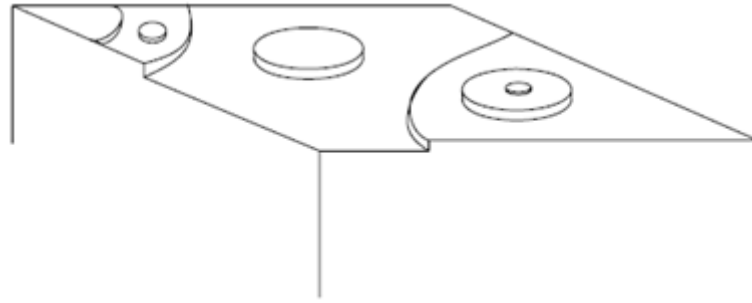
Figure 4.3 The crystal growth apparent by birth and spread model

(Adapted from Mullin, 2001).

4.3.2 General growth expression

The difficulty of using the previous theoretical models for estimating the crystal growth is that they cannot yet predict crystal growth constants for a particular substance.

To overcome to this issue, crystal growth rate studies for industrial crystallization processes usually use a power law model to empirically correlate the growth rate with the supersaturation (Myerson and Ginde, 2002) as described following

$$G = k_G \sigma^n \tag{4.9}$$

Where G is the growth rate, k_G is the growth rate constant, σ is relative supersaturation, and n is the growth rate order. The growth rate order indicates differences in the rate controlling mechanism of the growth process. If $n = 1$ the growth may be controlled by mass diffusion, and if the surface integration is rate controlling mechanism n usually $1 < n < 2$ (Flood, 2009; Randolph and Larson, 1988).

For protein crystallization n found to be equal to 2 (Carbone and Etzel, 2006; Judge, Johns, and White, 1995; Saikumar, Glatz, and Larson, 1998).

The growth rate is temperature dependent and can be expressed as equation (4.10) which is an Arrhenius relationship (Mullin, 2001).

$$k_G = k_G^0 \exp(-\frac{E_G}{RT}) \qquad (4.10)$$

where E_G is the activation energy of growth (kJ/mol), T is the temperature (K), k_g^0 is a pre-exponential constant (m/s), and R is the ideal gas constant (8.314 J/mol·K). The activation energies values are typically in the range 10 - 20 kJ/mol for the diffusion controlled mechanism and 40 - 60 kJ/mol for the surface integration controlled mechanism (Kramer and van Rosmalen, 2009).

4.4   Materials and Methods

4.4.1   Materials

Hen egg white lysozyme (HEWL, product No. 62971) and ovalbumin (product No. A5253) were purchased from Sigma-Aldrich. These two proteins were used without further purification since no other proteins were detected in a SDS-PAGE gel electrophoresis analysis (15% acrylamide).

Sodium chloride (purity ≥99.5%), sodium acetate trihydrate (purity ≥99.5%) and acetic acid (100%) were purchased from Carl Roth. All chemicals and deionized water were used without further purification to prepare buffer solution based on the method of Dawson et al. (1986) and salt solution as described in chapter II.

4.4.2   Preparation of Lysozyme Seed Crystal (Tetragonal Form)

Lysozyme seed crystals were prepared by mixing equal volumes of protein solution and salt solution. 100 mg/ml lysozyme in sodium acetate buffer pH 5.0 and 25 ml of 8% NaCl (g/100 mL) in the same buffer were mixed together. Mixing was done by adding the salt solution to the protein solution and keeping the solution at 8 °C overnight. The temperature of both protein solution and salt solution was kept at around 8°C (using a refrigerator) before mixing. After one week the lysozyme solution with tetragonal crystals was stirred at around 300 rpm for 10 min using a stirrer bar and a magnetic stirrer to cause crystal breakage. The fragment crystals were filtered using filter paper (Whatman) and dried with silica gel. The mean size of the seed crystals was approximately 8 μm (number- based) as determined by a laser diffraction particle size analyzer (LA-950, Horiba). This is consistent with the average particle size seen on a photograph of the seed crystals (Figure 4.6, left). The particle size distribution of the seed crystal is shown in Figure 4.4.
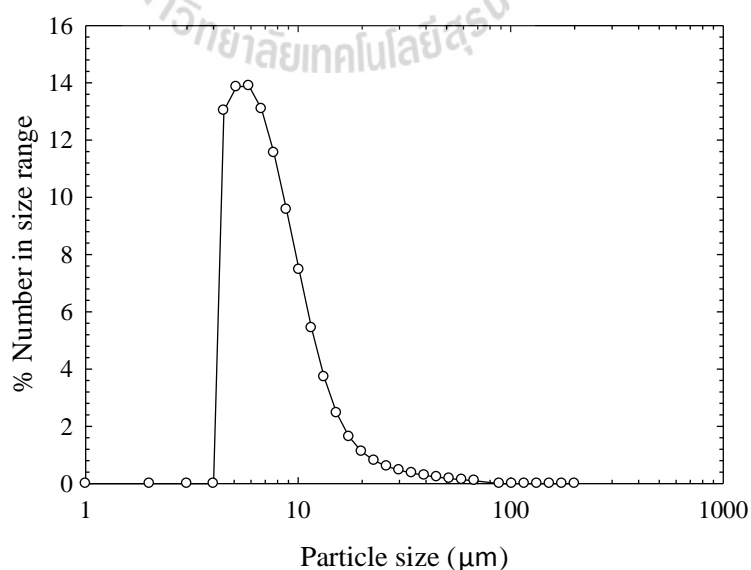
Figure 4.4 Particle size distribution (number-based) of the seed crystal.

4.4.3 Apparatus

A 100 mL batch crystallizer (Figure 4.5) that was modified from a Schott bottle was used to crystallize and measure the growth rate of lysozyme. The lysozyme protein slurry is continuously agitated at 100 rpm by a centrally located three-blade impeller driven by a connected motor gear. The crystallizer was placed inside a constant temperature water bath, where the temperature was controlled within ±0.5°C.
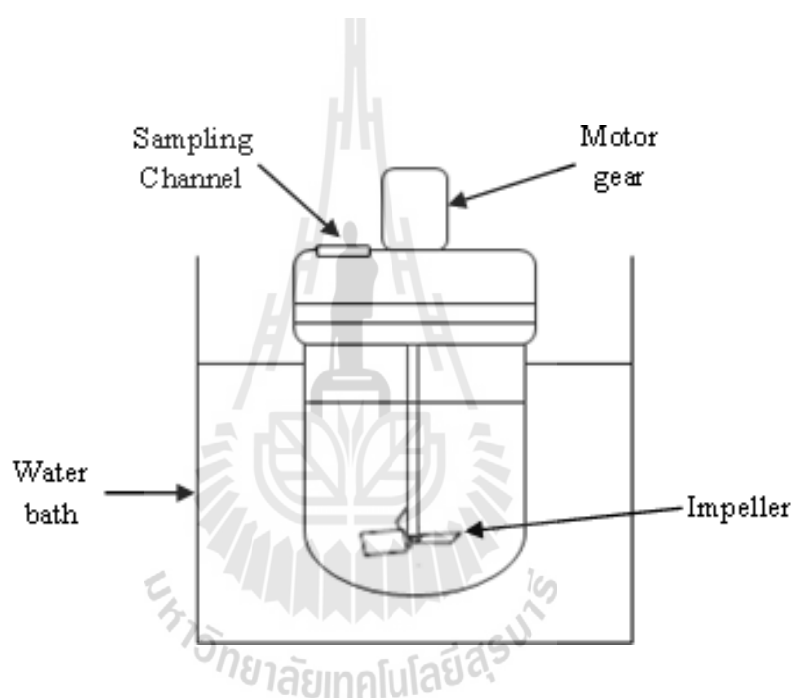
Figure 4.5 The 100 mL batch crystallizer.

4.4.4 Crystallization and Crystal Growth Rate Measurement

The crystallization and growth kinetics of lysozyme were studied using isothermal seeded batch crystallization. The experiments were performed at the temperature of 20°C in a 100 mL batch crystallizer agitated at 100 rpm by a centrally located three-blade impeller driven by a connected motor gear. To start the experiment 25 mL of 50 mg/mL lysozyme in 0.1M sodium acetate buffer pH 5.0 was

put into the crystallizer together with 25 mL of 8% NaCl in the same buffer and then 120 mg of lysozyme seed crystals was added. This initial experimental condition was performed to ensure that the crystallization occurred within the metastable zone to avoid the nucleation of new crystal (only crystal growth occurs); the estimated solubility was approximately 4 mg/mL (Forsythe, Judge, and Pusey, 1999; Maosoongnern, Borbon, Flood, and Ulrich, 2012).

The growth kinetics were studied using time dependent measurement of decline in protein concentration during crystallization (Carbone and Etzel, 2006; Carbone, Judge, and Etzel, 2005). The lysozyme solution was sampled and the concentration measured periodically using the UV absorbance technique at 280 nm wavelength. A UV photometer (HP 8453, Agilent) was used. The extinction coefficient of 2.4321 mL·mg^{-1}·cm^{-1} was obtained from a calibration curve. The concentrations were converted mathematically to size of the crystal (see section 4.4.5) in order to determine the number mean growth rate of the crystals. Three duplicates of two set of experiments were made. Approximately 24 hr and 6 hr crystallization times were used for each set of experiment.

4.4.5 Crystal Size Calculation

During crystallization the total mass of protein should be constant (no protein lose due to denaturation). Therefore, the size of the crystal can be calculated from the mass balance as given

$$m_s + m_{p.l}(t=0) = m_{cryst}(t=t) + m_{p,l}(t=t) \qquad (4.11)$$

where m_s is the seed crystal mass, $m_{p.l}(t=0)$ is the initial mass of protein in solution, $m_{cryst}(t=t)$ is the mass of protein crystal at time equal to t, and $m_{p.l}(t=t)$ is the mass of protein in solution at time equal to t.

Assuming no nucleation, no breakage, no agglomeration during crystallization (only crystal growth occurs) and the volume of solution is constant (no solvent evaporation). Then equation (4.11) become

$$m_s + c_i V = n\rho k_v L^3 + c_t V \tag{4.12}$$

where c_i is the initial protein concentration, c_t is the protein concentration at time t, V is volume the solution, n is the number of crystal, ρ is the density of protein, k_v is the volume shape factor of crystal, and L is the number mean size of the crystal. Thus equation (4.12) can be directly rearranged into equation (4.13) that is appropriate for the calculation of crystal size.

$$L^3 = \frac{m_s + (c_i - c_t)V}{n\rho k_v} \tag{4.13}$$

The term $\rho k_v L^3$ in equation (4.13) is the mass of a one crystal based on the characteristic size L (Mullin, 2001; Randolph and Larson 1988). Since assuming the number of crystal is constant then the term $n\rho k_v$ can be approximately calculated from the mass of seed divided by the cube of the number-based mean size of the seed.

4.5   Results and Discussions

4.5.1   Batch Crystallization of Lysozyme

Lysozyme was crystallized from a solution. Figure 4.6 shows an example of photographs of the seed crystals and the product crystals from the crystallization. A comparison of the photographs of seed and product crystals shows that there is no nucleation occurring during the growth process since no particle smaller than the seed crystal is observed
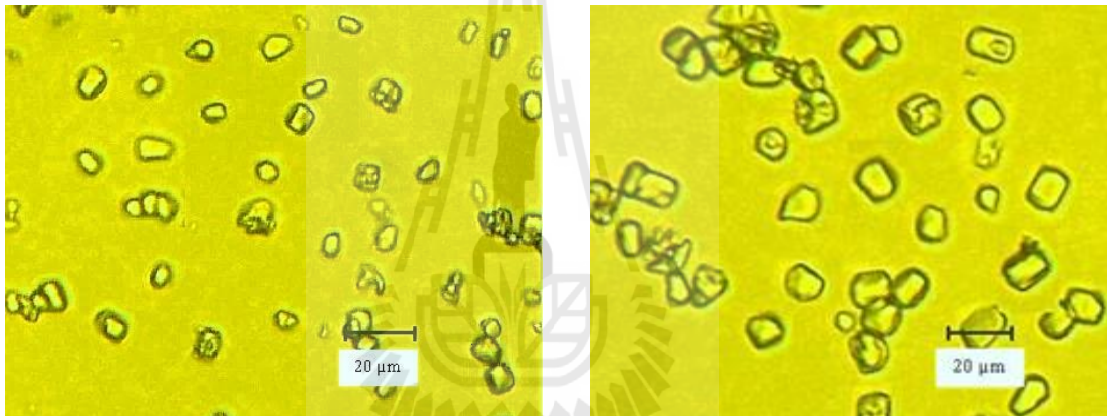
Figure 4.6 Photographs of lysozyme seed crystals (Left) and product crystals (Right). Crystallization of pure lysozyme, Exp. No.1-1.

Examples of concentration measurement during the isothermal seeded batch crystallization of lysozyme for two experiments (approximately 25 hr for Exp. No.1-1 and 6 hr for Exp. No.2-1) are shown in Table 4.1 and Table 4.2, respectively. The mass of the crystal appearing in the crystallizer can be directly calculated from the concentration via equation (4.11) and (4.12) as shown in the last column. The yield of the lysozyme crystallization can be calculated from the ratio between the

actual mass of lysozyme crystallized and the predicted mass of lysozyme crystallized

at equilibrium as expressed in equation (4.14).

$$Yield~(\%) = \frac{m_{cryst} - m_s}{(C_i - C^*)V} * 100\% \tag{4.14}$$

Where m_{cryst} is the mass of protein crystal at any time (t), m_s is the seed crystal

mass, c_i is the initial protein concentration, c^* is solubility of protein, and V is the

volume of solution. Since all of the parameters were known, this leads to 84.68%

yield for Exp. No.1-1 and 49.67% yield for Exp. No.2-1 were received, respectively.

This shows the behavior of general crystallization processes. Longer crystallization

time gives a higher yield (Mullin, 2001; Tung, Paul, Midler, and McCauley, 2009).

Table 4.1 Concentration measurement and calculation of total mass of crystal

(Exp. No.1-1), dilution factor = 50.

Time (hr)	Abs. 1	Abs. 2	Abs. 3	Ave. Abs.	C_t (mg/mL)	m_{cryst} (mg)
0	1.1960	1.1966	1.1962	1.1963	24.5933	120.00
1	1.0683	1.0690	1.0698	1.0690	21.9776	250.79
2	0.9980	0.9986	0.9990	0.9985	20.5282	323.25
3	0.9105	0.9098	0.9095	0.9099	18.7067	414.33
4	0.8372	0.8376	0.8366	0.8371	17.2101	489.16
5	0.7708	0.7711	0.7712	0.7710	15.8512	557.11
6	0.7196	0.7191	0.7195	0.7194	14.7897	610.18
8	0.6103	0.6107	0.6104	0.6105	12.5502	722.16
10	0.5519	0.5524	0.5526	0.5523	11.3544	781.95
12.5	0.4849	0.4839	0.4842	0.4843	9.9571	851.81
19.5	0.3850	0.3852	0.3857	0.3853	7.9211	953.61
25	0.3482	0.3485	0.3475	0.3481	7.1557	991.88

Table 4.2 Concentration measurement and calculation of total mass of crystal

(Exp. No.2-1), dilution factor = 50.

Time (hr)	Abs. 1	Abs. 2	Abs. 3	Ave. Abs.	C_t (mg/mL)	m_{cryst} (mg)
0.0	1.2168	1.2161	1.2159	1.2163	25.0045	70.0000
0.5	1.1773	1.1776	1.1779	1.1776	24.2095	109.7485
1.0	1.1358	1.1349	1.1336	1.1348	23.3292	153.7646
1.5	1.0835	1.0830	1.0841	1.0835	22.2757	206.4413
2.0	1.0387	1.0397	1.0376	1.0387	21.3538	252.5332
2.5	0.9870	0.9854	0.9849	0.9858	20.2658	306.9374
3.0	0.9351	0.9381	0.9324	0.9352	19.2267	358.8920
3.5	0.8921	0.8910	0.8913	0.8915	18.3271	403.8701
4.0	0.8392	0.8378	0.8410	0.8394	17.2557	457.4380
4.5	0.7900	0.7917	0.7925	0.7914	16.2699	506.7305
5.0	0.7455	0.7412	0.7408	0.7425	15.2648	556.9851
5.5	0.7043	0.7039	0.7040	0.7041	14.4744	596.5054
6.0	0.6608	0.6590	0.6605	0.6601	13.5709	641.6780

In the real crystallization process, a short time of operation with high yield (involving the consideration of operation cost) is required. Comparing the two experiments, the change in concentration of lysozyme is higher at the beginning period of the crystallization process and slower when the crystallization is continuing. The example plots of decline in concentration with time are shown in Figure 4.7 and Figure 4.8. As shown in Figure 4.8, the lysozyme concentration decay behavior of the 6 hr crystallization time is still almost linear. This indicates that the operation time of 6 hr is appropriate to use as a crystallization time. Although the yield of 6 hr operation time is less than the 25 hr operation time, it may be the process can be stopped and recrystallization begun again after adjusting the experimental conditions. Therefore the received product crystal for two cycling crystallization (e.g. 12 hr of crystallization time) might be higher than the product crystal with using only one cycle of crystallization (e.g. 12 hr of crystallization time)
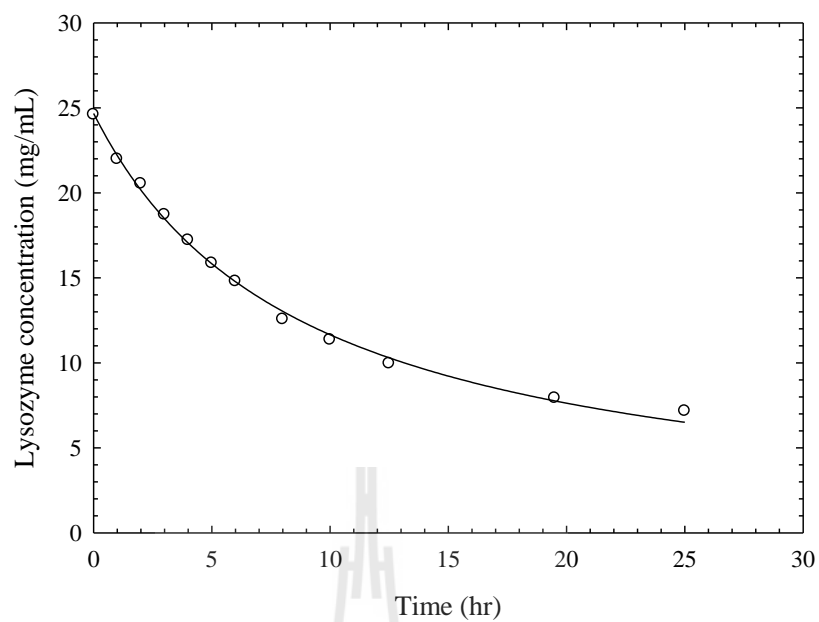
Figure 4.7 Concentration decay of lysozyme crystallization (Exp. No.1-1).
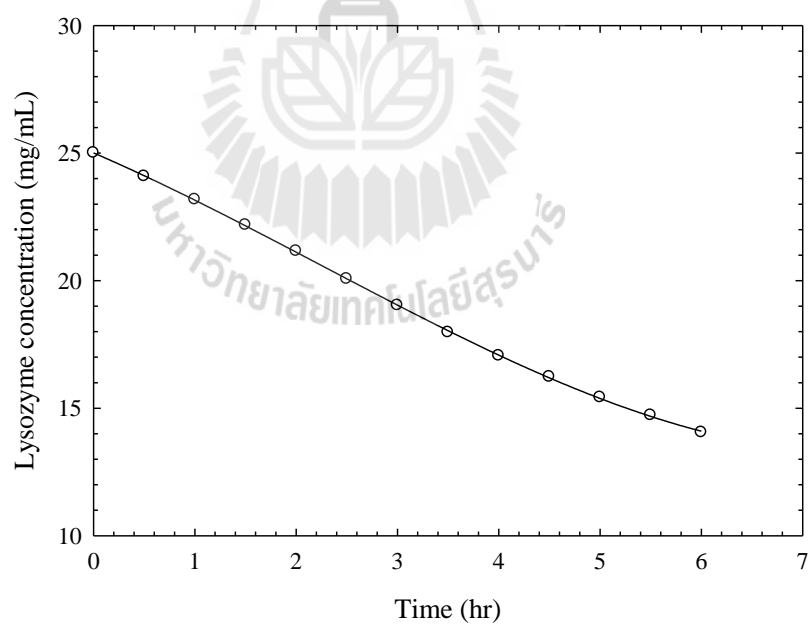
Figure 4.8 Concentration decay of lysozyme crystallization (Exp. No.2-1).

4.5.2 Crystal Growth Kinetics of Lysozyme

The mean crystal growth rate was determined as the ratio of the change in number mean crystal size vs time. The mean crystal size (number-based) was used to calculate the crystal growth rate since the crystal growth rate data can only be obtained from the batch crystal growth using the population balance, which is a number-based balance. If the volume or mass mean size is measured then the conversions of the others mean sizes to number mean size is required. The number-based mean size can be calculated from the following equation (Allen, 1997)

$$\ln x_{NL} = \ln x_{mV} - 2.5 \ln^2 \sigma_G \qquad (4.15)$$

where x_{NL} is the number-based mean crystal size, x_{mV} is the volume-based geometric mean crystal size, and σ_G is the geometric standard deviation of the volume-based particle size distribution.

The crystal growth rate can be calculated from the ratio of the change in number mean crystal size to the change of the time, and can be correlated to the change of supersaturation during periodic measurements. The examples of the crystal growth rate calculation procedure for two experiments are shown in Table 4.3 and 4.4. Concentrations are converted to number-based mean crystal size using equation (4.3) and shown in column 3. The growth rate was calculated directly from the rate of the change in a number-based mean crystal size with time for each measurement. These crystal growth rates values are shown in column 5. The corresponding relative supersaturation values for each crystal growth rate are also shown in column 4.

Table 4.3 Example of calculation for size and growth rate of the crystal (Exp. No.1-1

$c_{lys,0}$ = 25 mg/mL, Temp. = 20°C, 4% NaCl, pH 5.0).

Time (hr)	C_t (mg/mL)	L (μm)	Relative supersaturation, σ (-)	Growth rate, G (μm/hr)	log σ	log G
0	24.5933	8.0000				
1	21.9776	10.1476	5.1483	2.1776	0.7117	0.3380
2	20.5282	11.0436	4.4944	0.8960	0.6527	-0.0477
3	18.7067	11.9962	4.1321	0.9526	0.6162	-0.0211
4	17.2101	12.6789	3.6767	0.6826	0.5655	-0.1658
5	15.8512	13.2406	3.3025	0.5618	0.5188	-0.2504
6	14.7897	13.6484	2.9628	0.4078	0.4717	-0.3896
8	12.5502	14.4369	2.6974	0.3942	0.4309	-0.4043
10	11.3544	14.8248	2.1375	0.1940	0.3299	-0.7123
12.5	9.9571	15.2538	1.8386	0.1716	0.2645	-0.7655
19.5	7.9211	15.8387	1.4893	0.0836	0.1730	-1.0780
25	7.1557	16.0478	0.9803	0.0380	-0.0086	-1.4200

Table 4.4 Example of calculation for size and growth rate of the crystal (Exp. No.2-1,

$c_{lys,0}$ = 25 mg/mL, Temp. = 20°C, 4% NaCl, pH 5.0).

Time (hr)	C_t (mg/mL)	L (μm)	Relative supersaturation, σ (-)	Growth rate, G (μm/hr)	log σ	log G
0.0	25.0045	8.0000				
0.5	24.0855	8.8428	5.2511	1.7456	0.7203	0.2419
1.0	23.1796	9.5836	5.0214	1.4815	0.7008	0.1707
1.5	22.1763	10.2889	4.7949	1.4107	0.6808	0.1494
2.0	21.1546	10.9197	4.5441	1.2616	0.6574	0.1009
2.5	20.0650	11.5206	4.2886	1.2018	0.6323	0.0798
3.0	19.0275	12.0397	4.0162	1.0382	0.6038	0.0163
3.5	17.9680	12.5273	3.7569	0.9751	0.5748	-0.0110
4.0	17.0525	12.9200	3.4920	0.7854	0.5431	-0.1049
4.5	16.2315	13.2529	3.2631	0.6658	0.5136	-0.1767
5.0	15.4229	13.5652	3.0579	0.6246	0.4854	-0.2044
5.5	14.7246	13.8237	2.8557	0.5171	0.4557	-0.2864
6.0	14.0516	14.0641	2.6811	0.4807	0.4283	-0.3181

The behavior of the mean crystal growth rates were demonstrated as a function of relative supersaturation, as shown in Figures 4.9 and 4.10. These Figures show that the growth rates decrease with decreases in the relative supersaturation. The mean growth rates can be described by the power-law model as expressed in equation (4.9). Therefore, in this work the mean crystal growth rates (which were calculated using the approximation of the ratio of the number mean crystal size on the change of the time) can be expressed in the form

$$G = \frac{\Delta L}{\Delta t} = k_G \sigma^n \qquad (4.16)$$

Taking the logarithm of both sides of equation (4.16) gives

$$\log G = \log k_G + n \log \sigma \qquad (4.17)$$
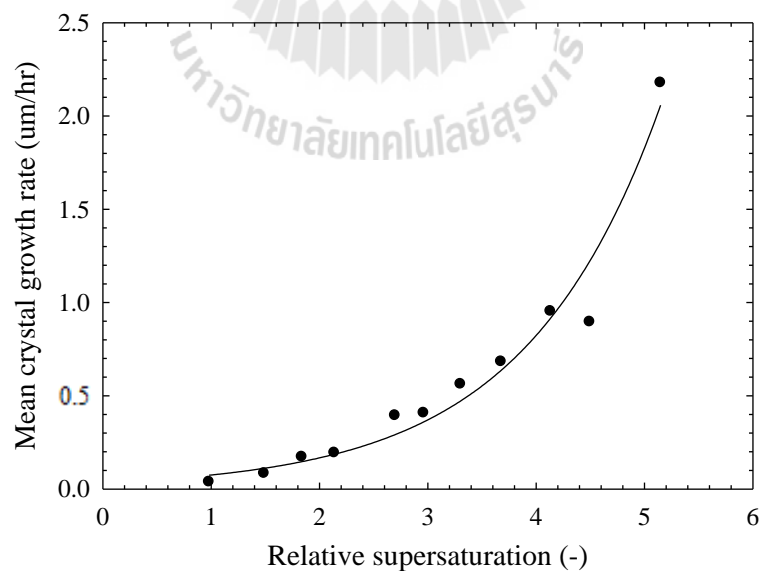
Figure 4.9 Mean crystal growth rates as a function of relative supersaturation

(Exp. No.1-1, $c_{lys,0} = 25$ mg/mL, Temp. = 20°C, 4% NaCl, pH 5.0).
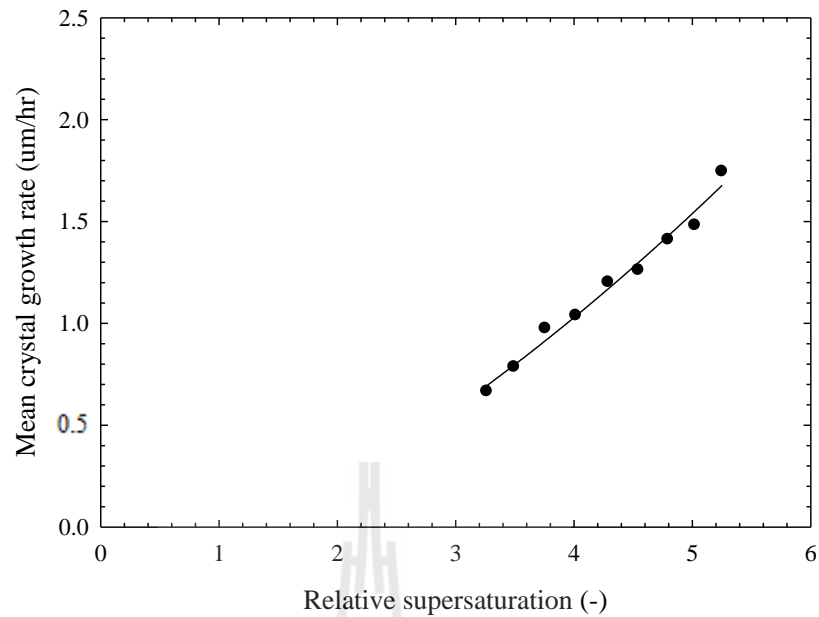
Figure 4.10 Mean crystal growth rates as a function of relative supersaturation

(Exp. No.2-1, $c_{lys,0} = 25$ mg/mL, Temp. = 20°C, 4% NaCl, pH 5.0).

Fitting the mean growth rate data in Table 4.3 and 4.4 to equation (4.17) ($\log G$ against $\log \sigma$) gives a straight line approximation with a high degree of linearity, as shown in Figure 4.11. Therefore n and $\log k_g$ can be directly obtained from the slope of the line and the intercept of the y axis, respectively. In the plots, the growth rate order $n = 2$ was used to fit the equation due to the results of Saikumar, Glatz, and Larson (1998). The plot showed a good fit of the straight line with the experimental mean growth rate data. The fitting equation is shown in equation (4.18) for the growth kinetics of tetragonal lysozyme crystal at 20°C, 4% NaCl, and pH 5.0. The seed size was 8 μm and the mass of 120 mg.

$$\log G = -1.248 (\pm 0.055) + 2\log \sigma \tag{4.18}$$

These equations show that the growth rate order is equal to 2. This indicates that the growth of the crystal is controlled by the surface integration mechanism as described in section 4.3.2. The growth rate constants values were calculated from the intercept of y axis which is results in the value of 5.65×10^{-6} cm/hr. The growth rate constant can be used to calculate the change in crystal size via the growth rate expression as equation (4.16) result in the average change of crystal size is 8.41 μm. Therefore the average final size of the growth crystal should be 16.41 μm (seed crystal size is 8 μm) which is agrees well with the photograph of the growth crystal as shown in Figure 4.6 (right). Generally, the growth rate constant is dependent of temperature and should be independent of the supersaturation. The difference of the value (crystallization time of 25 hr and 6 hr) may due to the measurements from different batches. Some slight difference in experimental conditions can make this occur. The comparison of the growth rate constant to previous work is shown in Table 4.5. The growth rate constant values agree well with others work. This indicates that this batch crystallization method can be used to accurately determine kinetics of pure lysozyme crystallization well.
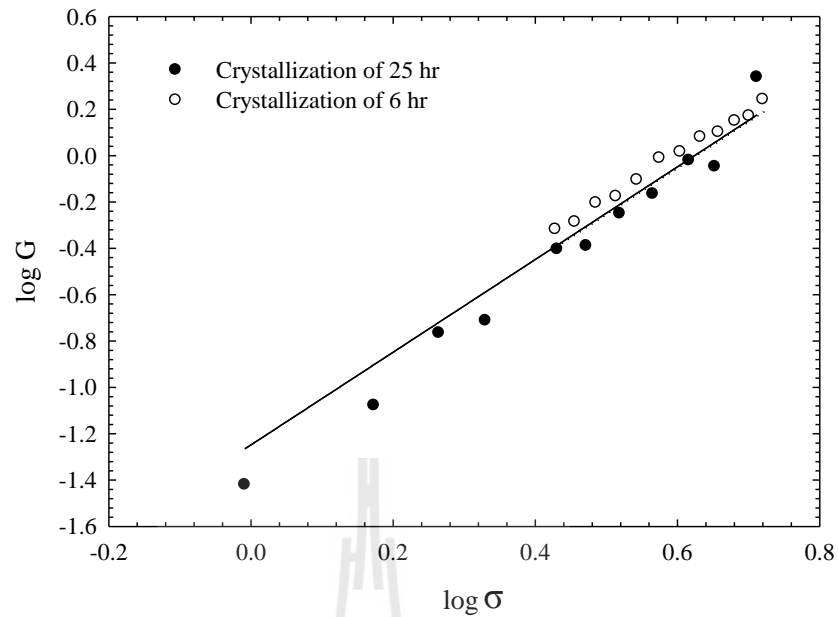
Figure 4.11 Plot of the growth rate and relative supersaturation ($c_{lys,0}$ = 25 mg/mL,

Temp. = 20°C, 4% NaCl, pH 5.0).

Table 4.5 Growth rate constant of lysozyme crystallization

Method of measurement	Average growth rate constant, k_g (cm/hr)	References
Measurement of solute concentration with time	5.65×10^{-6}	This work
Measurement of solute concentration with time	3.74×10^{-5}	Carbone and Etzel, 2006
Individual single crystal	11×10^{-5}	Saikumar et al., 1998
Individual single crystal	0.53×10^{-5}	Pusey et al., 1986

4.6 Conclusions

In this work, the isothermal batch crystallization of pure lysozyme protein has been studied at 20°C. The crystallization was carried out in a 100 mL agitated batch crystallizer that was modified from a Schott bottle. The product crystal yields were 84.68% and 49.67% using 25 hr and 6 hr operation time, respectively. The growth kinetics of the crystal has been studied by measurement of the change in lysozyme concentration with time. The crystal growth rate at higher supersaturation is higher than subsequent crystal growth rate at lower supersaturation. The growth rate order is equal to 2. This indicates that the growth kinetics is controlled by the surface integration mechanism. The calculated growth rate constant values was 5.67×10^{-6} cm/hr which agrees well with previous studies. This indicates that the batch crystallization method can be used to crystallize pure lysozyme well.

4.7 References

Allen, T. (1997). **Particle size measurement: Volume 1 powder sampling and particle size measurement** (5th ed.). London: Chapman&Hall.

Ataka, M., and Asai, M. (1990). Analysis of the nucleation and crystal growth kinetics of lysozyme by a theory of self-assembly. **Biophys. J.** 58: 807-811.

Ataka, M., and Tanaka, S. (1986). The growth of large single crystals of lysozyme, **Biopolymers** 25(2): 337-350.

Bessho, Y., Ataka, M., Asai, M., and Katsura, T. (1994). Analysis of the crystallization kinetics of lysozyme using a model with polynuclear growth mechanism. **Biophys. J.** 66(2): 310-313.

Carbone, M.N., and Etzel, M.R. (2006). Seeded Isothermal Batch Crystallization of Lysozyme. **Biotechnol. Bioeng.** 93(6): 1221-1224.

Carbone, M.N., Judge, R.A., and Etzel, M.R. (2005). Evaluation of a Model for Seeded Isothermal Batch Protein Crystallization. **Biotechnol. Bioeng.** 91(1): 84-90.

Dawson, R.M.C., Elliot, D.C., Elliot, W.H., and Jones, K.M. (1986). **Data for Biochemical Research** (3rd ed.). Oxford: Science Publication.

DeMattei, R.C., and Feigelson, R.S. (1986). Growth rate study of canavalin single crystals. **J. Cryst. Growth** 97(2): 333-336.

Flood, A.E. (2009). **Industrial crystallization from solution: A primer.** Thailand: Suranaree University of Technology.

Flood, A.E., Johns, M.R., and White, E.T. (2000). Crystal growth rates and dispersion for D-fructose from aqueous ethanol. **AIChE J.** 46(2): 239-246.

Forsythe, E.L., Ewing, F., and Pusey, M.L. (1994). Studies on tetragonal lysozyme crystal growth rates. **Acta Crystallogr.** D50: 614-619.

Forsythe E.L., Judge R.A., and Pusey M.L. (1999). Tetragonal chicken egg white lysozyme solubility in sodium chloride solutions. **J. Chem. Eng. Data.** 44: 637-640.

Garside, J., Mersmann, A., and Nyvlt, J. (2002). **Measurement of crystal growth and nucleation rates** (2nd ed.). UK: Institute of Chemical Engineering.

Glade, H., Ilyaskarov, A.M., and Ulrich, J. (2004). Determination of crystal growth kinetics using ultrasonic technique. **Chem. Eng. Technol.** 27(4): 736-740.

Gougazeh, M., Omar, W., and Ulrich, J. (2009). Growth and dissolution kinetics of potassium sulfate in pure solutions and in the presence of Cr3+ ions. **Cryst. Res. Technol.** 44(11): 1205-1210.

Jones, A.G. (2002). **Crystallization process systems** (1st ed.). Oxford: Butterworth-Heinemann.

Judge, R.A., Johns, M.R, and White E.T (1995). Protein Purification by Bulk Crystallization: The Recovery of Ovalbumin. **Biotechnol. Bioeng.** 48(4): 315-323.

Kitamura, M., and Ishizu, T. (1998). Kinetic effect of L-phenylalanine on growth process of L-glutamic acid polymorph. **J. Cryst. Growth** 192(1-2): 225-235.

Kramer, H.J.M., and van Rosmalen, G.M. (2009). Crystallization. In: I.A., Wilson and C.F., Poole (ed.). **Handbook of methods and instrumentation in separation science volume 2** (pp 1-20). London: Academic Press.

Li, M., Nadaraj, A., and Pusey, M.L. (1995). Modeling the growth rates of tetragonal lysozyme crystals. **J. Cryst. Growth** 156(1-2): 121-132.

Maosoongnern, S., Borbon, V.D., Flood, A.E., and Ulrich, J. (2012). Introducing a Fast Method to Determine the Solubility and Metastable Zone Width for Proteins: Case Study Lysozyme. **Ind. Eng. Chem. Res.** 2012(51): 15251−15257.

Mersmann, A. (1995). **Crystallization Technology Handbook**. New York: Mercel Dekker.

Monaco, L.A., and Rosenberger, F., (1993). Growth and etching kinetics of tetragonal lysozyme. **J. Cryst. Growth** 129: 465-484.

Mullin, J.W. (2001). **Crystallization** (4th ed.). Oxford: Butterworth-Heinemann.

Myerson, A.S., and Ginde, R. (2002). Crystals, crystal growth, and nucleation. In: A.S. Myerson (ed.). **Handbook of industrial crystallization** (2nd ed., pp 33-65). USA: Butterworth-Heinemann.

Ohara, M., and Reid, R.C. (1973). **Modeling crystal growth rates from solution**. Englewood Cliffs: Prentice-Hall.

Pantaraks, P., and Flood, A.E. (2005). Effect of growth rate history on current crystal growth: A second look at surface effects on crystal growth rates. **Cryst. Growth Des.** 5(1): 365-371.

Pusey, M.L., and Naumann, R. (1986). Growth kinetics of tetragonal lysozyme crystals. **J. Cryst. Growth** 76(3): 593-599.

Pusey, M.L., Snyder, R.S., and Naumann, R. (1986). Protein crystal growth: growth kinetics for tetragonal lysozyme crystals. **J. Biol. Chem.** 261(14): 6524-6529.

Randolph, A.D., and Larson, M.A. (1988). **Theory of particulate processes:Analysis and techniques of continuous crystallization** (2nd ed.). California: Academic Press.

Saikumar, M.V., Glatz C.E., and Larson M.A. (1998). Lysozyme crystal growth and nucleation kinetics. **J. Crystal. Growth** 187: 277–288.

Schöll, J., Lindenberg, C., Vicum, L., Brozio, J., and Mazzotti, M. (2007). Precipitation of α L-glutamic acid: determination of growth kinetics. **Faraday Disccuss.** 136: 247-264.

Srisa-nga, S., Flood, A.E., and White, E.T. (2006). The secondary nucleation threshold and crystal growth of α-glucose monohydrate in aqueous solution. **Cryst. Growth Des.** 6(3): 795-801.

Strickland-Constable, R.F. (1968). **Kinetics and Mechanism of Crystallization**. London: Academic Press.

Tanrikulu, S.Ü., Eroğlu, I., Bulutcu, A.N., and Özkar, S. (1998). The growth and dissolution of ammonium perchlorate crystals in a fuidized bed crystallizer. **J. Cryst. Growth** 194(2): 220-227

Tung, H.H., Paul, E.L., Midler, M., and McCauley J.A., (2009). **Crystallization of Organic Compounds: An Industrial Prespective.** New Jersey: John Wiley & Sons, Inc.

CHAPTER V

BATCH CRYSTALLIZATION AND GROWTH

KINETICS OF MIXED LYSOZYME-OVALBUMIN

5.1   Abstract

The batch crystallization of lysozyme from lysozyme-ovabumin mixtures was performed in a 100 mL agitated crystallizer that was modified from a Schott bottle. The experimental conditions used are varied to study the effect of each parameter on the growth kinetics of lysozyme crystal and the separation ability of the process. The initial relative supersaturations were 3.955 and 5.052, ovalbumin impurity concentrations were 28, 50, and 67.5% (based on the total weight of protein), temperature of 10 and 20 °C, and salt concentration of 3 and 4% NaCl. Experiments were performed using a solution volume of 50 ml, a seed with a mean crystal size of 8.0 μm (number-based) and 120 mg of seed in each experiment. The separation of lysozyme from the lysozyme-ovalbumin mixture was successful by crystallization. The fact that the product crystal was pure lysozyme was guaranteed by SDS-PAGE and activity tests, which showed that the purity of lysozyme product crystals is more than 96.5% and the remaining activity is greater than 97%. The product crystal yields (the ratio of mass of lysozyme crystallized on the total mass of lysozyme which can be crystallized at equilibrium) was greater than 80%. The growth kinetics of the crystallization process has been studied based on the measurement of the decline in lysozyme concentration with time. The crystal growth rate at higher supersaturation is

higher than subsequent crystal growth rate at lower supersaturation. There is no significant effect of the ovalbumin impurity up to the concentration of 67.5% ovalbumin (based on total protein). There is also no significant change in the growth kinetics of lysozyme when the NaCl concentration is changed from 3 to 4%. However, temperature has a significant effect on the growth of the crystal, with the growth rate constant being dependent on the temperature. The growth rates of lysozyme were found to be second order with respect to the relative supersaturation. Therefore the growth kinetics of the crystallization process is controlled by the surface integration mechanism. The calculated growth rate constants were 5.4×10^{-6} cm/hr and 2.5×10^{-6} cm/hr for the crystallization process at 20°C and 10°C, respectively. The calculated activation energy was 53.08 kJ/mol which supports the hypothesis that the crystallization process is controlled by the surface integration mechanism.

5.2   Introduction

Proteins are organic macromolecules and appear all around in our life. Examples of existing uses of protein are in food (Motoki and Seguro, 1998; Proctor and Cunningham, 1998; Yokoyama, Nio, and Kikuchi, 2004), in cosmetic products (Anton, Nau, and Nys, 2006; Chvapli and Eckmayer, 2007), in medicine and even nowadays in product such as packing film (Mecitoglu, Yemenicioglu, Arslanoglu, ElmacI, Korel, and Cetin, 2006; Stolte, Frohberg, Pietzsch, and Ulrich, 2010). To satisfy the increasing demand for proteins, method for protein extraction and purification are necessary on an industrial scale (Chang, Yang, and Chang, 2000; Tam, Chan, Ng, and Wibowo, 2011). Crystallization processes are one of the most

important separation and purification processes in the pharmaceutical, chemical, and food industries. In general, the main active pharmaceutical ingredients (APIs), and a large number of other chemicals are produced in the solid form (Tung, Paul, Midler, and McCauley, 2009). In addition, proteins are more stable in the crystalline state than in solution (Drenth and Haas, 1992).

In protein crystallization studies the thermodynamic and kinetics of the process is easily influenced by environmental and also experimental conditions such as supersaturation, protein impurity, temperature, solution pH, and salt concentration. When the supersaturation increases the induction time to form nuclei becomes shorter resulting in an increase in the number of crystals, and it also influences the growth and shape of the crystal (Burke, Leardi, Judge, and Pusey, 2001; Elgersma, Ataka, and Katsura, 1992; Judge, Jacobs, Frazier, Snell, and Pusey, 1999; Nadarajah, Forsythe, and Pusey, 1995; Ries-Kautt, Ducruix, 1992). For the effect of impurities of the kinetics of the process, impurities can affect the rate of nucleation and growth, often (or usually) with an effect out of proportion to the amount involved (Tung, Paul, Midler, and McCauley, 2009). The crystallization of lysozyme with conalbumin as an impurity is an example; conalbumin has an effect on the {110} face growth rate of lysozyme at concentrations larger than 30%, and has an obvious effect on the {101} face growth rate when the concentration is above 10% (Judge, Forsythe, and Pusey, 1998). However, there are some studies which reported that there was no effect of the presence of an impurity on the crystallization kinetics of a protein (Judge, Forsythe, and Pusey, 1998; Judge, Johns, and White, 1995). In crystallization of lysozyme with ovalbumin impurity, ovalbumin has no significant effect on the face (both 110 and 101 face) growth rate of lysozyme even with ovalbumin concentration up to 50%. In

the same way, for crystallization of ovalbumin there was no observed effect in the presence of both lysozyme and conalbumin with the concentration up to 14%. The effect of temperature on the kinetics of crystallization process is often quoted as a means for controlling supersaturation (Burke, Judge, and Pusey, 2001; Rosenberger, Howard, Sowers, and Nyce, 1993). Generally an increase in the temperature decreases the supersaturation because of the increasing solubility when the temperature is increased. However, in crystallization of lysozyme (with nucleation), increases in temperature when the concentration is held constant typically increases the number of nucleated crystal (Burke, Leardi, Judge, and Pusey, 2001; Judge, Jacobs, Frazier, Snell, and Pusey, 1999), decreases the growth rate (Nadarajah, Forsythe, and Pusey, 1995), and has a notable effect on habit of the crystal (Elgersma, Ataka, and Katsura, 1992; Lu, Wang, and Ching, 2002). High temperature gives an elongated rod/prism-like crystal, which become shorter and thicker when the temperature is decreasing. The solution pH has a notable effect on nucleation but not significant on growth of the crystal. In the crystallization of lysozyme at 4 °C, the number of crystal nucleating is increased with a decrease of the pH, while the {101} facial growth rate is also decreasing (Judge, Jacobs, Frazier, Snell, and Pusey, 1999). They reported that when the pH changed from 4.0 to 4.6, 4.6 to 4.8, and 4.8 to 5.2 the number of crystals nucleated drops by a factor of around 1.5, 20 and 2, respectively. However, Forsythe, Ewing, and Pusey (1994) proposed a dissimilar result for the effect of solution pH on the growth rate of tetragonal lysozyme crystal. At a specific supersaturation, at some point the growth rate increased with pH and a some point it decreased with increasing pH. Salt concentration always has an effect on protein solubility and can be predicated that it is a means for controlling supersaturation like temperature. An increase in salt

concentration decreases the solubility (Forsythe, Judge, and Pusey, 1999; Maosoongnern, Borbon, Flood, and Ulrich, 2012) and results in increasing of supersaturation, which must have an effect on the nucleation, growth, and habit of the crystal.

As mentioned above, there are several parameters that have an effect on the crystal growth kinetics of the process, and almost all of the prior literature studied the crystallization process involving pure (or single) protein solutions. Therefore, the crystal growth kinetics and crystallization of pure protein from a mixture of proteins will be studied in this chapter.

In this work, the isothermal seeded batch crystallization of lysozyme from mixed lysozyme-ovalbumin solutions has been study to determine the growth kinetics of the crystallization process and the ability to crystallize pure lysozyme from mixed protein solutions. The growth kinetics were determined based on the measurement of lysozyme concentration decay with time (observation of the desupersaturation curve) by assuming no nucleation, no breakage, and no agglomeration occurs during the crystallization process (only crystal growth occurs). This assumption was checked based on analysis of the crystal products and by checking for apparent nuclei in micrographs The measured concentrations are converted to predicted crystal mass, crystal size, and finally to the crystal growth rate by using the mass balance. A power-law model equation of the growth rate was used to fit the growth rate data as a function of relative supersaturation to determine the growth rate order and the growth rate constant. The batch crystallization experiments were performed at verified solution conditions (i.e. initial lysozyme concentration, initial ovalbumin concentration, temperature, salt concentration, and pH) to observe the behavior of the

growth kinetics. The nature of the lysozyme crystal was characterized by SDS-PAGE and an activity test to determine the purity and the remaining activity of the crystals.

5.3 Theory

In this section, the effect of impurities on the growth of a crystal is described. Other important phenomena or theories relating to crystallization from solution are described in previous Chapters. Solubility and the effect of solution conditions on solubility are discussed in Chapter II. Supersaturation, nucleation, and metastable zone width are discussed in Chapter III. Crystal growth is discussed in Chapter IV.

5.3.1 Effect of Impurity on Crystal Growth

In general crystallization processes the presence of impurity or chemical species in the solution can have a profound effect on the growth of a crystal (Mullin, 2001; Randolph and Larson 1988). Some impurities need to be present in moderately large amounts before having any effect, some impurities can influence the growth of the crystal at a very low concentration. However, some impurities may not have a significant effect on the growth. When the impurities influence the growth of a crystal, they are often adsorbed on to the crystal surface and reduce the growth rate of the crystal as seen in Figure 5.1. Based on the Kossel model there are three sites that need to be considered; kink site (Figure 5.1(a)), step site (Figure 5.1(b)), and flat site (Figure 5.1(c)). The impurity molecule may adsorb and cover all of the crystal surface or be adsorbed selectively at any site. Due to these mechanisms the crystal growth rate may be increased, decreased, or remain the same value as reviewed by Davey (1979) and Davey (1982). Theoretical considerations of adsorption (based on experimental observations) at three different sites which affect the growth rate

retardation can be classified into three level of present in impurity concentration (Davey and Mullin 1976). Firstly, adsorption selectively at a kink site; this adsorption may influence the growth at very low concentrations of impurity. Secondly, adsorption selectively at a step site; this adsorption may influence the growth if a larger amount of impurity is presented. Lastly, adsorption selectively at a flat site; a much higher level concentration of impurity may be needed to affect the growth rate.
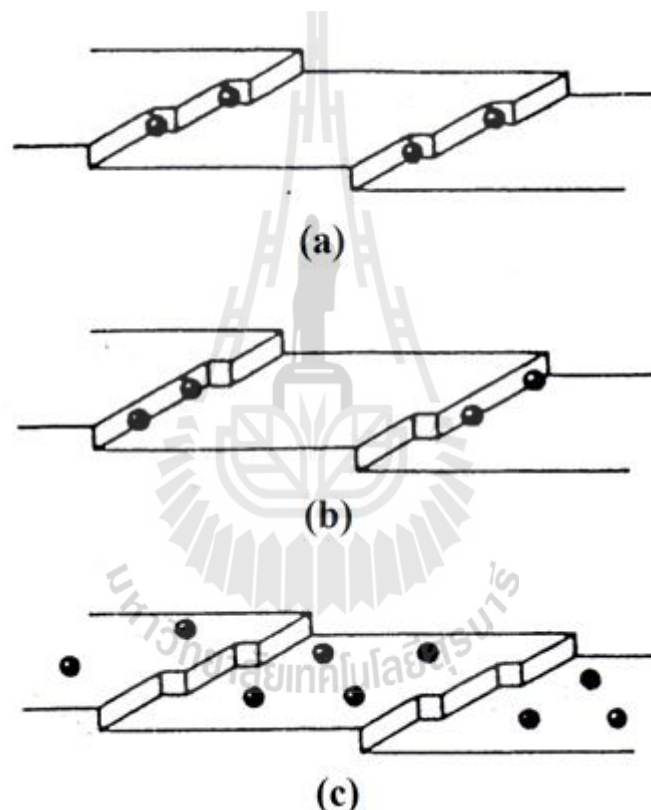
Figure 5.1 Sites for impurity adsorption on a growing crystal, based on Kossel

model: (a) kink site, (b) step site, (c) flat site (adapted from Davey

and Mullin, 1974).

Theoretical analyses of the effects of an impurity on the crystal growth rate have been studied by several work groups (Boistelle, 1982; Bunn, 1933; Cabrera and Vermilyea, 1958; Chernov, 1965; Davey, 1976; Lacmann and Stranski, 1958). They proposed that the progress of growth layers on a crystal surface is blocked by individually adsorbed impurity species.

The relative growth layer velocity in the present of an impurity and in pure solution can be expressed as following equation (Kubota and Mullin, 1995).

$$\frac{v}{v_0} = 1 - \alpha \theta_{eq} \qquad (5.1)$$

Where v is the growth layer velocity in the presence of an impurity, v_0 is the growth layer velocity in the pure solution, α is an impurity effectiveness factor, θ_{eq} is the fractional surface coverage by adsorbed impurity at equilibrium.

The number of active sites of the growth layer that are blocked by an impurity can be related to the impurity concentration in the solution using the Langmuir adsorption isotherm, and such models have been proposed (Black, Davey, and Halcrow, 1986; Davey and Mullin, 1974). Therefore, assuming the Langmuir adsorption isotherm is able to express the equilibrium fractional surface coverage as in equation 5.2

$$\theta_{eq} = \frac{Kc}{1 + Kc} \qquad (5.2)$$

Where K is the Langmuir constant and c is the impurity concentration. Therefore equation (5.1) becomes

$$\frac{v}{v_0} = 1 - \alpha\left(\frac{Kc}{1 + Kc}\right) \qquad (5.3)$$

Assuming the crystal face growth rate (G) is proportional to the growth layer velocity gives

$$\frac{G}{G_0} = 1 - \alpha\left(\frac{Kc}{1 + Kc}\right) \qquad (5.4)$$

The calculated relative growth layer velocity (step velocity) from equation (5.3) for several different effectiveness factors as a function of the dimensionless impurity concentration is shown in Figure 5.2. The three types of growth layer velocity were found and reported in the literature. For $\alpha = 1$, the growth layer velocity approaches zero asymptotically. An example is the effect of $FeCl_3$ and $AlCl_3$ on the growth velocity of ammonium dihydrogen phosphate (Davey and Mullin, 1974). For $\alpha < 1$, the growth layer velocity never approaches a zero value, however the impurity concentration is increases. An example is the effect of an aliphatic carboxylic acid on the growth velocity of KBr (Bliznakov and Nikolaeva, 1967). For $\alpha > 1$, the growth layer velocity decrease very rapidly with increasing impurity concentration. The example is the effect of raffinose on the growth velocity of sucrose (Albon and Dunning, 1962).
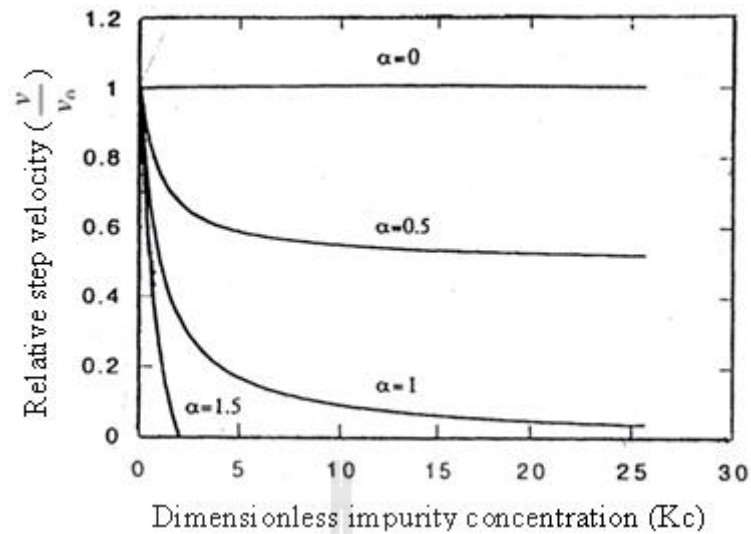
Figure 5.2 Relationship between the relative step velocity ($\frac{v}{v_0}$) and the

dimensionless impurity concentration (Kc) for different values

of the impurity effectiveness factor (α) (Mullin, 2001).

5.3.2 Effect of Temperature on Crystal Growth

The growth rate is temperature dependent and can be expressed as equation (5.5), the Arrhenius relationship (Mullin, 2001).

$$k_G = k_G^0 \exp(-\frac{E_G}{RT}) \tag{5.5}$$

where E_G is the activation energy of growth (kJ/mol), T is the temperature (K), k_g^0 is a pre-exponential constant (m/s), and R is the ideal gas constant (8.314 J/mol·K). The activation energies values are typically in the range 10 - 20 kJ/mol for a diffusion controlled mechanism and 40 - 60 kJ/mol for a surface integration controlled mechanism (Mullin, 2001).

5.4   Materials and Methods

5.4.1   Materials

Hen egg white lysozyme (HEWL, product No. 62971) and ovalbumin (product No. A5253) were purchased from Sigma-Aldrich. These two proteins were used without further purification since no other proteins were detected in a SDS-PAGE gel electrophoresis analysis (15% acrylamide).

Sodium chloride (purity ≥99.5%), sodium acetate trihydrate (purity ≥99.5%) and acetic acid (100%) were purchased from Carl Roth. All chemicals and deionized water were used without further purification to prepare buffer solution based on the method of Dawson et al. (1986) and salt solution as described in chapter II.

Micrococcus lysodeikticus (ATCC No. 4698) was purchased from Sigma-Aldrich. Potassium dihydrogen phosphate (purity ≥99%) and potassium hydroxide (RPE analytical) were purchased from Carlo. The bacteria and these chemical were used to prepare the reagent for the activity test for lysozyme.

Acrylamide (purity ≥99.5%), bis-acrylamide (purity ≥99.5%), SDS (purity ≥99.5%), Ammonium persulphate (purity ≥98%), Tris-base (purity ≥99.8%), TEMED (BioReagent), Laemmli Sample Buffer (BioReagent), and BME (purity ≥98%), were purchased from Bio-Rad. These chemicals were used to prepare the reagents for SDS-PAGE analysis.

5.4.2   Apparatus

A 100 mL batch crystallizer that was modified from a Schott bottle (Figure 4.5 in Chapter IV) was used to crystallize and measure the growth rate of lysozyme from the mixtures of lysozyme and ovalbumin. The lysozyme protein slurry

is continuously agitated at 100 rpm by a centrally located three-blade impeller driven by a connected motor gear. The crystallizer was placed inside a constant temperature water bath, where the temperature was controlled within ±0.5°C.

5.4.3 Preparation of Lysozyme Seed Crystal (Tetragonal Form)

Lysozyme seed crystals were prepared by mixing equal volumes of protein solution and salt solution, and keeping this solution at around 8°C (using a refrigerator) as described in Chapter IV section 4.4.2. The mean size of the seed crystals was approximately 8 μm (number- based) as determined by a laser diffraction particle size analyzer (LA-950, Horiba). This is consistent with the average particle size seen on a photograph of the seed crystals (Figure 5.4, left). The particle size distribution of the seed crystals is shown in Figure 5.3.
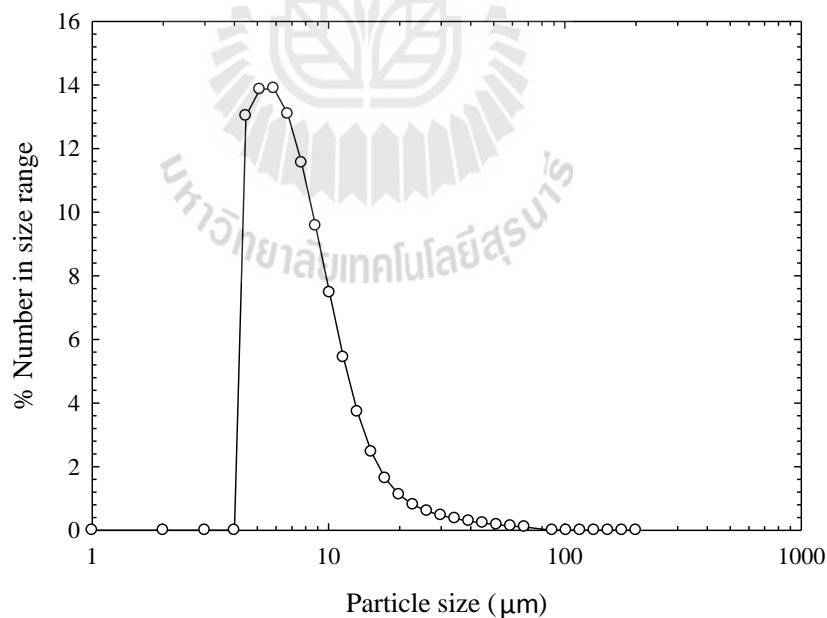
Figure 5.3 Particle size distribution (number-based) of the seed crystals.

5.4.4 Crystallization and Crystal Growth Rate Measurement

The crystallization and growth kinetics of lysozyme were studied using isothermal seeded batch crystallization. The experiments were performed in a 100 mL batch crystallizer agitated at 100 rpm by a centrally located three-blade impeller driven by a connected motor gear. The solution conditions were verified as following: the initial lysozyme concentration ranged from 10 to 25 mg/mL, the initial impurity concentration ranged from 28 to 66% (protein impurity on total protein), temperature of 20 and 10°C, salt concentration 3 and 4%, and pH value 5.0 and 5.6. Three solutions: lysozyme solution, ovalbumin solution, and salt solution were mixed together with the seed crystal to start each experiment. The experimental procedure will be described for experiment 1-1 (Table 5.1) as an example. A 10 mL solution of 125 mg/mL lysozyme in 0.1M sodium acetate buffer pH 5.0 and a 25 ml solution of 50 mg/mL ovalbumin in the same buffer were added together into the crystallizer and then 70 mg of lysozyme seed crystals was added. After seed was added, 2 g of NaCl in 15 mL of the same buffer was slowly put into the crystallizer as a last solution. This initial experimental condition was performed to ensure that the crystallization occurred within the metastable zone to avoid the nucleation of new crystal (only crystal growth occurs); the estimated solubility was approximately 4 mg/mL (Forsythe, Judge, and Pusey, 1999; Maosoongnern, Borbon, Flood, and Ulrich, 2012).

The growth kinetics were studied within 24 hr using time dependent measurement of decline in protein concentration during crystallization (Carbone and Etzel, 2006; Carbone, Judge, and Etzel, 2005) as described in Chapter IV section 4.4.4. However the UV absorbance technique for the mixed solution (see Chapter II section 2.4.5.2) was applied instead of UV the absorbance technique for pure solution.

All experimental conditions for the crystallization and crystal growth rate measurement of lysozyme from mixed protein solutions are shown in Table 5.1. These various experimental conditions are chosen to ensure that the crystallization occurred within the metastable zone and the crystals grew as the tetragonal crystal not the orthorhombic crystal: when the solution conditions were changed the crystals can growth into the different morphology.

Table 5.1 Experimental conditions for crystallization and growth experiments.

The number mean lysozyme seed size is 8 μm.

Exp. No.	$c_{lys,0}$ (mg/mL)	$c_{oval,0}$ (mg/mL)	Temp. (°C)	NaCl (%)	pH
1-1 to 1-3	25	25	20	4	5
2-1 to 2-3	20	20	20	4	5
3-1 to 3-3	25	10	20	4	5
4-1 to 4-3	25	50	20	4	5
5-1 to 5-3	10	10	10	4	5
6-1 to 6-3	25	25	20	3	5

5.4.5 Crystal Size Calculation

The calculated concentrations were converted mathematically to number mean size of lysozyme crystal in order to determine the number mean growth rate of the crystals (as in equation (4.13) in Chapter IV).

$$L^3 = \frac{m_s + (c_i - c_t)V}{n \rho k_v} \tag{5.5}$$

The term $\rho k_v L^3$ in the equation is the mass of a crystal based on the characteristic size L (Mullin, 2001; Randolph and Larson, 1988). Since assuming the number of crystal is constant then the term $n\rho k_v$ can be approximately calculated from the mass of seed (in all experiment 120 mg of seed was used) divided by the cube of the number-based mean size of the seed (approximately 8 µm), results in term $n\rho k_v$ is equal to 0.24. Since the solution volume of 50 mL was used, then the size of the crystals as expressed in equation (5.5) become

$$L^3 = \frac{120 + (c_i - c_t)50}{0.24} \tag{5.6}$$

5.4.6 Crystal Purity

The crystal purity was determined using the SDS-PAGE gel technique with 15% acrylamide as a separating gel and 5% acrylamide as a stacking gel based on the Mini-PROTEAN® Tetra Cell instruction manual (Cat. No. 165-8000 and 165-8001, Bio-Rad). The components of each gel are shown in Table 5.2 and 5.3.

Table 5.2 The components of the separating gel (15% acrylamide).

Component	Component Volume (mL)		
	5 mL	10 mL	20 mL
H_2O	1.2	2.3	4.6
30% Acrylamide mix	2.5	5	10
1.5 M Tris-Hcl, pH 8.8	1.3	2.5	5
10% SDS	0.1	0.1	0.2
10% Ammonium persulphate	0.1	0.1	0.2
TEMED	0.002	0.004	0.008

Table 5.3 The components of the stacking gel (5% acrylamide).

Component	Component Volume (mL)		
	2 mL	5 mL	10 mL
H$_2$O	1.4	3.4	6.8
30% Acrylamide mix	0.33	0.83	1.66
0.5 M Tris-Hcl, pH 6.8	0.25	0.63	1.26
10% SDS	0.02	0.05	0.1
10% Ammonium persulphate	0.02	0.05	0.1
TEMED	0.002	0.005	0.01

5.4.7 Activity of the Protein Crystal

The nature of the lysozyme product crystal was characterized by an activity test. Since lysozyme is an enzyme that can cause the lysis of bacteria, therefore the activity test is determined by measuring the UV absorbance decay in a suspension of micrococcus lysodeikticus bacteria resulting from their cell wall lysis in presence of lysozyme (Gorin, Wang, and Papapavlou, 1971; Shugar, 1952). In the test, the bacteria are treated by lysozyme powder and crystals in phosphate buffer pH 7.0. The UV absorbance measurements are carried out at a wavelength of 450 nm using a UV photometer (HP 8453, Agilent). The activity can be calculated by the following equation

$$Activity = \frac{(\Delta A_{450nm}/min\,Test - \Delta A_{450nm}/min\,Blank)}{(0.001)(C_{lys})(V_{lys})} \qquad (5.7)$$

Where $\Delta A_{450nm}/min\,Test$ is the change in an absorbance of the test solution (mixture of bacteria and lysozyme solution) per minute, $\Delta A_{450nm}/min\,Blank$ is the changed in an

absorbance of the reference solution (bacteria solution) per minute, C_{lys} is the concentration of lysozyme solution, and V_{lys} is the volume of lysozyme solution used. Assuming the powder has an activity of 100% then the calculated activity of the crystal is compared to the activity of the powder to determine the remaining activity of the crystals.

5.5   Results and Discussions

5.5.1   Batch Crystallization of Mixed Lysozyme-Ovalbumin

Lysozyme was crystallized from a mixture of lysozyme and ovalbumin. An example of photographs of the seed crystals and the product crystals from the crystallization is shown in Figure 5.4. A comparison of the photographs of seed and product crystals shows that there is no nucleation occurring during the growth process since no particle smaller than the seed crystal is observed. The examples of concentration measurement during the crystallization are shown in Table 5.4. The Mass of the crystal appearing in the crystallizer can be directly calculated from the concentration as in equation (4.11) and (4.12) in Chapter IV. The yield of the lysozyme for the crystallization can be calculated from the ratio between the actual mass of lysozyme crystallized and the predicted mass of lysozyme crystallized at equilibrium as expressed in equation (4.14) in Chapter IV. The calculation gives 84% yield for Exp. No.2-1.
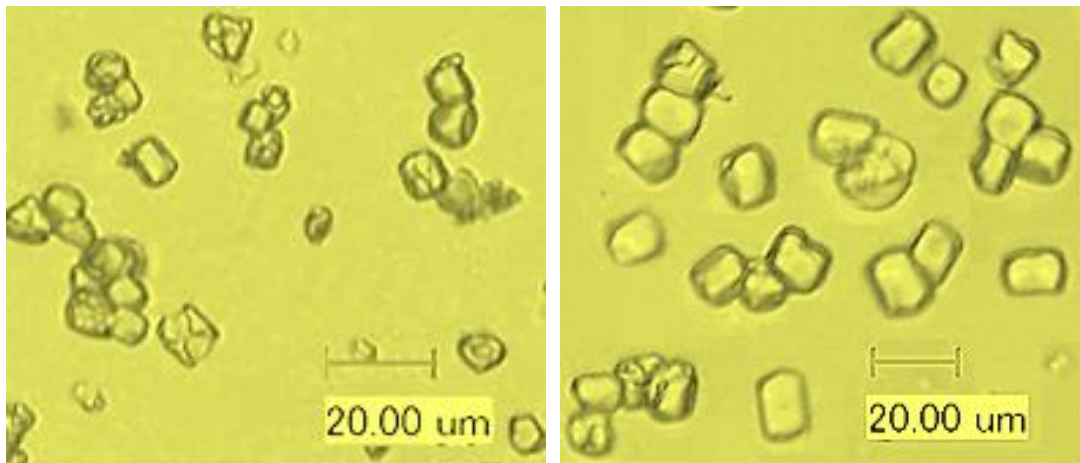
Figure 5.4 Photographs of Lysozyme seed crystals (Left) and product crystals

(Right). Crystallization of lysozyme from the mixed solution of

lysozyme-ovalbumin (Exp. No.2-1).

The example plots of decline in concentration with time are shown in Figure 5.5. As shows in Figure 5.5, the change in concentration of lysozyme is higher at the initial period of the crystallization process and becomes slower as the crystallization progresses.

Table 5.4 Concentration measurement and calculation of the total mass of crystal. Crystallization of lysozyme from the mixed solution

of lysozyme-ovalbumin (Exp. No.2-1).

t (hr)	Absorbance						C_{lys} (mg/mL)	C_{oval} (mg/mL)	m_{cryst} (mg)
	A250	A260	A270	A280	A290	A300			
0.00	0.3553	0.3774	0.6447	0.7438	0.5554	0.1209	24.2096	24.3725	120.0000
1.00	0.3339	0.3553	0.6041	0.6971	0.5193	0.1138	22.2500	24.4520	217.9800
2.00	0.3092	0.3297	0.5576	0.6437	0.4785	0.1056	20.1235	24.1286	324.3050
3.00	0.2894	0.3093	0.5196	0.6000	0.4447	0.0990	18.2287	24.4453	419.0450
4.00	0.2745	0.2939	0.4911	0.5673	0.4194	0.0941	16.8421	24.5478	488.3750
5.00	0.2568	0.2755	0.4577	0.5288	0.3900	0.0882	15.3000	24.3624	565.4800
6.00	0.2455	0.2637	0.4364	0.5044	0.3713	0.0844	14.3278	24.2085	614.0900
8.00	0.2276	0.2454	0.4023	0.4652	0.3410	0.0785	12.6470	24.4152	698.1300
10.00	0.2102	0.2274	0.3694	0.4274	0.3120	0.0727	11.1028	24.3258	775.3400
12.00	0.1982	0.2150	0.3466	0.4012	0.2919	0.0687	10.0156	24.3329	829.7000
15.00	0.1886	0.2049	0.3284	0.3803	0.2759	0.0655	9.1852	24.1952	871.2200
18.00	0.1782	0.1941	0.3087	0.3575	0.2584	0.0620	8.2350	24.2265	918.7300
21.00	0.1710	0.1868	0.2950	0.3418	0.2462	0.0597	7.5546	24.3278	952.7500
24.00	0.1681	0.1838	0.2892	0.3352	0.2410	0.0587	7.2340	24.5024	968.7800

* Dilution factor = 100
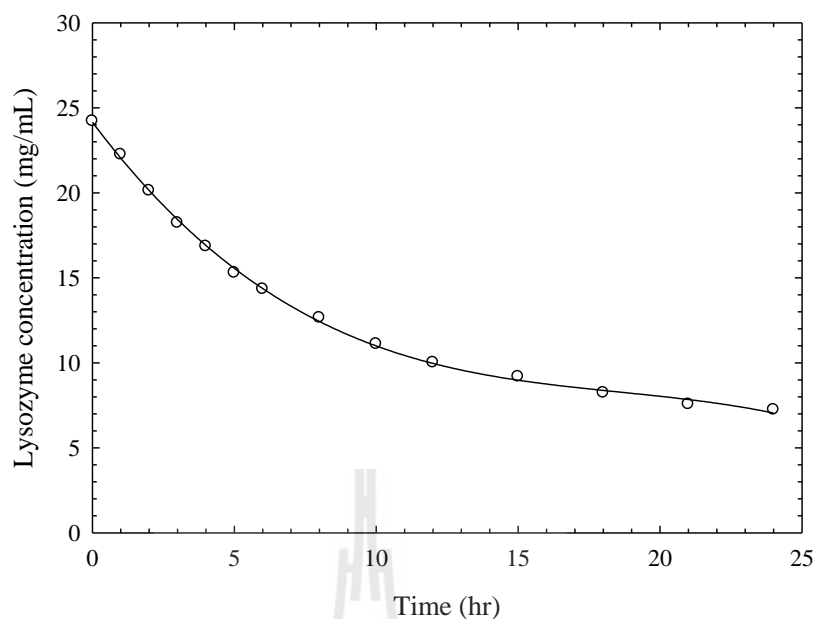
Figure 5.5 Concentration decay of lysozyme crystallization (Exp. No. 2-1).

5.5.2 Separation of Lysozyme and Ovalbumin.

In this section the possibility of separation of pure lysozyme from the mixed solution of lysozyme – ovalbumin using crystallization was investigated. In section 4.5.1, the measurement of the concentration decay with time of lysozyme was presented which indicating that lysozyme was crystallized out of the solution. However, we wanted to see whether it was possible to separate mixtures of lysozyme and ovalbumin by crystallization in cases where (a) only lysozyme was supersaturated (i.e. by knowing the phase diagram well enough we can choose a point where only lysozyme crystallizes), and (b) by preferential crystallization (with lysozyme seeding only) to achieve pure lysozyme crystals under conditions where both proteins are supersaturated.

To achieve this, the ovalbumin concentrations were varied at 10, 25, and 50 mg/mL as seen in Table 5.1, the initial condition of Exp. No.1, No.2, and No.3, respectively. Unfortunately, the solubilities of ovalbumin were prepared only at

25°C. Since during the early research the crystallization was designed to operate at 25°C but this criteria was changed later. Although, the solubility of ovalbumin at 20°C was not known, it can approximate from the solubility at 25°C using the van't Hoff relation. Figure 5.6 shows the solubility of ovalbumin at 25°C and 4% NaCl with points indicating the location of the initial ovalbumin concentration of the three experiments.
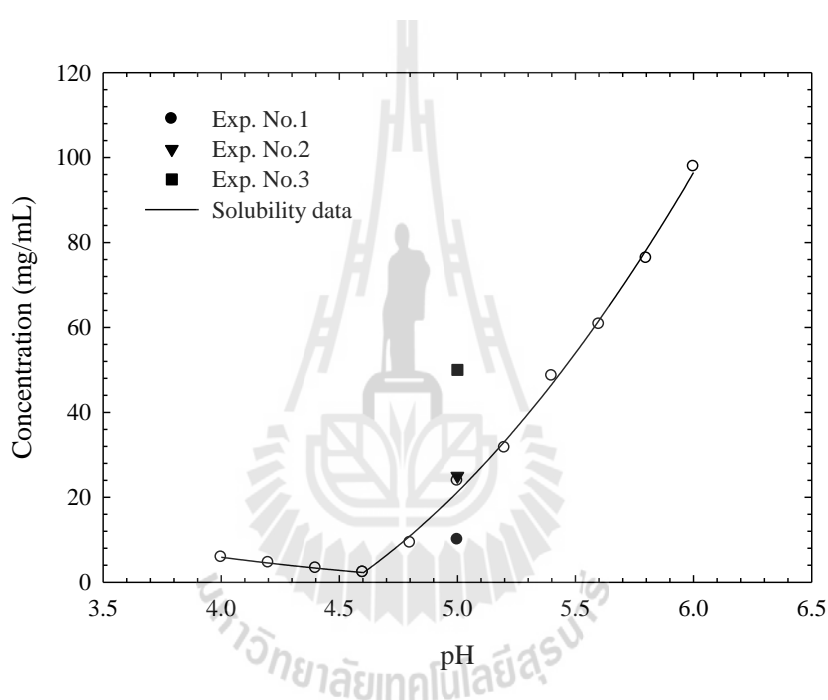
Figure 5.6 Solubility of ovalbumin at 25°C and 4% NaCl with points indicating the

    initial concentration of ovalbumin for three experiments.

The initial concentrations of ovalbumin compared to the solubility at 25°C shows that the ovalbumin concentration for Exp. No.1 is undersaturated while Exp. No.2 and Exp. No.3 are supersaturated. The solubility as a function of temperature can be determined via the van't Hoff equation (Broide, Tominc, and Saxowsky 1996; Flood 2009) which indicates that solubility is increasing with

increased temperature. Therefore, the solubility of ovalbumin at 20°C should be lower than the solubility at 25°C meaning the initial concentration of ovalbumin for Exp. No.2 and Exp. No.3 are certainly supersaturated. The concentration measurement and calculations for the crystallization of these three experiments are shown in the Appendix D. The mass of the protein crystallized are 869.32, 848.78, and 765.7 mg for Exp. No.1, No.2, and No.3, respectively. These results show that the protein can be crystallized from the mixture of lysozyme and ovalbumin. However, the purity of the protein product has to be verified; whether only pure lysozyme was crystallized, or both proteins were crystallized.

The composition of the protein product was determined by the SPS-PAGE gel technique as shown in Figure 5.7. The band appearing in well 2 is a low-range protein standard marker; well 4 is the protein product of Exp. No.1; well 6 is the protein product of Exp. No.2, and well 8 is the protein product of Exp. No.3. Different amounts of protein samples 30, 45, and 60 µg were overloaded (normally aproximately 15 µg was used) into well 4, 6, and 8, respectively. Only one band was detected in well 4, 6, and 8, and this band was lysozyme, however overloaded amounts of the protein samples were used. This indicates that only lysozyme was crystallized even when ovalbumin was also supersaturated. Therefore, this can guarantee that it is possible to separate pure lysozyme from the mixed solutions of lysozyme and ovalbumin using seeding crystallization, whether only lysozyme was supersaturated or when both protein were supersaturated.
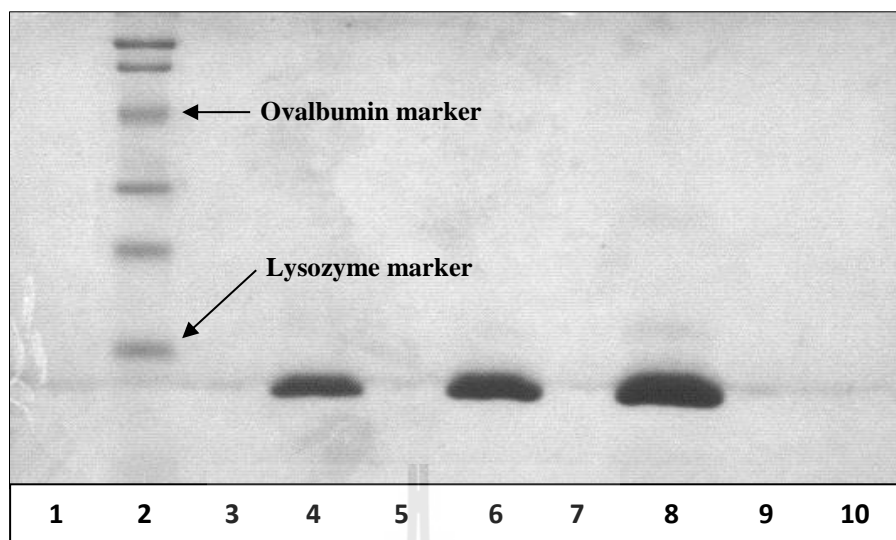
Figure 5.7 SDS-PAGE gel analysis of the product crystal for Exp. No. 1 (well 4),

Exp. No.2 (well 6), and Exp. No.3 (well 8) with an overloaded amount

of protein.

5.5.3 Purity and Activity of Lysozyme Product Crystal

The product purity was guaranteed by SDS-PAGE and the activity test.
An example of SDS-PAGE is shown in Figure 5.8; the different bands of each gel
contains a different protein. Well 2 is pure lysozyme, well 4 is pure ovalbumin, well 6
is the mixed solution before crystallization, and wells 8 and 9 contain product crystal.
The only band detected in wells 8 and 9 was lysozyme; this band is at the same
position with the lysozyme in well 2. This means that no other protein can be detected
in the product crystal. The purity of the product crystal can be described by the
intensity of the band using Coomassie Blue staining solution. The detection limit
when using this stain was approximately 0.5µg/well and the sample load for each well
was 15 µg. Consequently, the crystal contains lysozyme at approximately more than
96.5% of total protein.
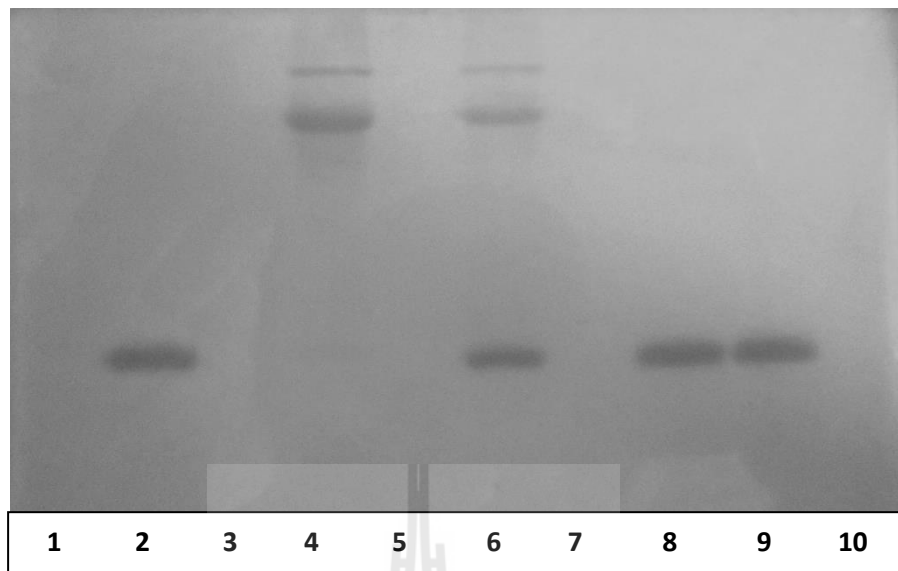
Figure 5.8 SDS-PAGE gel (Exp. No.2-1).

When the purity of the lysozyme crystal was confirmed, the remaining activity of the crystal was also determined by measuring the absorption decay of Micrococcus lysodeikticus with addition of lysozyme. Since lysozyme is a protein that can lysis the bacterial cell wall this test can measure lysozyme activity. The example of the activity of lysozyme powder and product crystal is shown in Figure 5.9.
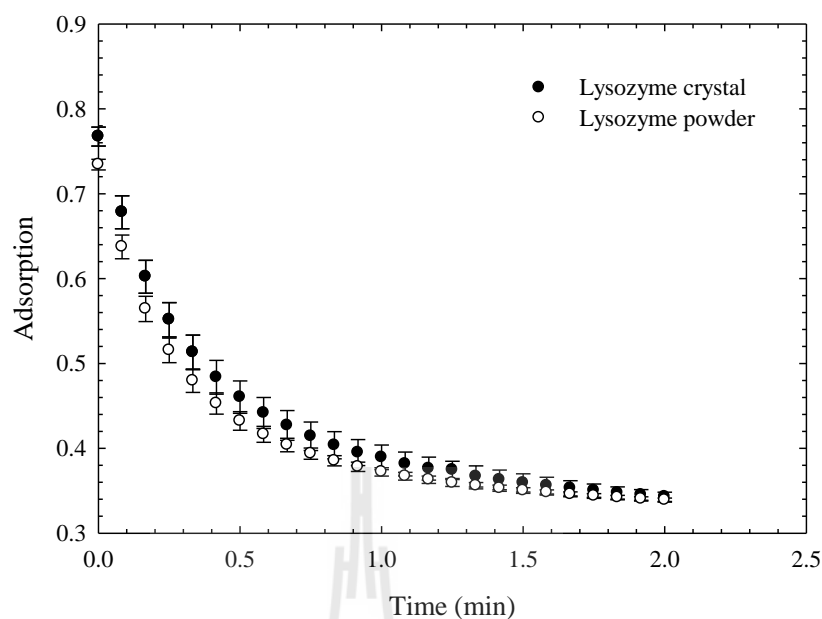
Figure 5.9 Activity test for Exp. No.2: adsorption decay of a *Micrococcus*

lysodeikticus.

The absorbance was measured three times for each experiment. At the beginning of the reaction the change in adsorption is very fast, and it tends to reach equilibrium within two or three minutes. However, in the calculation of activity, equation (5.6), the change in the absorbance used must be linear. Therefore the linear part of the curve at the beginning of reaction was used to calculate the activity. Assuming the activity of the lysozyme powder is 100%, the calculated remaining activity of the crystal is more than 97% (see Appendix C for example of calculation).

5.5.4 Crystal Growth Kinetics of Lysozyme

The mean crystal growth rate was determined as the ratio of the change in the number mean crystal size vs time. The number-based mean crystal size was used to calculate the crystal growth rate since the crystal growth rate data can only be obtained from the batch crystal growth using the population balance, which is a

number-based equation. The example of the crystal growth rate calculation procedure for Exp. No.2-1 is shown in Table 5.5. Concentrations are converted to number-based mean crystal size using equation (4.3) in Chapter IV. The growth rate was calculated directly from the rate of the change in a number-based mean crystal size with time for each measurement.

Table 5.5 Example of calculation in size and growth rate of the crystal (Exp. No.2-1, see Appendix D for other Exp. No.)

t (hr)	C_{lys} (mg/mL)	$\bar{L}$ (μm)	σ (-)	G (μm/hr)
0.00	24.2096	8.0000		
1.00	22.2500	9.6843	5.0524	1.6843
2.00	20.1235	11.0556	4.5625	1.3713
3.00	18.2287	12.0416	4.0309	0.9860
4.00	16.8421	12.6721	3.5572	0.6305
5.00	15.3000	13.3066	3.2105	0.6346
6.00	14.3278	13.6775	2.8250	0.3709
8.00	12.6470	14.2750	2.5820	0.2987
10.00	11.1028	14.7829	2.1618	0.2540
12.00	10.0156	15.1206	1.7757	0.1689
15.00	9.1852	15.3688	1.5039	0.0827
18.00	8.2350	15.6432	1.2963	0.0915
21.00	7.5546	15.8339	1.0588	0.0636
24.00	7.2340	15.9223	0.8887	0.0294

The mean crystal growth rates (which were calculated using the approximation of the ratio of the number mean crystal size on the change of the time) can be expressed in the form of power law model as described in Chapter IV.

$$G = \frac{\Delta L}{\Delta t} = k_G \sigma^n \tag{5.8}$$

and can be rearranged as

$$\log G = \log k_G + n \log \sigma \qquad (5.9)$$

Fitting the mean growth rate data and supersaturation with (5.9) gives a straight line approximation. Therefore n and $log\ k_g$ can be directly obtained from the slope of the line and the y-intercept, respectively. In crystallization of lysozyme, the growth rate order $n = 2$ was used to fit the equation since there are several works reporting a good fit with this value (Carbone and Etzel, 2006; Saikumar, Glatz, and Larson 1998).

5.5.4.1 Effects of Supersaturation

Figure 5.10 shows the mean crystal growth rate as a function of supersaturation at 20°C, 4% NaCl, pH 5.0, and around 50% ovalbumin impurity. The result shows that an increase in the supersaturation results in an increase in the mean crystal size. This is since the higher solute concentration in excess of the solubility leads to a higher amount of solute addition onto the surface of the crystal. However, an increase in the initial supersaturation from 3.955 to 5.052 did not have an effect on the mean size or growth of the crystal. This is because lysozyme has a large metastable zone width. At this experimental condition the metastable zone limit of lysozyme is a supersaturation of around 12.5 (Maosoongnern, Borbon, Flood, and Ulrich, 2012). The supersaturation in this experiment is changed from 31% to 40% (compared to the metastable zone limit) and no effect was observed on the growth of the crystal. Therefore if the change in initial supersaturation is not large enough it does not effect on the growth of the crystal.
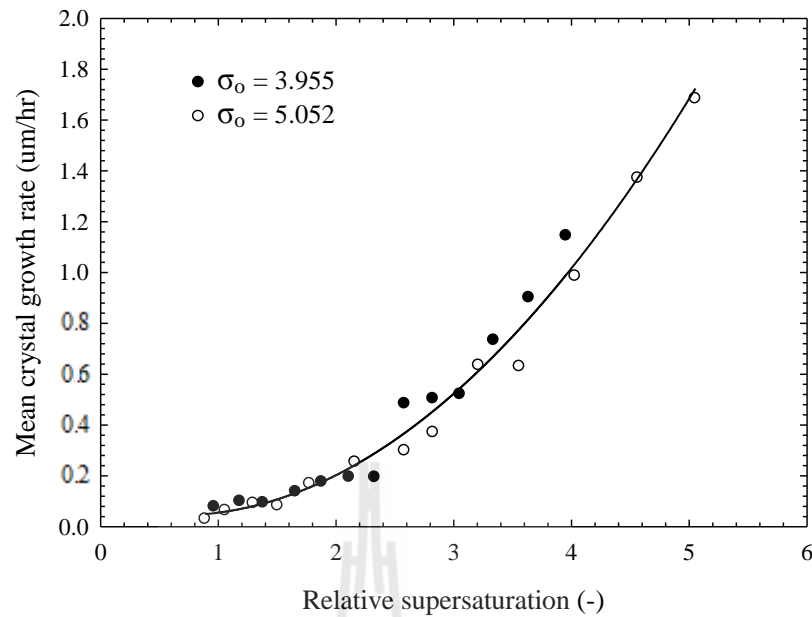
Figure 5.10 Mean crystal growth rates as a function of relative supersaturation

(Exp. No2-1. and No.4-1; 50% ovalbumin impurity, Temp. = 20°C,

4% NaCl, and pH 5.0).

5.5.4.2 Effects of Ovalbumin Impurity

The presence of ovalbumin as an impurity may have an effect

on the growth of a crystal lysozyme crystal. In this study, the crystallization process

was carried out at 20°C, 4% NaCl, and pH 5.0, with ovalbumin contents of 28%,

50%, and 67.5% (based on the ratio of the total protein). The growth data of lysozyme

crystal as a function of supersaturation were plotted and shown in Figure 5.11. The

results show that there is no significant effect of ovalbumin impurity (up to 67.5%) on

the growth of lysozyme crystals. It appears that a large amount of ovalbumin is

required before it has an effect on the growth of lysozyme crystal. Some impurities

need to be present in moderately large amounts before having any effect, some

impurities influence the growth of the crystal at a very low concentration and some

impurities may not have a significant effect on the growth. Based on the Kossel model, when the impurities influence the growth of a crystal, they are often adsorbed on to the kink site, step site, or the flat site of the crystal and reduce the growth rate of the crystal. In the case of ovalbumin impurity they would not adsorb/or adsorb selectively at a flat site, since the much higher level concentration of impurity are required to affect the growth rate.
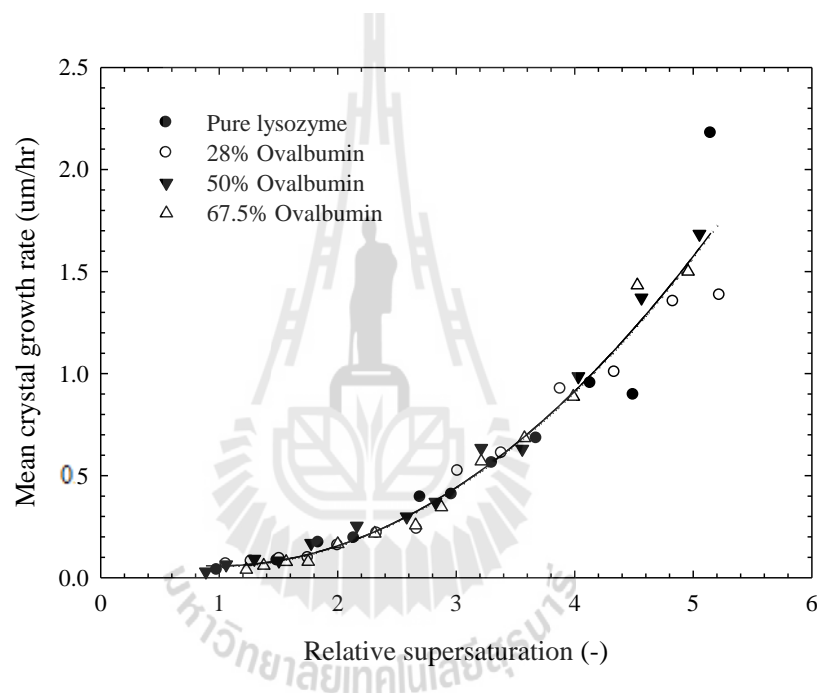
Figure 5.11 Mean crystal growth rates as a function of ovalbumin impurity (Exp. No.1-1, No.2-1, and No.3-1; Temp. = 20°C, 4 % NaCl, and pH 5.0).

5.5.4.3 Effects of Salt Concentration

Salt concentration always has an effect on the protein solubility and is a means for controlling supersaturation. Increasing salt concentration decreases the solubility (Forsythe, Judge, and Pusey, 1999; Maosoongnern, Borbon, Flood, and Ulrich, 2012) and results in an increase in the supersaturation which has an effect on

the nucleation, growth, and the habit of the crystal. However, in this study there was no observed effect on the growth rate of the lysozyme crystal (when it is calculated based on the relative supersaturation) when using 3% and 4% NaCl as a precipitant. The result is shown in Figure 5.12.
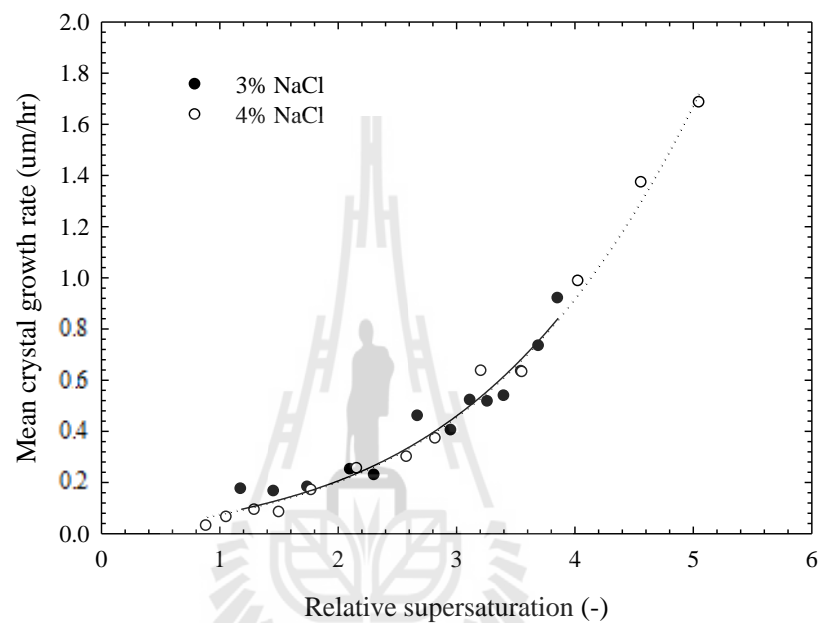
Figure 5.12 Mean crystal growth rates as a function of salt concentration and relative supersaturation (Exp.No.2-1 and No.6-1; 50% ovalbumin impurity, Temp. = 20°C, and pH 5.0).

5.5.4.4 Effects of Temperature

The growth rate is temperature dependent, and can be expressed as equation (4.10) which belongs to the Arrhenius relation (Mullin, 2001) and can be rearranged as equation (5.10).

$$\ln k_G = \ln k_G^0 - \frac{E_G}{RT} \tag{5.10}$$

Fitting the growth rate constant obtained from the plot of $\log G$ against $\log \sigma$ belong to the power-law model (equation (5.9)) and the temperature in the form of $\ln k_G$ against $\frac{1}{T}$ gives a straight line approximation with slope equal to the activation energy for crystal growth on the ideal gas constant ($\frac{E_G}{R}$). Figures 5.13 - 5.15 show plots of growth rate (in terms of $\log G$) as a function of relative supersatution which different initial condition at 20 °C. In the plots, the growth rate order $n = 2$ was used to fit the equation due to the results of Saikumar, Glatz, and Larson (1998). The plot showed a good fit of the straight line with the experimental mean growth rate data. Therefore the growth rate constant can be directly obtained from the y-intercept. The fitting equation (averaged value) is shown in equation (5.11) for the growth kinetics of tetragonal lysozyme crystal at 20 °C, pH 5.0. The seed size was 8 µm and the mass of 120 mg.

$$\log G = -1.2678(\pm 0.04) + 2\log \sigma \qquad (5.11)$$

This equation shows that the growth rate orders are equal to 2. This is indicates that the growth of the crystal is controlled by the surface integration mechanism as described in section Chapter IV. The growth constant in equation (5.11) was obtained from the crystallization at 20°C. Therefore, the average value of the growth rate constant at 20°C is 5.4×10^{-6} cm/hr.
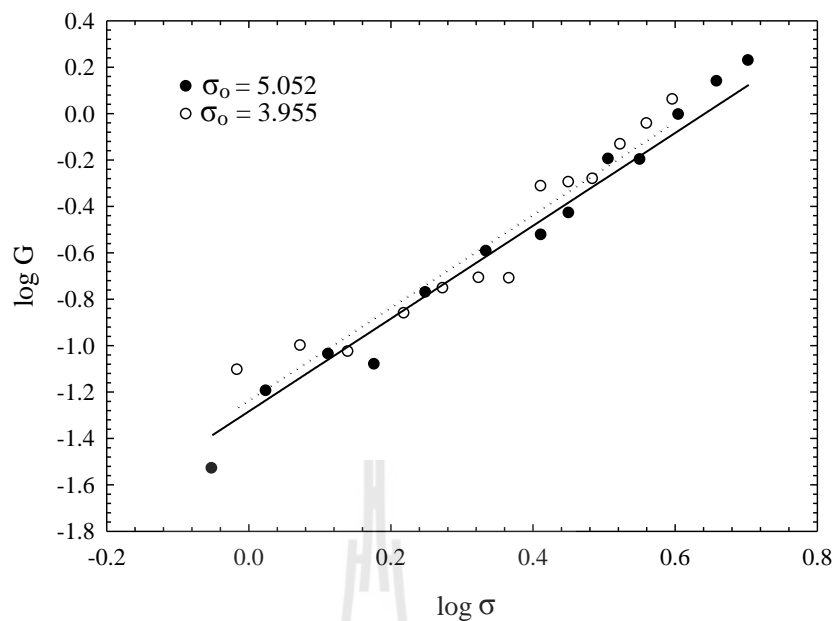
Figure 5.13 Plot of the growth rate and relative supersaturation with different initial

supersaturation (Exp. No.2-1 and No.4-1).
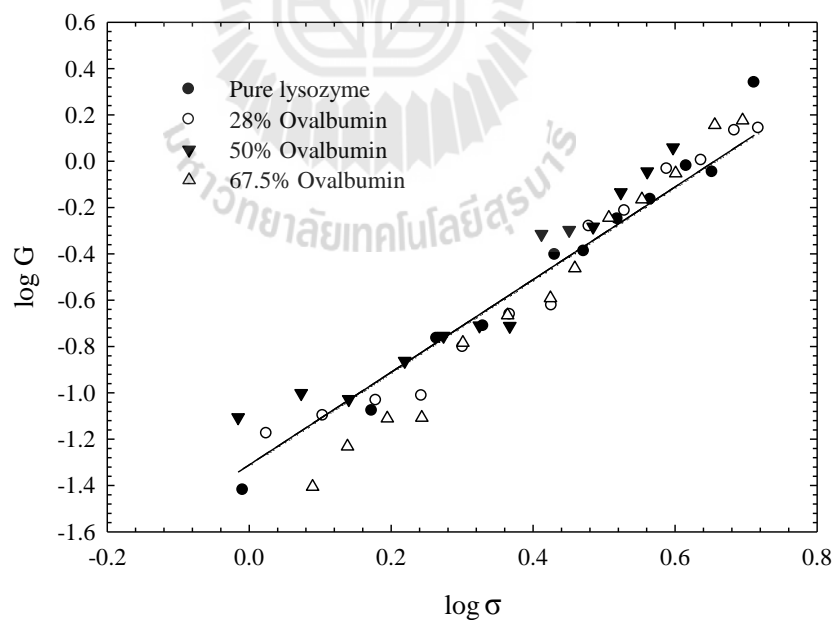
Figure 5.14 Plot of the growth rate and relative supersaturation with different

ovalbumin impurity concentration (Exp. No.1-1, No.2-1, No.3-1,

and pure lysozyme from Chapter IV).
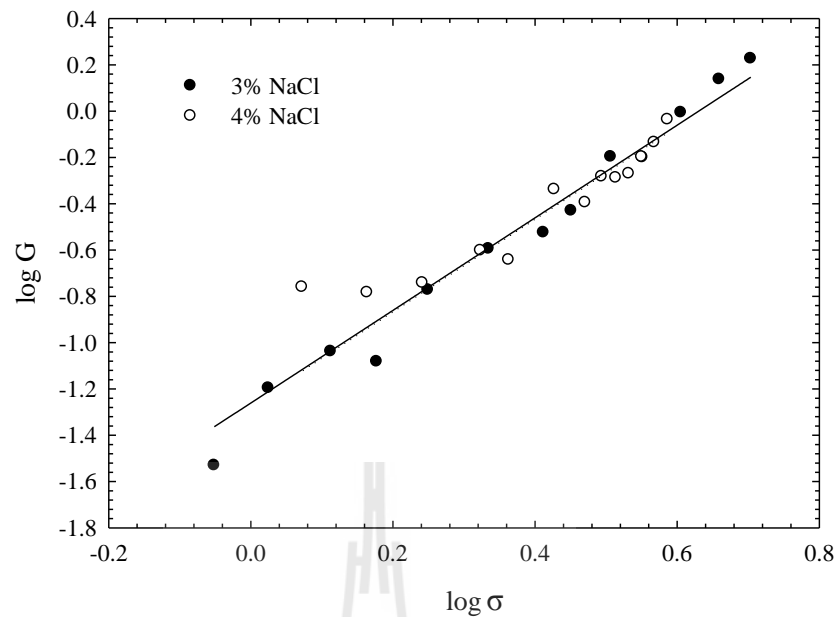
Figure 5.15 Plot of the growth rate and relative supersaturation with different salt

concentration (Exp. No.2-1 and No.6-1).

According to the Arrhenius relationship between growth rate

constant and temperature as described in equation (5.10): if only two measurement of

the growth rate constant at different temperature are available, the activation energy

of crystal growth can be estimated as following equation

$$E_G = \frac{RT_1 T_2}{T_2 - T_1} \ln \frac{K_{G,2}}{K_{G,1}} \tag{5.12}$$

Figure 5.16 shown the plots of growth rate as a function of

relative supersaturation at 10 °C. The fitting equation is show on equation (5.13).

Therefore, the growth rate constant calculated from the intercept of y-axis is 2.5×10^{-6}

cm/hr.

$$\log G = -1.6025 + 2\log \sigma \tag{5.13}$$
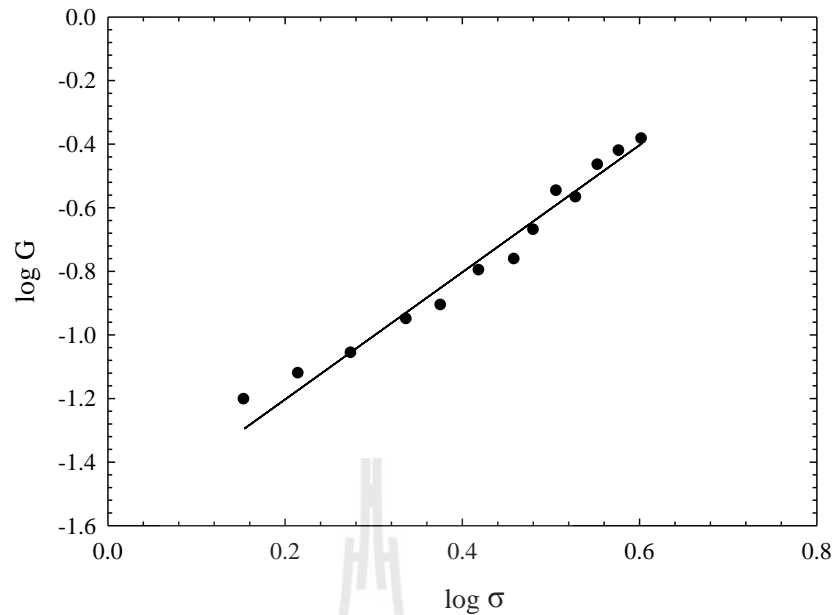
Figure 5.16 Plot of the growth rate and relative supersaturation at 10°C (Exp. No.6-1).

Since the growth rate constant at 10 and 20°C were known, the activation energy for crystal growth of lysozyme from the mixture of lysozyme-ovalbumin can be estimated by equation (5.14) and this gives the result of

$$E_G = 53.08 \text{ kJ/mol}$$

This value of activation energy can be used to support that crystal growth mechanism is controlled by surface integration mechanism. This is because if diffusion is controlling mechanism the activation energy usually around 10 - 20 kJ/mol, and if surface integration is controlled mechanism the activation energy usually around 40 – 60 kJ/mol (Mullin, 2001).

5.6 Conclusions

The batch crystallization of lysozyme from mixtures of lysozyme-ovabumin was performed in a 100 mL agitated crystallizer that was modified from a Schott bottle. The process was successful for crystallizing lysozyme out of the lysozyme − ovalbumin mixture using crystallization whatever only lysozyme was supersaturated or both protein were supersaturated (preferential crystallization with seeding with only lysozyme). The purity of the product crystal is greater than 96.5% guaranteed by SDS-PAGE, the remaining activity is greater than 97%, and the product crystal yield is up to 80%. The growth kinetics of the crystal has been studied by measurement of the decay in lysozyme concentration (or supersaturation) with time. Temperature and supersaturation has a notable effect on the growth of the crystal while ovalbumin impurity and NaCl concentration seem to have less effect (or need to present in large amount before influent the growth rate)

The growth rates order is equal to 2. This is indicating that the growth kinetics is controlled by the surface integration mechanism. The calculated growth rate constant values were 5.4×10^{-6} cm/hr and 2.5×10^{-6} cm/hr for the crystallization at 20°C and 10°C, respectively. The calculated activation energy was 53.08 kJ/mol which supports that the crystallization process is controlled by the surface integration mechanism.

5.7 References

Albon, N. and Dunning, W.J. (1962). Growth of sucrose crystals: the behavior of growth steps on sucrose crystals. **Acta Crystallographia** 15: 474-476.

Anton, M., Nau, F., and Nys, Y. (2006). Bioactive egg components and their potential uses. **World's Poultry Science Journal** 62: 429-438.

Black, S.N., Davey, R.J., and Halcrow, M. (1986). The kinetics of crystal growth in the presence of tailor-made additives. **J. Cryst. Growth** 79: 765-774.

Bliznakov, G. and Nikolaeva, R. (1967). Growth rate of {100} face of KBr. **Kristall und Tecknik.** 2: 161-166.

Boistelle, R. (1982). Impurity effects in crystal growth from solution. In **Interfacial aspects of phase transformations** (B. Mutaftschiev, ed.). Dordrecht: Reidel.

Bunn, C.W. (1933). Adsorption, oriented overgrowth and mixed crystal formation. **Proceedings of the Royal Society** 141: 567-593.

Burke, M.W., Judge, R.A., and Pusey, M.L. (2001). The effect of solution thermal history on chicken egg white lysozyme nucleation. **J. Cryst. Growth** 232(1-4): 301-307.

Burke, M.W., Leardi, R., Judge, R.A., and Pusey, M.L. (2001). Quantifying Main Trends in Lysozyme Nucleation: The Effect of Precipitant Concentration, Supersaturation, and Impurities. **Cryst. Growth Des.** 1(4): 333-337.

Cabrera, N. and Vermilyea, D.A. (1958). Growth of crystals from solution. **In Doremus, Roberts and Turnbull**: 393-410.

Carbone, M.N., and Etzel, M.R. (2006). Seeded Isothermal Batch Crystallization of Lysozyme. **Biotechnol. Bioeng.** 93(6): 1221-1224.

Carbone, M.N., Judge, R.A., and Etzel, M.R., (2005). Evaluation of a Model for Seeded Isothermal Batch Protein Crystallization. **Biotechnol. Bioeng.** 91(1): 84-90.

Chang, H.M., Yang, C.C., and Chang, Y.C. (2000). Rapid separation of lysozyme from chicken egg white by reductants and thermal treatment. **J Agric. Food Chem.** 48(2): 161-164.

Chernov, A.A. (1965). Some aspects of the theory on crystal growth forms in the presence of impurities. **In Kern** : 1-13.

Chvapli, M., and Eckmayer, Z. (2007). Role of protein in cosmatics. **Int. J. Cosmatic Sci.** 7(2): 41-49.

Davey, R.J. (1976). The effect of impurity adsorption on the kinetics of crystal growth from solution. **J. Cryst. Growth** 34: 109-119.

Davey, R.J. (1979). **Industrial Crystallization 78** (E.J. de Jong and S.J. Jancic, eds.). Amsterdam: North-Holland.

Davey, R.J. (1982). **Industrial Crystallization 81** (S.J. Jancic and E.J. de Jong, eds.). Amsterdam: North-Holland.

Davey, R.J. and Mullin, J.W. (1974). Growth of the {100} face of ADP crystals in the presence of ionic species. **J. Cryst. Growth** 26: 45-51.

Davey, R.J., and Mullin, J.W. (1976). A mechanism for the habit modification of ADP crystals in the present of ionic species in aqueous solution. **Kristall und Technik** (11): 229-233.

Dawson, R.M.C., Elliot, D.C., Elliot, W.H., and Jones, K.M. (1986). **Data for Biochemical Research** (3rd ed.). Oxford: Science Publication.

Drenth, J., and Haas, C. (1992). Protein crystals and their stability. **J. Crystal. Growth** 122(1-4): 107-109.

Elgersma, A.V., Ataka, M., and Katsura, T. (1992). Kinetic studies on the growth of three crystal forms of lysozyme based on the measurement of protein and Cl^- concentration changes. **J. Cryst. Growth** 122: 31-40.

Forsythe E.L., Judge R.A., and Pusey M.L. (1999). Tetragonal chicken egg white lysozyme solubility in sodium chloride solutions. **J. Chem. Eng. Data.** 44: 637-640.

Forsythe, E.L., Ewing, F., and Pusey, M.L., (1994). Studies on tetragonal lysozyme crystal growth rates. **Acta Cryst.** D50: 614-619.

Gorin, G., Wang, S.F., and Papapavlou, L. (1971). Assay of lysozyme by its lytic action on M. lysodeikticus cells. **Anal. Biochem.** 39(1): 113-27.

Judge, R.A., Forsythe, E.L., and Pusey, M.L. (1998). The Effect of Protein Impurities on Lysozyme Crystal Growth. **Biotechnol. Bioeng.** 59(6): 776-785.

Judge, R.A., Jacobs, R.S., Frazier, T., Snell, E.H., and Pusey, M.L. (1999). The effect of temperature and solution pH on the nucleation of tetragonal lysozyme crystals. **Biophys. J.** 77(3): 1585–1593.

Judge, R.A., Johns, M.R, and White, E.T. (1995). Protein Purification by Bulk Crystallization: The Recovery of Ovalbumin. **Biotechnol. Bioeng.** 48(4): 315-323.

Kubota, N. and Mullin, J.W. (1995). A kinetic model for crystal growth fron equeous solution in the presence of impurities. **J. Cryst. Growth** 152: 203-208.

Lacmann, R. and Stranski, I.N. (1958). The effect of adsorption of impurity on the equilibrium and growth forms of crystals. **In Doremus**, Roberts and Turnbull: 427-439.

Lu, J., Wang, X., and Ching, C.B. (2002). Batch crystallization of soluble proteins: effect of precipitant, temperature and additive**. Prog. Cryst. Growth Charact. Mater.** 45(3): 201-217.

Maosoongnern, S., Borbon, V.D., Flood, A.E., and Ulrich, J. (2012). Introducing a Fast Method to Determine the Solubility and Metastable Zone Width for Proteins: Case Study Lysozyme. **Ind. Eng. Chem. Res.** 2012(51): 15251−15257.

Mecitoglu, C., Yemenicioglu, A., Arslanoglu, A., ElmacI, Z.S., Korel, F., and Cetin, A.E. (2006). Incorporation of partially purified hen egg white lysozyme into zein films for antimicrobial food packaging. **Food Res. Int.** 39(1): 12-21.

Motoki, M., and Seguro, M. (1998). Transglutaminase and its use for food processing**. Trends Food Sci. Tech.** 9: 204–210.

Mullin, J.W. (2001). **Crystallization** (4th ed.). Oxford: Butterworth-Heinemann.

Myerson, A.S., and Ginde, R. (2002). **Handbook of industrial crystallization** (2nd ed.) USA: Butterworth-Heinemann.

Nadarajah, A., Forsythe, E.L., and Pusey, M.L. (1995). The averaged face growth rates of lysozyme crystals: the effect of temperature. **J. Cryst. Growth** 151: 163-172.

Proctor, V.A., Cunningham, F.E. (1998). The chemistry of lysozyme and its use as a food preservative and a pharmaceutical. **Crit. Rev. Food Sci. Nutr.** 26(4): 359-95.

Randolph, A.D., and Larson, M.A. (1988). **Theory of particulate processes: Analysis and techniques of continuous crystallization** (2nd ed.). California: Academic Press.

Ries-Kautt, M., Ducruix, A. (1992). **Crystallization of Nucleic Acids and Proteins: A Practical Approach.** New York: Oxford University Press.

Rosenberger, F., Howard, S.B., Sowers, J.W., and Nyce, T.A. (1993). Temperature dependence of protein solubility — determination and application to crystallization in X-ray capillaries. **J. Cryst. Growth** 129(1-2): 1-12.

Saikumar, M.V., Glatz, C.E., and Larson, M.A. (1998). Lysozyme crystal growth and nucleation kinetics. **J. Crystal. Growth** 187: 277–288.

Shugar, D. (1952). The measurement of lysozyme activity and the Ultra-violet inactivation of lysozyme. **Biochimica et Biophysica Acta** 8: 302-309.

Stolte, I., Frohberg, F., Pietzsch, M., and Ulrich, J. (2010). Crystal in protein films: what are they good for?. **Chem. Eng. Res. Des.** 88: 1148-1152.

Tam, S.K., Chan, H.C., Ng, K.M, and Wibowo, C. (2011). Design of Protein Crystallization Processes Guided by Phase Diagrams. **Ind. Eng. Chem. Res.** 50: 8163–8175.

Tung, H.H., Paul, E.L., Midler, M., and McCauley J.A. (2009). **Crystallization of Organic Compounds: An Industrial Prespective.** New Jersey: John Wiley & Sons, Inc.

Yokoyama, K., Nio, N., and Kikuchi, Y. (2004). Properties and applications of microbial transglutaminase. **Appl. Microbiol. Biotechnol.** 64: 447-454.

CHAPTER VI

CONCLUSIONS AND RECOMMENDATIONS

6.1 Conclusions

Proteins are value added products from simple agricultural materials and appear all around in our life. Proteins from a natural source have a diversity of the amino acid residue groups that can cause complexity in their structure which is easily influenced by environmental conditions. However, the separation and purification of proteins can be done using several methods. Examples of methods for separation of proteins are ion exchange chromatography, precipitation by salting-out, and crystallization. Each method have benefits and drawbacks. Therefore, the industrial scale demand gives the scientist or engineer a chance to select the method which best matches the needs of the process. Usually, the process which gives a high purity and stable product, low investment and operating cost, and is environmentally friendly is required in a variety of industrial applications.

Crystallization is one of the most important separation and purification processes in many industries, and is a simple and lower cost technique. It is particularly significant for the pharmaceutical industry. The main active pharmaceutical ingredients (APIs) and many other chemicals are produced in a solid form which is more stable than a chemical in solution. In the crystallization processes nucleation is hard to control, so that crystallization without nucleation is desired. To design and control crystallization process, knowledge of the thermodynamics and

kinetics of the process are of key importance and should be understood, be able to be predicted, and controlled. Thermodynamics is used to identify whether the solution is in an undersaturated or supersaturated state, while kinetics determine how fast the crystal can be grown at a certain driving force. This thesis focuses on a study of the possibility to separate pure lysozyme out of mixed lysozyme – ovalbumin solution by understanding the thermodynamic and kinetic behavior of the crystallization of lysozyme from both pure and mixed solution. The following conclusions can be made for this thesis.

1. The solubilties of pure lysozyme powder and lysozyme crystal were measured using both the well-known classical dissolution method and a miniature column method. The solubility of lysozyme increases with increasing temperature, decreases with increasing sodium chloride concentration, and is slightly reduced at higher values of the pH. The solubility data as a function of temperature are well fitted with both a third – order polynomial equation and the van't Hoff equation. The estimated enthalpy and entropy of dissolution are positive values and the average value of these parameters from the crystal form is higher than from the powder form. These values indicate that the dissolution is an endothermic process, where heat is required to make the lysozyme dissolve. Two modified techniques used to measure the concentration of mixed protein during crystallization were presented, the combination of the SDS-PAGE gel and UV-Vis techniques, and a UV-Vis technique for mixtures. These two techniques involve measuring the concentration in the solution phase and require only a very small volume of the solution. However, there are some limitations for their use. The techniques offer the opportunity to be used depending on the requirement of each project.

2. The concentration-temperature phase diagrams of lysozyme, containing besides thermodynamic data (solubility) also kinetic (nucleation) data were determined using temperature cycling control with an STEM integrity 10 system. This technique shows a rapid, precise and reliable determination of nucleation and solubility points. The width of the metastable zone depends on the solution conditions (e.g. initial protein concentration, salt concentration, and solution pH). The solubility of lysozyme was found to decrease with increasing salt concentration while the nucleation points were observed more early with respect to salt addition; as a consequence the metastable zone is narrower. The solubility of lysozyme is slightly reduced at higher values of the pH, and the nucleation point is observed later in time. The result is an increase of the metastable zone width. The presence of the phase diagram offers the possibility to use this information for design and control crystallization process. Since seed non-nucleating batch crystallizations are desirable it is preferable to work under conditions where the metastable zone is large.

3. The batch crystallization and growth kinetic studies for pure lysozyme were performed isothermally at 20°C in a 100 mL agitated crystallizer via a seeded batch crystallization process. The solution condition used is not the optimal condition for crystallizing pure lysozyme but in preparation for use in the crystallization of mixed protein. The successful crystallization of tetragonal lysozyme crystal was performed with a yield of around 50% in 6 hr and 85% in 25 hr. The crystal growth rates were found to be second order with respect to the relative supersaturation. This is indicating that the growth kinetics is controlled by the surface integration mechanism. This study gives the information background to the studies involving crystallization from mixed protein solutions.

4. The crystallization process was able to successfully separate pure lysozyme from the lysozyme – ovalbumin mixtures, using either crystallization from regions in the phase diagram where only lysozyme was supersaturated, or using preferential crystallization from regions where both proteins were supersaturated (using batch crystallization with seeding of only lysozyme). The batch crystallization and growth kinetic studies for lysozyme from mixed lysozyme – ovalbumin solutions was performed in a 100 mL agitated crystallizer via a seeded batch crystallization process. The successful crystallization of tetragonal lysozyme crystal from a lysozyme-ovalbumin mixture was performed within 24 hr with a yield of greater than 80%, purity more than 96.5%, and the remaining activity of lysozyme was more than 97%. The crystallization was performed within the metastable region to ensure that no nucleation occurs. The growth kinetics were measured based on the measurement of the decline in lysozyme concentration with time. The crystal growth rates were found to be second order with respect to the relative supersaturation, as in the case of crystallization of pure lysozyme. There is no significant effect of ovalbumin impurity up to the concentration of 67.5% (based on total protein) and NaCl concentration, for concentrations of 3 and 4% NaCl, on the growth of lysozyme crystal. The temperature has a greater effect on the growth of the crystal. The growth rate constants increase with increasing temperature and follow an Arrhenius relationship. The calculated activation energy supports the hypothesis from the growth rate order that the crystallization process is controlled by the surface integration mechanism.

6.2 Recommendations

The following recommendations may help for a deeper understanding of the protein crystallization process, and may be useful for future studies of the process.

1. The phase diagram should be determined and presented with also the secondary nucleation threshold (SNT). In this research, the crystallization experiments were carried out in the middle of the phase diagram (the region between solubility and primary nucleation) to ensure that no nucleation occurs. However, in seeding crystallization the growth of the crystal without nucleation usually occurs within the SNT region. Moving solution and experimental conditions close to the upper limit of the SNT can increase the supersaturation which is increasing the crystal growth rate. Therefore, the SNT should be studied further.

2. These crystallization processes were performed within the specific range of condition based on the preferred crystal type (tetragonal crystal). Therefore, if the shape of the product crystal is not of importance a wide range of solution and experimental conditions can be used. As seen in Chapter III, at low supersaturation the tetragonal crystals are crystallized while the orthorhombic crystals are crystallized at high supersaturation or at higher pH. Therefore, the solution and experimental conditions that can be used is dependent on the main results desired. For example; the type of the crystal, yield of the product, low energy consumption, and greater remaining activity.

3. The crystallization of lysozyme in the presence of several protein impurities should be studied. Egg white (a natural source of lysozyme), consists of approximately 40 proteins (with 6 main proteins). Adding other proteins into the solution as an impurity can make the solution behavior more like the natural egg.

4. In the further work, the population balance equation (PBE) may be used to model the crystallization of protein. Nowadays, there is a scant work on the modeling of crystallization process of protein due to the complexity of their structure. According to experimental results some parameters have no significant effect on the kinetics of the process (within a limited range). Therefore, some parameters or variables in the PBE may be neglected (with the range of validity) and therefore make it easier to solve.

APPENDIX A

RAW DATA OF SDS-PAGE GEL WITH INTENSITY
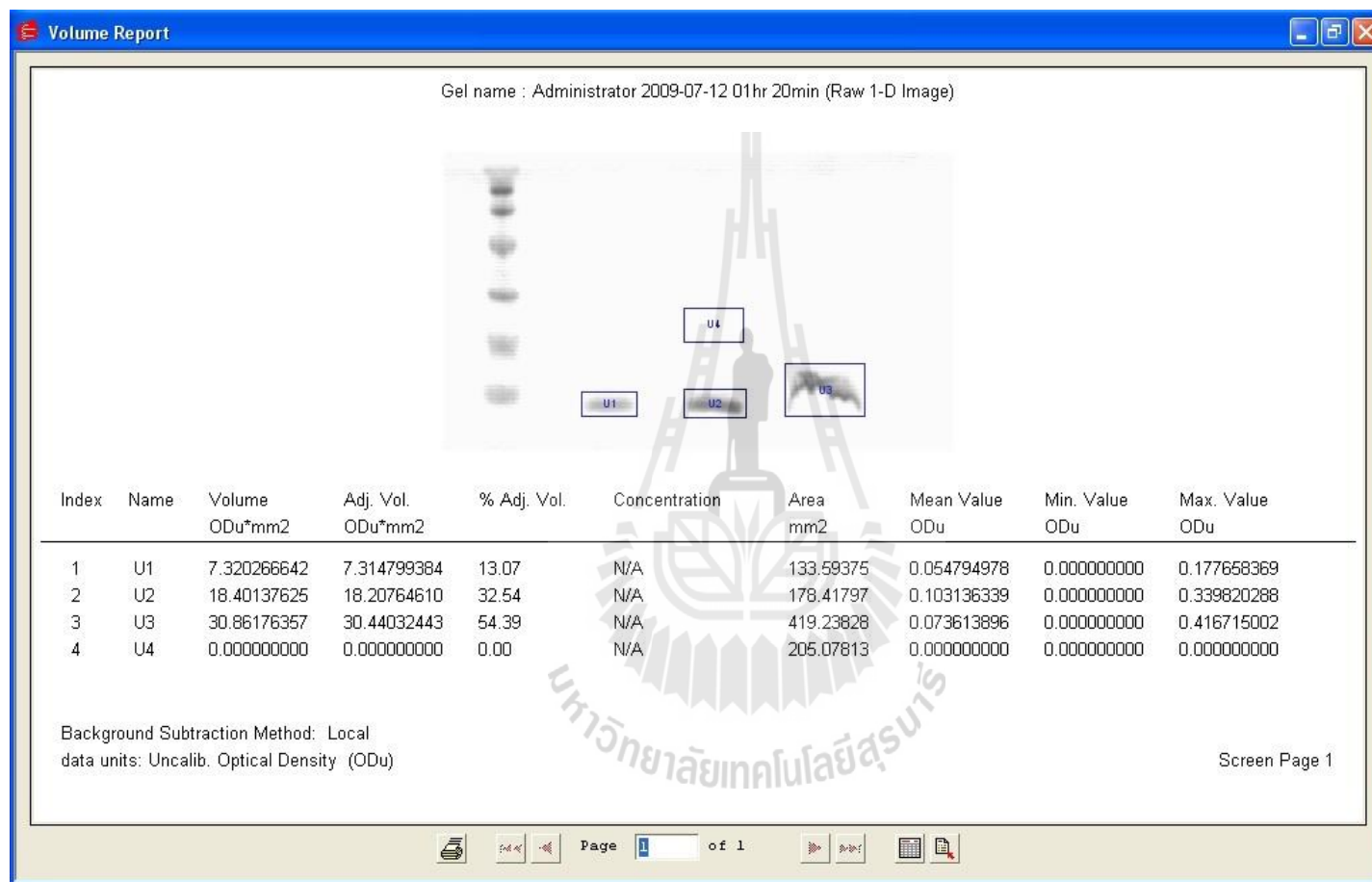
VOLUME ANALYSIS

Figure A.1 SDS-PAGE gel with intensity volume analysis for pure lysozyme (low concentration). U1 = 0.1 mg/mL, U2 = 0.2 mg/mL, U3 = 0.3 mg/mL.
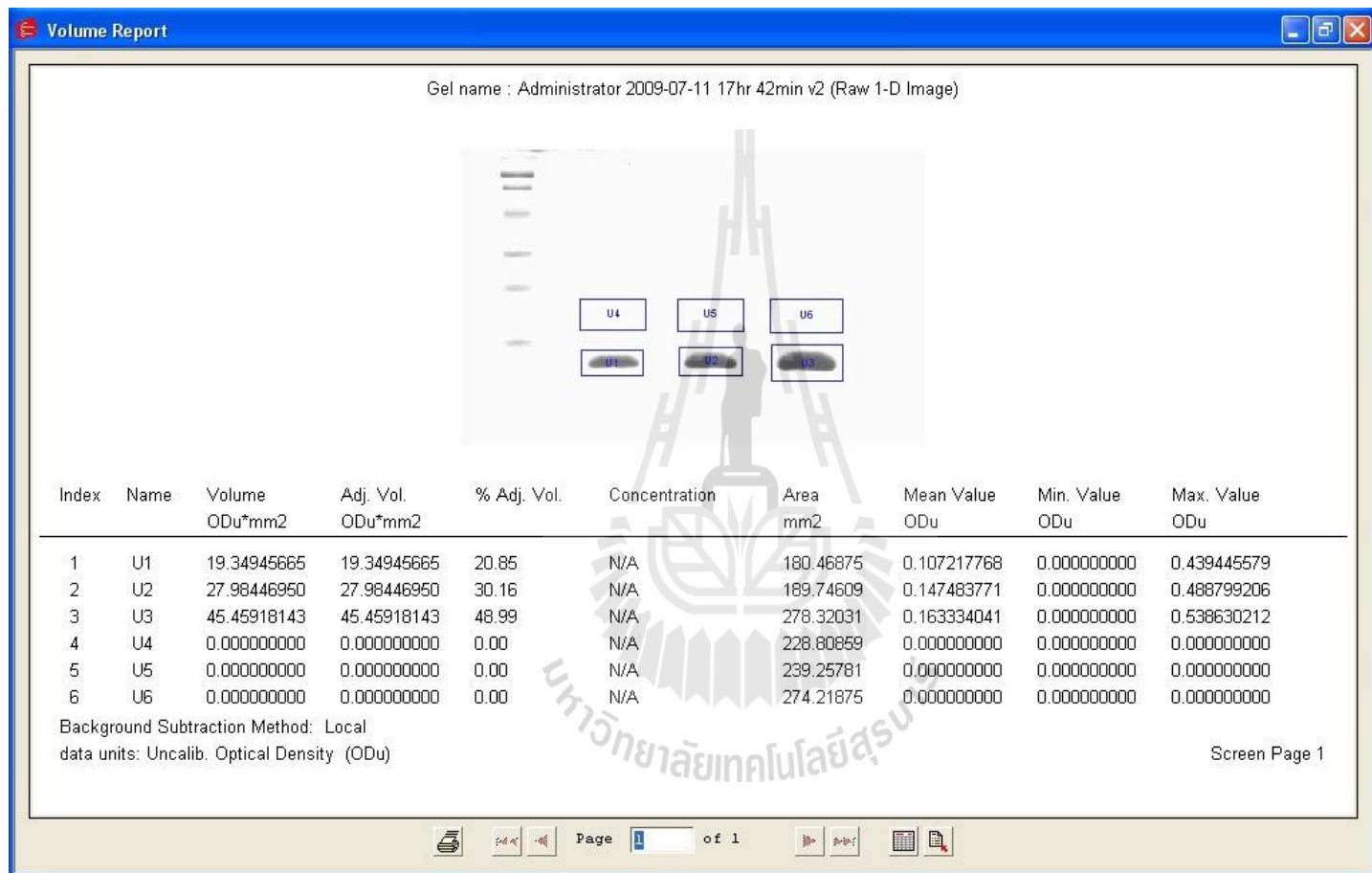
Figure A.2 SDS-PAGE gel with intensity volume analysis for pure lysozyme (high concentration). U1 = 0.3 mg/mL, U2 = 0.6 mg/mL, U3 = 1.2 mg/mL.
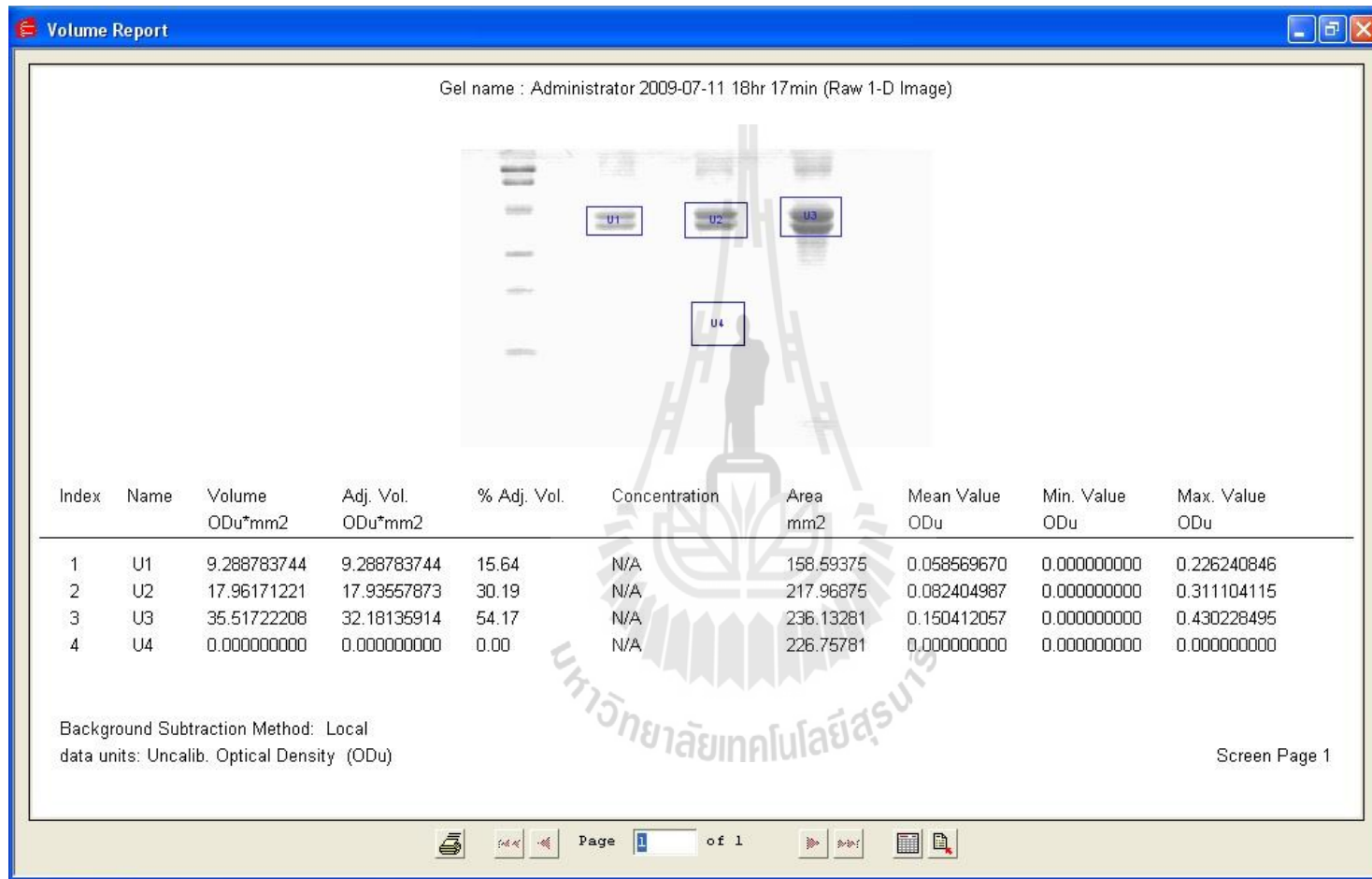
Figure A.3 SDS-PAGE gel with intensity volume analysis for pure ovalbumin. U1 = 0.25 mg/mL, U2 = 0.5 mg/mL, U3 = 1.0 mg/mL.
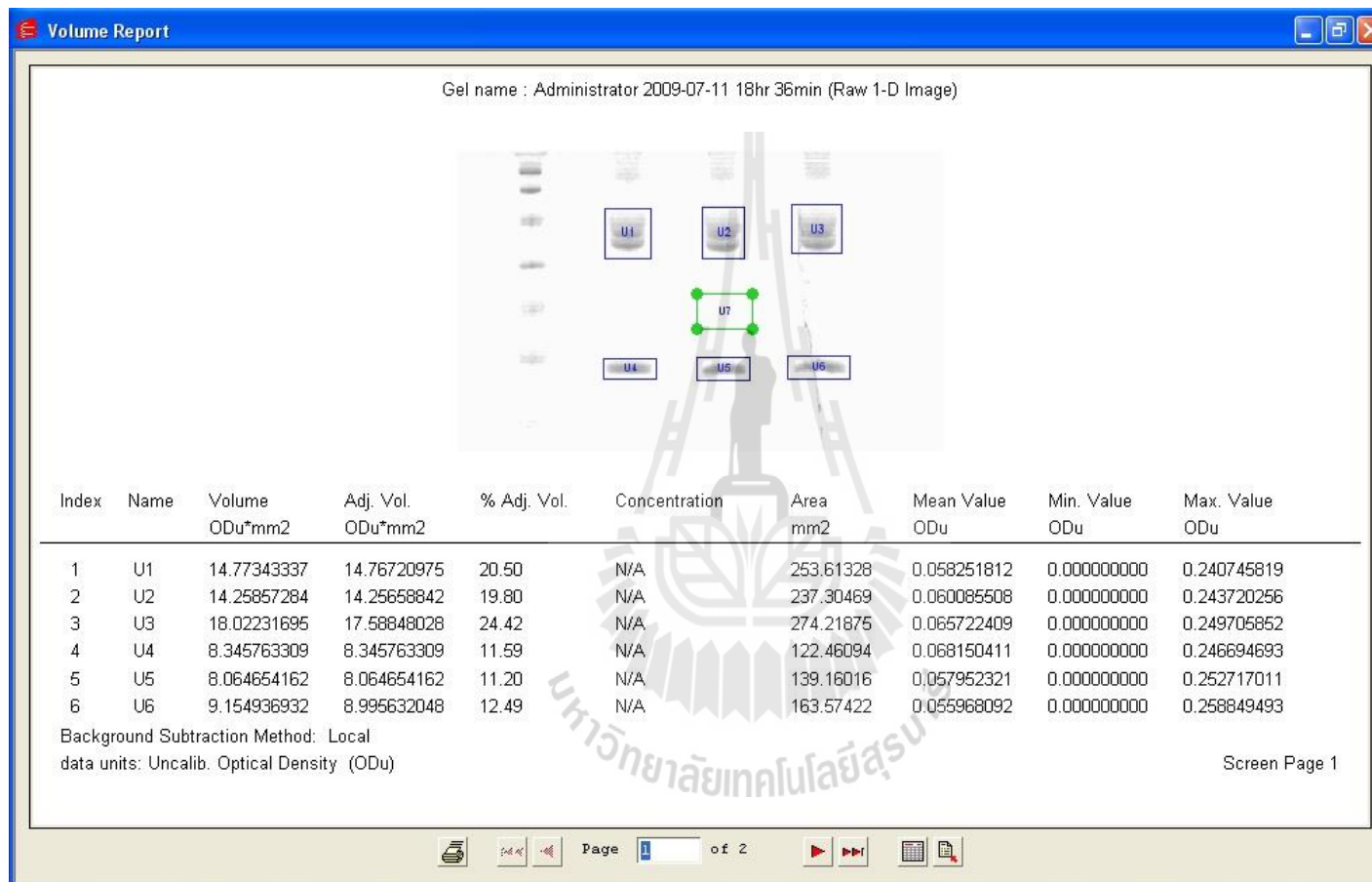
Figure A.4 SDS-PAGE gel with intensity volume analysis for mixed protein (20% lysozyme and 80% ovalbumin with the total concentration of 1 mg/mL).
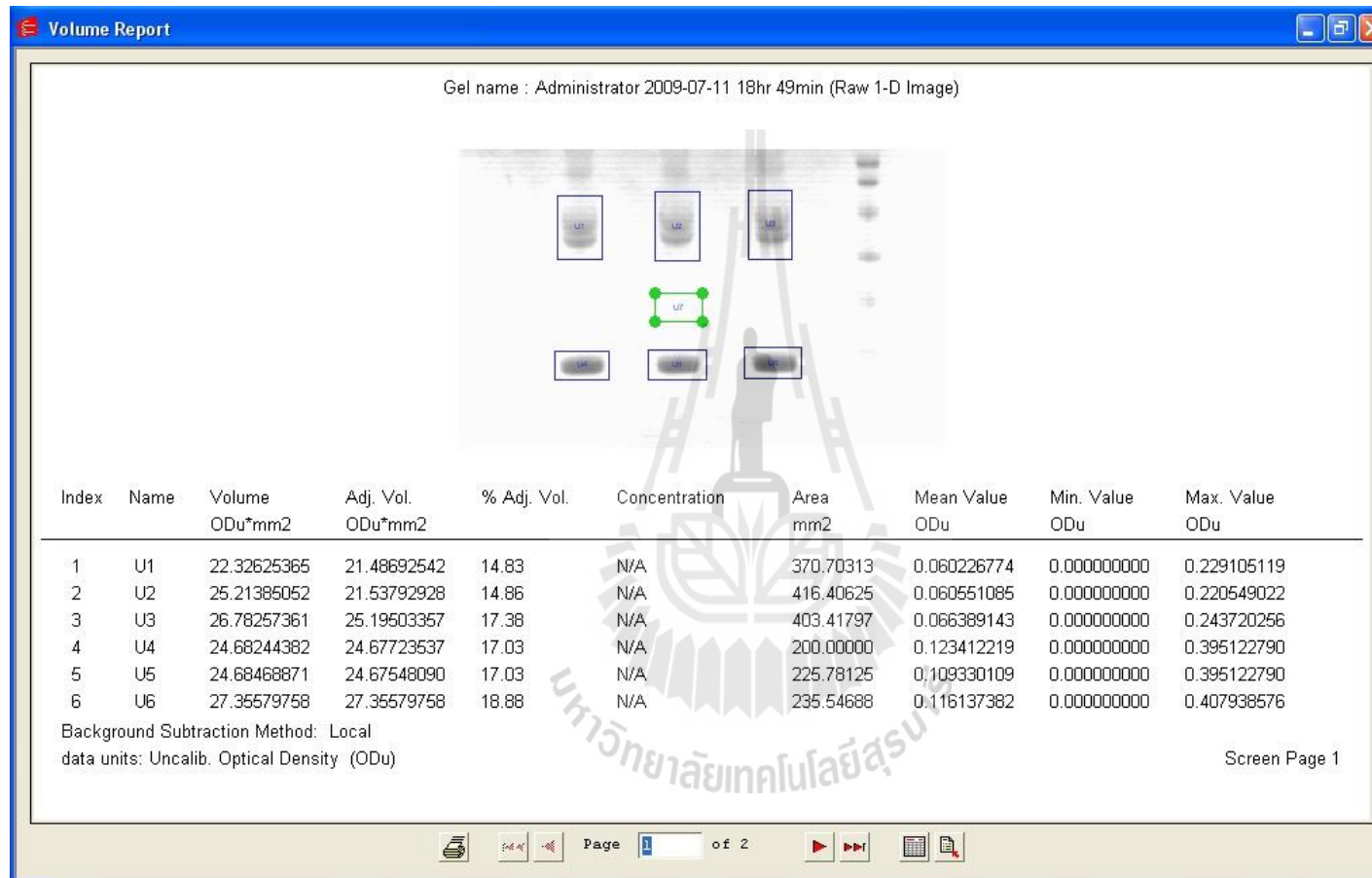
Figure A.5 SDS-PAGE gel with intensity volume analysis for mixed protein (40% lysozyme and 60% ovalbumin with the total concentration of 1 mg/mL).
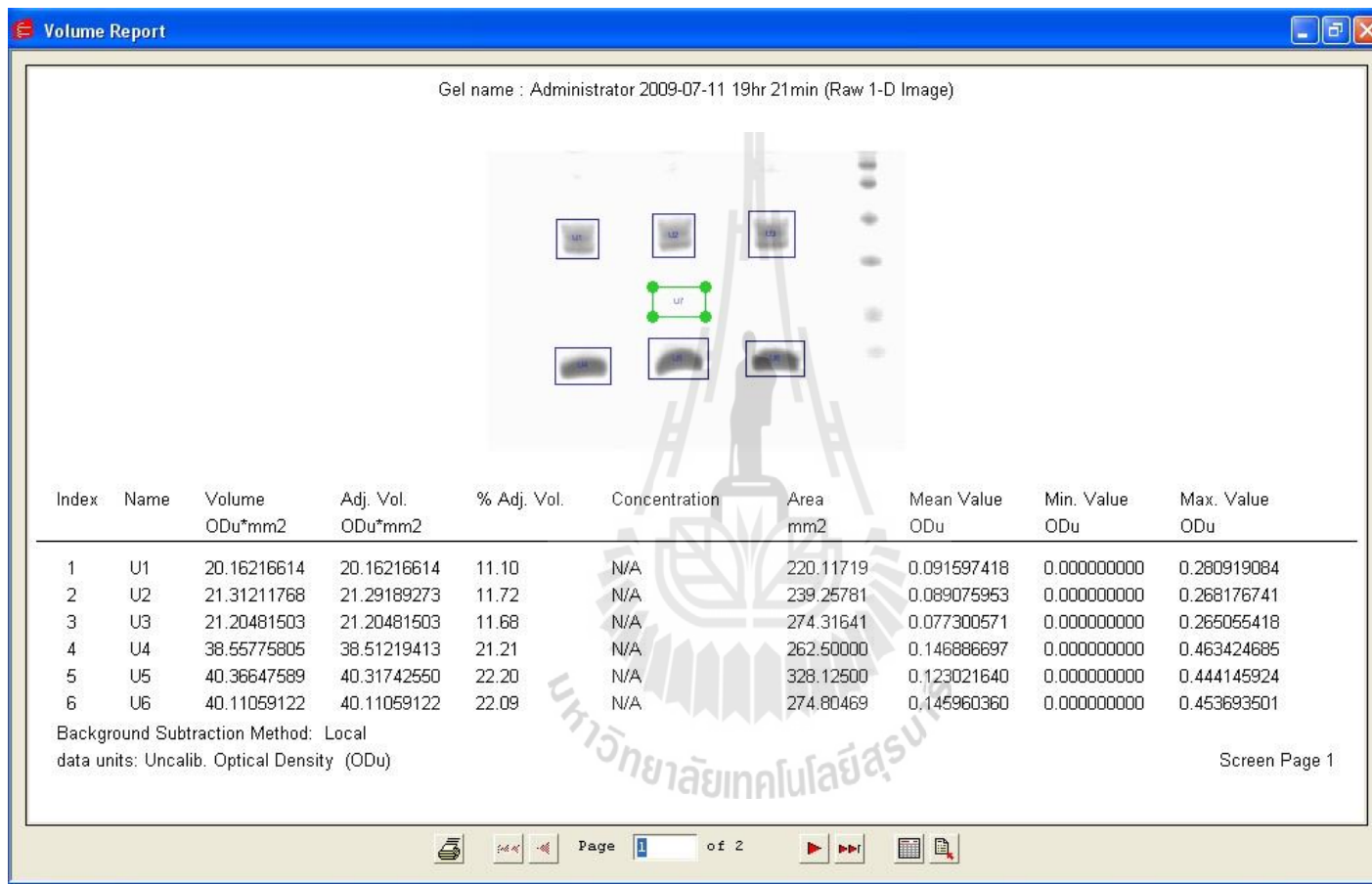
Figure A.6 SDS-PAGE gel with intensity volume analysis for mixed protein (60% lysozyme and 40% ovalbumin with the total

concentration of 1 mg/mL).
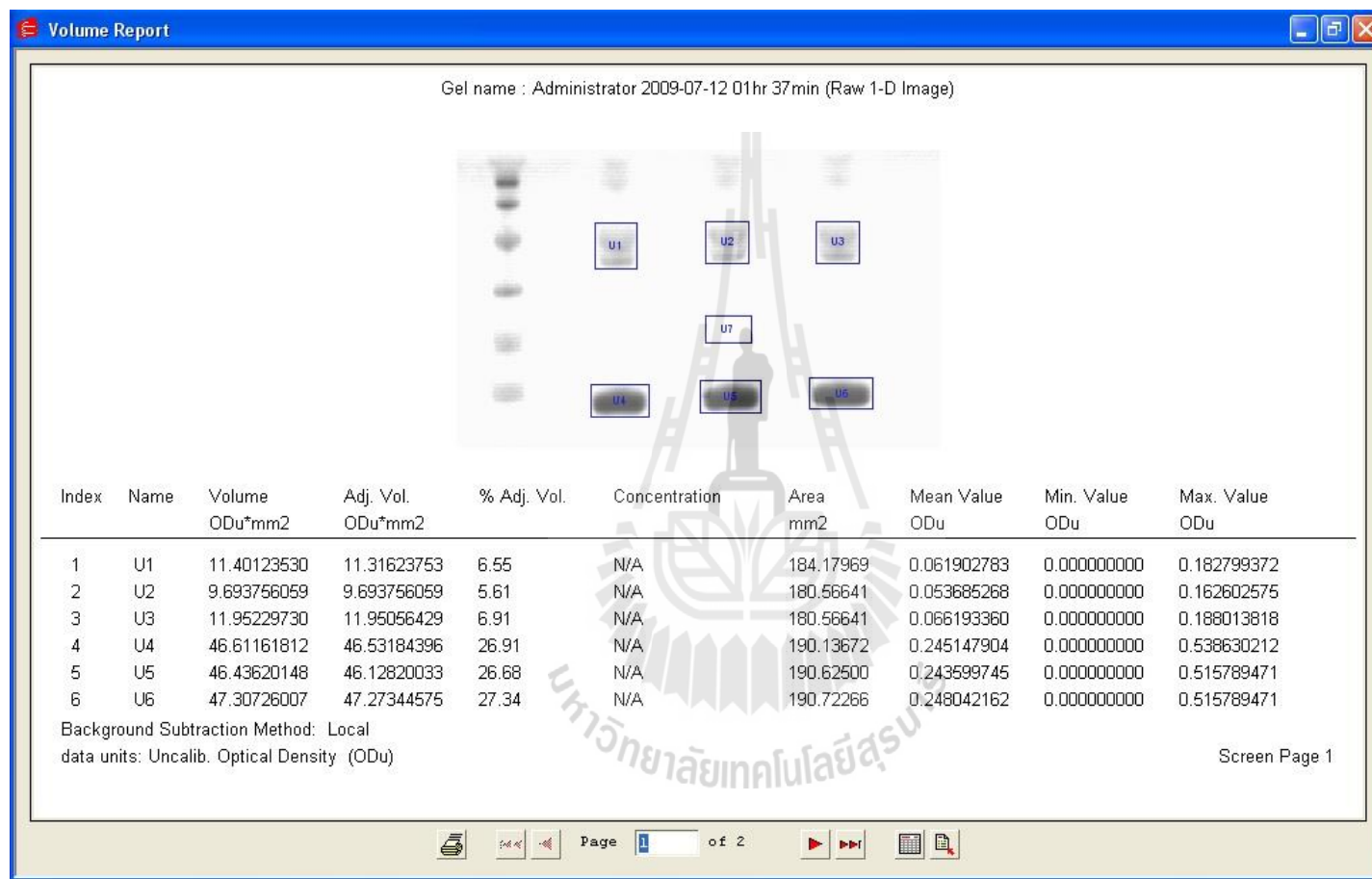
Figure A.7 SDS-PAGE gel with intensity volume analysis for mixed protein (70% lysozyme and 30% ovalbumin with the total concentration of 1 mg/mL).
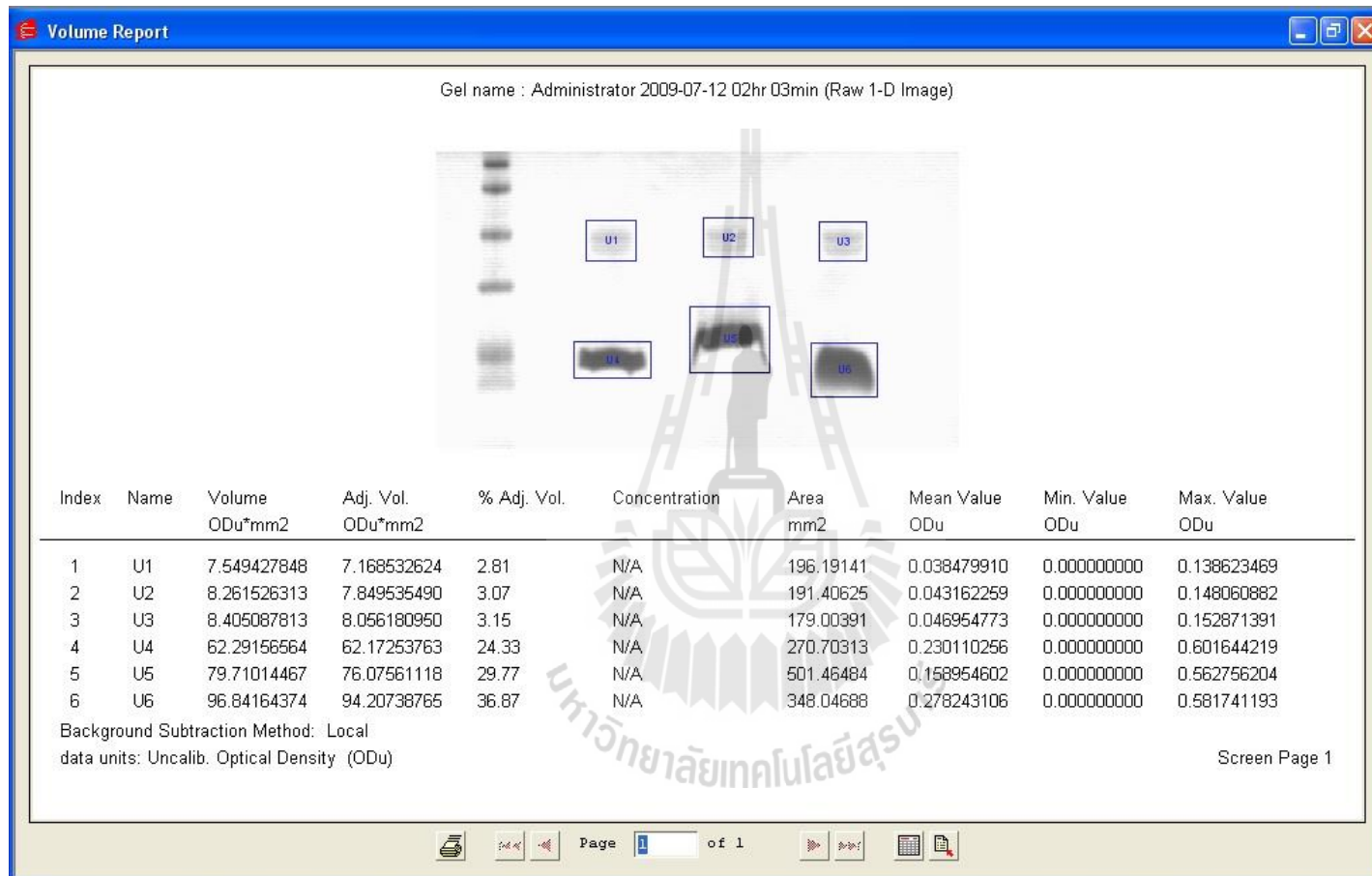
Figure A.8 SDS-PAGE gel with intensity volume analysis for mixed protein (90% lysozyme and 10% ovalbumin with the total concentration of 1 mg/mL).
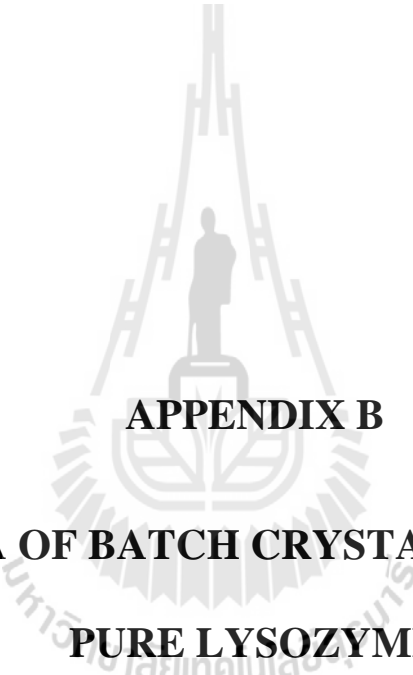
APPENDIX B

RAW DATA OF BATCH CRYSTALLIZATION OF

PURE LYSOZYME

Table B.1 Concentration measurement and calculation in total mass of crystal. Batch crystallization of pure lysozyme (Exp. No.1-1).

Time (hr)	Abs. 1	Abs. 2	Abs. 3	Ave. Abs.	C_t (mg/mL)	m_{cryst} (mg)
0	1.1960	1.1966	1.1962	1.1963	24.5933	120.00
1	1.0683	1.0690	1.0698	1.0690	21.9776	250.79
2	0.9980	0.9986	0.9990	0.9985	20.5282	323.25
3	0.9105	0.9098	0.9095	0.9099	18.7067	414.33
4	0.8372	0.8376	0.8366	0.8371	17.2101	489.16
5	0.7708	0.7711	0.7712	0.7710	15.8512	557.11
6	0.7196	0.7191	0.7195	0.7194	14.7897	610.18
8	0.6103	0.6107	0.6104	0.6105	12.5502	722.16
10	0.5519	0.5524	0.5526	0.5523	11.3544	781.95
12.5	0.4849	0.4839	0.4842	0.4843	9.9571	851.81
19.5	0.3850	0.3852	0.3857	0.3853	7.9211	953.61
25	0.3482	0.3485	0.3475	0.3481	7.1557	991.88

* Dilution factor = 50

Table B.2 Concentration measurement and calculation in total mass of crystal. Batch crystallization of pure lysozyme (Exp. No.1-2).

Time (hr)	Abs. 1	Abs. 2	Abs. 3	Ave. Abs.	C_t (mg/mL)	m_{cryst} (mg)
0	1.2275	1.2278	1.2296	1.2283	25.2518	120.00
1	1.0945	1.0952	1.0937	1.0945	22.5004	257.57
2	0.9980	0.9972	0.9990	0.9981	20.5186	356.66
3	0.9370	0.9382	0.9358	0.9370	19.2632	419.43
4	0.8530	0.8532	0.8550	0.8537	17.5514	505.02
5	0.7712	0.7695	0.7730	0.7712	15.8553	589.83
6	0.7105	0.7110	0.7128	0.7114	14.6259	651.29
9	0.5702	0.5719	0.5732	0.5718	11.7546	794.86
12	0.4839	0.4852	0.4823	0.4838	9.9461	885.28
15	0.4150	0.4137	0.4155	0.4147	8.5262	956.28
18	0.3805	0.3835	0.3820	0.3820	7.8533	989.93
24	0.3481	0.3493	0.3469	0.3481	7.1564	1024.77

* Dilution factor = 50

Table B.3 Concentration measurement and calculation in total mass of crystal. Batch crystallization of pure lysozyme (Exp. No.1-3).

Time (hr)	Abs. 1	Abs. 2	Abs. 3	Ave. Abs.	C_t (mg/mL)	m_{cryst} (mg)
0	1.2138	1.2148	1.2122	1.2136	24.9496	120.00
1	1.1290	1.1294	1.1305	1.1296	23.2234	206.31
2	1.0259	1.0270	1.0299	1.0276	21.1258	311.19
3	0.9240	0.9214	0.9205	0.9220	18.9541	419.77
4	0.8241	0.8245	0.8212	0.8233	16.9250	521.23
5	0.7550	0.7541	0.7562	0.7551	15.5236	591.30
6	0.6869	0.6872	0.6850	0.6864	14.1106	661.95
9	0.5865	0.5879	0.5885	0.5876	12.0808	763.44
15	0.4526	0.4550	0.4532	0.4536	9.3253	901.22
18.5	0.4049	0.4065	0.4028	0.4047	8.3207	951.45
21	0.3844	0.3862	0.3820	0.3842	7.8985	972.55
24.5	0.3605	0.3616	0.3591	0.3604	7.4092	997.02

* Dilution factor = 50

Table B.4 Concentration measurement and calculation in total mass of crystal. Batch crystallization of pure lysozyme (Exp. No.2-1).

Time (hr)	Abs. 1	Abs. 2	Abs. 3	Ave. Abs.	C_t (mg/mL)	m_{cryst} (mg)
0.0	1.2168	1.2161	1.2159	1.2163	25.0045	70.0000
0.5	1.1773	1.1776	1.1779	1.1776	24.2095	109.7485
1.0	1.1358	1.1349	1.1336	1.1348	23.3292	153.7646
1.5	1.0835	1.0830	1.0841	1.0835	22.2757	206.4413
2.0	1.0387	1.0397	1.0376	1.0387	21.3538	252.5332
2.5	0.9870	0.9854	0.9849	0.9858	20.2658	306.9374
3.0	0.9351	0.9381	0.9324	0.9352	19.2267	358.8920
3.5	0.8921	0.8910	0.8913	0.8915	18.3271	403.8701
4.0	0.8392	0.8378	0.8410	0.8394	17.2557	457.4380
4.5	0.7900	0.7917	0.7925	0.7914	16.2699	506.7305
5.0	0.7455	0.7412	0.7408	0.7425	15.2648	556.9851
5.5	0.7043	0.7039	0.7040	0.7041	14.4744	596.5054
6.0	0.6608	0.6590	0.6605	0.6601	13.5709	641.6780

* Dilution factor = 50

Table B.5 Concentration measurement and calculation in total mass of crystal. Batch

crystallization of pure lysozyme (Exp. No.2-2).

Time (hr)	Abs. 1	Abs. 2	Abs. 3	Ave. Abs.	C_t (mg/mL)	m_{cryst} (mg)
0.0	1.1585	1.1571	1.1612	1.1589	23.8258	120.00
0.5	1.1180	1.1190	1.1185	1.1185	22.9945	161.56
1.0	1.0756	1.0765	1.0744	1.0755	22.1105	205.76
1.5	1.0329	1.0340	1.0331	1.0333	21.2436	249.11
2.0	0.9939	0.9965	0.9955	0.9953	20.4617	288.20
2.5	0.9565	0.9549	0.9570	0.9561	19.6565	328.46
3.0	0.9200	0.9189	0.9213	0.9201	18.9151	365.54
3.5	0.8861	0.8876	0.8852	0.8863	18.2209	400.25
4.0	0.8530	0.8535	0.8514	0.8526	17.5287	434.85
4.5	0.8149	0.8175	0.8189	0.8171	16.7982	471.38
5.0	0.7893	0.7875	0.7899	0.7889	16.2185	500.37
5.5	0.7626	0.7635	0.7612	0.7624	15.6744	527.57
6.0	0.7379	0.7339	0.7348	0.7355	15.1214	555.22

* Dilution factor = 50

Table B.6 Concentration measurement and calculation in total mass of crystal. Batch

crystallization of pure lysozyme (Exp. No.2-3).

Time (hr)	Abs. 1	Abs. 2	Abs. 3	Ave. Abs.	C_t (mg/mL)	m_{cryst} (mg)
0.0	1.1975	1.1987	1.1999	1.1987	24.6433	120.00
0.5	1.1580	1.1598	1.1590	1.1589	23.8258	160.88
1.0	1.1200	1.1214	1.1235	1.1216	23.0589	199.22
1.5	1.0825	1.0832	1.0819	1.0825	22.2551	239.41
2.0	1.0414	1.0430	1.0440	1.0428	21.4383	280.25
2.5	1.0030	1.0021	1.0005	1.0019	20.5967	322.33
3.0	0.9618	0.9630	0.9645	0.9631	19.7998	362.18
3.5	0.9245	0.9258	0.9220	0.9241	18.9980	402.27
4.0	0.8860	0.8874	0.8851	0.8862	18.2181	441.26
4.5	0.8518	0.8521	0.8486	0.8508	17.4917	477.58
5.0	0.8123	0.8131	0.8150	0.8135	16.7235	515.99
5.5	0.7790	0.7801	0.7777	0.7789	16.0136	551.49
6.0	0.7420	0.7445	0.7410	0.7425	15.2646	588.94

* Dilution factor = 50
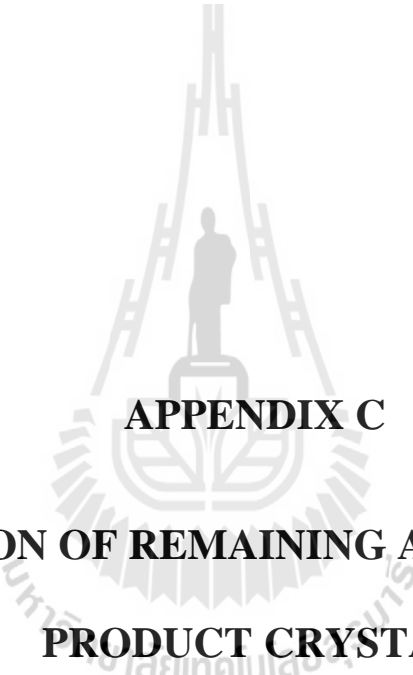
APPENDIX C

CALCULATION OF REMAINING ACTIVITY OF THE

PRODUCT CRYSTAL

C.1   Activity of the protein

According to equation (5.7) activity of the protein can be calculated from

$$\textbf{\textit{Activity}} = \frac{(\Delta A_{450nm}/\text{min Test} - \Delta A_{450nm}/\text{min Blank})}{(0.001)C_{lys})(V_{lys})} \qquad (C.1)$$

Where $\Delta A_{450nm}/\text{min Test}$ is the change in an absorbance of the test solution (mixture of bacteria and lysozyme solution) per minute, $\Delta A_{450nm}/\text{min Blank}$ is the changed in an absorbance of the reference solution (bacteria solution) per minute, C_{lys} is the concentration of lysozyme solution, and V_{lys} is the volume of lysozyme solution used. The value of $\Delta A_{450nm}/\text{min Test}$ and $\Delta A_{450nm}/\text{min Blank}$ can be directly estimated from the slope of the plot between absorbance and time (the linear part at the beginning). The values of the measured absorbance of Micrococcus lysodeikticus with adding lysozyme powder solution and product crystal solution are shown in table C.1 and C.2 and the plot are shown in Figure C.1 and C.2, respectively. As see in the plots,

$$\Delta A_{450nm}/\text{min Blank} = 0.0097$$

$$\Delta A_{450nm}/\text{min Test (with adding lysozyme powder solution)} = 1.0204$$

$$\Delta A_{450nm}/\text{min Test (with adding lysozyme crystal solution)} = 0.9910$$

Therefore, the calculated activities are

$$\text{Lysozyme powder: } \textbf{\textit{Activity}} = \frac{(1.0204 - 0.0097)}{(0.001)(0.3mg/mL)(50\,\mu L)} = 67,380 \text{ Units/mg}$$

Lysozyme crystal: $\textit{Activity} = \dfrac{(0.9910 - 0.0097)}{(0.001)(0.3\textit{mg}/\textit{mL})(50\,\mu\textit{L})} = 65{,}420$ Units/mg

The remaining activity is defined as $\dfrac{\text{Activity of lysozyme crystal}}{\text{Activity of lysozyme powder}} \times 100\%$

Then, the remaining activity $= \dfrac{65{,}420}{67{,}380} \times 100\% = 97\%$

Table C.1 Absorption decay of the Micrococcus lysodeikticus with adding lysozyme powder solution. C_{lyst} = 0.3 mg/mL, V_{lys} =50 μL.

Time		Absorbance (450 nm, 25°C)					
Sec	min	Blank	Rxn 1	Rxn 2	Rxn 3	Average Rxn	S.D.
0	0.000	0.8153	0.7257	0.7371	0.7402	0.7343	0.0062
5	0.083	0.8147	0.6189	0.6527	0.6405	0.6374	0.0140
10	0.167	0.8141	0.5462	0.5825	0.5641	0.5643	0.0148
15	0.250	0.8132	0.4975	0.5329	0.5160	0.5155	0.0145
20	0.333	0.8121	0.4624	0.4961	0.4805	0.4797	0.0138
25	0.417	0.8112	0.4372	0.4680	0.4532	0.4528	0.0126
30	0.500	0.8105	0.4189	0.4457	0.4321	0.4322	0.0109
35	0.583	0.8097	0.4054	0.4284	0.4157	0.4165	0.0094
40	0.667	0.8089	0.3951	0.4144	0.4024	0.4040	0.0080
45	0.750	0.8084	0.3867	0.4027	0.3918	0.3937	0.0067
50	0.833	0.8081	0.3794	0.3935	0.3830	0.3853	0.0060
55	0.917	0.8078	0.3730	0.3858	0.3758	0.3782	0.0055
60	1.000	0.8078	0.3679	0.3790	0.3697	0.3722	0.0049
65	1.083	0.8074	0.3635	0.3736	0.3645	0.3672	0.0045
70	1.167	0.8077	0.3598	0.3692	0.3601	0.3630	0.0044
75	1.250	0.8077	0.3565	0.3649	0.3561	0.3592	0.0041
80	1.333	0.8079	0.3538	0.3613	0.3528	0.3560	0.0038
85	1.417	0.8076	0.3512	0.3580	0.3498	0.3530	0.0036
90	1.500	0.8075	0.3489	0.3548	0.3471	0.3503	0.0033
95	1.583	0.8071	0.3470	0.3521	0.3448	0.3480	0.0031
100	1.667	0.8072	0.3452	0.3497	0.3427	0.3459	0.0029
105	1.750	0.8070	0.3434	0.3475	0.3408	0.3439	0.0028
110	1.833	0.8071	0.3416	0.3455	0.3390	0.3420	0.0027
115	1.917	0.8074	0.3403	0.3435	0.3374	0.3404	0.0025
120	2.000	0.8079	0.3390	0.3419	0.3362	0.3390	0.0023

Table C.2 Absorption decay of the Micrococcus lysodeikticus with adding lysozyme

crystal solution. C_{lyst} = 0.3 mg/mL, V_{lys} =50 µL.

Time		Absorbance (450 nm, 25°C)					
Sec	min	Blank	Rxn 1	Rxn 2	Rxn 3	Average Rxn	S.D.
0	0.000	0.8153	0.7608	0.7582	0.7830	0.7673	0.0111
5	0.083	0.8147	0.6780	0.6546	0.7021	0.6782	0.0194
10	0.167	0.8141	0.6062	0.5767	0.6236	0.6022	0.0194
15	0.250	0.8132	0.5553	0.5251	0.5742	0.5515	0.0202
20	0.333	0.8121	0.5163	0.4867	0.5362	0.5131	0.0203
25	0.417	0.8112	0.4858	0.4583	0.5070	0.4837	0.0199
30	0.500	0.8105	0.4613	0.4365	0.4833	0.4604	0.0191
35	0.583	0.8097	0.4418	0.4193	0.4640	0.4417	0.0182
40	0.667	0.8089	0.4268	0.4056	0.4486	0.4270	0.0176
45	0.750	0.8084	0.4127	0.3945	0.4355	0.4142	0.0168
50	0.833	0.8081	0.4009	0.3855	0.4245	0.4036	0.0160
55	0.917	0.8078	0.3918	0.3780	0.4152	0.3950	0.0154
60	1.000	0.8078	0.3888	0.3719	0.4074	0.3894	0.0145
65	1.083	0.8074	0.3771	0.3669	0.4006	0.3815	0.0141
70	1.167	0.8077	0.3716	0.3623	0.3945	0.3761	0.0135
75	1.250	0.8077	0.3667	0.3682	0.3889	0.3746	0.0101
80	1.333	0.8079	0.3623	0.3544	0.3838	0.3668	0.0124
85	1.417	0.8076	0.3587	0.3512	0.3787	0.3629	0.0116
90	1.500	0.8075	0.3552	0.3485	0.3740	0.3592	0.0108
95	1.583	0.8071	0.3524	0.3461	0.3695	0.3560	0.0099
100	1.667	0.8072	0.3495	0.3441	0.3652	0.3529	0.0089
105	1.750	0.8070	0.3472	0.3422	0.3610	0.3501	0.0080
110	1.833	0.8071	0.3447	0.3404	0.3573	0.3475	0.0072
115	1.917	0.8074	0.3428	0.3390	0.3536	0.3451	0.0062
120	2.000	0.8079	0.3407	0.3375	0.3505	0.3429	0.0055
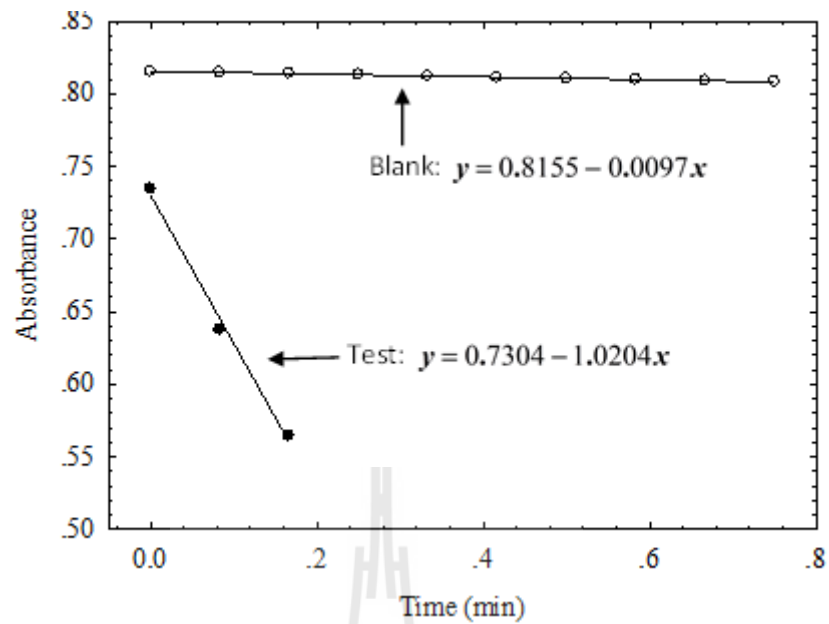
Figure C.1 Plot of absorption decay of bacteria as a function of time at the beginning

of reaction with adding lysozyme powder solution.
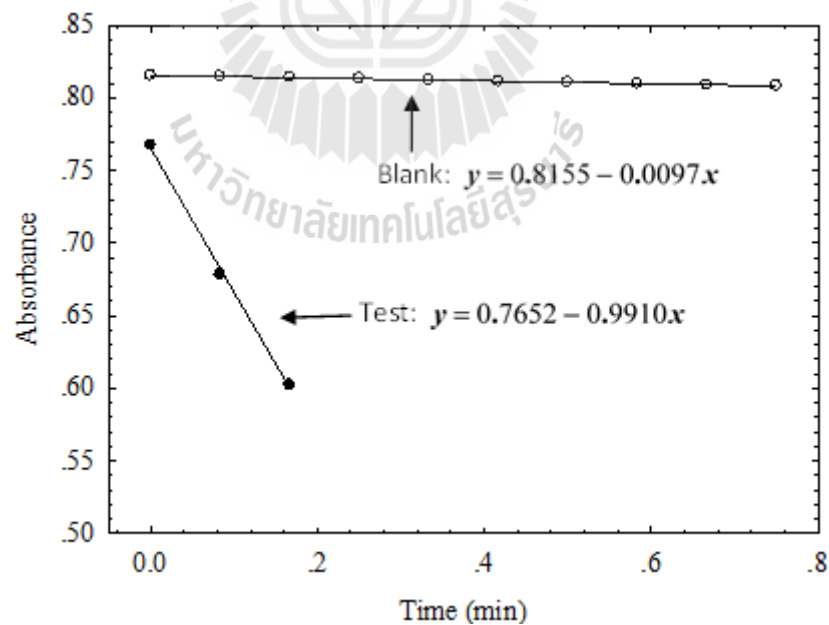
Figure C.2 Plot of absorption decay of bacteria as a function of time at the beginning

of reaction with adding lysozyme crystal solution.

APPENDIX D

RAW DATA OF BATCH CRYSTALLIZATION OF

MIXED LYSOZYME - OVALBUMIN

Table D.1 Concentration measurement and calculation in total mass of crystal. Batch crystallization of mixed lysozyme − ovalbumin

(Exp. No.1-1: $c_{lys,0}$ = 25 mg/mL, $C_{oval,0}$ = 10 mg/mL, Temp. = 20 °C, 4% NaCl, pH 5.0).

Time (hr)	Absorbance						C_{lys} (mg/mL)	C_{oval} (mg/mL)	m_{cryst} (mg)
	A250	A260	A270	A280	A290	A300			
0.0	0.3105	0.3253	0.5776	0.6650	0.5047	0.1043	24.8896	9.8542	120.0000
1.0	0.2931	0.3073	0.5446	0.6270	0.4755	0.0986	23.3230	9.8267	198.3300
2.0	0.2712	0.2845	0.5030	0.5792	0.4387	0.0913	21.3476	9.7965	297.1000
3.0	0.2509	0.2636	0.4645	0.5350	0.4047	0.0845	19.5151	9.8005	388.7250
4.0	0.2294	0.2413	0.4234	0.4878	0.3684	0.0774	17.5304	9.9005	487.9600
5.0	0.2128	0.2242	0.3921	0.4518	0.3407	0.0719	16.0520	9.8456	561.8800
6.0	0.1975	0.2083	0.3630	0.4184	0.3150	0.0668	14.6720	9.8267	630.8800
8.0	0.1825	0.1928	0.3346	0.3857	0.2899	0.0618	13.3210	9.8120	698.4300
10.0	0.1683	0.1781	0.3074	0.3544	0.2658	0.0571	12.0052	9.8880	764.2200
12.0	0.1568	0.1662	0.2858	0.3296	0.2468	0.0533	11.0025	9.7856	814.3550
15.0	0.1461	0.1551	0.2655	0.3063	0.2288	0.0497	10.0380	9.7800	862.5800
18.0	0.1358	0.1445	0.2458	0.2836	0.2114	0.0463	9.0826	9.8420	910.3500
21.0	0.1264	0.1347	0.2279	0.2631	0.1956	0.0431	8.2340	9.8336	952.7800
24.0	0.1182	0.1263	0.2124	0.2453	0.1819	0.0404	7.5032	9.8025	989.3200

* Dilution factor = 100

Table D.2 Concentration measurement and calculation in total mass of crystal. Batch crystallization of mixed lysozyme − ovalbumin

(Exp. No.1-2: $c_{lys,0}$ = 25 mg/mL, $C_{oval,0}$ = 10 mg/mL, Temp. = 20 °C, 4% NaCl, pH 5.0).

Time (hr)	Absorbance						C_{lys} (mg/mL)	C_{oval} (mg/mL)	m_{cryst} (mg)
	A250	A260	A270	A280	A290	A300			
0.0	0.3057	0.3203	0.5684	0.6544	0.4965	0.1027	24.4502	10.0120	120.0000
1.0	0.2920	0.3061	0.5424	0.6246	0.4736	0.0982	23.2215	10.0056	181.4350
2.0	0.2697	0.2830	0.5001	0.5759	0.4362	0.0908	21.2135	9.9854	281.8350
3.0	0.2504	0.2630	0.4634	0.5337	0.4038	0.0843	19.4621	9.9584	369.4050
4.0	0.2293	0.2413	0.4233	0.4877	0.3683	0.0774	17.5260	9.9756	466.2100
5.0	0.2136	0.2250	0.3936	0.4535	0.3420	0.0721	16.1245	10.0000	536.2850
6.0	0.1976	0.2084	0.3631	0.4185	0.3151	0.0668	14.6782	10.0115	608.6000
8.0	0.1827	0.1930	0.3348	0.3860	0.2901	0.0618	13.3325	9.9825	675.8850
10.0	0.1696	0.1795	0.3099	0.3573	0.2680	0.0575	12.1254	9.9682	736.2400
12.0	0.1580	0.1674	0.2880	0.3322	0.2488	0.0536	11.1103	10.0110	786.9950
15.0	0.1470	0.1560	0.2671	0.3081	0.2303	0.0500	10.1154	9.8995	836.7400
18.0	0.1366	0.1453	0.2473	0.2854	0.2127	0.0465	9.1548	9.9589	884.7700
21.0	0.1263	0.1347	0.2278	0.2629	0.1955	0.0431	8.2265	9.9256	931.1850
24.0	0.1199	0.1280	0.2156	0.2489	0.1847	0.0410	7.6548	9.8845	959.7700

* Dilution factor = 100

Table D.3 Concentration measurement and calculation in total mass of crystal. Batch crystallization of mixed lysozyme - ovalbumin

(Exp. No.1-3: $c_{lys,0}$ = 25 mg/mL, $C_{oval,0}$ = 10 mg/mL, Temp. = 20 °C, 4% NaCl, pH 5.0).

Time (hr)	Absorbance						C_{lys} (mg/mL)	C_{oval} (mg/mL)	m_{cryst} (mg)
	A250	A260	A270	A280	A290	A300			
0.0	0.3122	0.3269	0.5810	0.6689	0.5079	0.1049	25.1204	9.5996	120.0000
1.0	0.2934	0.3074	0.5453	0.6278	0.4763	0.0986	23.4126	9.6215	205.3900
2.0	0.2739	0.2873	0.5084	0.5854	0.4436	0.0921	21.6548	9.6125	293.2800
3.0	0.2521	0.2647	0.4669	0.5377	0.4069	0.0849	19.6780	9.6087	392.1200
4.0	0.2323	0.2442	0.4293	0.4945	0.3737	0.0783	17.8854	9.6114	481.7500
5.0	0.2117	0.2229	0.3901	0.4495	0.3391	0.0715	16.0236	9.6050	574.8400
6.0	0.1950	0.2056	0.3585	0.4131	0.3111	0.0659	14.5126	9.6112	650.3900
8.0	0.1846	0.1949	0.3388	0.3905	0.2937	0.0625	13.5789	9.5995	697.0750
10.0	0.1700	0.1798	0.3111	0.3586	0.2692	0.0576	12.2546	9.6102	763.2900
12.0	0.1552	0.1644	0.2829	0.3262	0.2443	0.0527	10.9112	9.6135	830.4600
15.0	0.1462	0.1551	0.2658	0.3066	0.2292	0.0497	10.1010	9.5985	870.9700
18.0	0.1392	0.1479	0.2525	0.2914	0.2175	0.0474	9.4658	9.6103	902.7300
21.0	0.1282	0.1365	0.2316	0.2673	0.1990	0.0437	8.4687	9.6054	952.5850
24.0	0.1226	0.1308	0.2211	0.2552	0.1897	0.0419	7.9658	9.6146	977.7300

* Dilution factor = 100

Table D.4 Concentration measurement and calculation in total mass of crystal. Batch crystallization of mixed lysozyme - ovalbumin

(Exp. No.2-1: $c_{lys,0}$ = 25 mg/mL, $C_{oval,0}$ = 25 mg/mL, Temp. = 20 °C, 4% NaCl, pH 5.0).

Time (hr)	Absorbance						C_{lys} (mg/mL)	C_{oval} (mg/mL)	m_{cryst} (mg)
	A250	A260	A270	A280	A290	A300			
0.0	0.3553	0.3774	0.6447	0.7438	0.5554	0.1209	24.2096	24.3725	120.0000
1.0	0.3339	0.3553	0.6041	0.6971	0.5193	0.1138	22.2500	24.4520	217.9800
2.0	0.3092	0.3297	0.5576	0.6437	0.4785	0.1056	20.1235	24.1286	324.3050
3.0	0.2894	0.3093	0.5196	0.6000	0.4447	0.0990	18.2287	24.4453	419.0450
4.0	0.2745	0.2939	0.4911	0.5673	0.4194	0.0941	16.8421	24.5478	488.3750
5.0	0.2568	0.2755	0.4577	0.5288	0.3900	0.0882	15.3000	24.3624	565.4800
6.0	0.2455	0.2637	0.4364	0.5044	0.3713	0.0844	14.3278	24.2085	614.0900
8.0	0.2276	0.2454	0.4023	0.4652	0.3410	0.0785	12.6470	24.4152	698.1300
10.0	0.2102	0.2274	0.3694	0.4274	0.3120	0.0727	11.1028	24.3258	775.3400
12.0	0.1982	0.2150	0.3466	0.4012	0.2919	0.0687	10.0156	24.3329	829.7000
15.0	0.1886	0.2049	0.3284	0.3803	0.2759	0.0655	9.1852	24.1952	871.2200
18.0	0.1782	0.1941	0.3087	0.3575	0.2584	0.0620	8.2350	24.2265	918.7300
21.0	0.1710	0.1868	0.2950	0.3418	0.2462	0.0597	7.5546	24.3278	952.7500
24.0	0.1681	0.1838	0.2892	0.3352	0.2410	0.0587	7.2340	24.5024	968.7800

* Dilution factor = 100

Table D.5 Concentration measurement and calculation in total mass of crystal. Batch crystallization of mixed lysozyme − ovalbumin

(Exp. No.2-2: $c_{lys,0}$ = 25 mg/mL, $C_{oval,0}$ = 25 mg/mL, Temp. = 20 °C, 4% NaCl, pH 5.0).

Time (hr)	Absorbance						C_{lys} (mg/mL)	C_{oval} (mg/mL)	m_{cryst} (mg)
	A250	A260	A270	A280	A290	A300			
0.0	0.3600	0.3825	0.6535	0.7539	0.5630	0.1225	24.5602	24.6254	120.0000
1.0	0.3346	0.3561	0.6054	0.6987	0.5206	0.1140	22.3152	24.4552	232.2500
2.0	0.3119	0.3326	0.5622	0.6489	0.4823	0.1065	20.2269	24.5524	336.6650
3.0	0.2909	0.3109	0.5223	0.6031	0.4470	0.0995	18.3256	24.5629	431.7300
4.0	0.2731	0.2925	0.4884	0.5641	0.4170	0.0936	16.6985	24.6010	513.0850
5.0	0.2565	0.2752	0.4571	0.5282	0.3895	0.0881	15.2638	24.3956	584.8200
6.0	0.2472	0.2657	0.4393	0.5078	0.3737	0.0850	14.3658	24.5827	629.7200
8.0	0.2296	0.2474	0.4059	0.4693	0.3441	0.0791	12.7895	24.5163	708.5350
10.0	0.2129	0.2302	0.3741	0.4327	0.3160	0.0736	11.2526	24.5958	785.3800
12.0	0.2000	0.2169	0.3498	0.4049	0.2946	0.0693	10.1254	24.4896	841.7400
15.0	0.1906	0.2071	0.3318	0.3842	0.2787	0.0662	9.2658	24.4993	884.7200
18.0	0.1780	0.1941	0.3081	0.3569	0.2577	0.0620	8.1365	24.4895	941.1850
21.0	0.1707	0.1865	0.2940	0.3407	0.2452	0.0596	7.4569	24.5257	975.1650
24.0	0.1686	0.1844	0.2901	0.3362	0.2418	0.0589	7.2598	24.5662	985.0200

* Dilution factor = 100

Table D.6 Concentration measurement and calculation in total mass of crystal. Batch crystallization of mixed lysozyme - ovalbumin

(Exp. No.2-3: $c_{lys,0}$ = 25 mg/mL, $C_{oval,0}$ = 25 mg/mL, Temp. = 20 °C, 4% NaCl, pH 5.0).

Time (hr)	Absorbance						C_{lys} (mg/mL)	C_{oval} (mg/mL)	m_{cryst} (mg)
	A250	A260	A270	A280	A290	A300			
0.0	0.3663	0.3891	0.6651	0.7673	0.5731	0.1246	25.0426	24.8896	120.0000
1.0	0.3461	0.3682	0.6268	0.7233	0.5392	0.1179	23.2260	24.8594	210.8300
2.0	0.3173	0.3384	0.5720	0.6603	0.4908	0.1084	20.5984	24.9215	342.2100
3.0	0.2924	0.3127	0.5247	0.6059	0.4489	0.1001	18.3345	24.9564	455.4050
4.0	0.2760	0.2957	0.4935	0.5701	0.4213	0.0946	16.8456	24.9703	529.8500
5.0	0.2575	0.2765	0.4583	0.5296	0.3902	0.0885	15.1689	24.9665	613.6850
6.0	0.2467	0.2653	0.4380	0.5063	0.3723	0.0849	14.2256	24.8746	660.8500
8.0	0.2314	0.2495	0.4087	0.4726	0.3463	0.0798	12.7895	25.0256	732.6550
10.0	0.2131	0.2306	0.3740	0.4327	0.3156	0.0737	11.1259	25.0548	815.8350
12.0	0.2018	0.2189	0.3527	0.4082	0.2969	0.0700	10.1450	24.9264	864.8800
15.0	0.1914	0.2081	0.3329	0.3855	0.2794	0.0665	9.1987	24.9385	912.1950
18.0	0.1811	0.1975	0.3133	0.3630	0.2620	0.0631	8.2569	24.9762	959.2850
21.0	0.1727	0.1887	0.2974	0.3447	0.2481	0.0603	7.5254	24.8812	995.8600
24.0	0.1690	0.1850	0.2901	0.3363	0.2414	0.0591	7.1164	25.1002	1016.3100

* Dilution factor = 100

Table D.7 Concentration measurement and calculation in total mass of crystal. Batch crystallization of mixed lysozyme - ovalbumin

(Exp. No.3-1: $c_{lys,0}$ = 25 mg/mL, $C_{oval,0}$ = 50 mg/mL, Temp. = 20 °C, 4% NaCl, pH 5.0).

Time (hr)	Absorbance						C_{lys} (mg/mL)	C_{oval} (mg/mL)	m_{cryst} (mg)
	A250	A260	A270	A280	A290	A300			
0.0	0.4416	0.4769	0.7778	0.8997	0.6580	0.1525	23.8240	49.5540	120.0000
1.0	0.4230	0.4577	0.7424	0.8590	0.6266	0.1464	22.1092	49.6524	205.7400
2.0	0.3992	0.4331	0.6972	0.8070	0.5866	0.1384	19.9524	49.6672	313.5800
3.0	0.3810	0.4143	0.6626	0.7673	0.5560	0.1324	18.3000	49.6823	396.2000
4.0	0.3645	0.3972	0.6315	0.7315	0.5286	0.1269	16.8421	49.5842	469.0950
5.0	0.3496	0.3817	0.6031	0.6989	0.5035	0.1219	15.5000	49.5534	536.2000
6.0	0.3403	0.3721	0.5853	0.6784	0.4877	0.1188	14.6278	49.6342	579.8100
8.0	0.3250	0.3564	0.5564	0.6452	0.4621	0.1138	13.2470	49.6455	648.8500
10.0	0.3111	0.3420	0.5300	0.6148	0.4389	0.1092	12.0000	49.6101	711.2000
12.0	0.3002	0.3307	0.5093	0.5910	0.4205	0.1055	11.0000	49.6528	761.2000
15.0	0.2920	0.3222	0.4936	0.5731	0.4067	0.1028	10.2600	49.6374	798.2000
18.0	0.2834	0.3133	0.4775	0.5545	0.3924	0.1000	9.5020	49.5920	836.1000
21.0	0.2771	0.3068	0.4654	0.5406	0.3818	0.0979	8.9124	49.6520	865.5800
24.0	0.2725	0.3020	0.4567	0.5306	0.3741	0.0963	8.5100	49.6000	885.7000

* Dilution factor = 100

Table D.8 Concentration measurement and calculation in total mass of crystal. Batch crystallization of mixed lysozyme - ovalbumin

(Exp. No.3-2: $c_{lys,0}$ = 25 mg/mL, $C_{oval,0}$ = 50 mg/mL, Temp. = 20 °C, 4% NaCl, pH 5.0).

Time (hr)	Absorbance						C_{lys} (mg/mL)	C_{oval} (mg/mL)	m_{cryst} (mg)
	A250	A260	A270	A280	A290	A300			
0.0	0.4504	0.4859	0.7951	0.9194	0.6734	0.1554	24.7526	49.1525	120.0000
1.0	0.4316	0.4664	0.7592	0.8783	0.6417	0.1492	23.0256	49.2236	206.3500
2.0	0.4056	0.4396	0.7098	0.8215	0.5980	0.1405	20.6540	49.2854	324.9300
3.0	0.3880	0.4213	0.6766	0.7833	0.5687	0.1346	19.1200	49.1023	401.6300
4.0	0.3700	0.4027	0.6426	0.7441	0.5387	0.1287	17.5123	49.0523	482.0150
5.0	0.3558	0.3880	0.6155	0.7130	0.5147	0.1240	16.2015	49.1275	547.5550
6.0	0.3449	0.3767	0.5946	0.6890	0.4962	0.1203	15.1856	49.2037	598.3500
8.0	0.3331	0.3645	0.5722	0.6633	0.4764	0.1164	14.1257	49.1824	651.3450
10.0	0.3229	0.3540	0.5529	0.6411	0.4594	0.1130	13.2105	49.1654	697.1050
12.0	0.3109	0.3415	0.5301	0.6149	0.4392	0.1090	12.1203	49.1712	751.6150
15.0	0.3007	0.3310	0.5109	0.5928	0.4223	0.1056	11.2254	49.0986	796.3600
18.0	0.2909	0.3209	0.4923	0.5715	0.4058	0.1024	10.3356	49.1154	840.8500
21.0	0.2823	0.3120	0.4758	0.5524	0.3912	0.0995	9.5241	49.2022	881.4250
24.0	0.2760	0.3055	0.4639	0.5388	0.3807	0.0975	8.9552	49.2150	909.8700

* Dilution factor = 100

Table D.9 Concentration measurement and calculation in total mass of crystal. Batch crystallization of mixed lysozyme − ovalbumin

(Exp. No.3-3: $c_{lys,0}$ = 25 mg/mL, $C_{oval,0}$ = 50 mg/mL, Temp. = 20 °C, 4% NaCl, pH 5.0).

Time (hr)	Absorbance						C_{lys} (mg/mL)	C_{oval} (mg/mL)	m_{cryst} (mg)
	A250	A260	A270	A280	A290	A300			
0.0	0.4485	0.4841	0.7907	0.9144	0.6692	0.1548	24.3820	49.7525	120.0000
1.0	0.4344	0.4695	0.7640	0.8837	0.6456	0.1501	23.1214	49.7068	183.0300
2.0	0.4091	0.4433	0.7160	0.8286	0.6032	0.1417	20.8564	49.6254	296.2800
3.0	0.3909	0.4245	0.6816	0.7891	0.5729	0.1357	19.2258	49.5989	377.8100
4.0	0.3732	0.4062	0.6480	0.7504	0.5431	0.1298	17.6253	49.5898	457.8350
5.0	0.3580	0.3905	0.6189	0.7171	0.5174	0.1247	16.2245	49.6582	527.8750
6.0	0.3458	0.3779	0.5959	0.6905	0.4970	0.1207	15.1186	49.6825	583.1700
8.0	0.3258	0.3571	0.5577	0.6467	0.4633	0.1140	13.2952	49.7015	674.3400
10.0	0.3116	0.3425	0.5307	0.6156	0.4394	0.1093	12.0025	49.7234	738.9750
12.0	0.3009	0.3314	0.5106	0.5925	0.4217	0.1058	11.0658	49.6413	785.8100
15.0	0.2905	0.3207	0.4909	0.5699	0.4042	0.1023	10.1203	49.6643	833.0850
18.0	0.2796	0.3094	0.4701	0.5460	0.3859	0.0987	9.1265	49.6838	882.7750
21.0	0.2706	0.3000	0.4529	0.5262	0.3706	0.0957	8.3002	49.7022	924.0900
24.0	0.2673	0.2966	0.4466	0.5190	0.3651	0.0946	8.0036	49.6991	938.9200

* Dilution factor = 100

Table D.10 Concentration measurement and calculation in total mass of crystal. Batch crystallization of mixed lysozyme - ovalbumin

(Exp. No.4-1: $c_{lys,0}$ = 20 mg/mL, $C_{oval,0}$ = 20 mg/mL, Temp. = 20 °C, 4% NaCl, pH 5.0).

Time (hr)	Absorbance						C_{lys} (mg/mL)	C_{oval} (mg/mL)	m_{cryst} (mg)
	A250	A260	A270	A280	A290	A300			
0.0	0.2893	0.3072	0.5254	0.6061	0.4528	0.0984	19.8206	19.5200	120.0000
1.0	0.2750	0.2924	0.4984	0.5750	0.4289	0.0937	18.5502	19.4522	183.5200
2.0	0.2619	0.2789	0.4735	0.5464	0.4069	0.0893	17.3544	19.4905	243.3100
3.0	0.2487	0.2652	0.4486	0.5178	0.3850	0.0849	16.2087	19.3398	300.5950
4.0	0.2390	0.2552	0.4301	0.4965	0.3685	0.0817	15.2946	19.4552	346.3000
5.0	0.2281	0.2438	0.4094	0.4727	0.3503	0.0781	14.3258	19.3871	394.7400
6.0	0.2173	0.2327	0.3888	0.4491	0.3320	0.0745	13.3145	19.5008	445.3050
8.0	0.2073	0.2223	0.3699	0.4274	0.3154	0.0712	12.4428	19.3986	488.8900
10.0	0.1972	0.2119	0.3507	0.4053	0.2984	0.0678	11.5126	19.4531	535.4000
12.0	0.1873	0.2017	0.3319	0.3837	0.2818	0.0645	10.6245	19.4279	579.8050
15.0	0.1753	0.1892	0.3090	0.3574	0.2615	0.0605	9.5240	19.4662	634.8300
18.0	0.1663	0.1799	0.2921	0.3379	0.2466	0.0575	8.7335	19.4008	674.3550
21.0	0.1571	0.1704	0.2743	0.3176	0.2308	0.0545	7.8590	19.5126	718.0800
24.0	0.1487	0.1617	0.2586	0.2995	0.2170	0.0517	7.1453	19.3800	753.7650

* Dilution factor = 100

Table D.11 Concentration measurement and calculation in total mass of crystal. Batch crystallization of mixed lysozyme - ovalbumin

(Exp. No.4-2: $c_{lys,0}$ = 20 mg/mL, $C_{oval,0}$ = 20 mg/mL, Temp. = 20 °C, 4% NaCl, pH 5.0).

Time (hr)	Absorbance						C_{lys} (mg/mL)	C_{oval} (mg/mL)	m_{cryst} (mg)
	A250	A260	A270	A280	A290	A300			
0.0	0.2931	0.3110	0.5329	0.6147	0.4596	0.0996	20.2500	19.2528	120.0000
1.0	0.2785	0.2959	0.5054	0.5830	0.4352	0.0948	18.9502	19.2026	184.9900
2.0	0.2633	0.2802	0.4763	0.5497	0.4095	0.0897	17.5523	19.2524	254.8850
3.0	0.2509	0.2674	0.4529	0.5227	0.3888	0.0856	16.4210	19.3025	311.4500
4.0	0.2384	0.2545	0.4293	0.4956	0.3680	0.0815	15.3265	19.1895	366.1750
5.0	0.2276	0.2433	0.4088	0.4720	0.3499	0.0779	14.3487	19.1956	415.0650
6.0	0.2159	0.2312	0.3863	0.4462	0.3299	0.0740	13.2458	19.3125	470.2100
8.0	0.2033	0.2182	0.3625	0.4189	0.3089	0.0698	12.1254	19.2687	526.2300
10.0	0.1959	0.2104	0.3484	0.4026	0.2965	0.0673	11.4689	19.2050	559.0550
12.0	0.1882	0.2024	0.3338	0.3859	0.2836	0.0648	10.7856	19.1682	593.2200
15.0	0.1765	0.1904	0.3115	0.3603	0.2638	0.0609	9.6874	19.3021	648.1300
18.0	0.1675	0.1810	0.2944	0.3406	0.2487	0.0579	8.8825	19.2558	688.3750
21.0	0.1573	0.1705	0.2750	0.3183	0.2316	0.0545	7.9562	19.2743	734.6900
24.0	0.1529	0.1660	0.2669	0.3089	0.2244	0.0531	7.5846	19.2100	753.2700

* Dilution factor = 100

Table D.12 Concentration measurement and calculation in total mass of crystal. Batch crystallization of mixed lysozyme - ovalbumin

(Exp. No.4-3: $c_{lys,0}$ = 20 mg/mL, $C_{oval,0}$ = 20 mg/mL, Temp. = 20 °C, 4% NaCl, pH 5.0).

Time (hr)	Absorbance						C_{lys} (mg/mL)	C_{oval} (mg/mL)	m_{cryst} (mg)
	A250	A260	A270	A280	A290	A300			
0.0	0.2931	0.3110	0.5329	0.6147	0.4596	0.0996	20.2500	19.8456	120.0000
1.0	0.2785	0.2959	0.5054	0.5830	0.4352	0.0948	18.9502	19.8025	184.9900
2.0	0.2633	0.2802	0.4763	0.5497	0.4095	0.0897	17.5523	19.7521	254.8850
3.0	0.2509	0.2674	0.4529	0.5227	0.3888	0.0856	16.4210	19.7026	311.4500
4.0	0.2384	0.2545	0.4293	0.4956	0.3680	0.0815	15.3265	19.7225	366.1750
5.0	0.2276	0.2433	0.4088	0.4720	0.3499	0.0779	14.3487	19.7865	415.0650
6.0	0.2159	0.2312	0.3863	0.4462	0.3299	0.0740	13.2458	19.8512	470.2100
8.0	0.2033	0.2182	0.3625	0.4189	0.3089	0.0698	12.1254	19.8257	526.2300
10.0	0.1959	0.2104	0.3484	0.4026	0.2965	0.0673	11.4689	19.7598	559.0550
12.0	0.1882	0.2024	0.3338	0.3859	0.2836	0.0648	10.7856	19.7156	593.2200
15.0	0.1765	0.1904	0.3115	0.3603	0.2638	0.0609	9.6874	19.6559	648.1300
18.0	0.1675	0.1810	0.2944	0.3406	0.2487	0.0579	8.8825	19.6987	688.3750
21.0	0.1573	0.1705	0.2750	0.3183	0.2316	0.0545	7.9562	19.7598	734.6900
24.0	0.1529	0.1660	0.2669	0.3089	0.2244	0.0531	7.5846	19.8125	753.2700

* Dilution factor = 100

Table D.13 Concentration measurement and calculation in total mass of crystal. Batch crystallization of mixed lysozyme – ovalbumin

(Exp. No.5-1: $c_{lys,0}$ = 10 mg/mL, $C_{oval,0}$ = 10 mg/mL, Temp. = 10 °C, 4% NaCl, pH 5.0).

Time (hr)	Absorbance						C_{lys} (mg/mL)	C_{oval} (mg/mL)	m_{cryst} (mg)
	A250	A260	A270	A280	A290	A300			
0.0	0.1449	0.1538	0.2635	0.3040	0.2272	0.0493	10.0125	9.5214	120.0000
1.0	0.1395	0.1481	0.2533	0.2922	0.2183	0.0474	9.5545	9.4126	142.9000
2.0	0.1355	0.1441	0.2456	0.2834	0.2114	0.0461	9.1510	9.5512	163.0750
3.0	0.1308	0.1392	0.2368	0.2732	0.2037	0.0446	8.7556	9.4587	182.8450
4.0	0.1272	0.1354	0.2299	0.2654	0.1976	0.0434	8.4214	9.4862	199.5550
5.0	0.1228	0.1309	0.2217	0.2559	0.1903	0.0419	8.0500	9.4057	218.1250
6.0	0.1198	0.1278	0.2160	0.2493	0.1852	0.0409	7.7554	9.4872	232.8550
8.0	0.1144	0.1222	0.2055	0.2373	0.1760	0.0391	7.2512	9.5126	258.0650
10.0	0.1088	0.1165	0.1950	0.2253	0.1667	0.0373	6.7546	9.5024	282.8950
12.0	0.1041	0.1116	0.1862	0.2151	0.1589	0.0357	6.3474	9.4462	303.2550
15.0	0.0978	0.1050	0.1741	0.2012	0.1482	0.0336	5.7651	9.4703	332.3690
18.0	0.0926	0.0997	0.1642	0.1898	0.1395	0.0319	5.2840	9.5126	356.4250
21.0	0.0878	0.0947	0.1551	0.1793	0.1314	0.0303	4.8510	9.5024	378.0750
24.0	0.0836	0.0904	0.1472	0.1703	0.1244	0.0289	4.4790	9.4857	396.6750

* Dilution factor = 100

Table D.14 Concentration measurement and calculation in total mass of crystal. Batch crystallization of mixed lysozyme – ovalbumin

(Exp. No.5-2: $c_{lys,0} = 10$ mg/mL, $C_{oval,0} = 10$ mg/mL, Temp. $= 10$ °C, 4% NaCl, pH 5.0).

Time (hr)	Absorbance						C_{lys} (mg/mL)	C_{oval} (mg/mL)	m_{cryst} (mg)
	A250	A260	A270	A280	A290	A300			
0.0	0.1428	0.1516	0.2595	0.2993	0.2237	0.0486	9.8200	9.7426	120.0000
1.0	0.1370	0.1456	0.2486	0.2868	0.2142	0.0466	9.3322	9.6854	144.3900
2.0	0.1327	0.1412	0.2403	0.2773	0.2067	0.0452	8.8974	9.7025	166.1300
3.0	0.1275	0.1357	0.2305	0.2660	0.1981	0.0435	8.4560	9.6125	188.2000
4.0	0.1237	0.1318	0.2233	0.2577	0.1917	0.0422	8.1054	.9.6548	205.7300
5.0	0.1203	0.1283	0.2169	0.2503	0.1861	0.0411	7.8213	9.7516	219.9350
6.0	0.1176	0.1255	0.2117	0.2444	0.1815	0.0402	7.5525	9.7423	233.3750
8.0	0.1126	0.1204	0.2022	0.2335	0.1731	0.0385	7.0942	9.7015	256.2900
10.0	0.1083	0.1159	0.1940	0.2241	0.1658	0.0371	6.7054	9.6429	275.7300
12.0	0.1039	0.1113	0.1857	0.2145	0.1585	0.0356	6.3245	9.6052	294.7750
15.0	0.0981	0.1053	0.1747	0.2019	0.1488	0.0337	5.7946	9.6378	321.2700
18.0	0.0924	0.0994	0.1638	0.1893	0.1391	0.0318	5.2626	9.7125	347.8700
21.0	0.0878	0.0947	0.1551	0.1794	0.1314	0.0303	4.8523	9.7029	368.3850
24.0	0.0848	0.0916	0.1495	0.1729	0.1265	0.0293	4.5887	9.6282	381.5650

* Dilution factor = 100

Table D.15 Concentration measurement and calculation in total mass of crystal. Batch crystallization of mixed lysozyme - ovalbumin

(Exp. No.5-3: $c_{lys,0}$ = 10 mg/mL, $C_{oval,0}$ = 10 mg/mL, Temp. = 10 °C, 4% NaCl, pH 5.0).

Time (hr)	Absorbance						C_{lys} (mg/mL)	C_{oval} (mg/mL)	m_{cryst} (mg)
	A250	A260	A270	A280	A290	A300			
0.0	0.1432	0.1522	0.2599	0.2998	0.2239	0.0487	9.7512	9.8550	120.0000
1.0	0.1393	0.1482	0.2523	0.2911	0.2171	0.0475	9.3524	9.9942	139.9400
2.0	0.1353	0.1440	0.2447	0.2824	0.2104	0.0461	9.0026	9.9532	157.4300
3.0	0.1314	0.1400	0.2373	0.2739	0.2038	0.0448	8.6512	9.9415	175.0000
4.0	0.1264	0.1348	0.2279	0.2630	0.1955	0.0432	8.2024	9.9364	197.4400
5.0	0.1223	0.1305	0.2202	0.2542	0.1887	0.0418	7.8556	9.8654	214.7800
6.0	0.1185	0.1266	0.2128	0.2457	0.1822	0.0405	7.4996	9.8854	232.5800
8.0	0.1130	0.1209	0.2024	0.2337	0.1730	0.0387	6.9913	9.9247	257.9950
10.0	0.1089	0.1167	0.1945	0.2247	0.1660	0.0373	6.6058	9.9624	277.2700
12.0	0.1044	0.1121	0.1861	0.2151	0.1586	0.0359	6.2089	9.9545	297.1150
15.0	0.0989	0.1064	0.1757	0.2030	0.1493	0.0340	5.7123	9.9468	321.9450
18.0	0.0947	0.1019	0.1676	0.1938	0.1423	0.0326	5.3458	9.8856	340.2700
21.0	0.0902	0.0974	0.1593	0.1842	0.1349	0.0311	4.9512	9.8712	360.0000
24.0	0.0871	0.0941	0.1532	0.1773	0.1295	0.0301	4.6589	9.8925	374.6150

* Dilution factor = 100

Table D.16 Concentration measurement and calculation in total mass of crystal. Batch crystallization of mixed lysozyme - ovalbumin

(Exp. No.6-1: $c_{lys,0}$ = 30 mg/mL, $C_{oval,0}$ = 30 mg/mL, Temp. = 20 °C, 3% NaCl, pH 5.0).

Time (hr)	Absorbance						C_{lys} (mg/mL)	C_{oval} (mg/mL)	m_{cryst} (mg)
	A250	A260	A270	A280	A290	A300			
0.0	0.4382	0.4652	0.7962	0.9185	0.6863	0.1490	30.1254	29.2450	120.0000
1.0	0.4267	0.4533	0.7746	0.8937	0.6673	0.1452	29.1200	29.1586	170.2700
2.0	0.4169	0.4432	0.7559	0.8722	0.6507	0.1420	28.2103	29.2257	215.7550
3.0	0.4069	0.4329	0.7369	0.8503	0.6339	0.1386	27.3040	29.2329	261.0700
4.0	0.3974	0.4230	0.7188	0.8295	0.6179	0.1355	26.4426	29.2251	304.1400
5.0	0.3873	0.4126	0.6997	0.8075	0.6010	0.1321	25.5321	29.2208	349.6650
6.0	0.3765	0.4014	0.6790	0.7837	0.5827	0.1285	24.5241	29.3012	400.0650
8.0	0.3568	0.3810	0.6418	0.7410	0.5499	0.1220	22.7800	29.1958	487.2700
10.0	0.3393	0.3629	0.6085	0.7027	0.5204	0.1162	21.1844	29.2256	567.0500
12.0	0.3246	0.3476	0.5805	0.6706	0.4957	0.1113	19.8548	29.2205	633.5300
15.0	0.3076	0.3300	0.5482	0.6334	0.4671	0.1056	18.3154	29.2198	710.5000
18.0	0.2924	0.3143	0.5194	0.6003	0.4417	0.1006	16.9432	29.2195	779.1100
21.0	0.2809	0.3024	0.4975	0.5752	0.4223	0.0967	15.8987	29.2256	831.3350
24.0	0.2724	0.2936	0.4814	0.5567	0.4081	0.0939	15.1295	29.2301	869.7950

* Dilution factor = 50

Table D.17 Concentration measurement and calculation in total mass of crystal. Batch crystallization of mixed lysozyme - ovalbumin

(Exp. No.6-2: $c_{lys,0}$ = 30 mg/mL, $C_{oval,0}$ = 30 mg/mL, Temp. = 20 °C, 3% NaCl, pH 5.0).

Time (hr)	Absorbance						C_{lys} (mg/mL)	C_{oval} (mg/mL)	m_{cryst} (mg)
	A250	A260	A270	A280	A290	A300			
0.0	0.4350	0.4620	0.7899	0.9112	0.6806	0.1480	29.7540	29.5024	120.0000
1.0	0.4274	0.4542	0.7755	0.8947	0.6678	0.1455	29.0548	29.5526	154.9600
2.0	0.4171	0.4435	0.7558	0.8720	0.6504	0.1421	28.1024	29.6014	202.5800
3.0	0.4075	0.4336	0.7375	0.8510	0.6342	0.1389	27.2256	29.6250	246.4200
4.0	0.3994	0.4252	0.7223	0.8335	0.6208	0.1362	26.5126	29.5784	282.0700
5.0	0.3898	0.4152	0.7039	0.8124	0.6046	0.1330	25.6423	29.5628	325.5850
6.0	0.3807	0.4058	0.6866	0.7925	0.5892	0.1299	24.8120	29.5813	367.1000
8.0	0.3632	0.3877	0.6534	0.7543	0.5599	0.1241	23.2245	29.6005	446.4750
10.0	0.3444	0.3683	0.6178	0.7135	0.5285	0.1179	21.5468	29.5429	530.3600
12.0	0.3259	0.3491	0.5826	0.6730	0.4973	0.1117	19.8540	29.5861	615.0000
15.0	0.2992	0.3215	0.5318	0.6146	0.4524	0.1029	17.4256	29.6236	736.4200
18.0	0.2823	0.3041	0.4998	0.5778	0.4241	0.0973	15.9025	29.6145	812.5750
21.0	0.2723	0.2937	0.4808	0.5560	0.4073	0.0939	15.0012	29.6025	857.6400
24.0	0.2641	0.2852	0.4652	0.5381	0.3936	0.0912	14.2654	29.5784	894.4300

* Dilution factor = 50

Table D.18 Concentration measurement and calculation in total mass of crystal. Batch crystallization of mixed lysozyme - ovalbumin

(Exp. No.6-3: $c_{lys,0}$ = 30 mg/mL, $C_{oval,0}$ = 30 mg/mL, Temp. = 20 °C, 3% NaCl, pH 5.0).

Time (hr)	Absorbance						C_{lys} (mg/mL)	C_{oval} (mg/mL)	m_{cryst} (mg)
	A250	A260	A270	A280	A290	A300			
0.0	0.4300	0.4569	0.7802	0.9001	0.6719	0.1463	29.2526	29.6524	120.0000
1.0	0.4191	0.4456	0.7594	0.8762	0.6535	0.1427	28.2520	29.6874	170.0300
2.0	0.4064	0.4325	0.7354	0.8486	0.6324	0.1385	27.1200	29.6514	226.6300
3.0	0.3954	0.4211	0.7145	0.8246	0.6138	0.1349	26.1103	29.6923	277.1150
4.0	0.3846	0.4099	0.6940	0.8010	0.5957	0.1313	25.1456	29.6518	325.3500
5.0	0.3742	0.3991	0.6744	0.7785	0.5784	0.1278	24.2356	29.5587	370.8500
6.0	0.3650	0.3896	0.6570	0.7585	0.5631	0.1248	23.4060	29.5613	412.3300
8.0	0.3488	0.3729	0.6263	0.7232	0.5359	0.1194	21.9520	29.5248	485.0300
10.0	0.3378	0.3614	0.6053	0.6990	0.5174	0.1157	20.9564	29.5069	534.8100
12.0	0.3283	0.3517	0.5869	0.6779	0.5010	0.1126	20.0042	29.7895	582.4200
15.0	0.3126	0.3355	0.5571	0.6437	0.4746	0.1074	18.5640	29.8654	654.4300
18.0	0.3000	0.3224	0.5332	0.6162	0.4535	0.1031	17.4589	29.7423	709.6850
21.0	0.2885	0.3105	0.5115	0.5913	0.4344	0.0993	16.4326	29.7151	761.0000
24.0	0.2784	0.3001	0.4924	0.5693	0.4175	0.0960	15.5246	29.7016	806.4000

* Dilution factor = 50

APPENDIX E

LIST OF PUBLICATIONS

List of Publications

Maosoongnern, S., Borbon, V.D., Flood, A.E., and Ulrich, J. (2012). Introducing a Fast Method to Determine the Solubility and Metastable Zone Width for Proteins: Case Study Lysozyme. **Ind. Eng. Chem. Res.** 2012(51): 15251−15257.

Maosoongnern, S., Borbon, V.D., Pertig, D., and Ulrich, J. (2011). **Determination of metastable zone width: case study lysozyme.** 18th BIWIC International Workshop on Industrial Crystallization. Delft, The Netherlands.

Introducing a Fast Method to Determine the Solubility and Metastable Zone Width for Proteins: Case Study Lysozyme

Somchai Maosoongnern,[†] Viviana Diaz Borbon,[‡] Adrian E. Flood,[†] and Joachim Ulrich[‡,*]

[†]School of Chemical Engineering, Suranaree University of Technology, Nakhon Ratchasima 30000, Thailand

[‡]Martin-Luther-Universität Halle-Wittenberg, Zentrum für Ingenieurwissenschaften, Verfahrenstechnik/TVT, D-06099 Halle (Saale), Germany

ABSTRACT: The phase diagrams of tetragonal hen egg white lysozyme containing besides thermodynamic (solubility) also kinetic (nucleation) data were determined for pH values of 4.4, 5.0, and 6.0, 3 to 7 wt % sodium chloride concentrations and lysozyme concentrations from 5 to 70 mg/mL by the use of a turbidity technique. This new technique offers a rapid, precise and reliable determination of nucleation and solubility points. These points can be obtained simultaneously within 6 h. The errors of measurements are less than ± 0.9 °C for the solubility temperature and less than ± 1.0 °C for the nucleation temperature. The solubility data obtained could be extended and described by a good correlation with literature data. The solubility of lysozyme was found to decrease with increasing salt concentration while the nucleation points were observed more early with respect to salt addition; as a consequence the metastable zone is more narrow. The solubility of lysozyme is slightly reduced at higher values of the pH, and the nucleation point is observed later in time. The result is an increase of the metastable zone width.

1. INTRODUCTION

Knowledge of the phase diagram has key importance when designing and controlling a crystallization process for a substance. In the case of proteins, accurate phase diagram data is limited due to the complexity of their structure caused by the diversity of the amino acid residue groups that form proteins, with this process being easily influenced by environmental conditions. Natural proteins contain 20 standard amino acids.[1] A significant characteristic for the biological function as well as for the crystallization of proteins is that the residues consist of polar functional groups and nonpolar functional groups. The polar groups prefer to associate with water. In contrast to these hydrophilic groups, the nonpolar hydrophobic groups prefer to associate with themselves. The hydrophilic groups result in proteins having finite water solubility despite being very large molecules. The solubility of a protein depends strongly on the protein–protein interactions as well as on the protein–solvent interactions.[2] Any slight modification of the composition can influence the solubility dramatically, or even alter the nature of these macromolecules. Independently of the complexity of protein behavior, the phase transformation is still governed by both the thermodynamics and the kinetics of the system. It is still possible to describe all this information in phase diagrams. In the case that crystallization conditions or nucleation points are identified the information can be plotted in phase diagrams, and in this case the information that is provided relates to both thermodynamics and kinetics.

There is a well studied protein from which a large set of reported data on solubility and crystallization conditions is available: hen egg white lysozyme (HEWL). This protein is composed of 129 amino acids and it has molecular weight of 14.3 kDa.[3–5] It is a basic protein with an approximate isoelectric point value of 11.3 and belongs to the group of globular proteins.[6] HEWL has often been used in thermodynamic and kinetic crystallization studies.[2,7–17,19–24] In order to

control the isothermal batch crystallization within specific conditions the phase diagram of HEWL is required. Even though it is one of the most studied proteins, phase diagrams which contain solubility and nucleation curves (which is kinetic information rather than thermodynamic) for pH 4.4, 5.0, and 6.0, with NaCl from 3 to 7 wt % and with a temperature range of 2−45 °C are not available. However, for instance, the solubility of HEWL at pH 4.4 and 5 and temperatures between 2 and 25 °C have been reported,[7–9] but for higher temperatures there is no data. This has been the impulse which brought the present work to be conducted. It is necessary to complete these solubility curves up to the operating temperatures of the desired batch crystallization process or any other further interest, as well as the nucleation points for the whole range of conditions in order to control the crystallization process.

Several methods have been used to measure the solubility of proteins, such as the well-known classical dissolution and crystallization methods.[10–12] These methods have the disadvantage of requiring long times due to the slow diffusivity of proteins in the solution and also resulting in very imprecise measurements. The measured solubility points by these methods might have a concentration higher or lower than the equilibrium concentration. One good alternative for measuring the solubility of proteins is the use of a miniature column technique.[8,13] This technique is known as a rapid determination technique with high reliability (the solubility data can be obtain within 24 h with an error less than ± 1 mg/mL)[9] and requires only a small amount of material. Therefore the use of this method allows a larger number of experiments in the same

amount of materials, and thus a better data set. However, it is not possible to carry out more than one experiment at one time. In order to measure the nucleation point, some methods such as microtiter plates or micofluidic tools[14] are used. Both crystallizations require only a small volume of solution. However, these methods have precision limitations because they are based on optical observations.

Here the turbidity measurement method for detection of the nucleation and solubility points of proteins is introduced using lysozyme as a model substance. The principle of this method consists of the application of an IR signal through a protein solution, and the detection of changes in the signal produced by changes in the mixture caused by thermal changes. This signal has 100% transmission when the solution is clear. If the solution is cooled down and the nucleation temperature is reached, the transmission decreases due to the scattering of the signal by particles formed within the solution (protein nuclei). It is assumed that this corresponds to the formation of the protein crystals which may nucleate within the drops rich with protein. Images of the solution were acquired to ensure the formation of the crystal. The protein nuclei grow further during the cooling process, up to crystals with significant size. It is therefore possible to increase the temperature of the solution and induce the dissolution of the crystals until the equilibrium is reached. At this point the formed particles are totally dissolved and the transmission of the IR signal is again 100%. This temperature corresponds to the solubility point. The method offers furthermore the possibility to measure the nucleation and solubility points simultaneously in one experiment, and it is possible to carry out up to 10 experiments simultaneously. The required solution volume is only 1 mL and the duration for one cycle (nucleation and solubility measurement) is just 6 h.

In the present work the phase diagrams are reported for lysozyme, and contain the thermodynamic data (solubility, either obtained from literature or self-measured) and the kinetic data (nucleation points) for pH values of 4.4, 5.0 and 6.0, 3−7 wt % sodium chloride concentrations and lysozyme concentrations from 5 to 70 mg/mL. In the operation of a crystallization process the kinetic data are vital to observe the change in the crystallizing system over time, and are equally important as the thermodynamic data which are used to observe the behavior of the system at equilibrium. Therefore, the positioning of these data together in the phase diagram is very useful. For example, in the solvent freeze out crystallization process of lysozyme[15] the particle size or size distribution of the crystals can be controlled by changing the process conditions from the nucleating region to the middle of the metastable region, which is only possible if the phase diagram is known. In an isothermal crystallization the supersaturation value has a strong effect on the growth rate and the habit of the growing protein crystals.[16,17] Therefore, the operation time, size and quality of the crystals can be directly controlled by the supersaturation value.

Furthermore, the metastable zone widths (MZW) are presented and offer the opportunity to be used to control isothermal or cooling crystallization processes.

2. MATERIALS AND METHODS

Hen egg white lysozyme (HEWL) (product no. 62971, Fluka) was used without further purification since no other proteins were detected in a SDS-PAGE gel electrophoresis analysis (15% acrylamide). Sodium chloride, NaCl (≥99.5%, Carl Roth)

was used as a crystallizing agent. 0.1 M sodium acetate buffer stock solutions were prepared with sodium acetate trihydrate (≥99.5%, Carl Roth) and acetic acid (100%, Carl Roth) based on the method of Dawson et al.[18] 100 mg/mL lysozyme stock solution was prepared by dissolving 2 g of lysozyme into enough 0.1 M sodium acetate buffer to obtain a final volume of 20 mL at the desired pH. After dissolution (approximately 3 h), the solution was centrifuged at 9000 rpm for 15 min by the use of a 2−16K centrifuge (Sigma, Germany) in order to remove any undissolved particles that cannot be observed by the naked eye. There was no significant amount of protein removed by the centrifuge since the lysozyme concentration after centrifuge was 99.87 ± 0.21 mg/mL (using the UV absorbance technique, see Section 2.2). The solution was then kept at 4−8 °C in a refrigerator. A 0.2 g/mL salt stock solution was prepared by dissolving 4 g of NaCl into enough 0.1 M sodium acetate buffer to obtain a final volume of 20 mL at the desired pH.

Solutions with pH of 4.4, 5.0, and 6.0, salt concentrations of 3, 4, 5, and 7 wt %, and with 5−70 mg/mL of lysozyme were prepared by appropriate mixing of the stock solutions (0.1 M sodium acetate buffer, lysozyme stock solution, and salt stock solution).

2.1. Measurements of Nucleation and Solubility Points via the Turbidity Method. The temperatures of nucleation and solubility points were measured by the detection of turbidity changes in the solutions through temperature variations. All experiments were performed in a STEM Integrity 10 system (Electro Thermal, England) depicted in Figure 1.
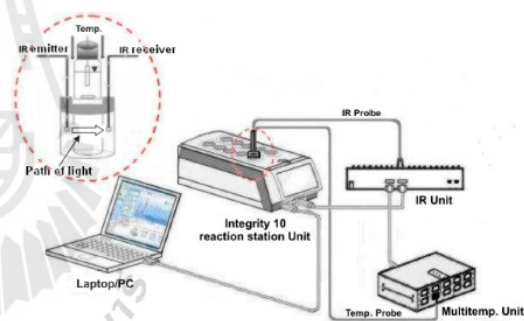
Figure 1. STEM Integrity 10 system (Electro Thermal).

This device can run up to 10 experiments (one experiment per cell of the STEM Integrity 10 reaction station) at the same time with independent control of temperature and stirring speed. The operating ranges of the device are stirring speed from 250 to 1200 rpm, temperature from −30 to 150 °C and maximum cooling and heating rates of 5 °C/min.

To start the experiment a 1.5 mL glass bottle containing 1 mL of lysozyme solution (with known concentration) was inserted in an IR probe (part code ATS10360) which was placed in a cell of a STEM Integrity 10 reaction station. This IR probe was designed as a miniature transmission probe for operation in the wavelength range of 920−960 nm and with a light pathway of 8 mm. The light was passed through the solution from the IR emitter channel to the IR receiver channel. The temperature sensor was immersed into the solution through the cap of the glass bottle. The solution was stirred at 350 rpm while it was cooled or heated. The STEM Integrity 10 reaction station is controlled by the STEM Integrity 10
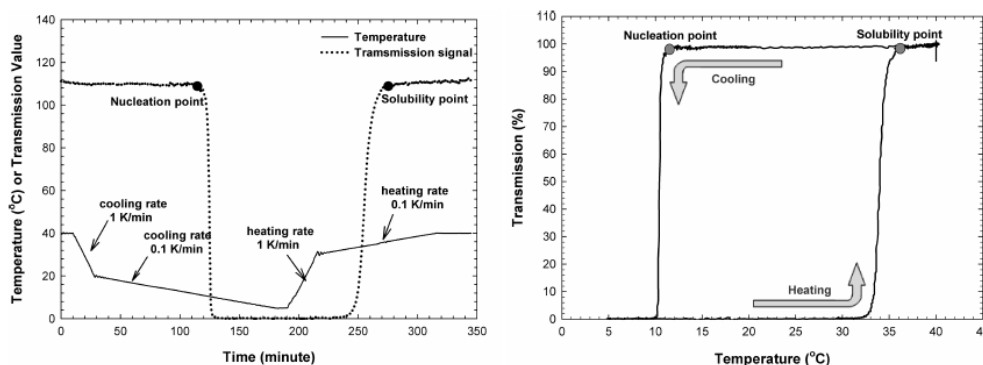
Figure 2. Left: Temperature profile. Right: Change in turbidity of a lysozyme solution with temperature. Lysozyme concentration 25 mg/mL, 4 wt % NaCl, and pH 4.4.

software. The real time turbidity (the ratio of the light intensity before and after passing through the solution) and temperature of the solutions are collected by connecting the IR probe to the Multi-IR box (part code ATS10232) and the temperature sensor to the Multi-Temp 10 Module (part code ATS10001). Both IR Unit and Multi-Temp 10 Module were connected to the computer through the STEM Integrity 10 reaction station block.

To determine the nucleation point, the temperature of the determined solution is increased to 35, 40, 45, or 50 °C (depending on pH, lysozyme concentration and salt concentration) and kept constant for 10 min. Then, the temperature is decreased to the set temperature of 0, 5, 10, or 15 °C (depend on the nucleation point) and kept constant again at this set temperature for 10 min. Two cooling rates are applied to the system: 1.0 K/min and 0.1 K/min. The faster cooling rate is applied when the temperature of the solution is far from the set temperature and the slower cooling rate when the temperature of the system approaches it. The changing point of the cooling rate is approximately 5 °C higher than the nucleation point. This is an approximation of the researcher based on preliminary experiments. The MZW changes with respect to a slower cooling rate. The example of a temperature profile for the experiment with lysozyme concentration of 25 mg/mL, 4 wt % NaCl and pH 4.4 is given in Figure 2 (left). The solution was heated up to 40 °C for 10 min. Then the temperature was decreased to 20 °C within 20 min (cooling rate = 1 K/min). After that the solution was cooled again to 5 °C within 150 min and kept at constant temperature at this point for 10 min. The nucleation point is defined as the first point at which a distinct drop in transmission is measured while the temperature is decreasing. A VHX-500F microscope (Keyence, Germany) was used to analyze the morphology of the nucleated crystals.

To determine the solubility point, after the cooling process and the formation of the crystals the solution is heated up to a set temperature (the same point as the start of the cooling process). The temperature profile was also divided into 2 steps, as in the cooling process (using a heating rate of 1.0 K/min when the temperature is far from the set point and 0.1 K/min when the temperature is near to the set point). The solubility point is defined as the point at which the transmission reaches a stable plateau while the temperature is increasing. The plot of transmission against temperature gives clear information on nucleation and solubility points (see Figure 2, right).

2.2. Solubility Measurement by the Miniature Column Technique (Low Temperature, pH 6.0). Tetragonal lysozyme crystals were prepared by mixing equal volumes of 100 mg/mL lysozyme solution and 8 wt % sodium chloride solution and keeping the mixture at 4–8 °C overnight. The solubility of tetragonal lysozyme crystals at pH 6.0 was measured at 5, 10, 15, 20, and 25 °C with sodium chloride concentration of 3, 4, and 5 wt % using the miniature column technique as described by Cacioppo et al.[8] and Pusey and Gernert.[13] The temperature of the column was maintained within ±0.1 °C using a thermostat (F12 ED, Julabo).

The concentrations of dissolved lysozyme were measured using a UV photometer (Carry 50, Varian) at 280 nm. An extinction coefficient of 2.4321 mL·mg^{-1}·cm^{-1} was used (obtained from a calibration curve of 9 measurements).

3. RESULTS AND DISCUSSION

3.1. Phase Diagrams. The measured nucleation (kinetic) and solubility (thermodynamic) points for the lysozyme systems were plotted in phase diagrams. Each data point is the average of three replicate experiments (the samples used in each replicate experiment were fresh prepared from the stock solution). The nucleation points are corresponding to a cooling rate of 0.1 K/min since this cooling rate was applied to the system at least 5 °C higher than the nucleation point.

The preliminary experiments showed that there is no effect of a cooling rate of 1 K/min on the MZW if the cooling rate was changed to 0.1 K/min at a point at least 5 °C higher than the nucleation. We compared the result from this experiment to the result of an experiment at a constant cooling rate equal to 0.1 K/min and obtained the same nucleation temperature to within ±1.0 K.

In Figure.3 the applied cooling rates in the second step of the cooling process were 0.1, 0.2, 0.3, and 0.4 K/min. The detected nucleation and the solubility temperatures are nearly the same (an error of less than 1 °C is observed). In some conditions the induction time is expected to be very long because the nucleation is very difficult at high pH. This result shows that it is also possible to increase the second cooling rate up to 0.4 K/min and still obtain results consistent with 0.1 K/min cooling rate.

The maximum error (the difference between the measured value and the average value) of the measurement is ±0.9 °C for the solubility temperature and ±1.0 °C for the nucleation
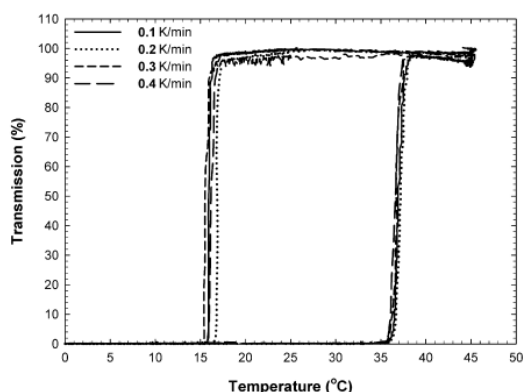
Figure 3. Change in turbidity of a lysozyme solution with temperature. Different cooling rates (0.1, 0.2, 0.3, and 0.4 K/min) were applied in the second step of the cooling process. Lysozyme concentration 40 mg/mL, 4 wt % NaCl and pH 4.4.

temperature. The phase diagrams of lysozyme for different sodium chloride concentrations at pH 4.4, 5.0, and 6.0 are shown in Figures 4, 5 and 6, respectively. The solubility data
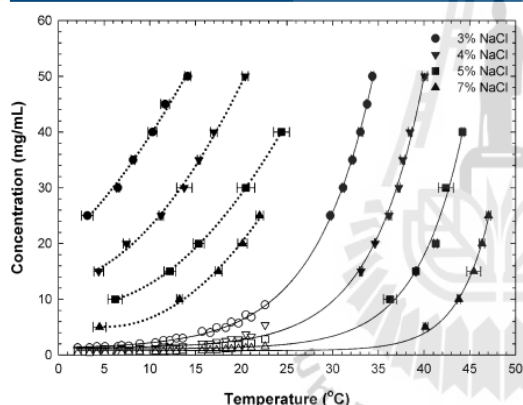
Figure 4. Phase diagram of HEWL for pH 4.4, open symbols are solubility data from literature.[9] The dashed lines represent the fitted nucleation data. The solid lines represent the fitted solubility data.

obtained from the turbidity measurements for pH values of 4.4 and 5.0 were plotted with the solubility data from the literature.[9] The solubility for systems at pH 6.0 and low temperatures was measured as described in the previous section (Section 2.2). There are no literature data for these conditions to be found. The reliability of the measurements was shown by a good correlation of the solubility data (solid line) with an exponential growth ($R^2 \geq 0.99$). The literature solubility data[9] which was obtained by the use of the miniature column technique has been compared with the solubility data of Apgar[19] (who determined the solubility of lysozyme crystals by observation of the rate of change of scattering intensity of the sample) and it was found to be in good agreement. Therefore, the solubility data measured in this work is consistent with the experimental results of Apgar. The solubility is a thermodynamic property of a substance, and the Van't Hoff equation can
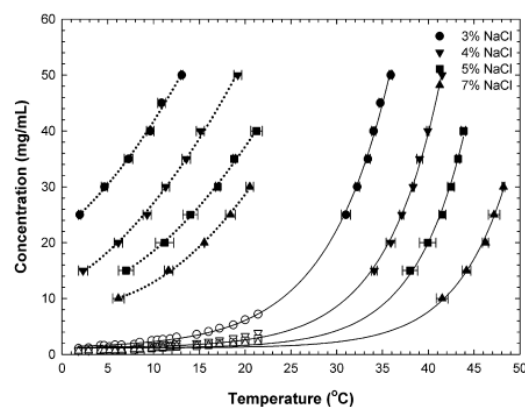
Figure 5. Phase diagram of HEWL for pH 5.0, open symbols are the solubility data from literature.[9] The dash lines represent the fitted nucleation data. The solid lines represent the fitted solubility data.
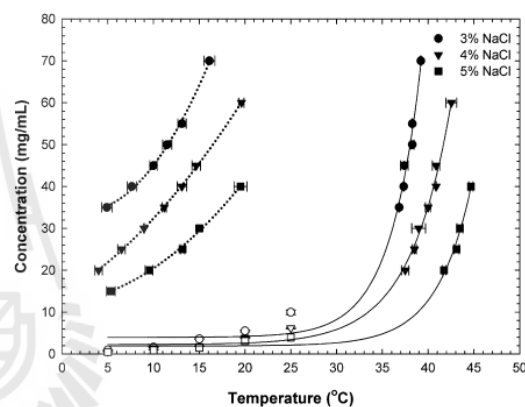
Figure 6. Phase diagram of HEWL for pH 6.0, open symbols are the solubility data obtained by the use of a miniature column technique. The dash lines represent the fitted nucleation data. The solid lines represent the fitted solubility data.

be used to describe the changes in solubility with temperature. The exponential growth equation can be linearized into the Van't Hoff equation. Therefore the solubility data can be represented with a curve of exponential type. A second order polynomial was used to fit the onset of the nucleation data, which are indicated as dotted lines in the phase diagrams.

To verify the morphology of the crystals formed during the cooling step (nucleation), the crystals were observed under a microscope. In Figure 7(a), small crystals obtained shortly after the end of the cooling process are shown as an example. The size of the crystals is less than 10 μm and it was difficult to identify their morphology. Therefore, a sample of those crystals has been kept for three days at 4−8 °C in order to let them grow. In Figure 7(b), crystals with sizes around 100 μm are shown. Due to the larger size of the crystals, the tetragonal shape is easily recognized for this example as well as for almost all the crystals analyzed in the measurement of the nucleation points. However, for 7 wt % of NaCl and 40 mg/mL of
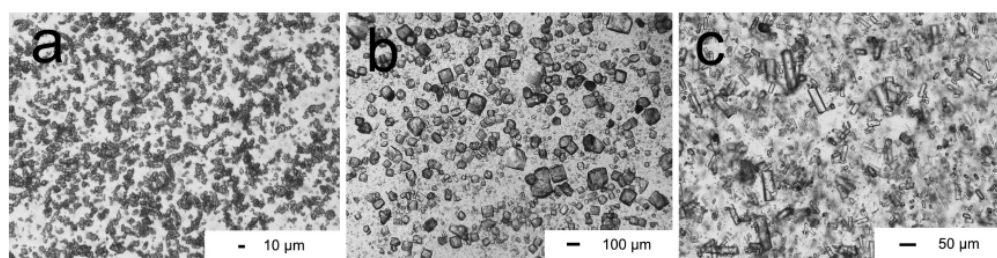
Figure 7. Lysozyme crystals (30 mg/mL, pH 5.0, 4 wt % NaCl): (a) after end of cooling process, (b) after three days growth at 4 °C. Lysozyme crystals (40 mg/mL, pH 5.0, 7 wt % NaCl): (c) after three days growth at 4 °C.
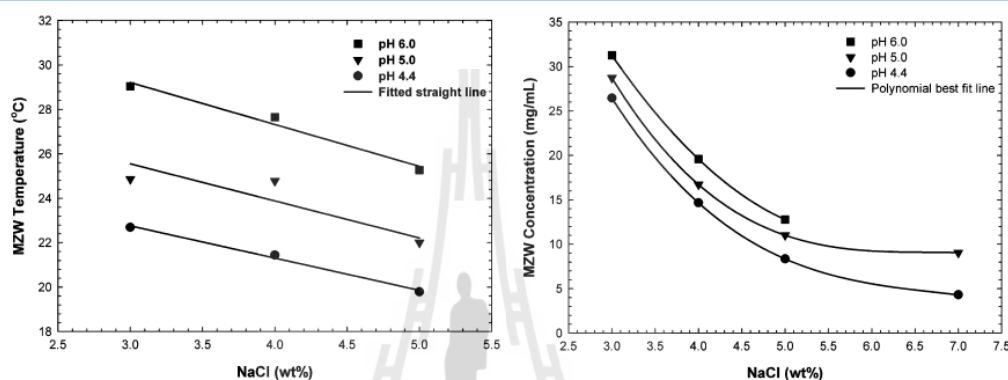
Figure 8. Left: Influence of NaCl concentration and solution pH on the MZW with respect to temperature level. Lysozyme concentration: 40 mg/mL. Right: Influence of NaCl concentration and solution pH on the MZW with respect to protein concentration at 5 °C.

lyosozyme at pH 5.0, the crystals show an orthorhombic shape (see Figure 7(c)).

In the phase diagrams (Figures 4, 5, and 6) it can be observed that there is a concurrent shift in nucleation and solubility points with salt concentration. This phenomenon was also observed and reported by other authors.[7,20,21] Therefore, with increasing salt concentration the nucleation temperature approaches to 25 °C, the temperature at which there is a phase transformation from the tetragonal lysozyme crystals form into the orthorhombic form.[22−24] This explains the formation of the orthorhombic crystals at higher concentrations of lysozyme for 7 wt % of NaCl at pH 5.0 (Figure 7(c)).

As it can be observed in Figure 6 (pH 6.0), experimental data for 7 wt % sodium chloride are missing. Well shaped tetragonal crystals were not obtained after the end of the cooling process for these conditions. The formation of particles in the solution took place after the end of the cooling process, but once the temperature of the system was increased (the heating process) the particles were immediately dissolved. In this case it was not possible to further analyze the particles by microscopy to determine which morphology they presented. The measured solubility and nucleation values are not reliable, and are therefore not reported for these conditions. The possible explanation of this phenomenon is the occurrence of liquid−liquid phase separation (LLPS) without nucleation of protein crystals. In general LLPS occurs at a very high supersaturation and can occasionally be observed by changing the solution condition.[25] When LLPS occurred liquid drops were formed containing a high concentration of protein. These drops may separate from the rest of the solution, which now contains a lower concentration of protein. The many small drops can scatter light, resulting in a drop in the transmission of light detected by the device, similar to the nucleation of a crystal. However, when the solution was heated up the solution immediately become clear liquid because LLPS is inherently a metastable transition in protein solution.[26] In this case it is considered that the LLPS occurred without the nucleation of protein crystals taking place within the protein-rich droplets.

At pH 6.0 it is barely possible to crystallize lysozyme in tetragonal shape from sodium acetate solutions. This behavior was also reported by Alderton and Fevold.[27] They observed a copious crystallization at pH 3.5, moderate at pH 4.8 and very slight at pH 5.8, by using 5 wt % sodium chloride and an initial lysozyme concentration of 40 mg/mL. It indicates that the crystallization of HEWL in the tetragonal form is less probable at high pH values and high salt concentrations (>5 wt %).

In all cases the nucleation point is reached more early with increasing salt concentration. The solubility decreases with increasing salt concentration. This is due to the salting out effect, therefore, the crystallization is easier to perform.[20] The solution pH also has an influence on the nucleation point of lysozyme crystals as shown in the phase diagrams. The nucleation temperature and concentration decreases with increasing pH as can be observed if Figures 4, 5, and 6 are compared. The pH has a stronger effect on the nucleation points than on the solubility. The solubility slightly decreases with increasing pH due to the low ionic strength,[7] a behavior that was also observed by Ataka et al.[28]

The phase diagrams shown in Figures 4 and 5 as well as in Figure 6 supply information for a study of the behavior of the process when the experimental conditions change with respect to time. The location of the nucleation line indicates the border of the nucleation region and the upper limit of the metastable region. In the metastable region the nucleated crystals can grow without the formation of new crystals. In protein crystallization, the growth of a protein crystal to a suitable size for structural determination is still difficulty. The presence of the nucleation line in the phase diagram helps to know how to change the solution conditions to allow the crystals grow after they have been nucleated.

3.2. Metastable Zone Width (MZW). Nucleation, one of the two phenomena in crystallization, gives one boundary of the metastable zone; the zone width is therefore strongly kinetically influenced. The information on the metastable zone is limited by the precision of the method to detect the presence of particles with determined size. There are no fluctuations of the turbidity signal during the cooling process. It is assumed that this corresponds to the formation of the protein crystals which probably nucleate within the drops rich with protein. These nuclei probably have an inherent growth and this nucleation point should carry the inherent uncertainly of the exact nucleation point. Nevertheless, it is consider a good estimation of the nucleation point for phase diagrams that will be used as guide in crystallization.

The width of the metastable zone is determined as the distance between the solubility and the corresponding nucleation points. The MZW are shown in the phase diagrams for the evaluated pH values and sodium chloride concentrations in Figure 8. Depending on the arrangements of the axis, the width can be expressed, for example, with respect to temperature for 40 mg/mL of lysozyme (Figure 8, left) or concentration at 5 °C (Figure 8, right).

In Figure 8 it can be observed that the increasing of salt concentration causes the narrowing of the MSW. This phenomenon can be described by linking protein−protein interaction with the classical nucleation theory.[17] Increasing salt concentration can reduce the energy barrier of the diffusion of protein molecules from the bulk solution to the cluster (more ions represent less protein − solvent interaction). Therefore, the strength of protein − protein interaction is increased with increasing salt concentration. The increasing of pH value causes an increase in the width of the MZW. One explanation of this is that lysozyme is a protein that consists of a number of side-chain groups that have pK_a values close to or within the pH range of 4.0−5.2.[29] The titration of side chains at increment of pH value can form intermolecular interactions which may increase the interfacial tension.[30] Therefore, the nucleation rate may be reduced. This behavior of the metastable zone width is expected and is to be found for all the other conditions evaluated in Section 3.1. The narrowing of the metastable zone with increasing salt concentration results from a shift of the nucleation curve together with a smaller shift of the solubility line. This has been previously observed and reported by other authors.[15,17,21]

4. CONCLUSIONS

The concentration−temperature phase diagrams enriched by the kinetic data necessary to design crystallization processes are here determined for lysozyme as a function of sodium chloride concentration and solution pH, by the use of a turbidity measurement technique. This technique shows a rapid and reliable determination of nucleation and solubility points. The use of this technique allows the collection of data of the metastable zone width within a few hours rather than days, and with a high precision compared to conventional methods.[10−12] The presence of the kinetic data in the phase diagram offers the possibility to use this information for design and control crystallization process. To maintain the right modification, tetragonal rather than orthorhombic, was an aim. The width of the metastable zone of lysozyme in sodium acetate buffer depends on the solution conditions (in this study: initial protein concentration, salt concentration, and solution pH). The knowledge of the influence of these variables on the metastable zone width can be used to predict the phase diagram for another set of conditions. For example, using seeded isothermal batch crystallization at 5 °C, pH 5.4, and 4 wt % NaCl the upper limit of MZW concentration would be approximately 18 mg/mL higher than the solubility (see Figure 8, right). Or using the cooling batch crystallization for the 40 mg/mL initial lysozyme concentration, pH 5.4, and 4 wt % NaCl the MZW temperature is approximately 25 °C lower than the solubility temperature (see Figure 8, left).

■ AUTHOR INFORMATION

Corresponding Author
*Tel.: +49 345 55 - 28400. Fax: +49 345 55 - 27358. E-mail: Joachim.ulrich@iw.uni-halle.de.

Notes
The authors declare no competing financial interest.

■ REFERENCES

(1) Rosenberger, F. Protein crystallization. *J. Cryst. Growth* **1996**, *166* (1−4), 40−54.

(2) Curtis, R. A.; Lue, L. A Molecular Approach to Bioseparations: Protein−Protein and Protein−salt Interactions. *Chem. Eng. Sci.* **2006**, *61* (3), 907−923.

(3) Blake, C. C. F.; Koenig, D. F.; Mair, G. A.; North, A .C. T.; Phillips, D. C.; Sarma, V. R. Structure of Hen Egg-White Lysozyme: A Three-Dimensional Fourier Synthesis at 2 Å Resolution. *Nature* **1965**, *206* (4986), 757−761.

(4) Canfield, R. E. The Amino Acid Sequence of Egg White Lysozyme. *J. Biol. Chem.* **1963**, *238* (8), 2698−2707.

(5) Jolles, P. Lysozymes: A Chapter of Molecular Biology. *Angew. Chem., Int. Ed.* **1969**, *8* (4), 227−239.

(6) Wetter, L. R.; Deutsch, H. F. Immunological studies on egg white proteins 0.4. Immunochemical and physical studies of lysozyme. *J. Biol. Chem.* **1951**, *192*, 237−242.

(7) Cacioppo, E.; Pusey, M. L. The Solubility of the Tetragonal Form of Hen Egg White Lysozyme From pH 4.0 to 5.4. *J. Cryst. Growth* **1991**, *114*, 286−292.

(8) Cacioppo, E.; Munson, S.; Pusey, M. L. Protein Solubilities Determined by a Rapid Technique and Modification of That Technique to a Micro-Method. *J. Cryst. Growth* **1991**, *110*, 66−71.

Industrial & Engineering Chemistry Research Article

(9) Forsythe, E. L.; Judge, R. A.; Pusey, M. L. Tetragonal Chicken Egg White Lysozyme Solubility in Sodium Chloride Solutions. *J. Chem. Eng. Data* 1999, *44*, 637−640.

(10) Ataka, M.; Asai, M. Systematic Studies on the Crystallization of Lysozyme Determination and Use of Phase Diagrams. *J. Cryst. Growth* 1988, *90*, 86−93.

(11) Retailleau, P.; Ries-Kautt, M.; Ducruix, A. No Salting-In of Lysozyme Chloride Observed at Low Ionic Strength over a Large Range of pH. *Biophys. J.* 1997, *73*, 2156−2163.

(12) Howard, S. B.; Twigg, P. J.; Baird, J. K.; Meehan, E. J. The Solubility of Hen Egg-Whjte Lysozyme. *J. Cryst. Growth* 1988, *90*, 94−104.

(13) Pusey, M. L.; Gernert, K. A Method for Rapid Liquid-Solid Phase Solubility Measurements Using the Protein Lysozyme. *J. Cryst. Growth* 1988, *88*, 419−424.

(14) Ildefonso, M.; Revalor, E.; Punniama, P.; Salmon, J. B.; Candoni, N.; Veesler, S. Nucleation and Polymorphism Explored via an Easy-to-Use Microfluidic Tool. *J. Cryst. Growth* 2012, *342*, 9−12.

(15) Diaz Borbon, V.; Ulrich, J. Solvent Freeze out Crystallization of Lysozyme from a Lysozyme-Ovalbumin Mixture. *Cryst. Res. Technol.* 2012, *47* (5), 541−547.

(16) Elgersma, A. V.; Ataka, M.; Katsura, T. Kinetic Studies on the Growth of Three Crystal Forms of Lysozyme Based on the Measurement of Protein and Cl⁻ Concentration Changes. *J. Cryst. Growth* 1992, *122* (1−4), 31−40.

(17) Liu, Y.; Wang, X.; Ching, C. B. Toward Further Understanding of Lysozyme Crystallization: Phase Diagram, Protein-Protein Interaction, Nucleation Kinetics, and Growth Kinetics. *Cryst. Growth Des.* 2010, *10*, 548−558.

(18) Dawson, R. M. C.; Elliot, D. C.; Elliot, W. H.; Jones, K. M. *Data for Biochemical Research*, 3rd ed.; Science Publication: Oxford, 1986.

(19) Apgar, M. C. *Graduate School Theses and Dissertations*, University of South Florida (USF), 2008.

(20) Ries-Kautt, M. M.; Ducruix, A. F. Relative Effectiveness of Various Ions on the Solubility and Crystal Growth of Lysozyme*. *J. Biol. Chem.* 1989, *264* (2), 745−748.

(21) Muschol, M.; Rosenberger, F. Liquid−liquid Phase Separation in Supersaturated Lysozyme Solutions and Associated Precipitate Formation/Crystallization. *J. Chem. Phys.* 1997, *107* (6), 1953−1962.

(22) Jollbs, P.; Berthou, J. High Temperature Crystallization of Lysozyme: An Example of Phase Transition*. *FEBS Lett.* 1972, *23* (1), 21−23.

(23) Berthou, J.; Jolies, P. A Phase Transition in a Protein Crystal: The Example of Hen Lysozyme*. *Biochim. Biophys. Acta* 1974, *336*, 222−227.

(24) Ewing, F.; Forsythe, E.; Pusey, M. L. Orthorhombic Lysozyme Solubility. *Acta Crystallogr.* 1994, *D50*, 424−428.

(25) Asherie, N. Protein Crystallization and Phase Diagrams. *Methods* 2004, *34*, 266−272.

(26) Asherie, N.; Lomakin, A.; Benedek, G. B. Phase diagram of colloidal solutions. *Phys. Rev. Lett.* 1996, *77* (23), 4832−4835.

(27) Alderton, G.; Fevold, H. L. Direct Crystallization of Lysozyme from Egg White and Some Crystalline Salts of Lysozyme. *J. Biol. Chem.* 1946, *146*, 1−5.

(28) Ataka, M.; Tanaka, S. The Growth of Large Single Crystals of Lysozyme. *Biopolymers* 1986, *25*, 337−350.

(29) Kuramitsu, S.; Hamaguchi, K. Analysis of the Acid-Base Titration Curve of Hen Lysozyme. *J. Biochem.* 1980, *87* (4), 1215−1219.

(30) Mullin, J. W. *Crystallization*, 3rd ed.; Butterworth-Heinemann: Ox-ford, 1993.

BIOGRAPHY

Mr. Somchai Maosoongnern was born on October 1, 1983 in Nakhon Ratchasima. He earned his bachelor's degree in Chemical Engineering from Suranaree University of Technology (SUT), Nakhon Ratchasima in 2006. He has received the RGJ-Ph.D. scholarship from the Thailand Research Fund (TRF) in co-operation with SUT to study in the doctoral degree in Chemical Engineering under the supervision of Prof. Dr. Adrian E. Flood since 2006. He has also had additional laboratory experience as an exchange scholar at the Institute of Thermal Process Technology at Martin Luther University Halle-Wittenberg, Halle (Saale), Germany, in 2011 with the cooperative supervision of Prof. Dr. Joachim Ulrich.